Une approche globale pour caractériser les matériaux massifs anisotropes: quelques exemples d'Analyse Combinée par diffraction-diffusion

D. Chateigner

Normandie Université, IUT-Univ. Caen

CRISMAT-CNRS, ENSICAEN

Saint Gobain CREE, Cavaillon, 7th Feb. 2017

<u>Diffraction “sees”</u>

Texture
$f(g)_{\Phi,L}$

Structure
$|F_{\mathbf{h}}|^2_{\Phi,L}$

Real samples
Layered samples
thicknesses
roughnesses
$\rho(z)$…

Residual Stress
$\langle C_{ijkl}(g) \rangle_{\Phi,L}$

Phase
$S_{\Phi,L}$

defects (0D .. nD)
broadening
asymmetry

Rietveld: Acta Cryst. (1967), J. Appl. Cryst (1969)

computers, neutrons (Gaussian peaks): powders !

Lutterotti, Matthies, Wenk: Rietveld Texture Analysis, J. Appl. Phys. (1997)

classical Rietveld + QTA (WIMV)

Morales, Chateigner, Lutterotti, Ricote: Mat. Sci. For. (2002)

Rietveld of layers (QTA, QMA) + E-WIMV

ESQUI EU FP6 project (ended Jan. 2003)

Lutterotti, Chateigner, Ferrari, Ricote: Thin Sol. Films (2004)

E-WIMV + RSA + XRR + Geom. Mean: Extended Rietveld

Chateigner, Combined Analysis, Wiley-ISTE (2010)

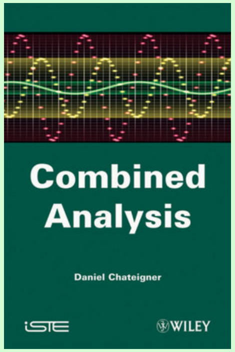

Soon in International Tables Vol H

Boullay, Lutterotti, Chateigner, Sicard: Acta Cryst A (2014)

Electron Diffraction Pattern – 2-waves Blackman correction

Why not benefit of texture in Structure determination ?

Perfect powders:
- overlaps (intra- and inter-p
- no angular constrain
- anisotropy difficult to reso

Single pattern

Single crystals:
- reduced overlaps
- max angular constrains
- Perfect texture: max anisotropy

Many individual diffracted peaks

Textured powders:
- reduced overlaps
- angular constrain = f(texture strength)
- Intermediate anisotropy

Many patterns to measure and analyse

Rietveld: extended to lots of spectra

$$y_c(\mathbf{y}_S,\theta,\eta) = y_b(\mathbf{y}_S,\theta,\eta) + I_0 \sum_{i=1}^{N_L} \sum_{\Phi=1}^{N_\Phi} \frac{\nu_{i\Phi}}{V_{c\Phi}^2} \sum_h Lp(\theta) j_{\Phi h} \left|F_{\Phi h}\right|^2 \Omega_{\Phi h}(\mathbf{y}_S,\theta,\eta) P_{\Phi h}(\mathbf{y}_S,\theta,\eta) A_{i\Phi}(\mathbf{y}_S,\theta,\eta)$$

Texture:

$$P_h(\mathbf{y}_S) = \int_{\tilde{\varphi}} f(g,\tilde{\varphi})\, d\tilde{\varphi}$$

E-WIMV, components, Harmonics, Exp. Harmonics …

Strain-Stress:

$$\langle S \rangle_{geo}^{-1} = \left[\prod_{m=1}^{N} S_m^{\nu_m}\right]^{-1} = \prod_{m=1}^{N} S_m^{-\nu_m} = \prod_{m=1}^{N} \left(S_m^{-1}\right)^{\nu_m} = \left\langle S^{-1} \right\rangle_{geo} = \langle C \rangle_{geo}$$

Geometric mean, Voigt, Reuss, Hill …

Layering:

$$A_{i\Phi} = \frac{\nu_{i\Phi} \sin\theta_i \sin\theta_o}{\mu_i (\sin\theta_i + \sin\theta_o)} \left\{1 - e^{-\bar{\mu}_i \tau_i W}\right\} \prod_{k<i} e^{-\bar{\mu}_k \tau_k W}$$

$$W = \frac{1}{\sin\theta_i} + \frac{1}{\sin\theta_o}$$

Stacks, coatings, multilayers …

Line Broadening:

Popa, Delft: Crystallite sizes, shapes, microstrains, distributions
0D-3D defects

X-Ray Reflectivity (specular):

Matrix, Parrat, DWBA, EDP …

X-Ray Fluorescence/GiXRF:

De Boer

Electron Diffraction Patterns:

2-waves Blackman

Line Broadening:

Crystallite sizes, shapes, μstrains, distributions

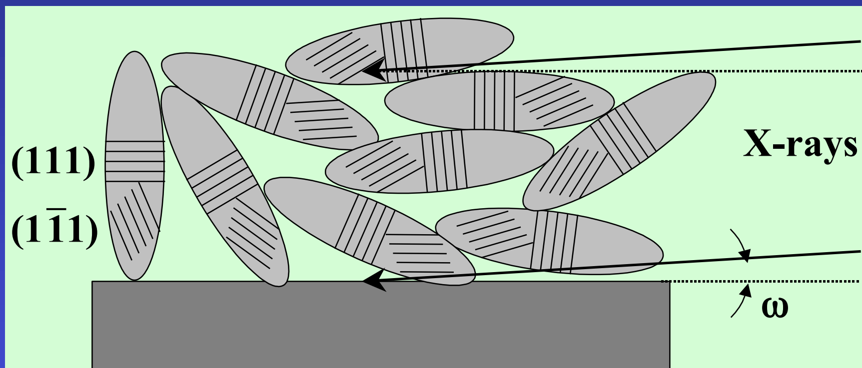

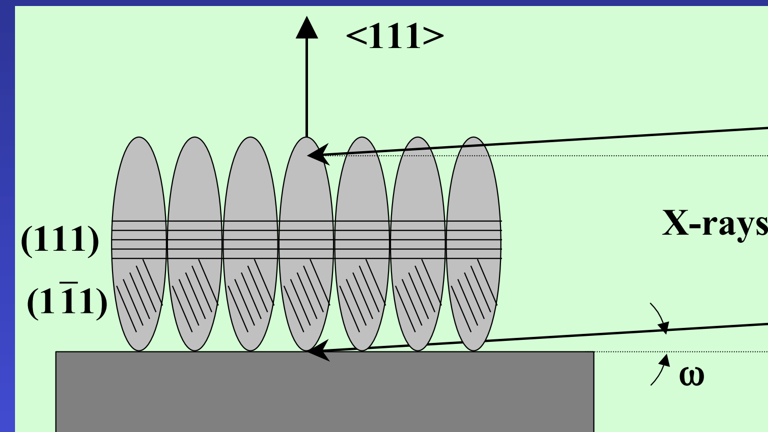

- Texture helps the "real" mean shape determination

$$\langle R_{\vec{h}} \rangle = \sum_{\ell=0}^{L} \sum_{m=0}^{\ell} R_\ell^m K_\ell^m(\chi,\varphi)$$

Symetrised spherical harmonics

$$K_\ell^m(\chi,\varphi) = P_\ell^m(\cos\chi)\cos(m\varphi) + P_\ell^m(\cos\chi)\sin(m\varphi)$$

$$<R_{\mathbf{h}}> = R_0 + R_1 P_2^0(x) + R_2 P_2^1(x)\cos\varphi + R_3 P_2^1(x)\sin\varphi + R_4 P_2^2(x)\cos 2\varphi + R_5 P_2^2(x)\sin 2\varphi + \ldots$$

$$<\varepsilon_{\mathbf{h}}^2> E_{\mathbf{h}}^4 = E_1 h^4 + E_2 k^4 + E_3 \ell^4 + 2E_4 h^2 k^2 + 2E_5 \ell^2 k^2 + 2E_6 h^2 \ell^2 + 4E_7 h^3 k + 4E_8 h^3 \ell + 4E_9 k^3 h + 4E_{10} k^3 \ell + 4E_{11} \ell^3 h + 4E_{12} \ell^3 k + 4E_{13} h^2 k \ell + 4E_{14} k^2 h \ell + 4E_{15} \ell^2 kh$$

$\bar{1}$

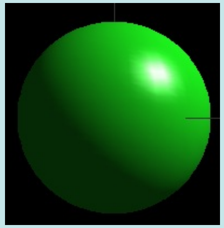

R_0

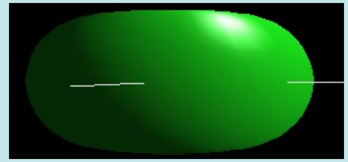

R_0, $R_1 < 0$

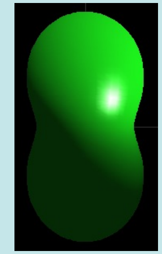

R_0, $R_1 > 0$

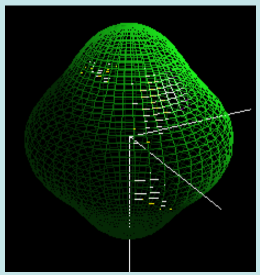

R_0, $R_6 > 0$

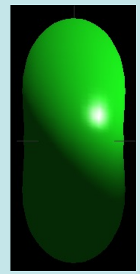

R_0,
R_2 and $R_6 > 0$

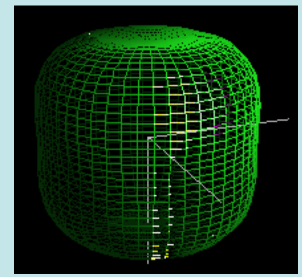

R_0, $R_6 < 0$

6/m

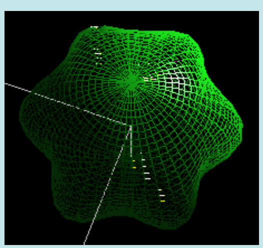

R_0, $R_4 > 0$

m3m

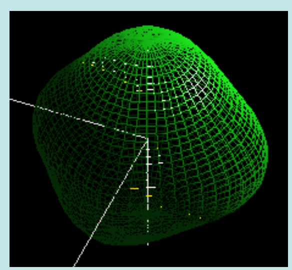

R_0, $R_1 > 0$

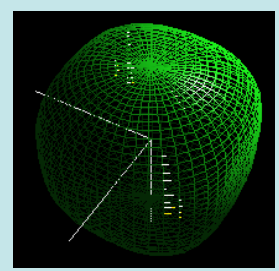

R_0, $R_1 < 0$

EMT nanocrystalline zeolite

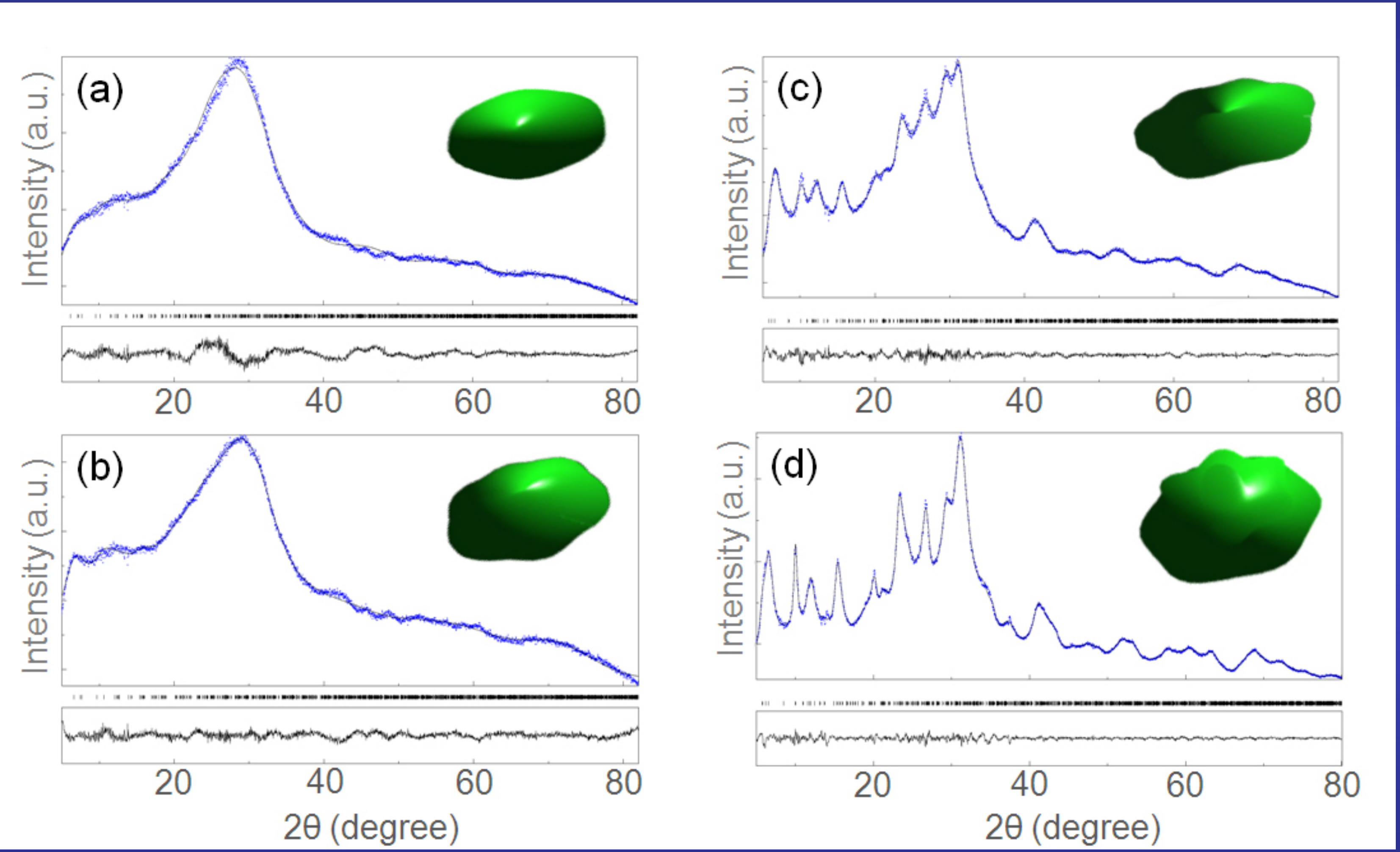

Ng, Chateigner, Valtchev, Mintova: *Science* **335** (2012) 70

Combined Analysis approach

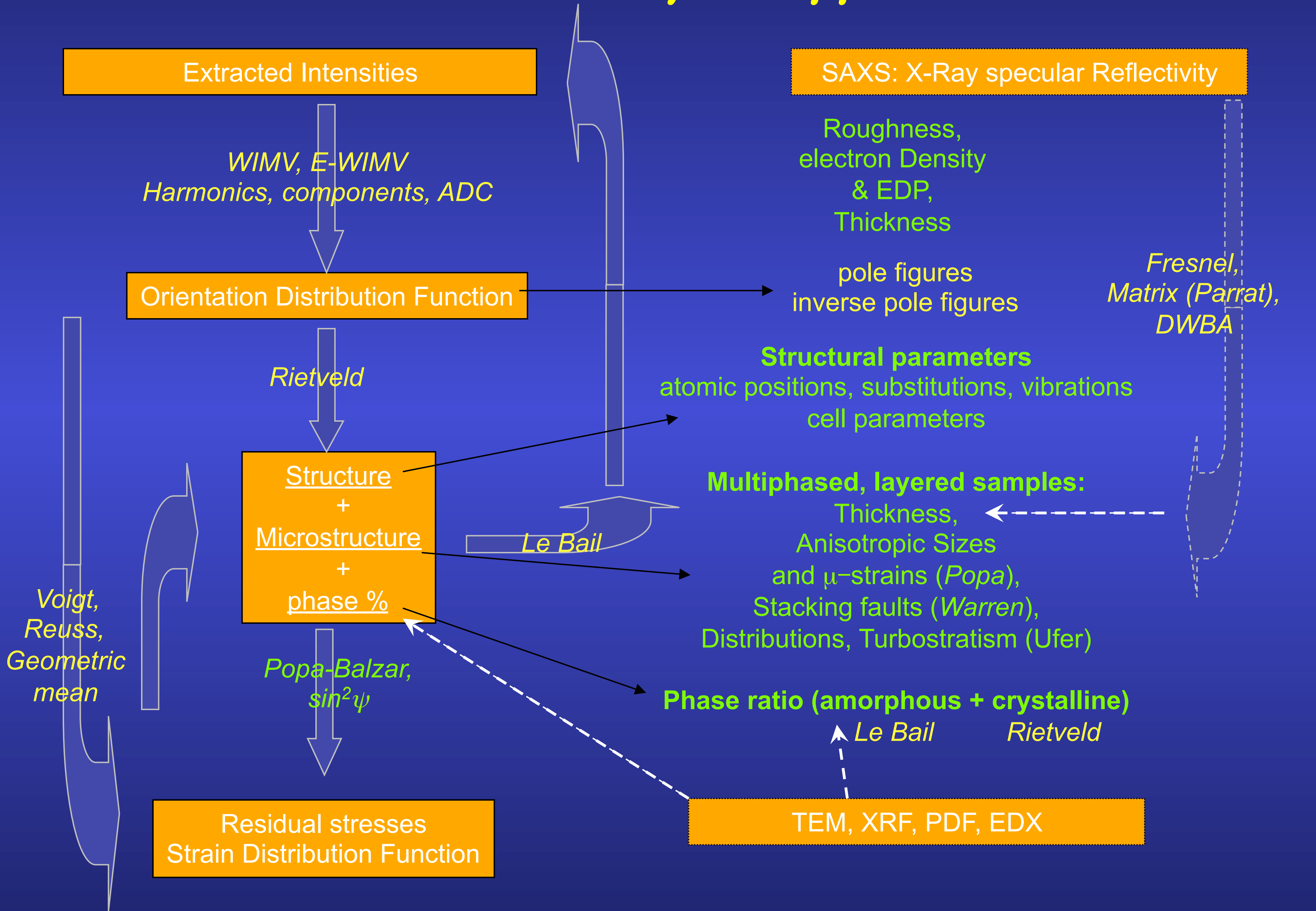

Minimum experimental requirements

1D or 2D Detector +
4-circle diffractometer
(CRISMAT – ANR EcoCorail)

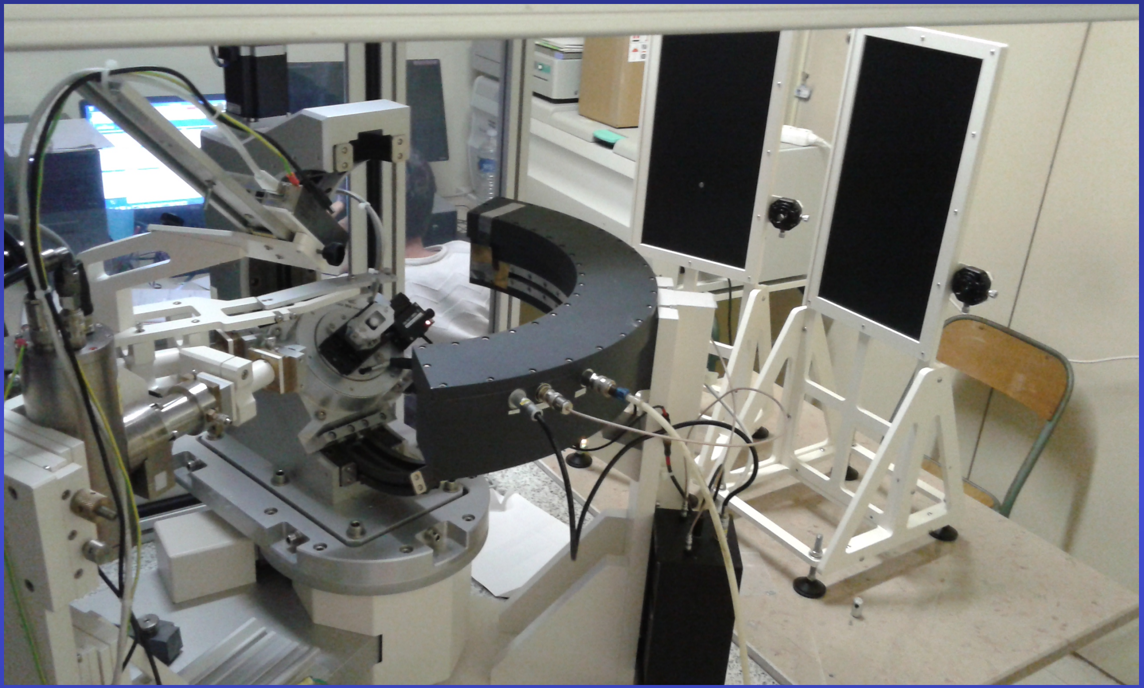

~1000 experiments (2θ diagrams)
in as many sample orientations

+

Instrument calibration
(peaks widths and shapes,
misalignments, defocusing …)

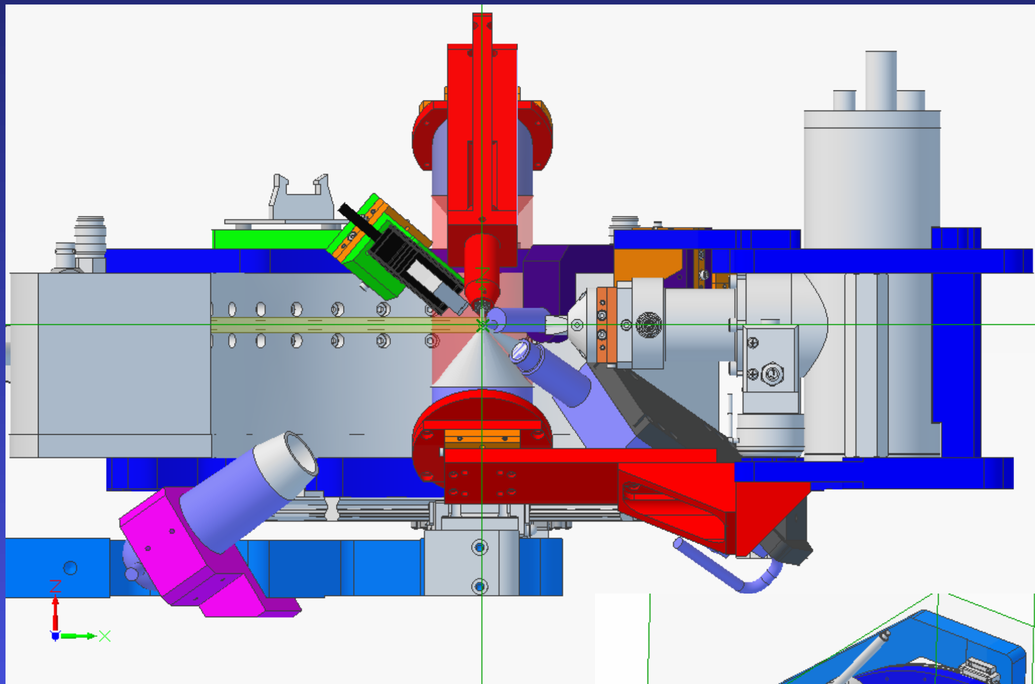

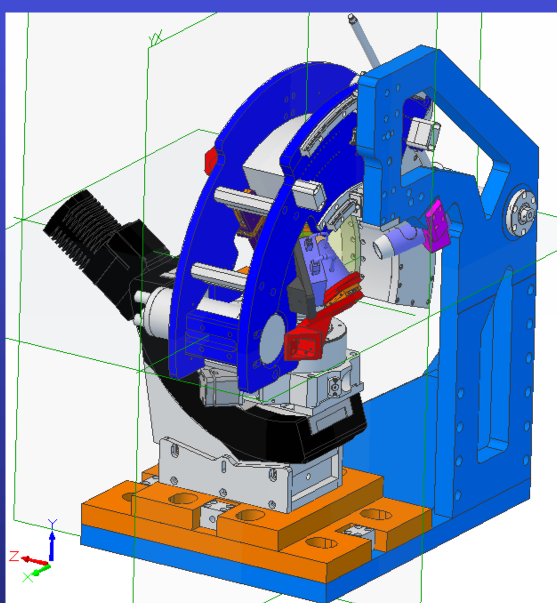

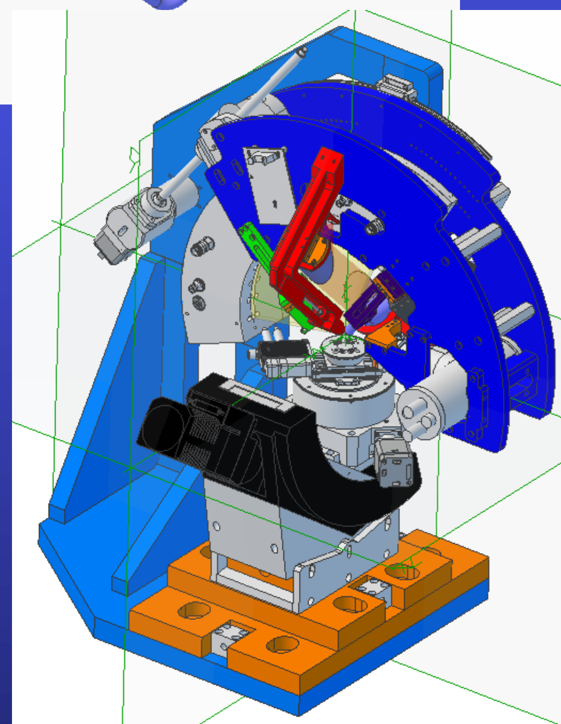

XRD-XRF-Raman-FTIR Combined Analysis (SOLSA EU projet)

Independent measurements

Different wavelengths and rays

Reflectivity: thickness, roughness, electron density profiles

X-ray Fluorescence: composition

Spectroscopies: local structures (PDF, FTIR, Mossbauer …), eventually anisotropic (P-EXAFS, ESR, Raman …), Element profiles (SIMS, RBS …) …

Physical models: magnetisation, conductivity …

Environments: applied fields

Combined Analysis cost function

$$WSS = \sum_{t=1}^{N_p} u_t \sum_{i=0}^{N_t} w_{it} \left(y_{itc} - y_{ito} \right)^2$$

For each pattern t: w_{it} : weight, usually $1/y_i = \sigma^2$.

u_t : weight of each pattern t
should be used to adjust the importance we want to give to a particular technique or pattern with respect to the others

Grinding-Spinning to powderise another problem !

Grinding: removes angular relationship, adds correlations

Spinning: what if the fiber texture axis // spinning axis ?

Texture and strains:
- not measured, not removed ?
- added ?

Same sample ? Rare samples ?
Impossible to grind ?

Correction: without measuring it ? (March-Dollase)

XRD Calibration

ω = 20°

60°

χ

0°

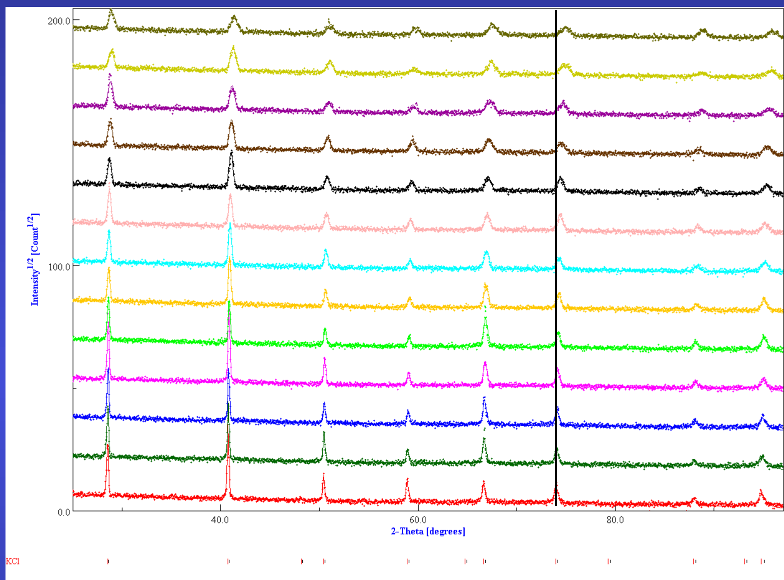

ω = 40°

60°

χ

0°

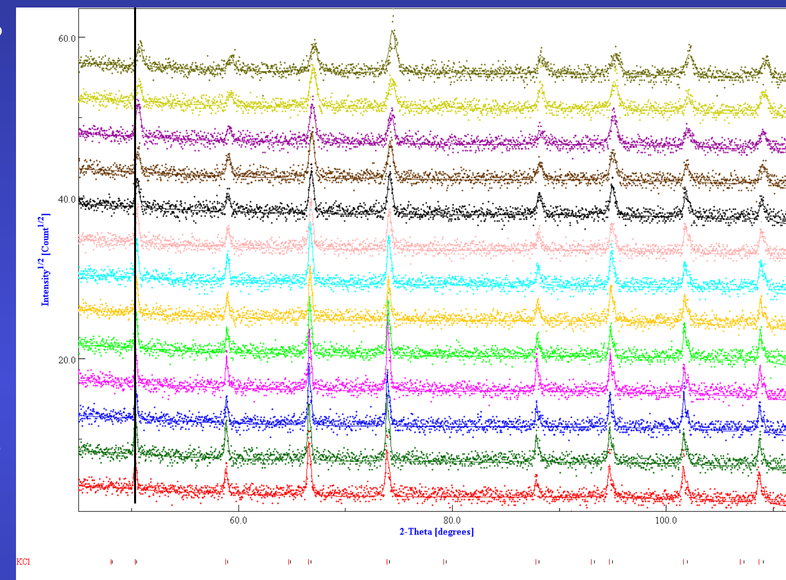

KCl, LaB_6 …

FWHM (ω, χ, 2θ, η …)
2θ shift
gaussianity
asymmetry
misalignments ...

Minimization algorithms

- Can be fully used in the method (everywhere)

- Marquardt Least Squares (based on steepest decrease and Gauss-Newton)
  - Efficient, best with few parameters, near the solution
- Evolutionary computation (or genetic algorithm)
  - Slow, not efficient, requires a lot of resources
  - Unlimited number of parameters
  - Can start far from the solution
- Simulated annealing (the solution proceed like a random walk, but the walking step decreases as temperature decreases)
  - In between the Marquardt and evolutionary algorithms
- Simplex (generates n+1 starting solutions as vertices of a polygon, n number of parameters, and contract/expand the polygon around the minima)
  - Slow on convergence
  - Remains close to the solution, but explore more minima with respect to the Marquardt

$Ca_3Co_4O_9$ thermoelectrics

$Ca_3Co_4O_9$: Misfit lamellar and modulated Structure, with high thermopower

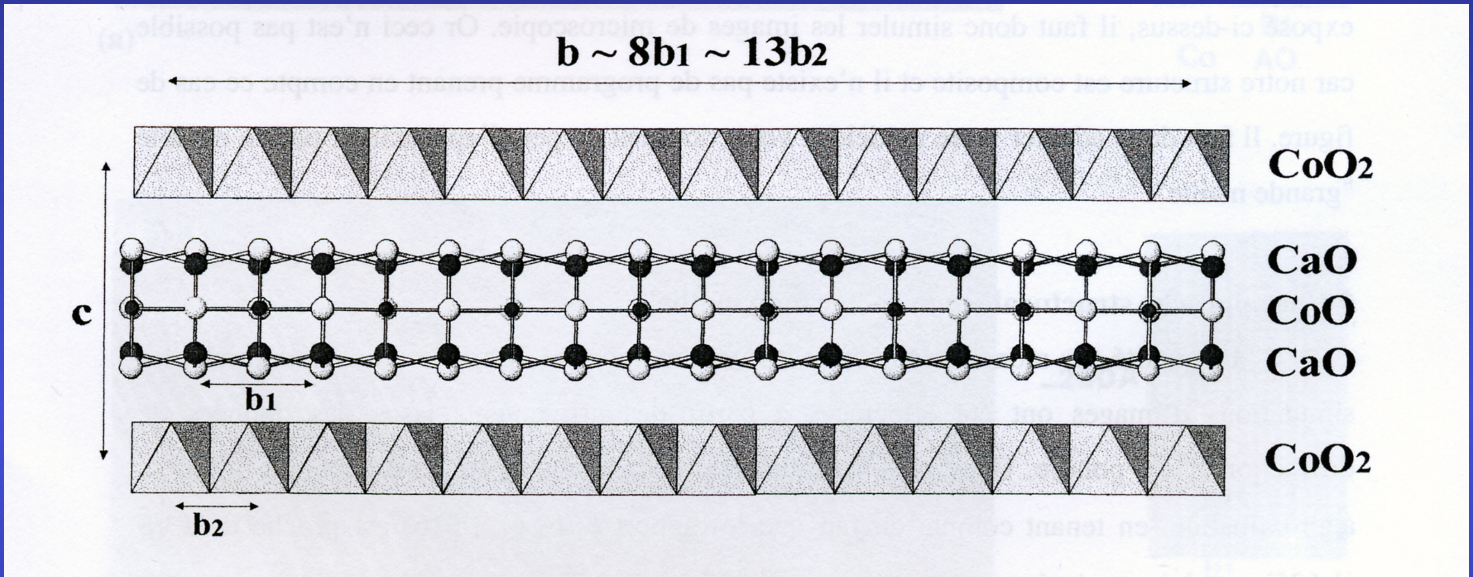

Two monoclinic sub-systems:
S1 with a ~ 4.8Å, b_1 ~ 4.5Å, c ~ 10.8Å et β ~ 98° (NaCl-type)
S2 with a ~ 4.8Å, b_2 ~ 2.8Å, c ~ 10.8Å et β ~ 98° (CdI_2-type)

$\Gamma = \sigma_{ab}/\sigma_c \sim 10$ → Texture

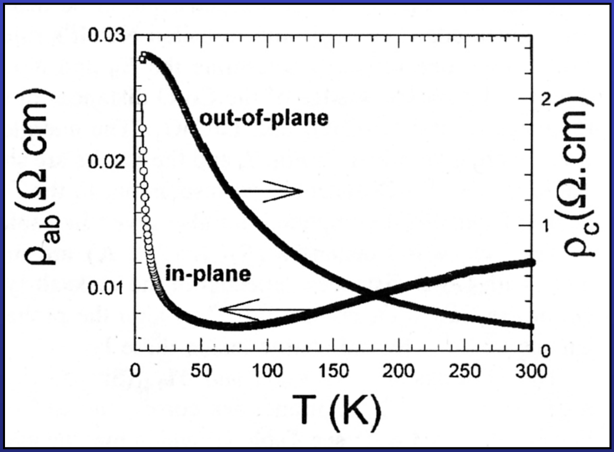

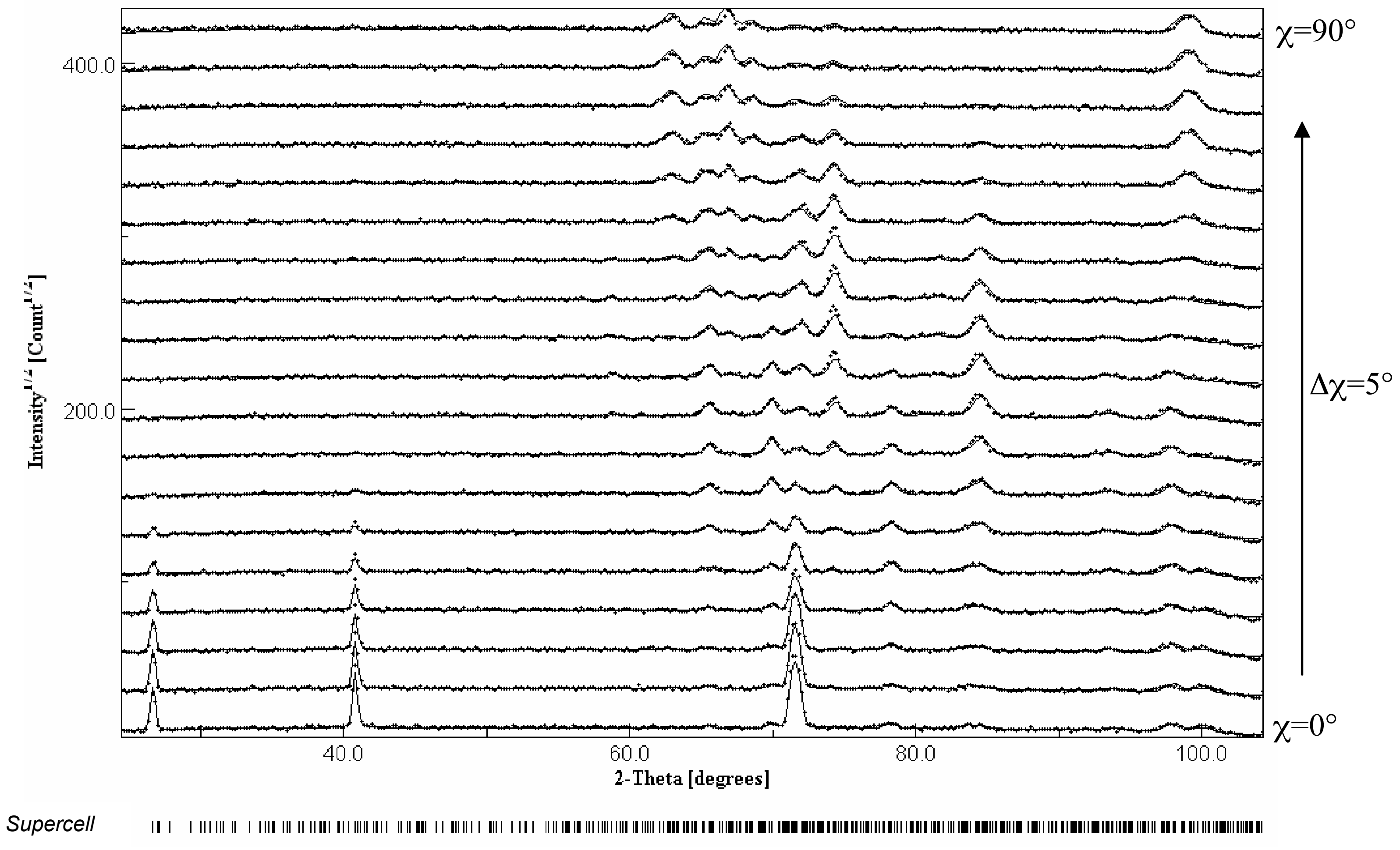

χ=90°
400.0
200.0
Intensity^1/2 [Count^1/2]
Δχ=5°
χ=0°
40.0
60.0
80.0
100.0
2-Theta [degrees]
Supercell

RP=19.7%, Rw=11.9%

9.8 MPa for 2 h

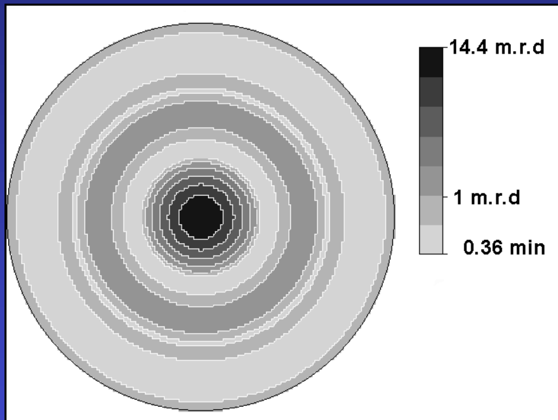

19.6 MPa for 6 h

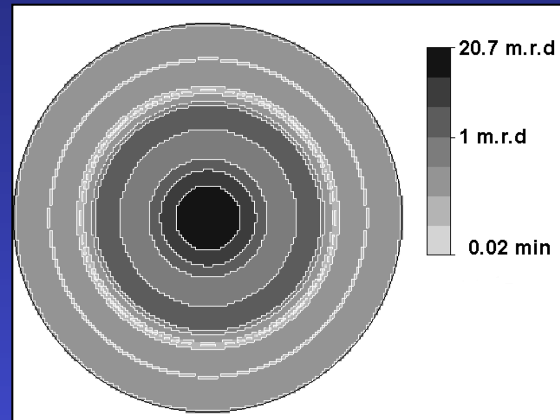

19.6 MPa for 20 h

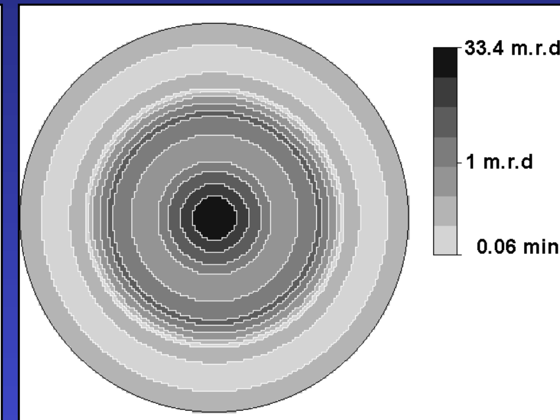

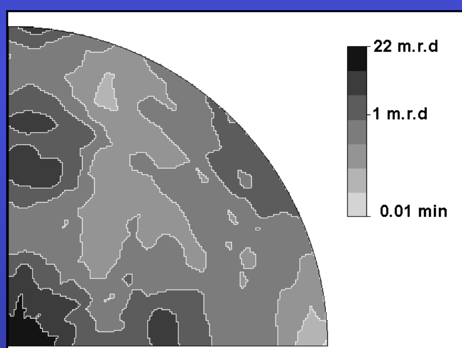

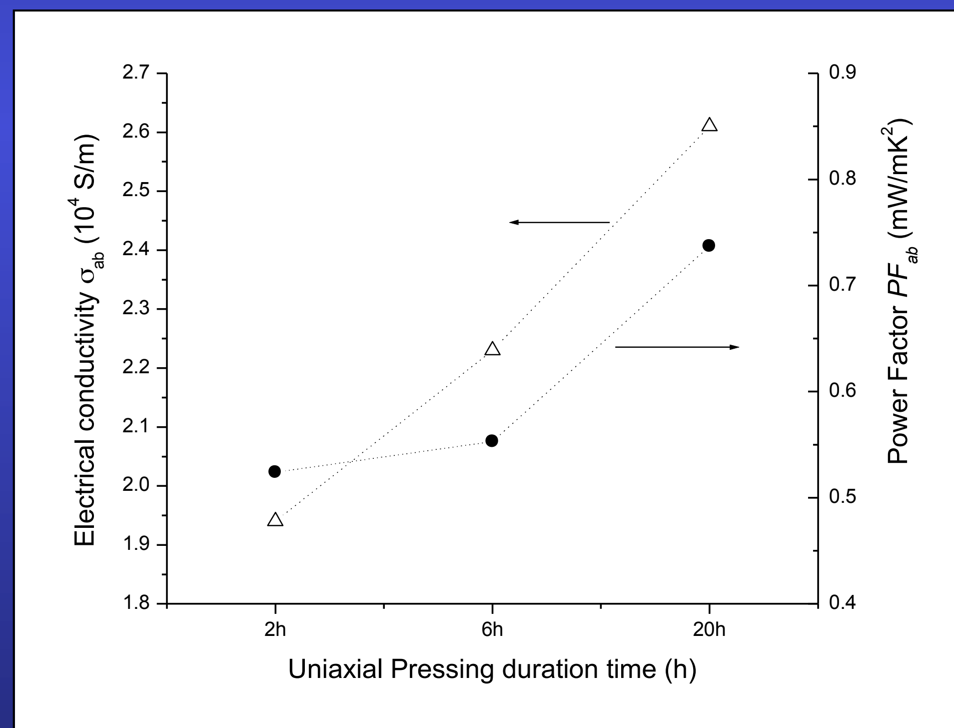

Templated Growth Method

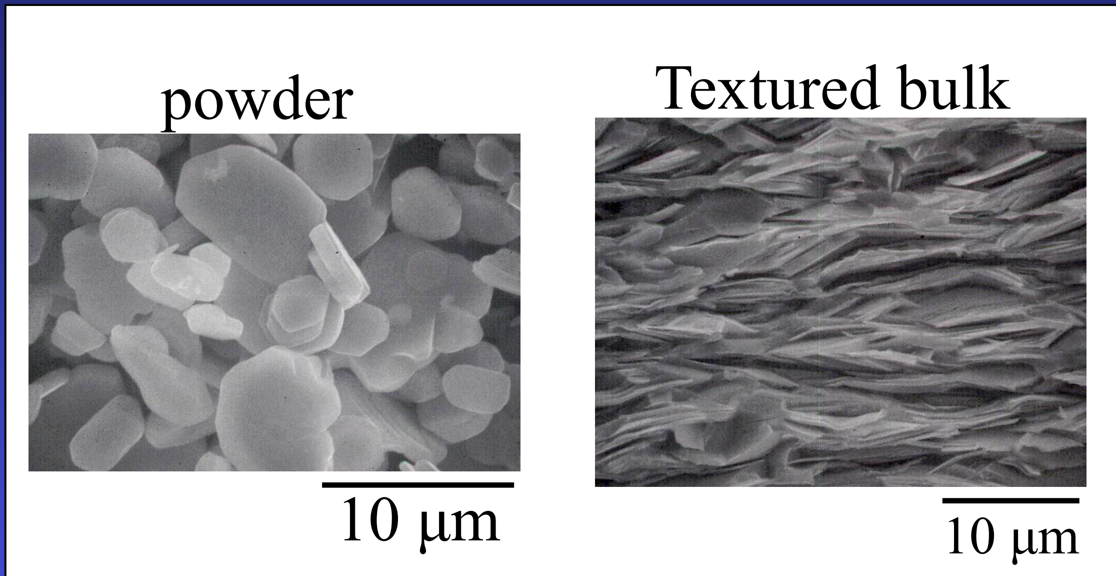

Magnetic alignment
and
Templated Growth
method

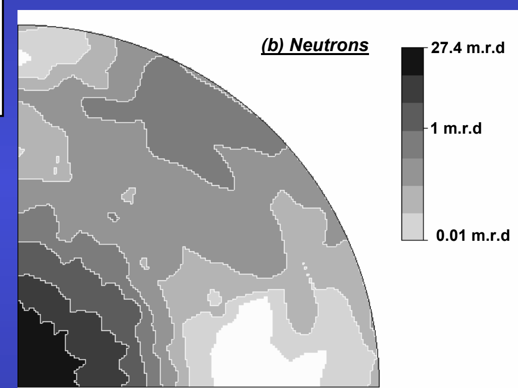

- neutrons
- 3D Supercell: a=4.8309Å, b~8b1~13b2~36.4902Å, c=10.8353Å, β=98.13°
174 atoms/cell
-Sample : 0.6 cm^3

SPS (Spark Plasma Sintering)

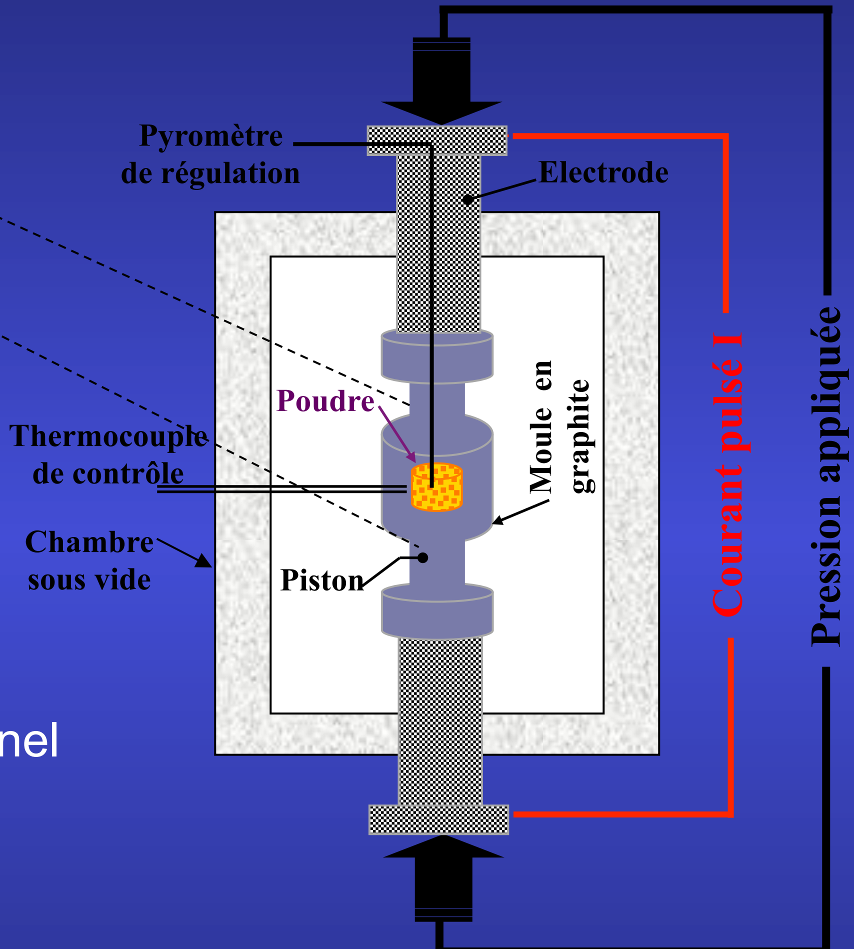

[M. Tokita-1999]

- Technique de frittage non conventionnel

✓ Cinétique de frittage très rapide

✓ Température de frittage plus basse

✓ Densification plus importante

X Frittage sous vide (risque de réduction)

X Matrice en graphite (risque de contamination)

→ Effet de la pression σ_{SPS}

Pression, σ_{SPS}

30 MPa

(900°C;2min)

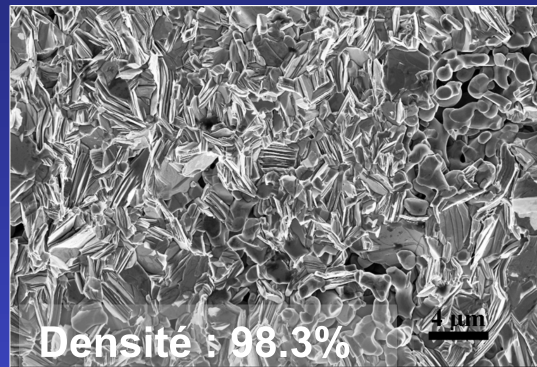

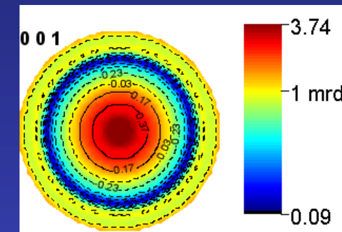

- Le max. de pôles {001} : 3.74 mrd

50 MPa

(900°C;2min)

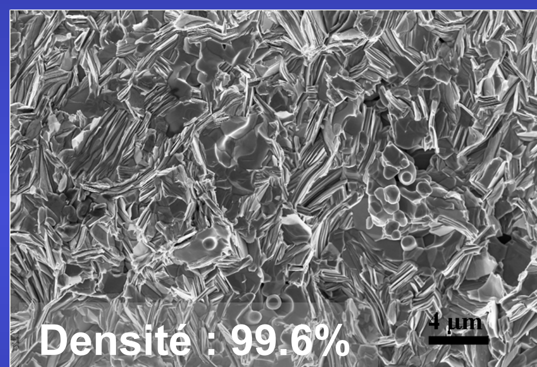

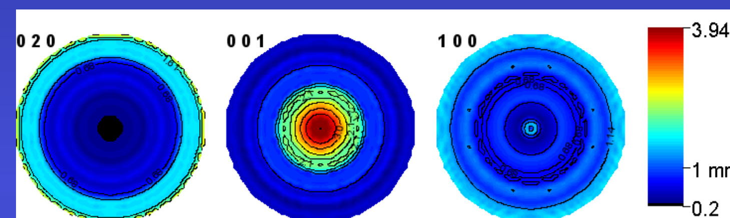

- Le max. de pôles {001} : 3.94 mrd

75 MPa

(900°C;2min)

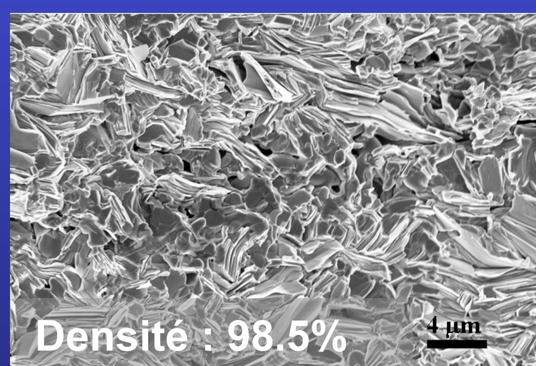

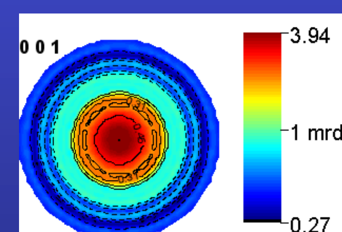

- Le max. de pôles {001} : 4.05 mrd

Effets de bords de cellules SPS → Spark Plasma Texturing

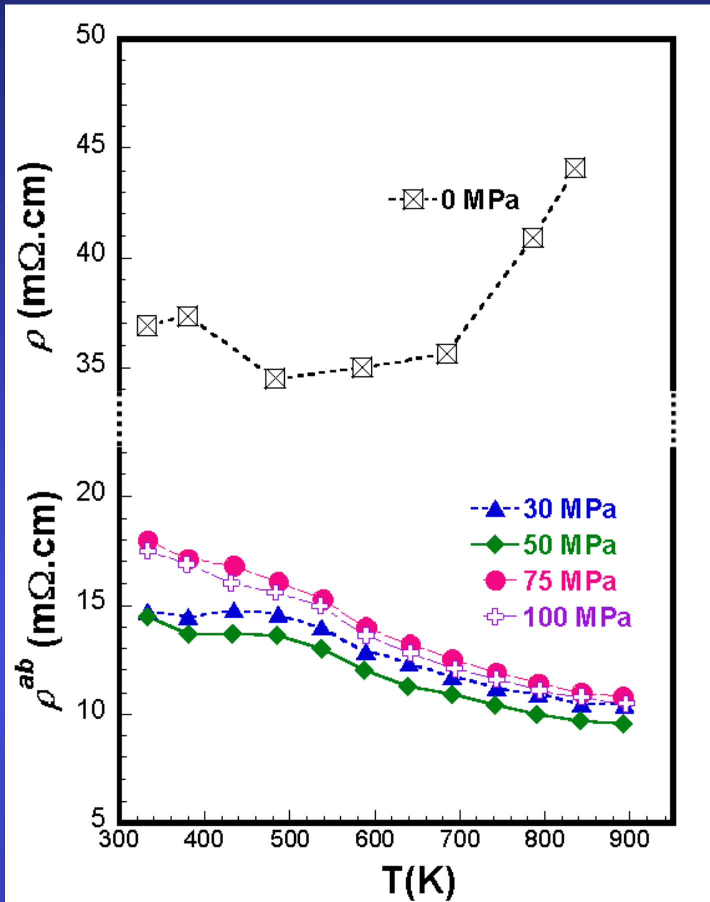

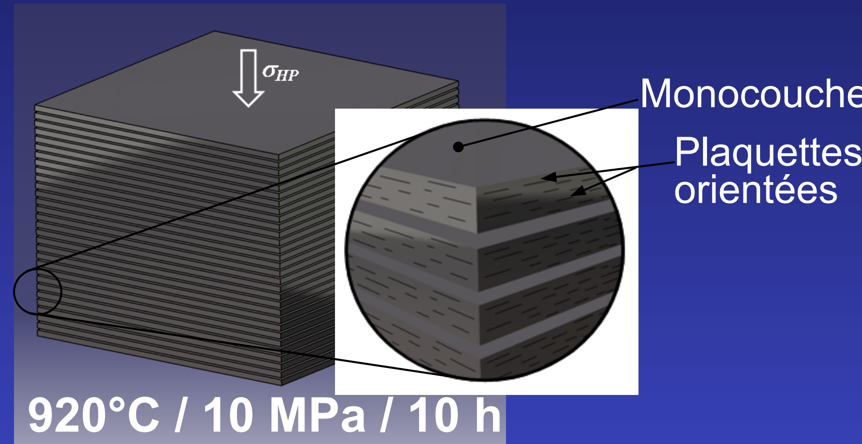

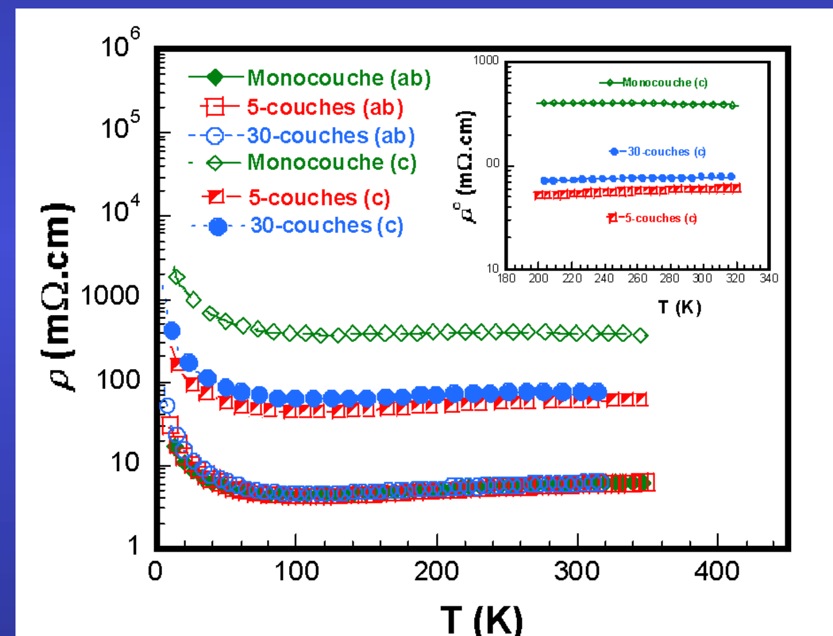

❑ Texture

- Diffraction neutronique

  → Texture dans le volume

- Le max. de pôles {001} : 42.73 mrd

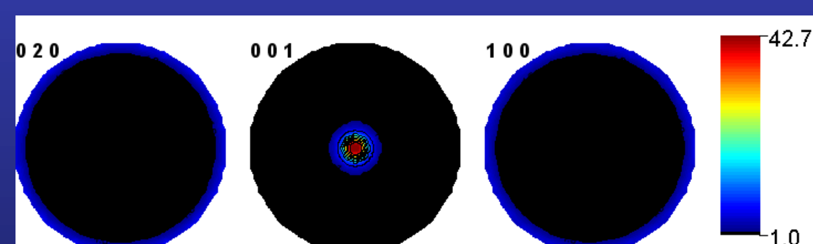

$Bi_2Te_{3-x}Se_x$ thermoelectrics
By double SPS

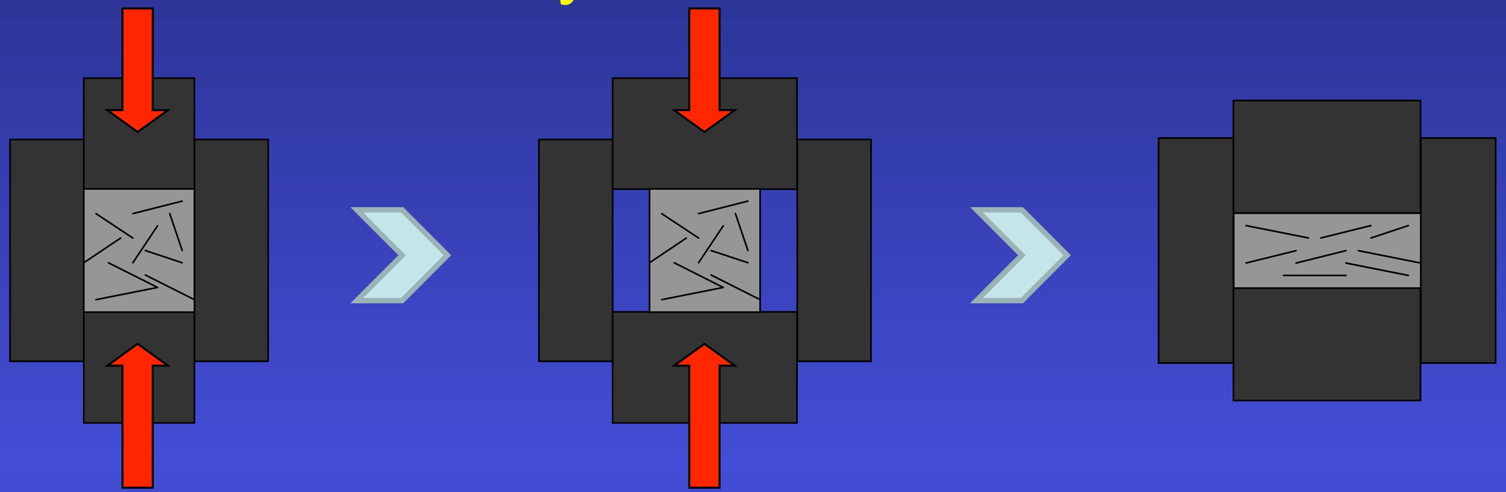

15 mm, 450°C, 5kN, 30'

20 mm, 450°C, 9kN, 30'

Pastille « texturée »

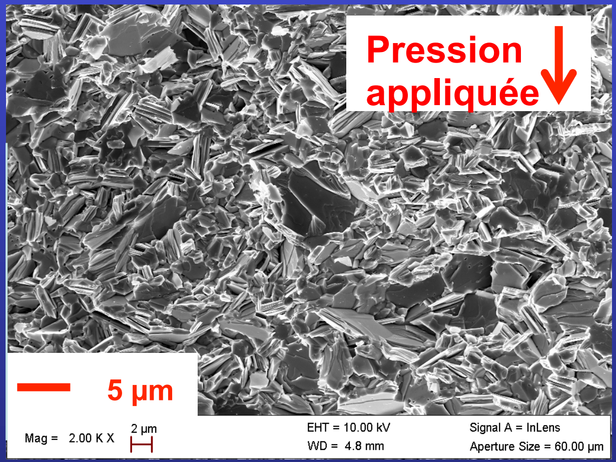

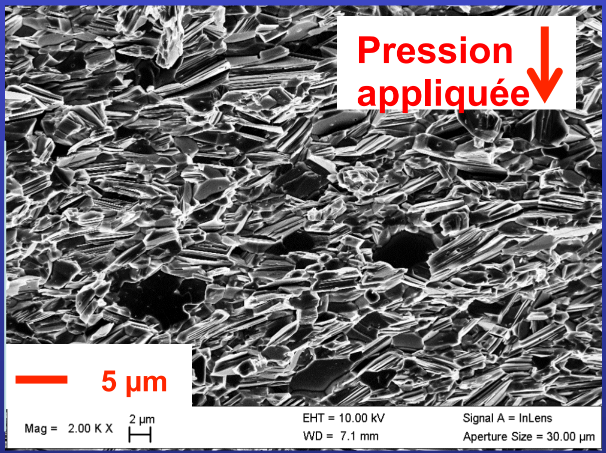

Kenfaui *et al*., J. Europ. Ceram. Soc. 32, 2012, 2405

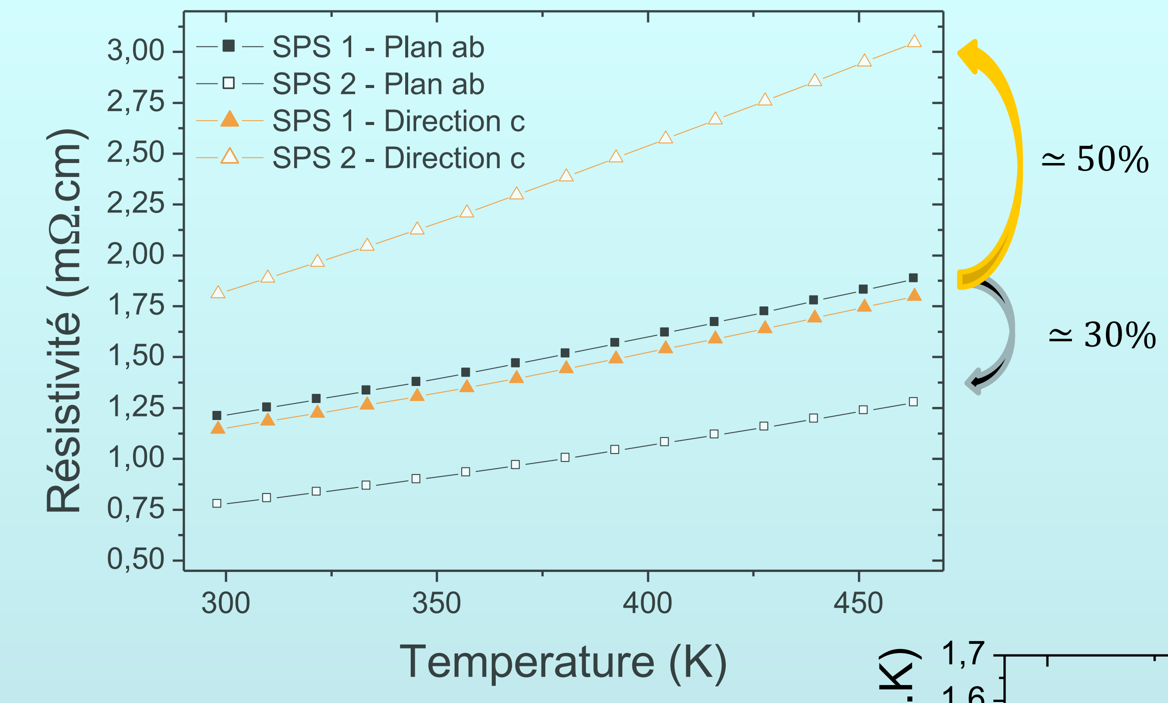

→ Forte augmentation/ diminution de la résistivité
→ Facteur d'anisotropie : de 1 à 2,5 à 300K

- $\kappa_{élec}$ augmente : due à la loi de W-F (nombre de Lorenz utilisé: 2.10^{-8} $W.\Omega.K^{-2}$)
- κ_{tot} augmente **légèrement**: due à l'augmentation de $K_{élec}$ compensée par la diminution de $K_{rés}$
- $\kappa_{rés}$ diminue : due à ???

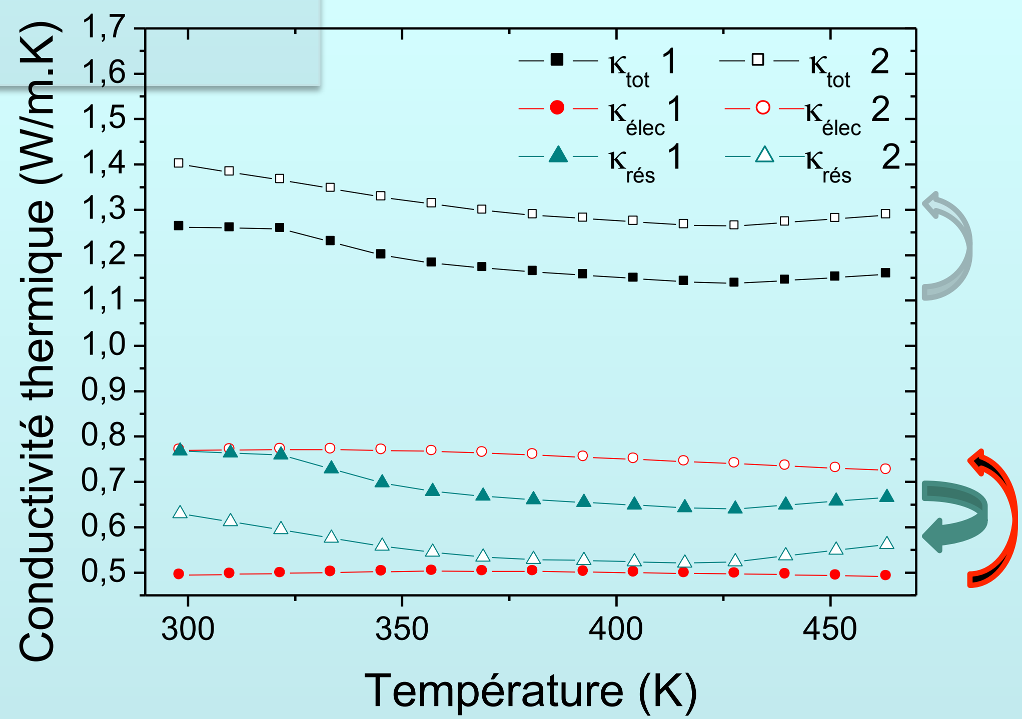

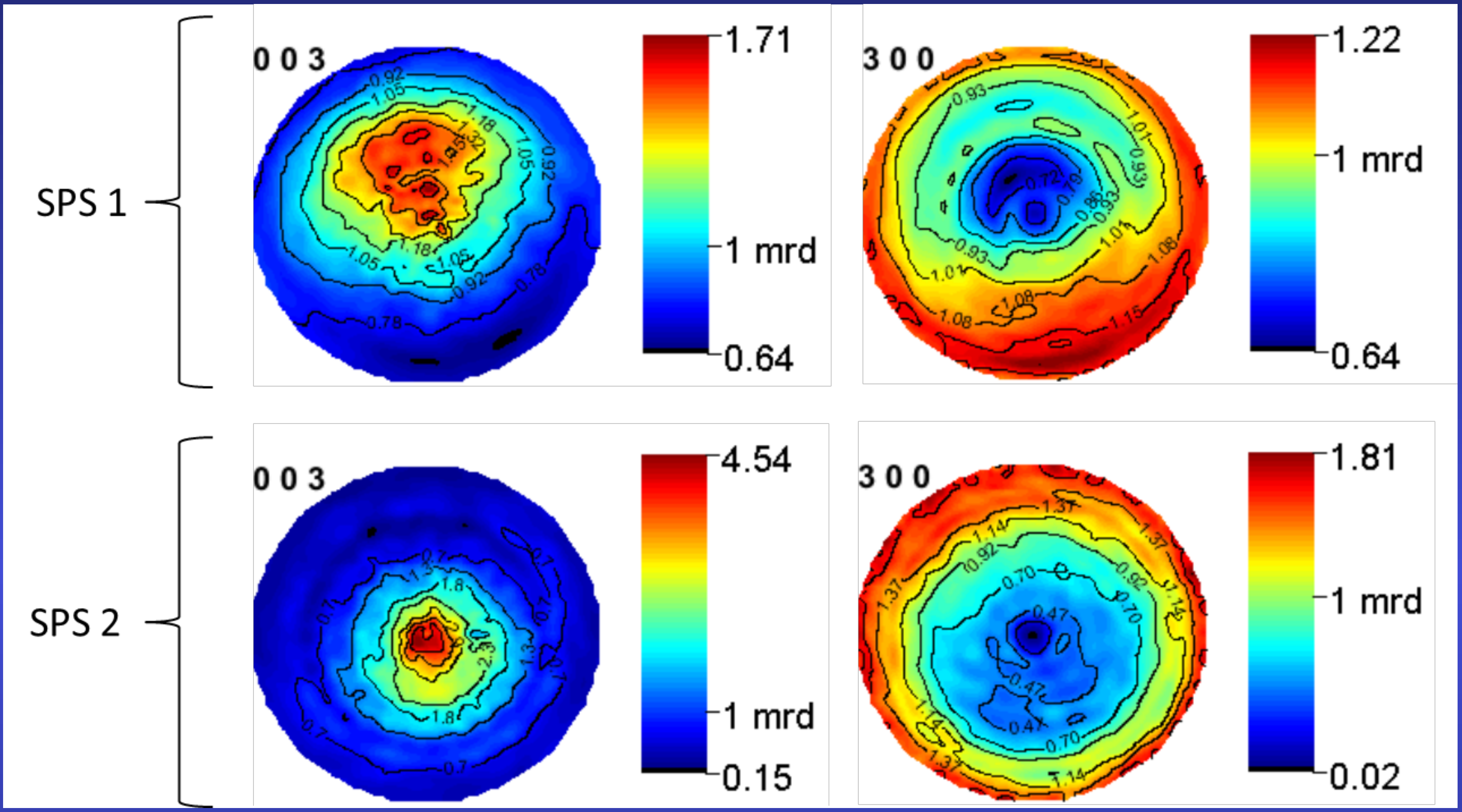

Weak texture increase

Cristallites orientation is not the sole cause for resistivity increase : (ρ_c/ρ_{ab}) calculated = 1,1

1^er^ SPS

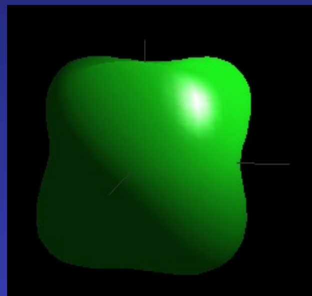

370 Å

470 Å

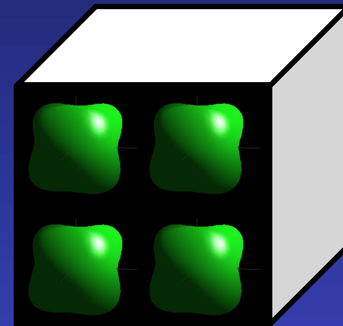

Grain après 1er SPS

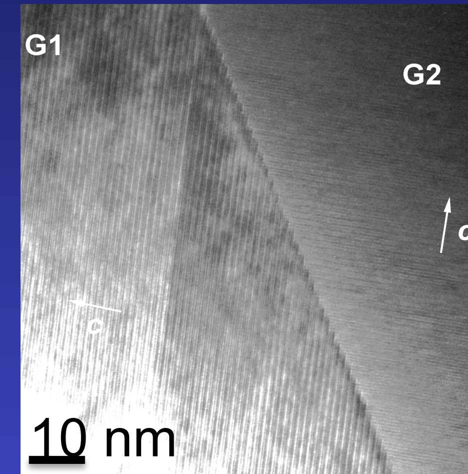

$$\rho_{ij}^{M} = \begin{vmatrix} 17.31 & . & . \\ . & 17.31 & . \\ . & . & 17.32 \end{vmatrix} ; \kappa_{ij}^{M} = \begin{vmatrix} 2.33 & . & . \\ . & 2.33 & . \\ . & . & 2.33 \end{vmatrix} ; \alpha_{ij}^{M} = \begin{vmatrix} 211 & . & . \\ . & 211 & . \\ . & . & 211 \end{vmatrix}$$

$$\rho_{ij}^{M} = \begin{vmatrix} 16.79 & . & . \\ . & 16.79 & . \\ . & . & 18.39 \end{vmatrix} ; \kappa_{ij}^{M} = \begin{vmatrix} 2.20 & . & . \\ . & 2.20 & . \\ . & . & 2.30 \end{vmatrix} ; \alpha_{ij}^{M} = \begin{vmatrix} 210.8 & . & . \\ . & 210.8 & . \\ . & . & 211.5 \end{vmatrix}$$

2nd SPS

1085 Å

250 Å

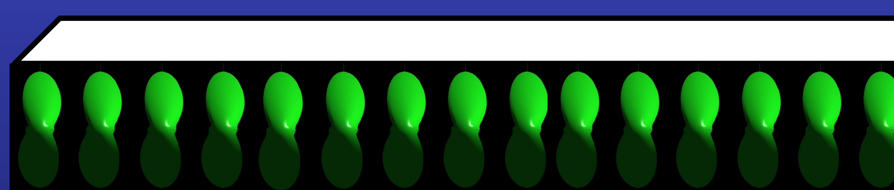

Grain après 2nd SPS

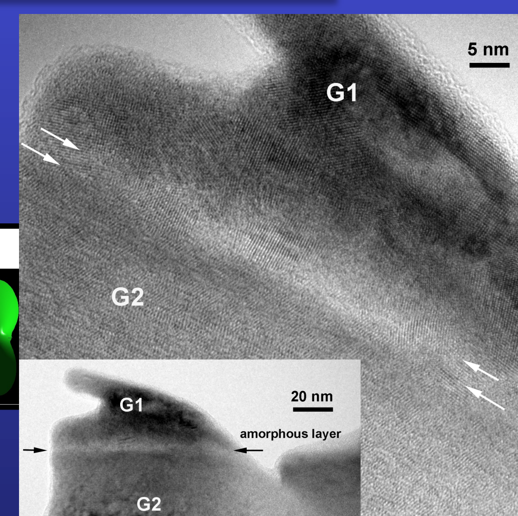

Artificial Coral Reefs from electrochemistry

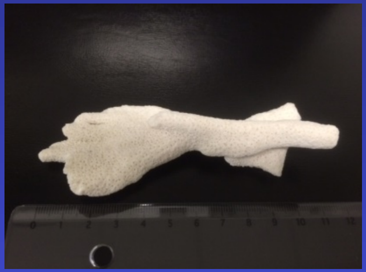

Millepora sp.

Natural sea water

$Mg(OH)_2$ – mediated $CaCO_3$ precipitation

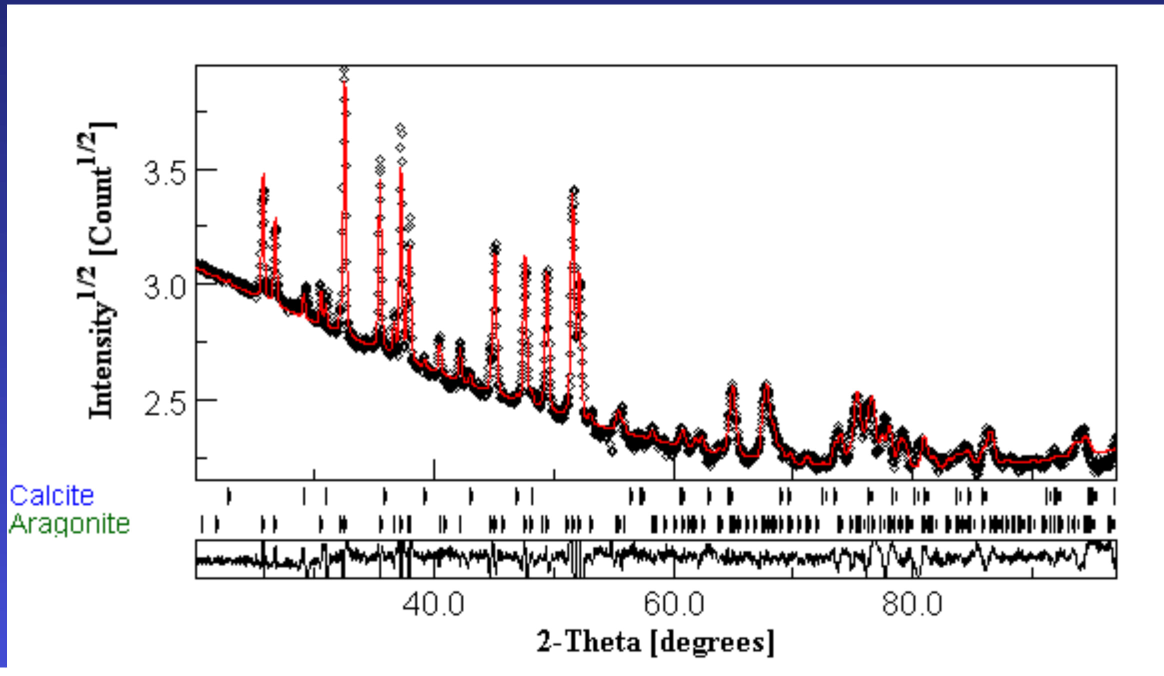

***Millepora* sp.**

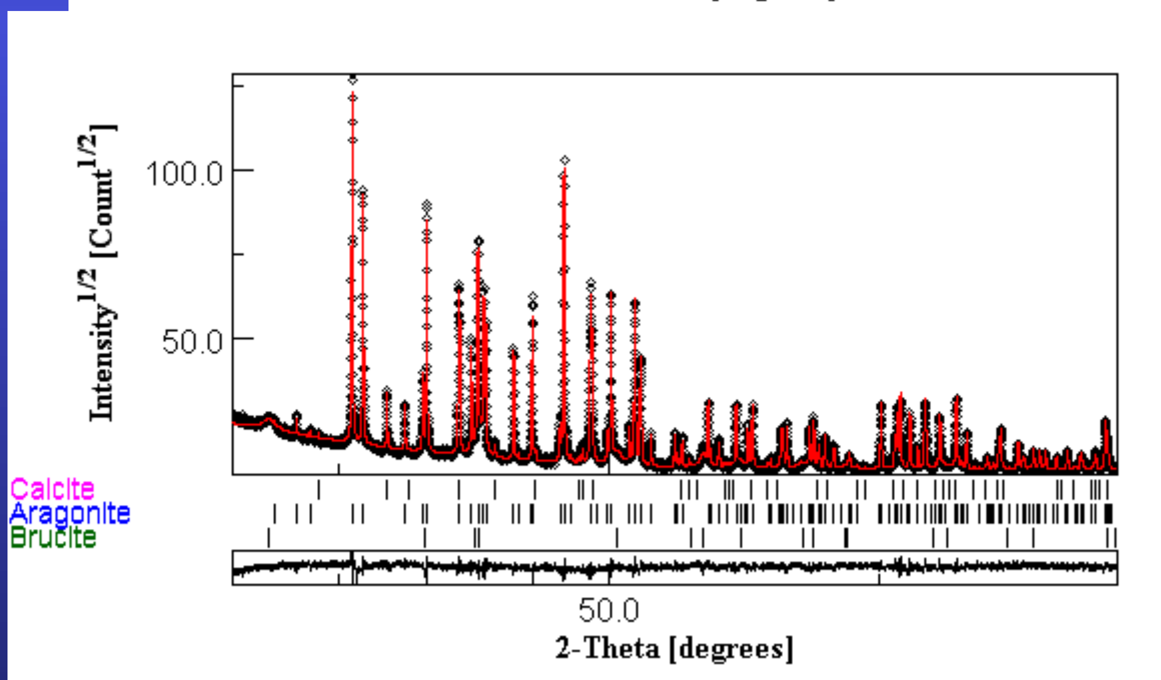

Dépôt 51 jours

26508

α-Al_2O_3 Slip-casted + magnetically aligned ceramics

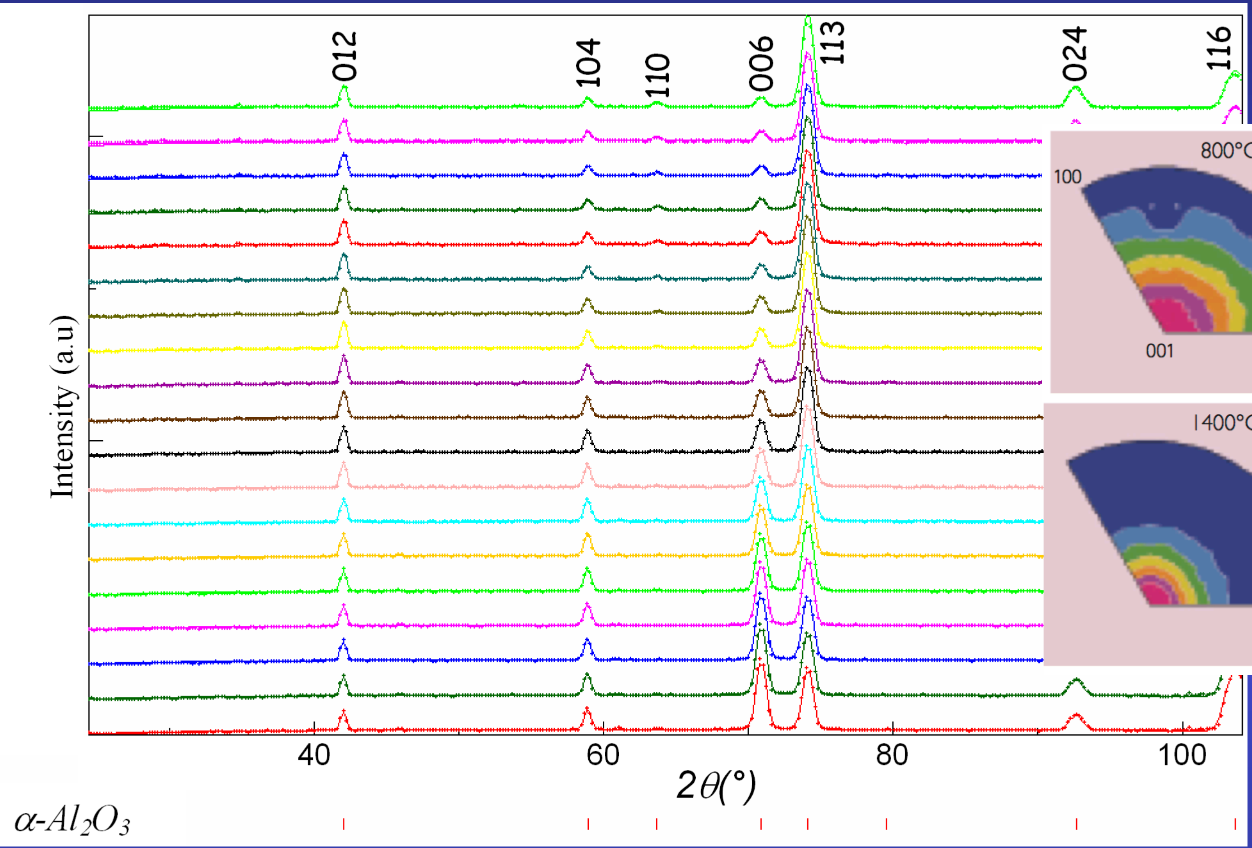

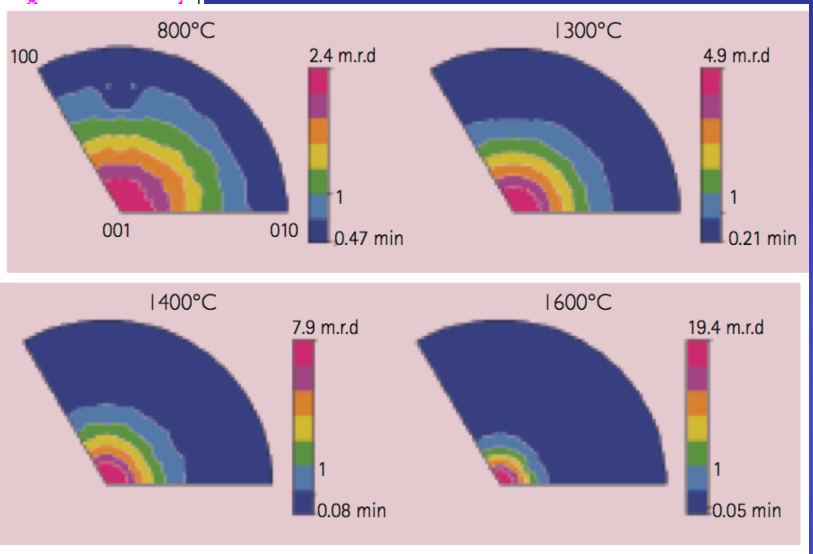

Specimens (Sintering Temperature)	ODF (001) inverse pole figure		Texture Index (F2)	Refined crystallite size (nm)	SEM Calculated grain size (nm)		Aspect Ratio
	Min	Max			$d_{//}$	$d_{\perp}$	$(d_{\perp}/d_{//})$
800°C	0.47	2.4	1.24	137 (13)	~150	~150	1
1300°C	0.21	4.9	2.13	> 1μm	1100	1170	1.063
1400°C	0.08	7.9	3.16	> 1μm	2610	2970	1.138
1600°C	0.05	19.4	7.78	> 1μm	7300	8800	1.205

Irradiated FluorApatite (FAp) ceramics

Self-recrystallisation under irradiation, depending on SiO_4 / PO_4 ratio (FAp / Nd-Britholite) and on irradiating species

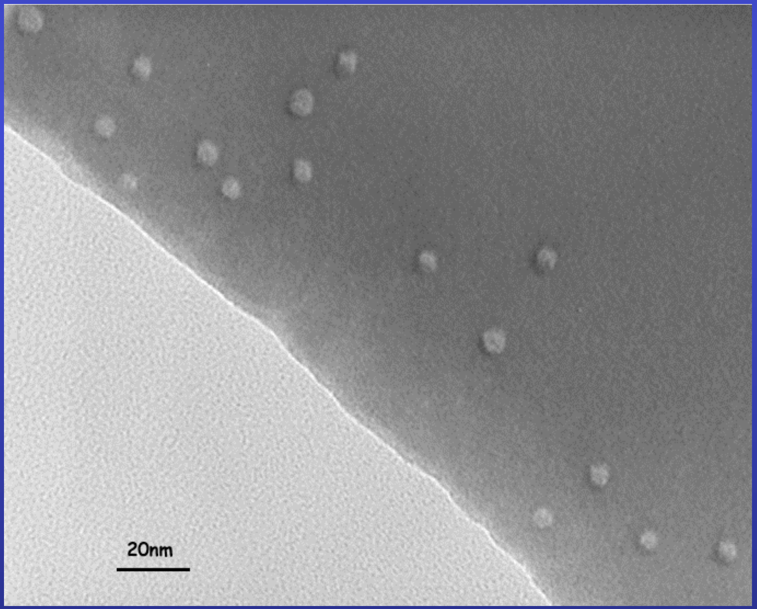

TEM of FAp irradiated with 70 MeV, 10^{12} Kr cm^{-2} ions

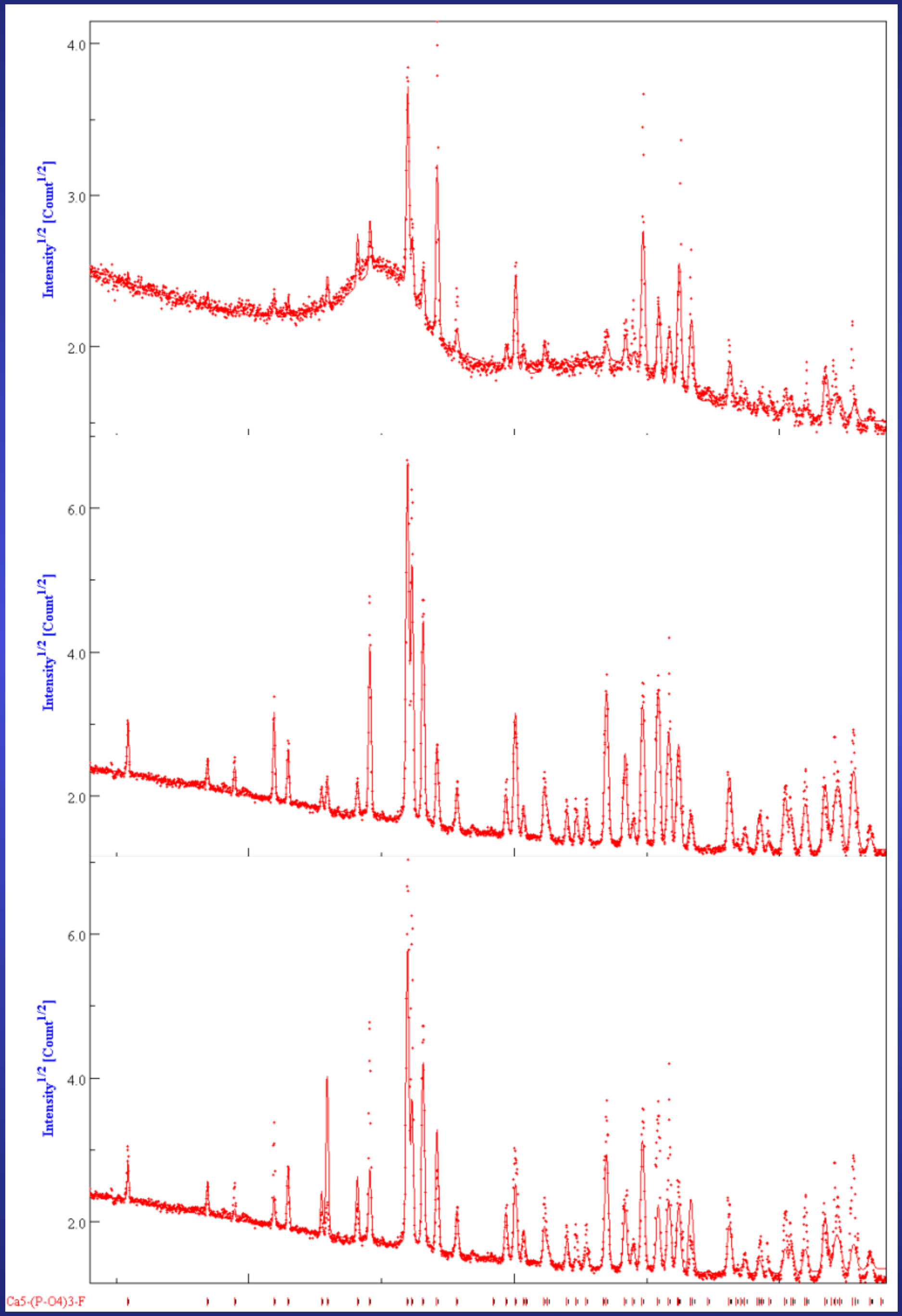

texture corrected,

10^{13} Kr cm^{-2}

Virgin, with texture correction

Virgin, no texture correction

Fluence (ions.cm^{-2})	Vc/V (%)	A (Å)	c (Å)	<t> (nm)	$\Delta a/a_0$ (%)	$\Delta c/c_0$ (%)	R_w (%)	R_B (%)
0	100	9.3365(3)	6,8560(5)	294(22)	-	-	14.6	9.1
Kr								
10^{11}	100	-	-	-	-	-		
10^{12}	100	-	-	-	-	-		
5.10^{12}	49(1)	9.3775(9)	6.8912(8)	294(20)	0.44	0.53	24	15
10^{13}	20(1)	9.4236(5)	6.9105(5)	291(20)	0.94	0.82	9.9	6
5.10^{13}	14(1)	9.3160(4)	6.8402(5)	294(22)	-0.21	-0.22	10.5	5.9
I								
10^{11}	-	-	-	-	-	-		
5.10^{11}	86(2)	9.3603(3)	6.8790(5)	90(10)	0.26	0.35	23.9	15.1
10^{12}	-	-	-	-	-	-		
3.10^{12}	47(2)	9.3645(3)	6.8840(5)	91(6)	0.30	0.42	13.3	9
5.10^{12}	29.2(5)	9.3765(5)	6.8881(6)	77(11)	0.44	0.48	10.4	7.3
10^{13}	13.2(2)	9.3719(4)	6.8857(6)	82(9)	0.38	0.45	6.7	4.9

Single impact model associated to crystal size reduction

Cell parameters and volume increase, then relax

Amorphisation / recrystallisation competition: single or double impact

Amorphous/crystalline volume fraction (damaged fraction Fd = Va / V) as determined by x-ray diffraction

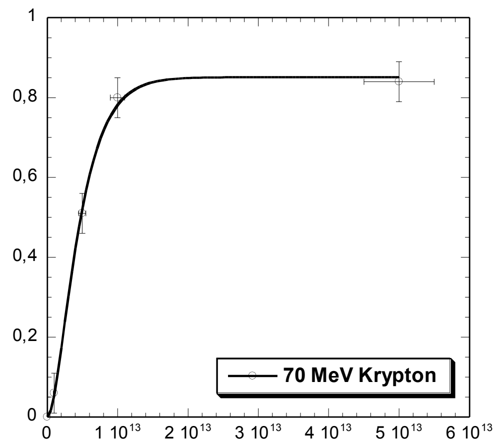

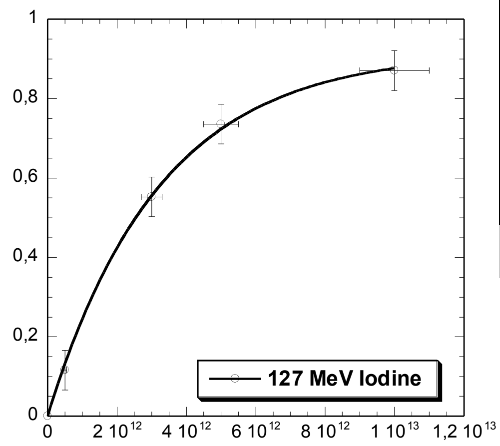

B

Fitting parameters	Krypton		Iodine
	Single impact Fd = B(1- exp(-AΦt))	**Double impact** Fd = B(1 – (1+ AΦt) exp(-AΦt))	**Single impact** Fd = B(1- exp(-AΦt))
A = πR² (cm²)	$1.85 \pm 0.15\ 10^{-13}$	$4.1 \pm 0.15\ 10^{-13}$	$3.3 \pm 0.15\ 10^{-13}$
Radius R (nm)	2.4 ± 0.2	3.6	3.2
B (Max.damage rate)	0.87	0.85 ± 0.2	0.92 ± 0.2
χ2	0.013	0.0006	0.0004

Mullite-silica composites

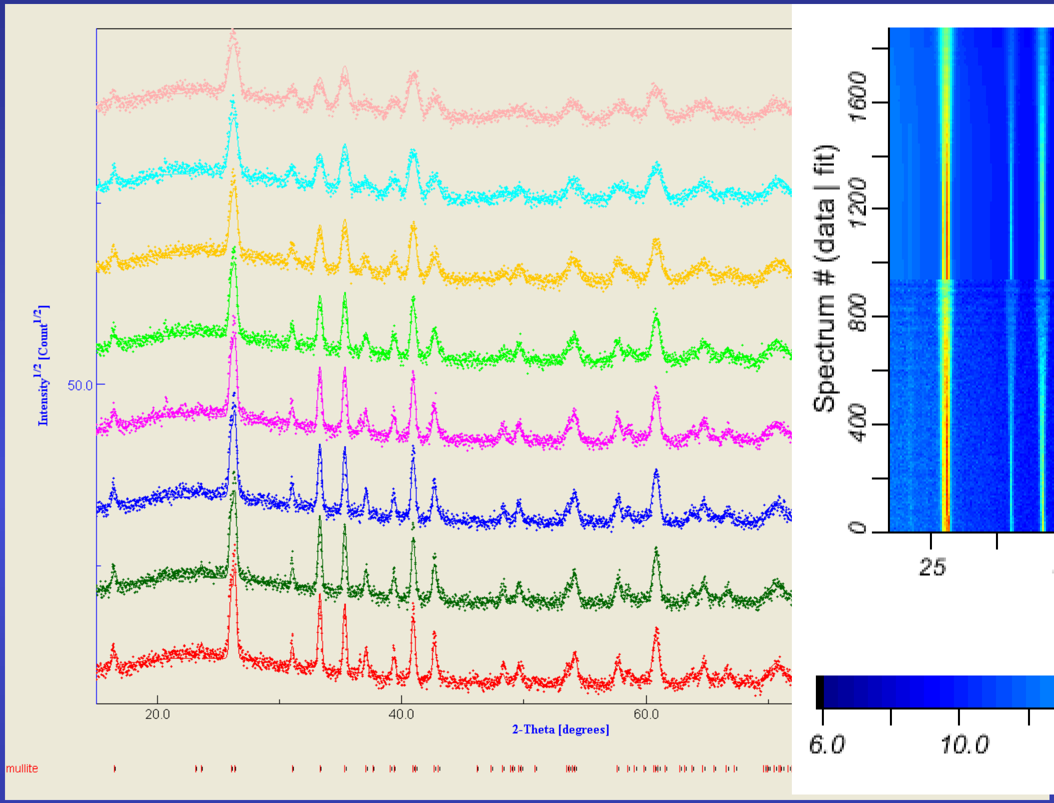

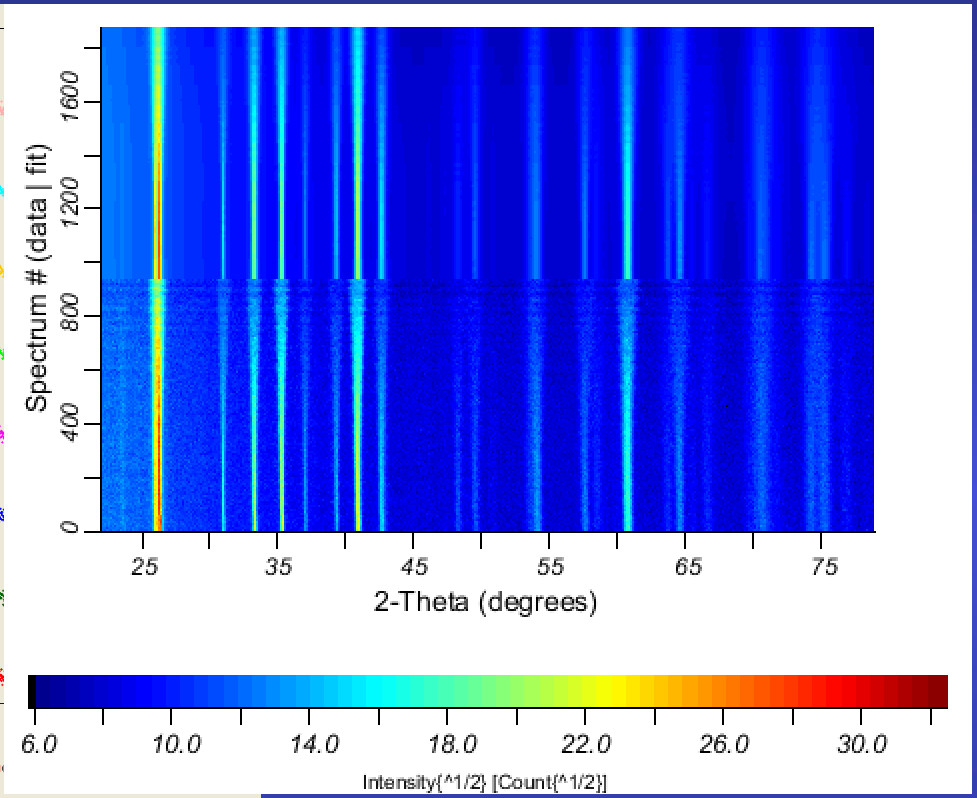

ODF: R_w = 4.87 %, R_B = 4.01 %

Rietveld: R_w = 12.90 %, GoF = 1.77

Mullite: a = 7.56486(5) Å; b = 7.71048(5) Å; c = 2.89059(1)Å

Uniaxially pressed

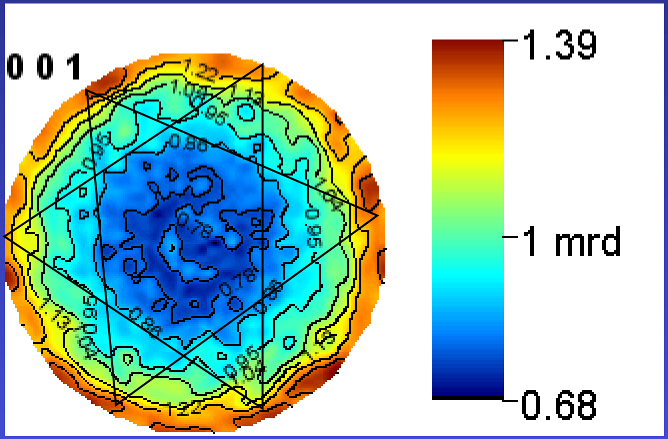

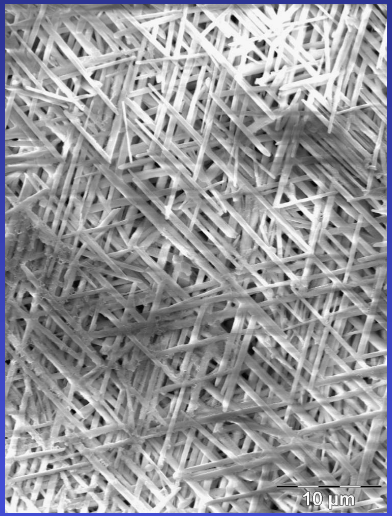

Centrifugated

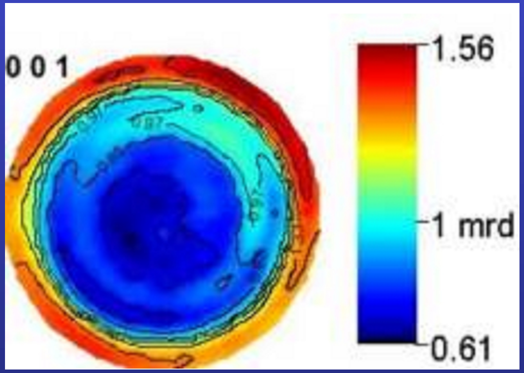

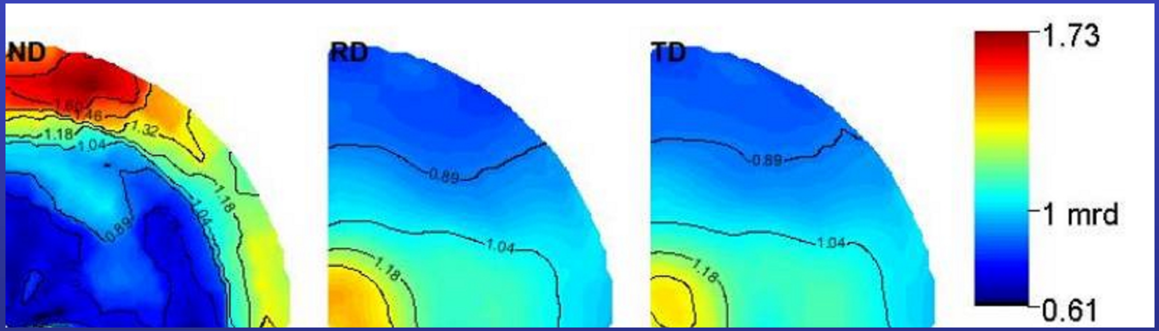

Carbon nanofibre

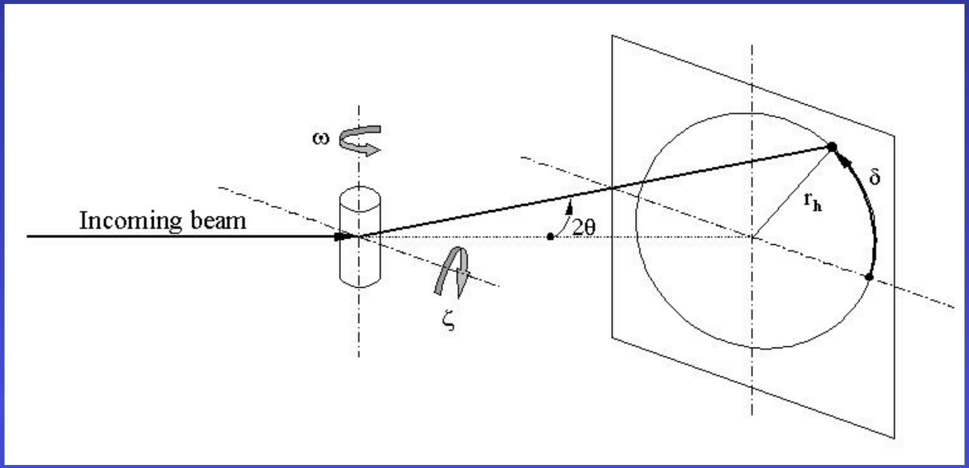

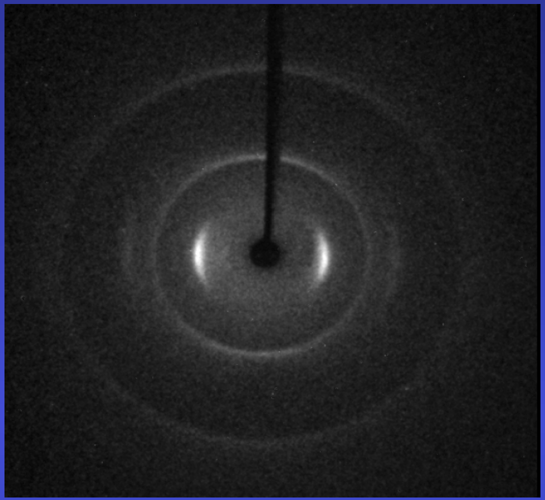

1 fibre (7 microns diameter): CCD Kappa diffractometer

Planar texture Component
Ufer turbostractic model

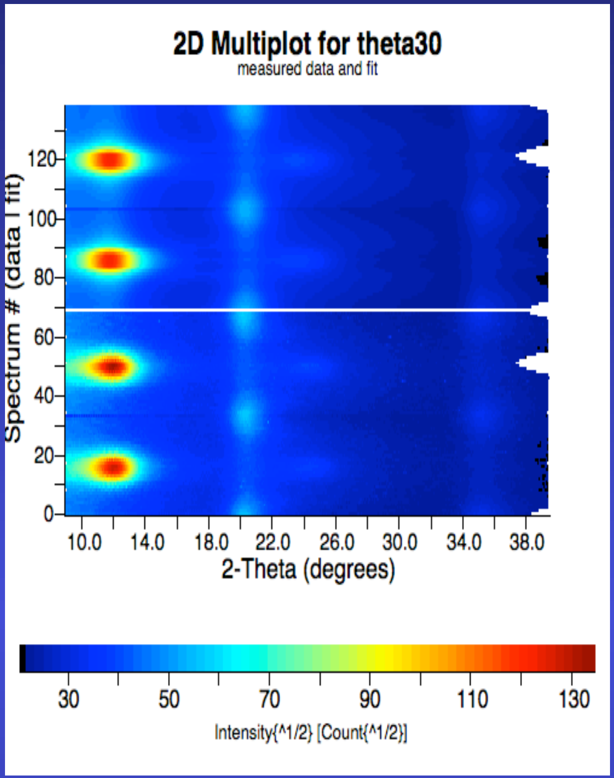

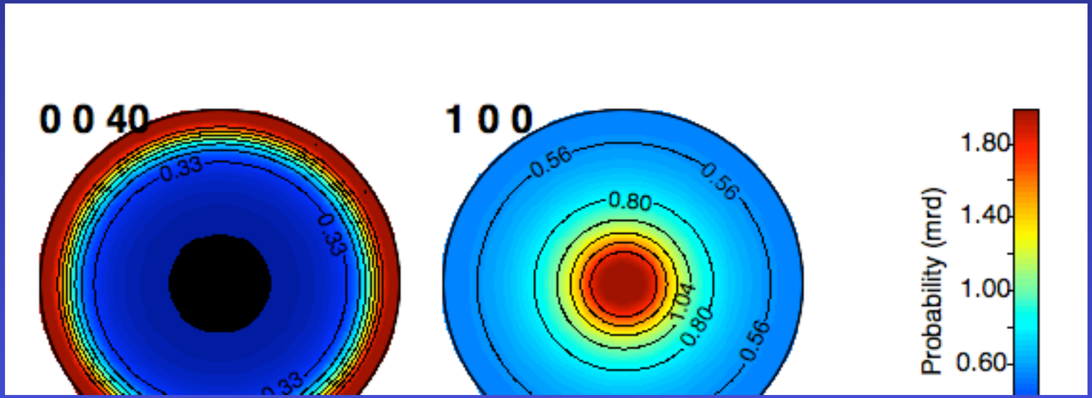

	A(nm)	C(nm)	Orientation FWHM(°)	Max 00l pole figure (m.r.d.)	Crystallite size along c (nm)	Crystallite size along a (nm)	Global microstrain (rms)
C1B1	0.23589(7)	0.6821(1)	21.6(1)	1.95	2.1(4)	2.2(4)	0.0152(10)
C2B1	0.23746(5)	0.68915(8)	18.75(6)	2.05	2.3(2)	2.5(2)	0.0154(11)
C3B1	0.23734(5)	0.69233(9)	18.63(6)	2.04	2.4(3)	2.7(5)	0.0136(6)
C3B2	0.23716(4)	0.69389(9)	19.87(7)	1.98	2.4(4)	2.5(4)	0.0150(4)
C3B3	0.23656(4)	0.68980(8)	19.16(6)	1.99	2.5(6)	2.3(5)	0.0168(8)

Turbostratic phyllosilicate aggregates

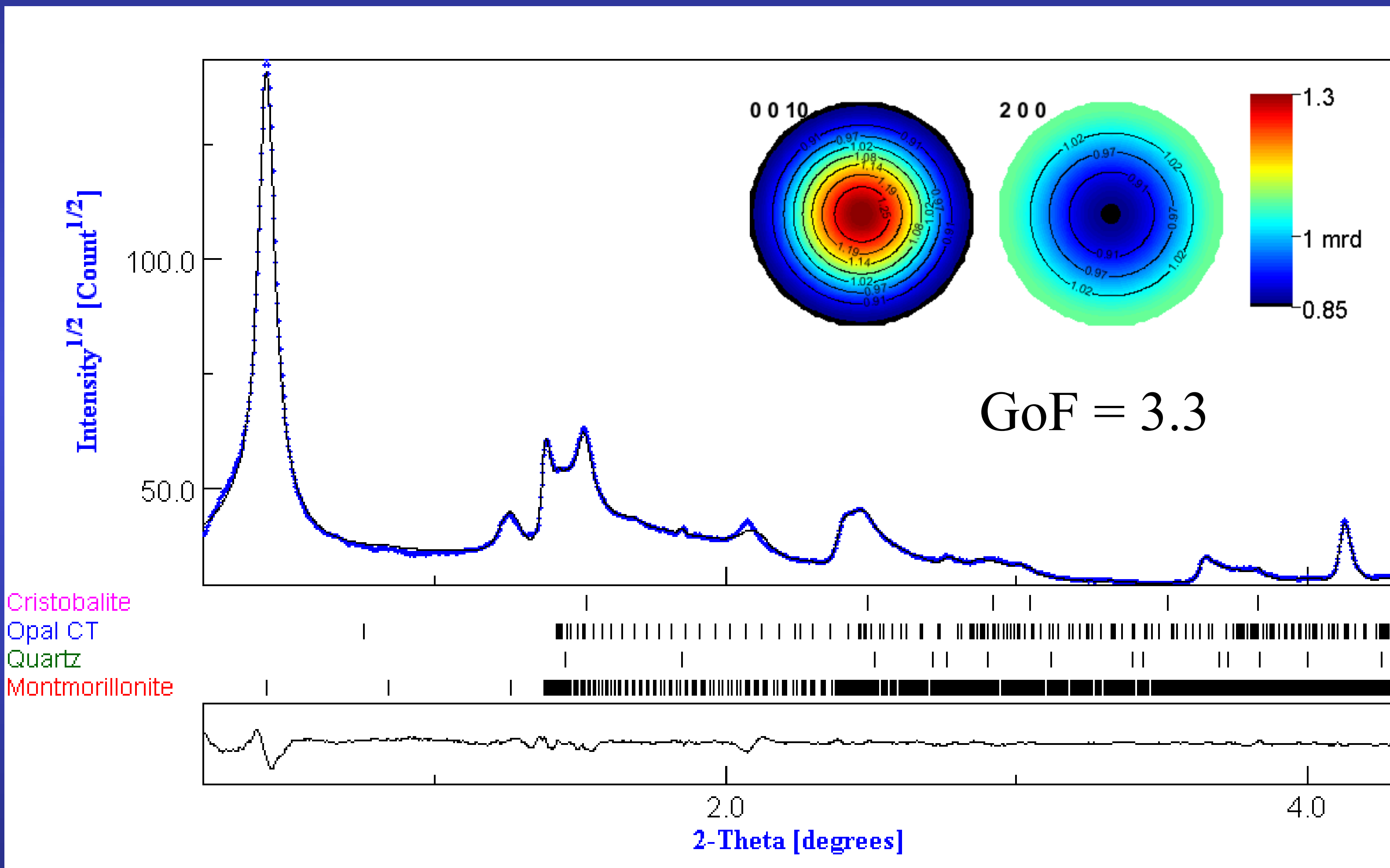

V%
1.45(2)
6.6(1)
0.19(1)
91.8(3)

$Mg_{0.75}Fe_{0.25}O$ high pressure experiments

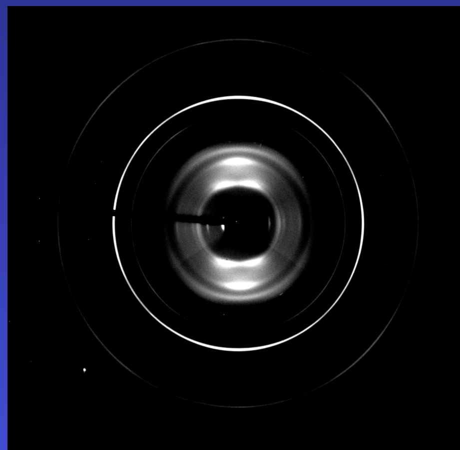

E-WIMV + geo

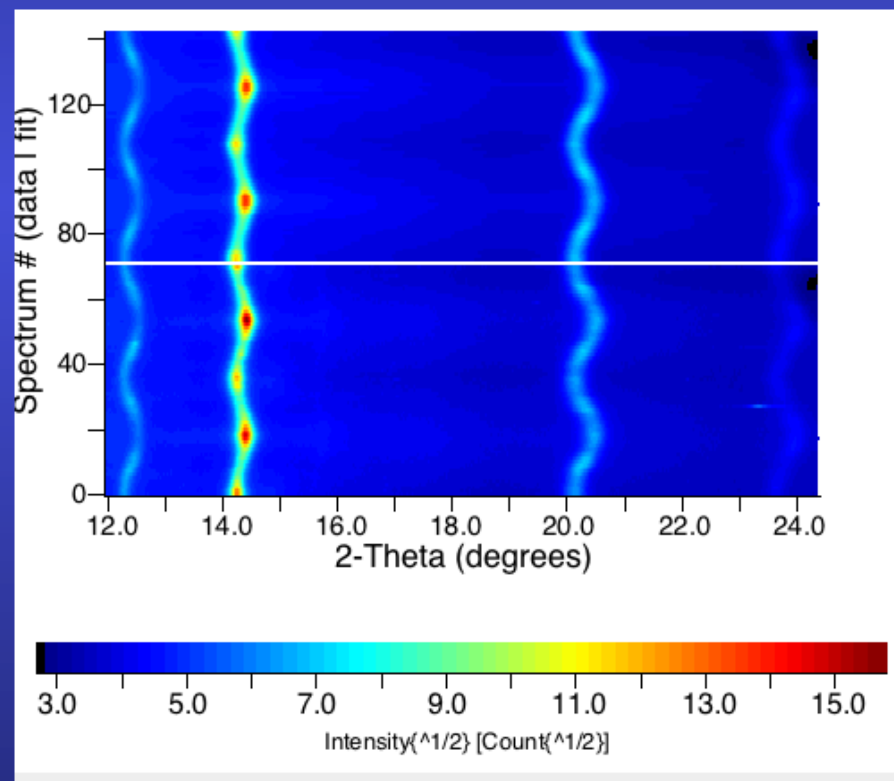

a = 3.98639(3) Å
<t> = 46.8(3) Å
$\langle\varepsilon\rangle$ = 0.00535(1)
σ_{33} = -861(3) MPa

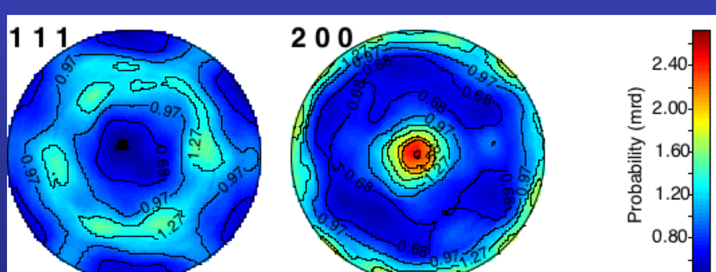

$LiNbO_3$

- Predict macroscopic anisotropic properties: BAW

Propagation equation

$$\rho \frac{\partial^2 u^i}{\partial t^2} = \left[C^{i\ell mn} \right] \frac{\partial^2 u_n}{\partial x^m \partial x^\ell}$$

Propagation direction	V_P	V_{S1}	V_{S2}
[100]	$\sqrt{\frac{c^M{}_{11}}{\rho}}$	$\sqrt{\frac{c^M{}_{44}}{\rho}}$	$\sqrt{\frac{c^M{}_{44}}{\rho}}$
[110]	$\sqrt{\frac{c^M{}_{11} + 2c^M{}_{44} + c^M{}_{12}}{2\rho}}$	$\sqrt{\frac{c^M{}_{11} - c^M{}_{12}}{2\rho}}$	$\sqrt{\frac{c^M{}_{44}}{\rho}}$
[111]	$\sqrt{\frac{c^M{}_{11} + 4c^M{}_{44} + 2c^M{}_{12}}{3\rho}}$	$\sqrt{\frac{c^M{}_{11} + c^M{}_{44} - c^M{}_{12}}{3\rho}}$	$\sqrt{\frac{c^M{}_{11} + c^M{}_{44} - c^M{}_{12}}{3\rho}}$

Cubic crystal system

	c_{11} or c_{11}^M	c_{12} or c_{12}^M	c_{13} or c_{13}^M	c_{14} or c_{14}^M	c_{33} or c_{33}^M	c_{44} or c_{44}^M
Single crystal	201	54.52	71.43	8.4	246.5	60.55
$LiNbO_3$/Si	206.4	68.5	67.6	0.48	216.5	64
$LiNbO_3$/Al_2O_3	204	65.7	69.7	1.1	219.9	63.2

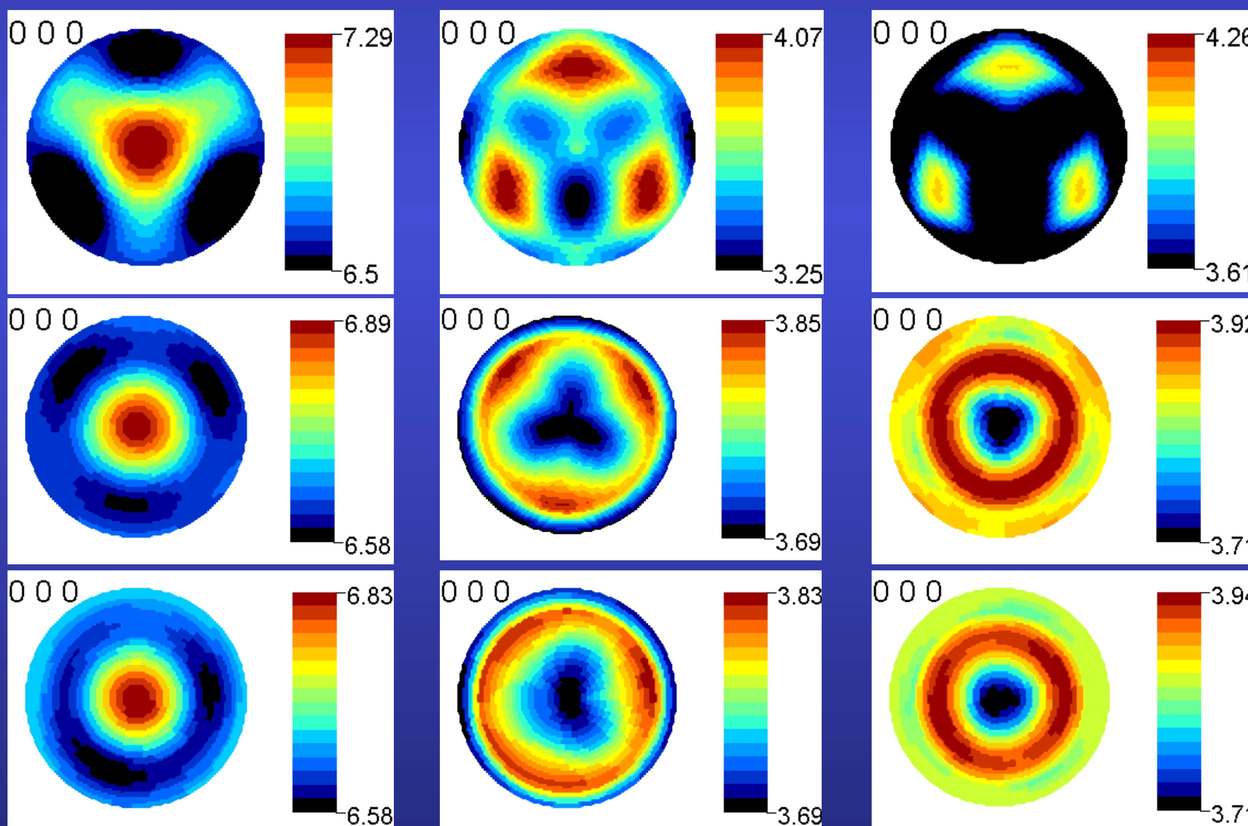

Single crystal

$LiNbO_3$/Si

$LiNbO_3$/Al_2O_3

$ErMn_3Fe_9C$ ferrimagnet

Predict macroscopic anisotropic properties: Magnetisation

$$\frac{M_{\perp}}{M_S} = 2\pi \int_0^{\frac{\pi}{2}} (1-\rho_0) PV(\theta_g) \sin\theta_g \cos(\theta_g - \theta)\, d\theta_g + \rho_0 M_{random}$$

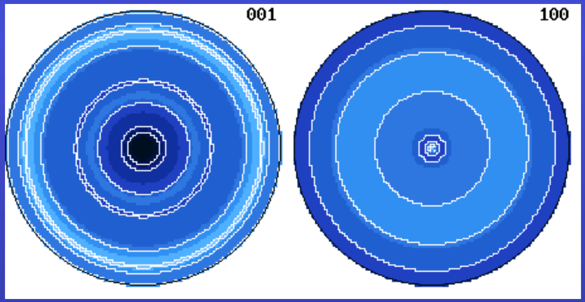

max {001}: 3.9 mrd
min: 0.5 mrd

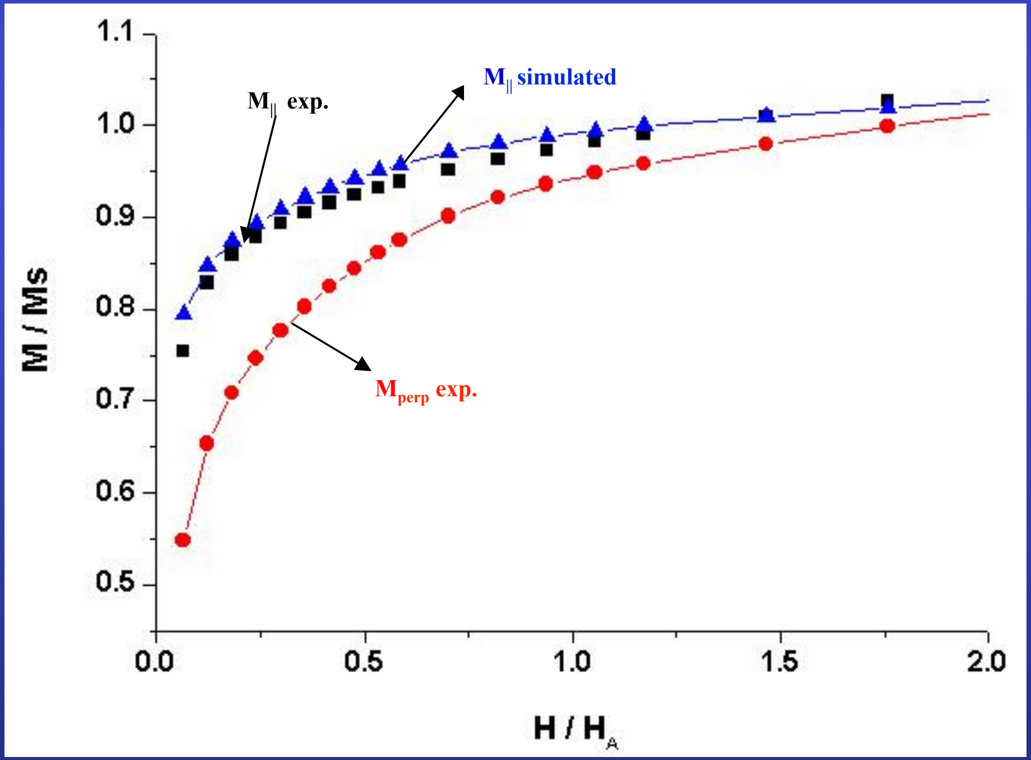

Why not more ?

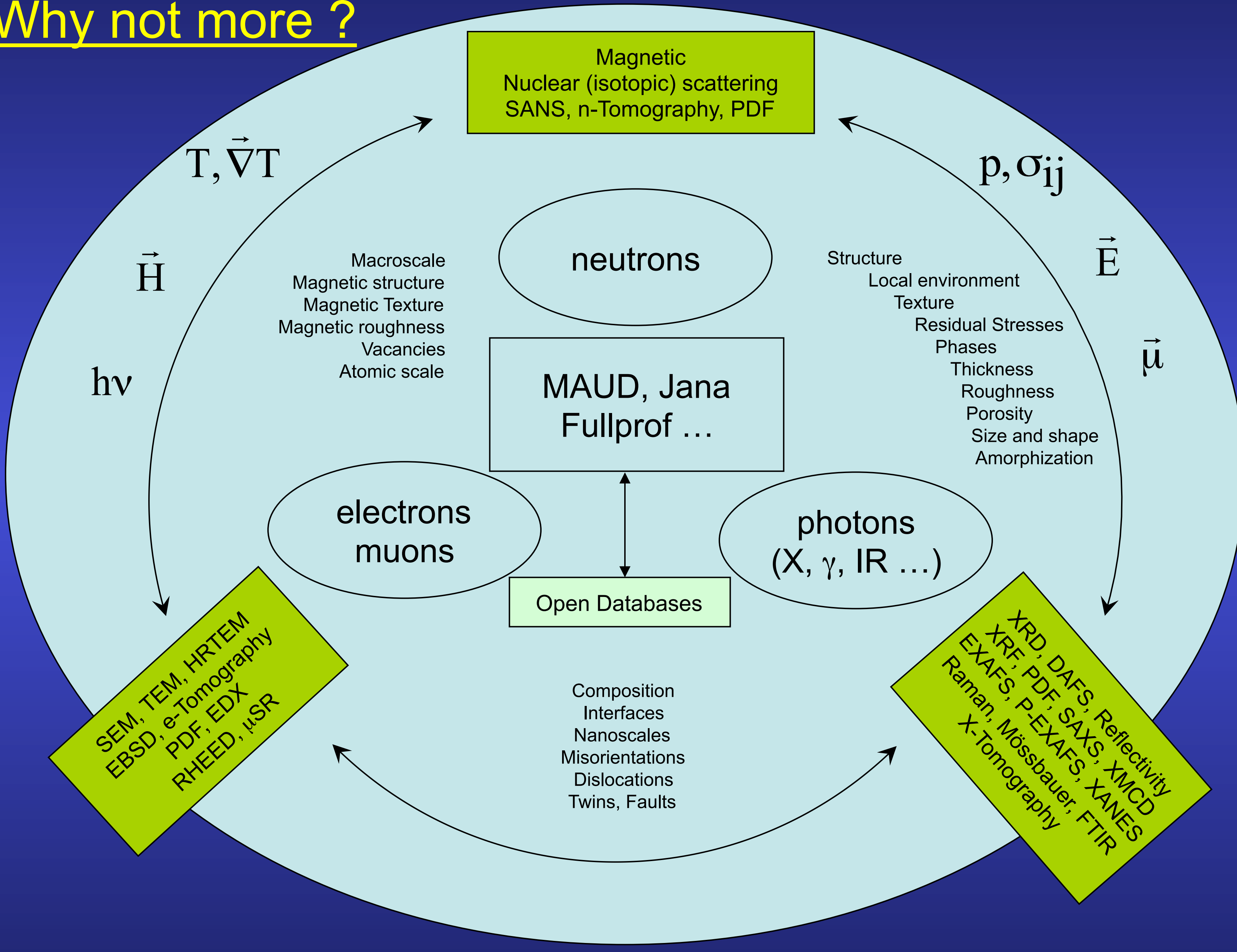

Magnetic
Nuclear (isotopic) scattering
SANS, n-Tomography, PDF
$T, \vec{\nabla} T$
p, σ_{ij}
$\vec{H}$
$\vec{E}$
$h\nu$
$\vec{\mu}$
neutrons
Macroscale
Magnetic structure
Magnetic Texture
Magnetic roughness
Vacancies
Atomic scale
Structure
Local environment
Texture
Residual Stresses
Phases
Thickness
Roughness
Porosity
Size and shape
Amorphization
MAUD, Jana
Fullprof …
electrons
muons
photons
(X, γ, IR …)
Open Databases
SEM, TEM, HRTEM
EBSD, e-Tomography
PDF, EDX
RHEED, μSR
XRD, DAFS, Reflectivity
XRF, PDF, SAXS, XMCD
EXAFS, P-EXAFS, XANES
Raman, Mössbauer, FTIR
X-Tomography
Composition
Interfaces
Nanoscales
Misorientations
Dislocations
Twins, Faults

Conclusions

A lot of problems can be solved !

Texture helps to resolve them: good for real samples

Anisotropy favours higher resolutions

Combined analysis may be a solution, unless you can destroy your sample or are not interested in macroscopic anisotropy ...

If you think you can destroy it, perhaps think twice

Combined Analysis Workshop in Caen:
3rd - 7th July 2017 !
www.ecole.ensicaen.fr/~chateign/formation/

Thanks !

UNION EUROPENNE

ESQUI
SOLSA

MEET
XMAT
MIND
COSTs

l'Europe s'engage en Basse-Normandie avec le FEDER

COMBIX: Chair of Excellence

AGENCE NATIONALE DE LA RECHERCHE ANR

FURNACE
ECOCORAIL

DAME
SEMOME

Région Centre

SMAM

EXPERIMENTS

Minimum experimental requirements

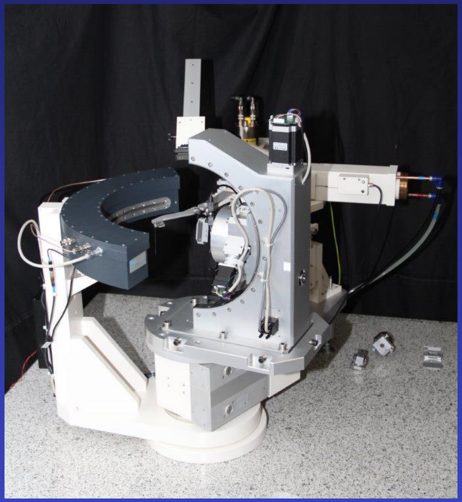

1D or 2D Detector + 4-circle diffractometer
(X-rays and neutrons)
CRISMAT, ILL

+

~1000 experiments (2θ diagrams)
in as many sample orientations

+

Instrument calibration
(peaks widths and shapes,
misalignments, defocusing …)

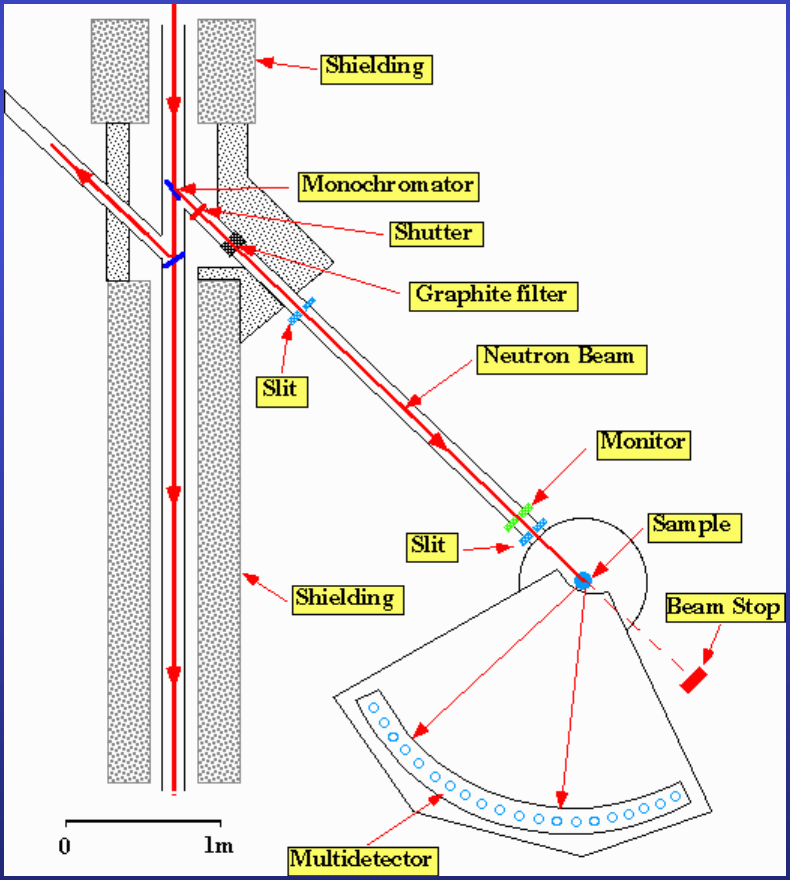

2D Curved Area Position Sensitive Detector

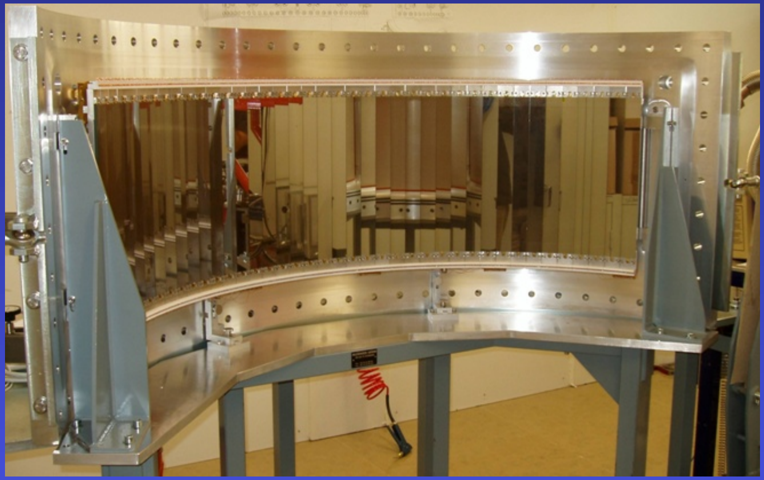

D19 - ILL

+

~100 experiments (2D Debye-Scherrer diagrams)

in as many sample orientations

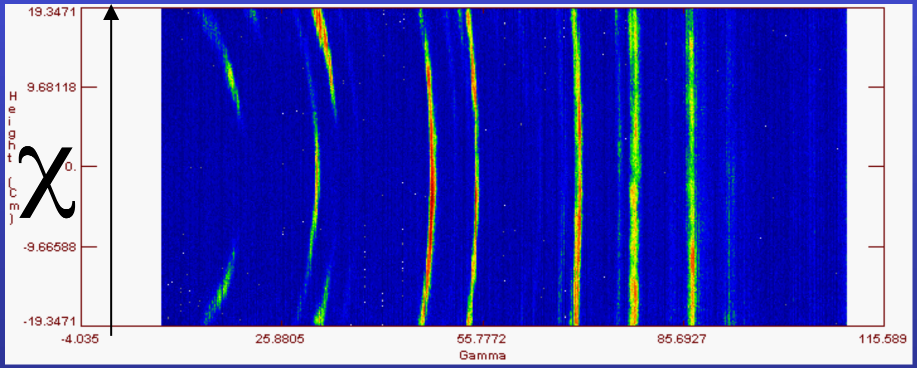

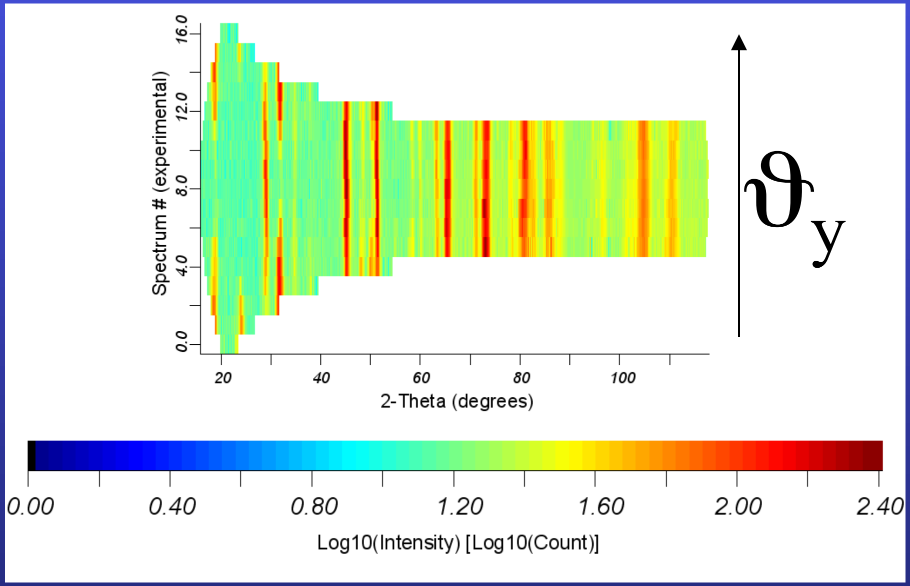

STRUCTURE

Structure determination on real (textured) samples
Problem 1

Structure and QTA: correlations ?

f(g) and $|F_{\mathbf{h}}|^2$ are different !

f(g):

-Angularly constrained: $[h_1k_1l_1]^*$ and $[h_2k_2l_2]^*$ make a given angle: more determined if F^2 high

- lot of data (spectra) needed

$|F_{\mathbf{h}}|^2$:

-Position, f_i, and Debye-Waller constrained

- work on the sum of all diagrams on average

Structure and Residual Stresses (shift peaks with **y**)
Problem 5

Stress and cell parameters: correlations: peak positions and C_{ijkl}

Cell parameters:
- Measured at high angles
- Bragg law evolution

strains:
- Measured precisely at high angles
- stiffness-based variation, also with Ψ

How it works

Le Bail extraction

$$T_{hkl}^{k} = T_{hkl}^{k-1} \frac{\sum_i I_i^{exp} S_{hkl}^{i}}{\sum_i I_i^{calc} S_{hkl}^{i}}$$

- Starts with nominal intensities (T_{hkl})
- Computes the full pattern (I^{calc})
- Uses the formula to compute next T_{hkl}
- Cycle the last two steps until convergence

- In Maud, options:
  - Only few cycles for texture (3-5) necessary
  - The range for the weighting of the profile can be reduced
  - Background subtracted or not

QTA

Texture from Spectra

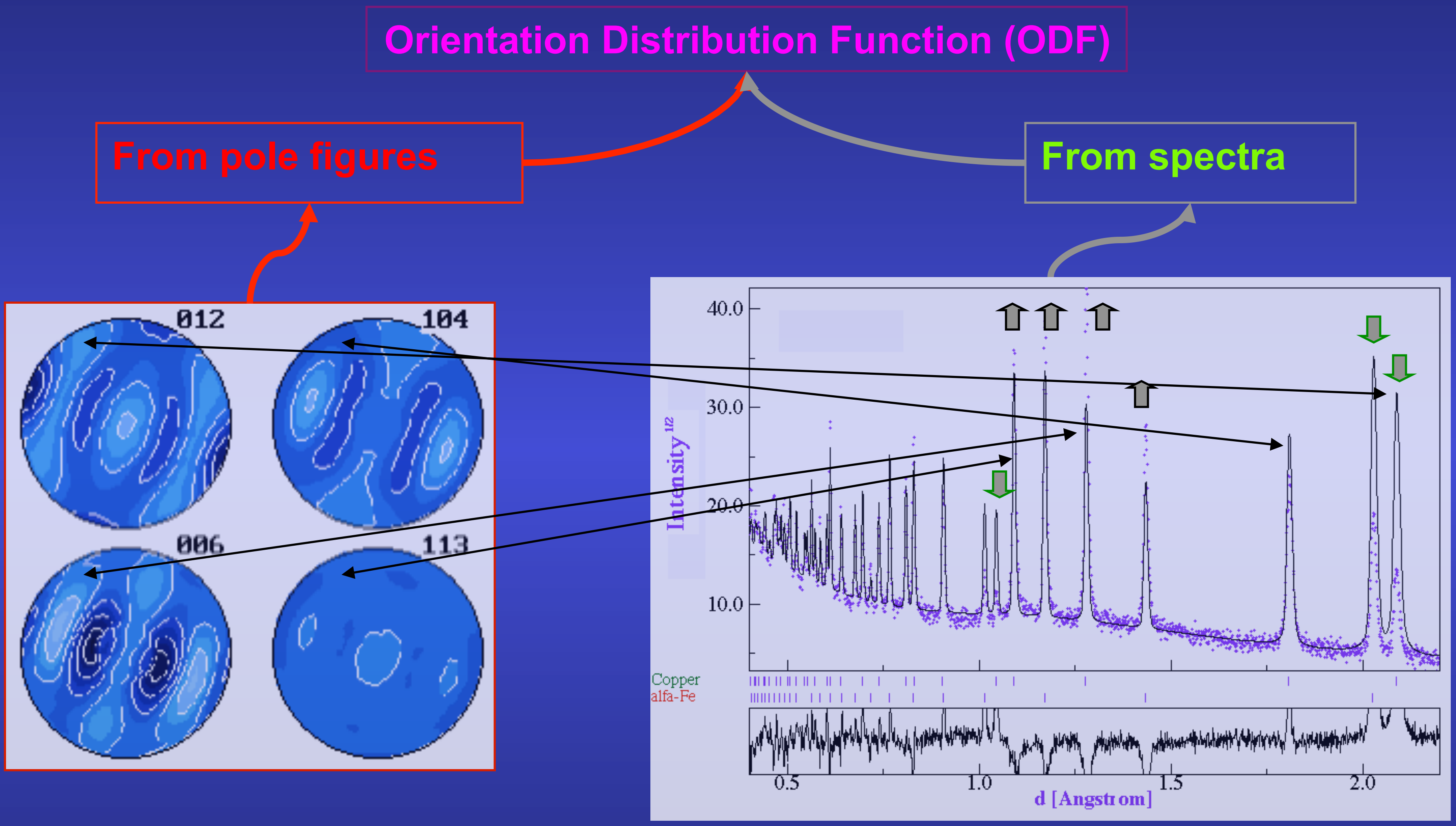

Le Bail extraction + ODF: WMV, E-WIMV, Generalized spherical harmonics, components, ADC, entropy maximisation …

Rietveld-Structure

$$y_c(\mathbf{y_S},\theta,\eta) = y_b(\mathbf{y_S},\theta,\eta) + I_0 \sum_{i=1}^{N_L} \sum_{\Phi=1}^{N_\Phi} \frac{\nu_{i\Phi}}{V_{c\Phi}^2} \sum_h Lp(\theta) j_{\Phi h} \left|F_{\Phi h}\right|^2 \Omega_{\Phi h}(\mathbf{y_S},\theta,\eta) P_{\Phi h}(\mathbf{y_S},\theta,\eta) A_{i\Phi}(\mathbf{y_S},\theta,\eta)$$

Texture

$$P_k(\chi,\phi) = \int_\varphi f(g,\varphi)\,d\varphi$$

- Generalized Spherical Harmonics (Bunge):

$$P_k(\chi,\phi) = \sum_{l=0}^{\infty} \frac{1}{2l+1} \sum_{n=-l}^{l} k_l^n(\chi,\phi) \sum_{m=-l}^{l} C_l^{mn} k_n^{*m}(\Theta_k \phi_k)$$

$$f(g) = \sum_{l=0}^{\infty} \sum_{m,n=-l}^{l} C_l^{mn} T_l^{mn}(g)$$

- Components (Helming):

$$f(g) = F + \sum_c I^c f^c(g)$$

- WIMV (William, Imhof, Matthies, Vinel) iterative process:

$$f^{n+1}(g) = N_n \frac{f^n(g) f^0(g)}{\left(\prod_{\mathbf{h}=1}^{I} \prod_{m=1}^{M_h} P_{\mathbf{h}}^n(\mathbf{y}) \right)^{\frac{1}{IM_h}}}$$

$$f^0(g) = N_0 \left(\prod_{\mathbf{h}=1}^{I} \prod_{m=1}^{M_h} P_{\mathbf{h}}^{exp}(\mathbf{y}) \right)^{\frac{1}{IM_h}}$$

E-WIMV (Rietveld only):

$$f^{n+1}(g) = f^n(g) \prod_{m=1}^{M_h} \left(\frac{P_{\mathbf{h}}(\mathbf{y})}{P_{\mathbf{h}}^n(\mathbf{y})} \right)^{r_n \frac{w_h}{M_h}}$$

with $0 < r_n < 1$, relaxation parameter,
$M_{\mathbf{h}}$ number of division points of the integral around k,
$w_{\mathbf{h}}$ reflection weight

- Entropy maximisation (Schaeben):

$$f^{n+1}(g) = f^n(g) \prod_{m=1}^{M_h} \left(\frac{P_{\mathbf{h}}(\mathbf{y})}{P_{\mathbf{h}}^n(\mathbf{y})} \right)^{\frac{r_n}{M_h}}$$

- arbitrarily defined cells (ADC, Pawlik): Very similar to E-WIMV, with integrals along path tubes

QMA

Shapes, microstrains, defaults, distributions
Problem 6

Shapes …. and stress-texture-structure: correlations ?

Shapes …:
- line broadening problem
- average positions modified
- if anisotropic: modification changes with **y**

Stress-texture-structure:
- need "true" peak positions and intensities
- need deconvoluted signals

Line Broadening causes

- Instrumental broadening

- Finite size of the crystals
  acts like a Fourier truncation: size broadening

- Imperfection of the periodicity
  due to d_h variations inside crystals: microstrain effect

- Generally: 0D, 1D, 2D, 3D defects

- All quantities are average values over the probed volume
  electrons, x-rays, neutrons: complementary
  distributions: mean values depend on distributions' shapes

Irradiated Fluorapatites

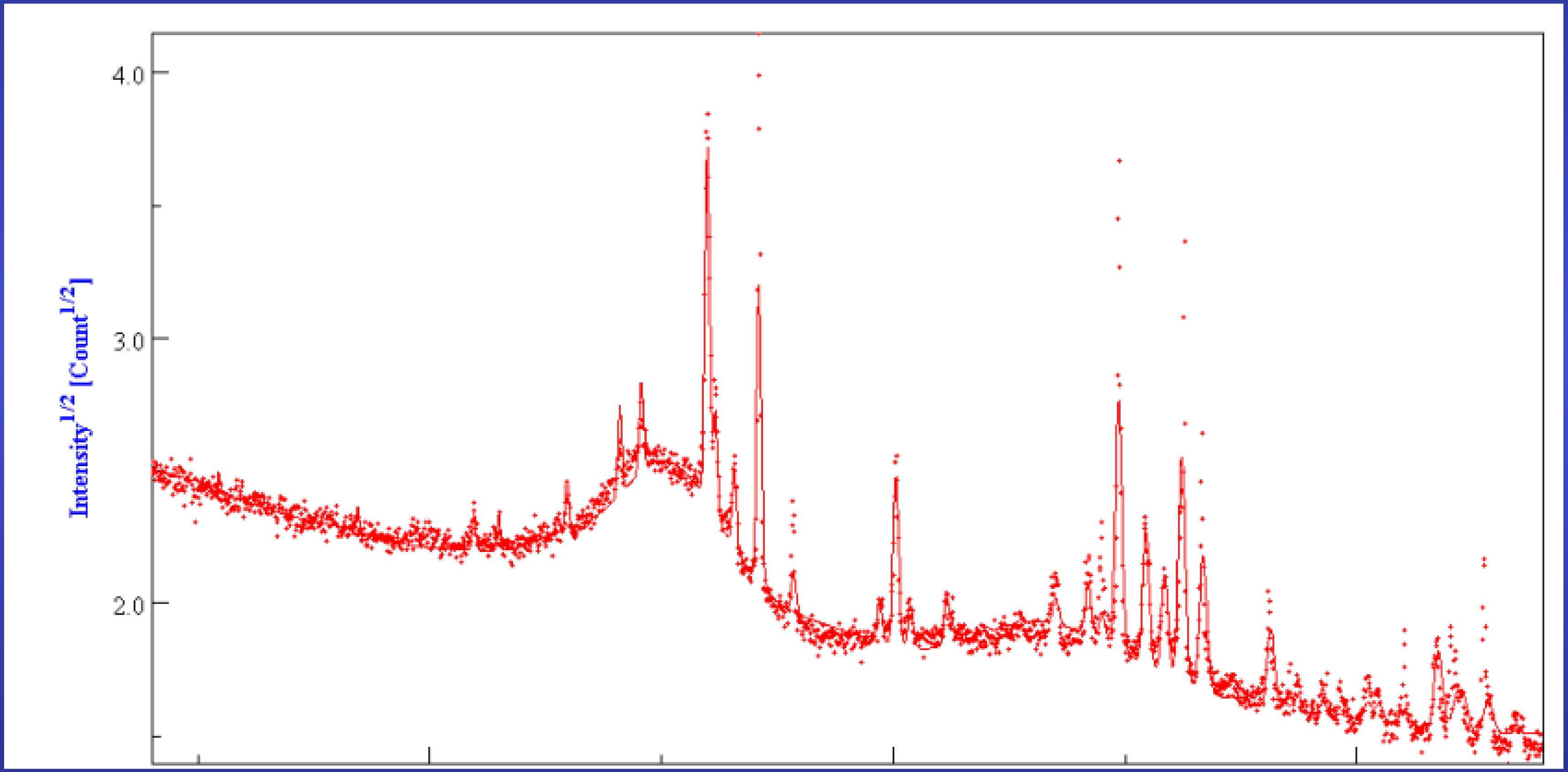

Instrumental broadening

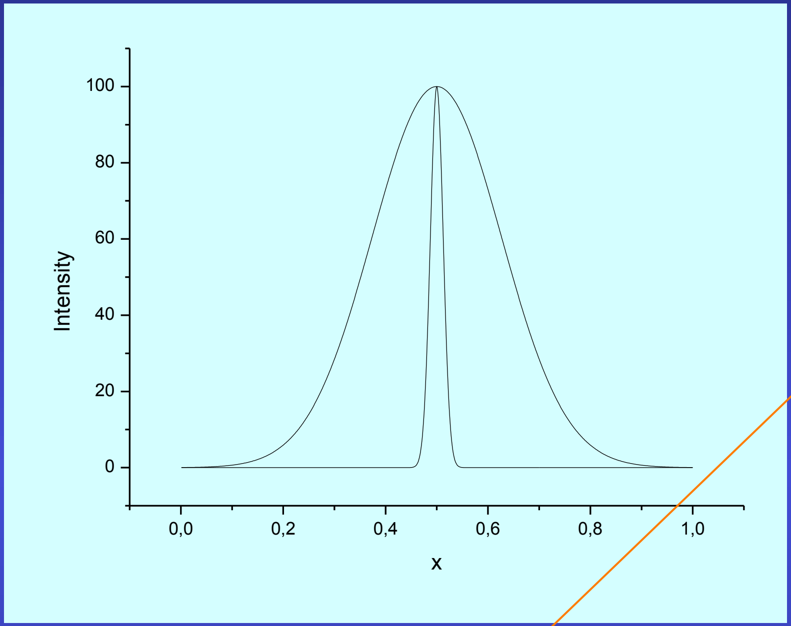

$$g(x) = g_{\lambda}(x) \otimes g_{g}(x)$$

Energy dispersion

Geometrical aberrations

$$h(x) = f(x) \otimes g(x) + b(x) = b(x) + \int_{-\infty}^{+\infty} f(y)g(x-y)dy$$

Measured profile

Sample contribution

Background

Back on diffraction expression

$$A_{\vec{h}} = F_{\vec{h}} T_{\vec{a}\vec{b}\vec{c}}(\vec{h})$$

$$T_{\vec{a}\vec{b}\vec{c}}(\vec{h}) = \frac{\sin[\pi(n+1)\vec{a}.\vec{h}]}{\sin[\pi\vec{a}.\vec{h}]} \frac{\sin[\pi(p+1)\vec{b}.\vec{h}]}{\sin[\pi\vec{b}.\vec{h}]} \frac{\sin[\pi(q+1)\vec{c}.\vec{h}]}{\sin[\pi\vec{c}.\vec{h}]}$$

$A_{\vec{h}}$: scattered amplitude

$F_{\vec{h}}$: structure factor

$T_{\vec{a}\vec{b}\vec{c}}(\vec{h})$: interference function

n, p, q : number of periods in the $\vec{a}$, $\vec{b}$, $\vec{c}$ directions

$$H(\alpha) = \frac{\sin^2[\pi(n+1)\alpha]}{\sin^2[\pi\alpha]}$$

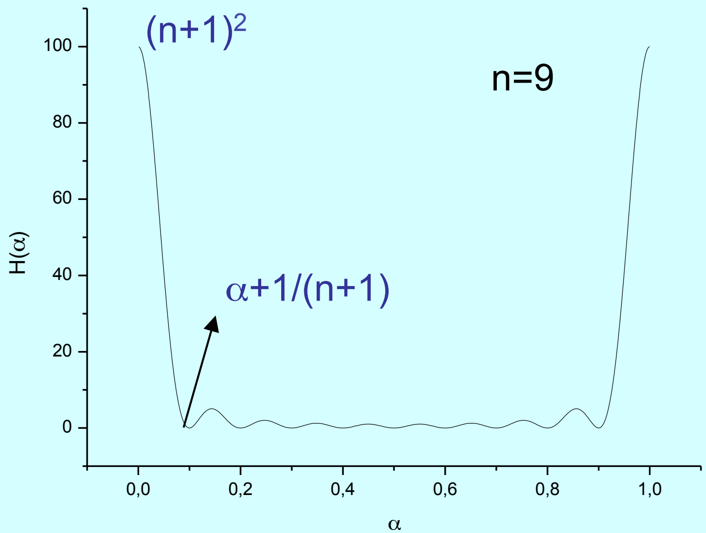

$$\text{infinite crystal}: \left| \begin{array}{l} \vec{a}.\vec{h} = h \\ \vec{b}.\vec{h} = k \\ \vec{c}.\vec{h} = l \end{array} \right.$$

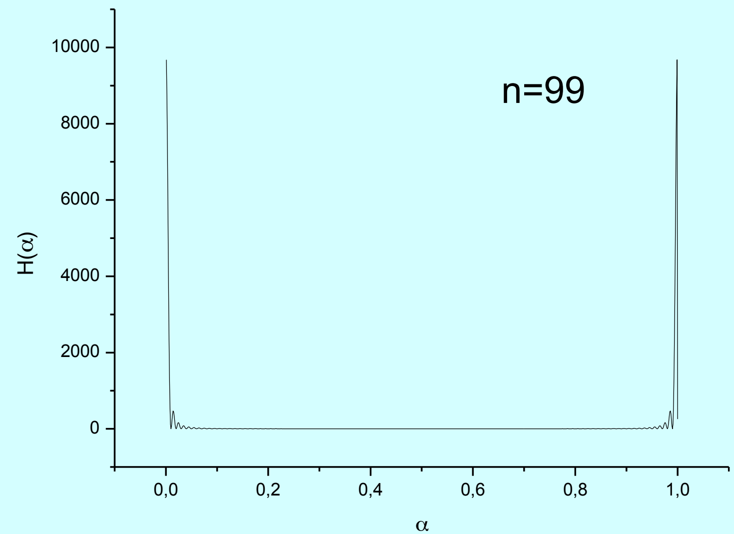

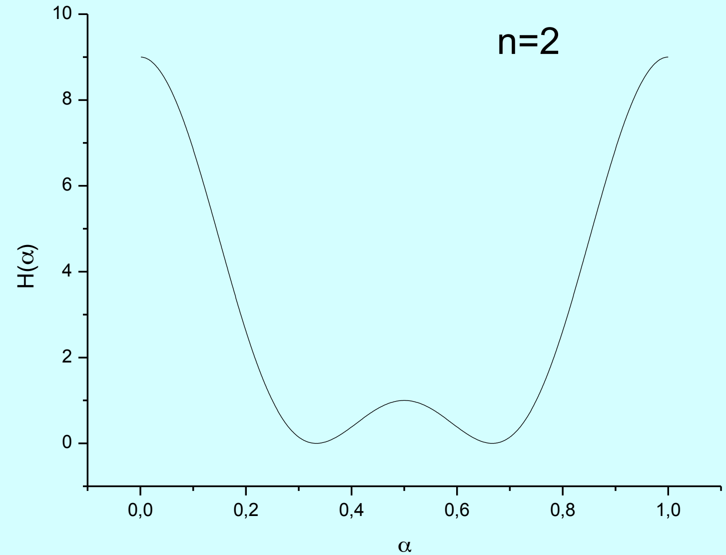

Crystallite's size-shape effect

Scherrer analysis:

Scherrer formula (1918):

$$R_{\vec{h}} = \frac{K\lambda}{\omega \cos\theta_0}$$

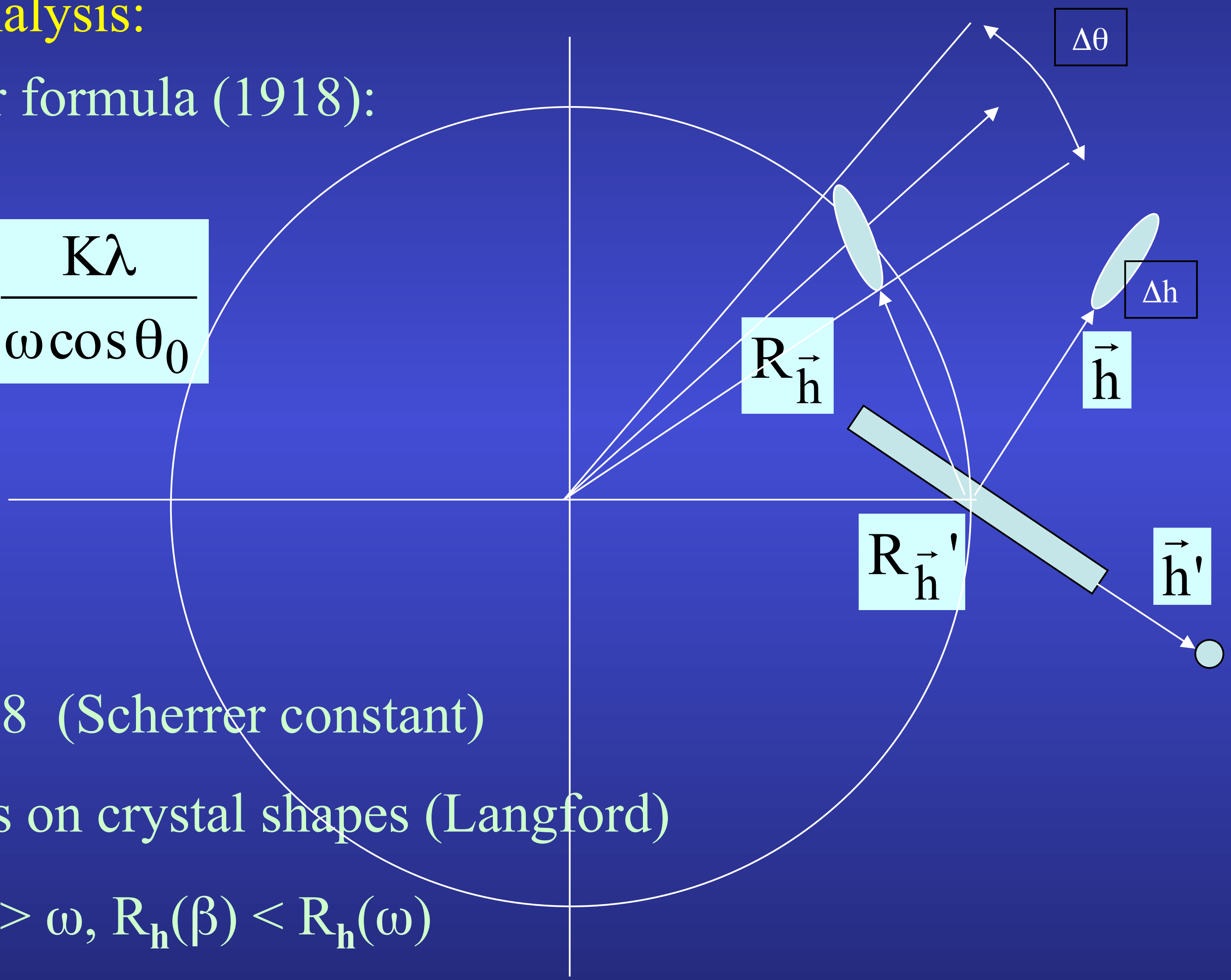

K= 0.888 (Scherrer constant)

Depends on crystal shapes (Langford)

Since $\beta > \omega$, $R_{\mathbf{h}}(\beta) < R_{\mathbf{h}}(\omega)$

After Scherrer analysis …

Williamson-Hall (1949)

Warren-Averback-Bertaut (1952)

Whole-Pattern analysis: Langford (1978), de Keijser (1982), Balzar et Ledbetter (1982) …

But deconvolution of contributions (Stokes 1948) !

Rietveld (1969): convolution !

More infos: http://www.ecole.ensicaen.fr/~chateign/formation/course/Classical_Microstructure.pdf

Scherrer, Integral breadth, Williamson-Hall …

$$<D>_v = \frac{K\lambda}{\beta_S(2\theta)\ \cos\theta}$$

More elegant, mandatory for whole-pattern: Stokes deconvolution
Bertaut-Warren-Averbach treatment, e.g. for a 00l peak:

$$A_n = A_n^S A_n^D = \frac{N_n}{N_3}\langle \cos 2\pi l Z_n \rangle$$

$$A_n^S = \frac{N_n}{N_3} = \frac{1}{N_3}\sum_{i=|n|}^{\inf}(i-|n|)p(i)$$

$$\left(\frac{dA_n^S}{dn}\right)_{n\to 0} = -\frac{1}{N_3}$$

Second derivative: distribution of column lengths

QPA

Phase and Texture

Problem 4

Phase and QTA: correlations: f(g), S_Φ

f(g):
- angular relationships
- plays on individual spectra
- essential to operate on textured sample

S_Φ:
- plays on overall scale factor (sum diagram)

Phase analysis

- Volume fraction

$$V_{\Phi} = \frac{S_{\Phi} V_{uc\Phi}^{2}}{\sum_{\Phi} \left(S_{\Phi} V_{uc\Phi}^{2} \right)_{\Phi}}$$

- Weight fraction

$$m_{\Phi} = \frac{S_{\Phi} Z_{\Phi} M_{\Phi} V_{uc\Phi}^{2}}{\sum_{\Phi} \left(S_{\Phi} Z_{\Phi} M_{\Phi} V_{uc\Phi}^{2} \right)_{\Phi}}$$

Z = number of formula units

M = mass of the formula unit

V = cell volume

RESIDUAL STRESSES

Residual Stresses shift peaks with y

Problem 2

Stress and QTA: correlations ? f(g) and $<C_{ijkl}>$

f(g):

- Moves the $\sin^2\Psi$ law away from linear relationship
- Needs the integrated peak (full spectra)

strains:

- Measured with pole figures
- needs the mean peak position

Isotropic samples: triaxial, biaxial, uniaxial stress states

Textured samples: Reuss, Voigt, Hill, Bulk geometric mean approaches

Residual Stresses and Rietveld

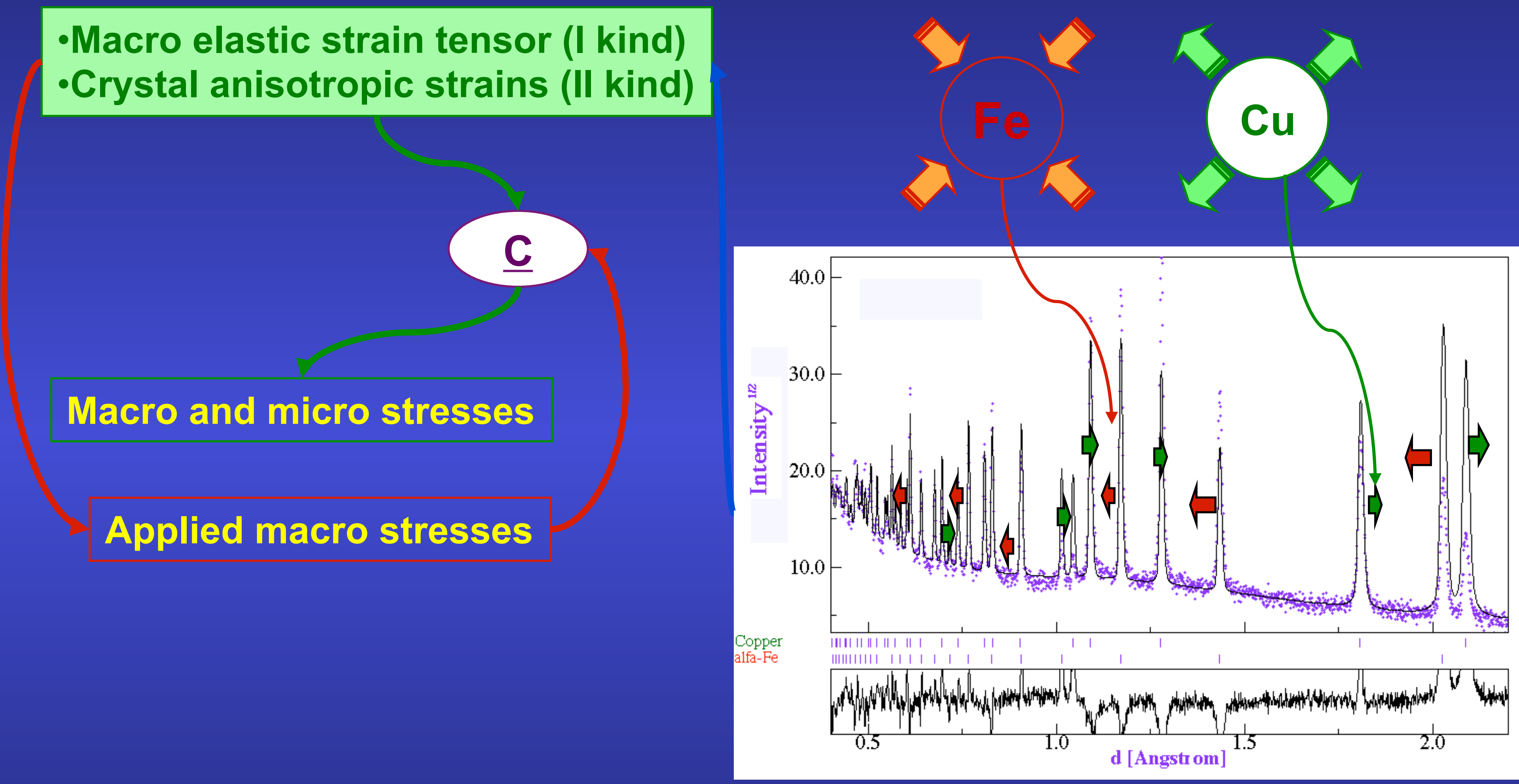

Isotropic samples: triaxial, biaxial, uniaxial stress states

Textured samples: Reuss, Voigt, Hill, Bulk geometric mean approaches

Strain-Stress

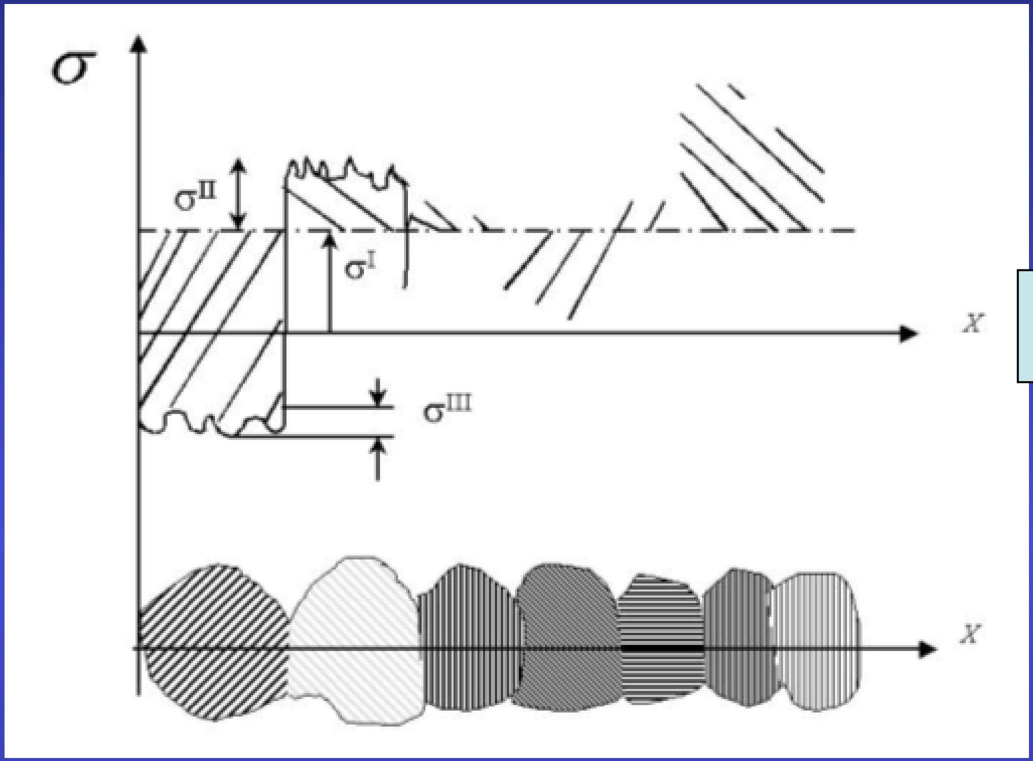

$$\varepsilon(\mathbf{X}) = \varepsilon^{I} + \varepsilon^{II}(\mathbf{X}) + \varepsilon^{III}(\mathbf{X})$$

$$\langle S\rangle_{geo}^{-1} = \exp\left[-\sum_{m=1}^{N}\nu_m \ln S_m\right] = \exp\left[\sum_{m=1}^{N}\nu_m \ln S_m^{-1}\right] = \left\langle S^{-1}\right\rangle_{geo} = \langle C\rangle_{geo}$$

or

$$\langle S\rangle_{geo}^{-1} = \left[\prod_{m=1}^{N} S_m^{\nu_m}\right]^{-1} = \prod_{m=1}^{N} S_m^{-\nu_m} = \prod_{m=1}^{N}\left(S_m^{-1}\right)^{\nu_m} = \left\langle S^{-1}\right\rangle_{geo} = \langle C\rangle_{geo}$$

Strain-Stress by diffraction

Microstress (II)

Macrostress (I)

rms Microstress (III)

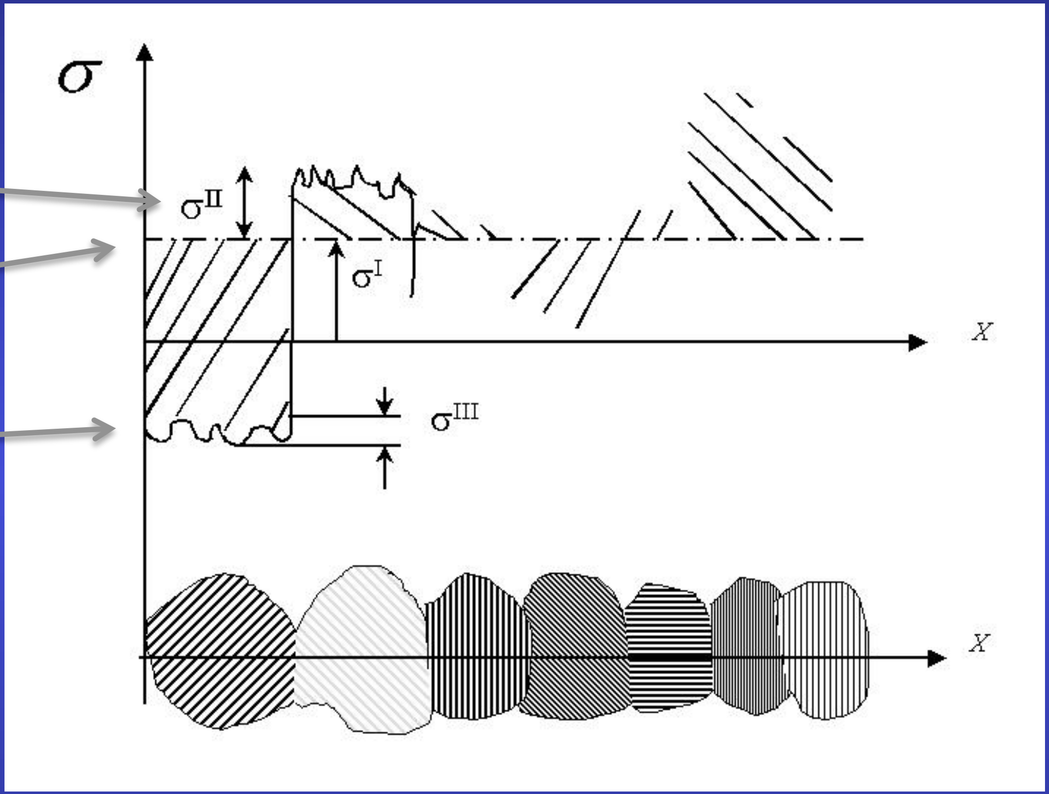

We measure strains !

For each **h** and **y** directions

$\varepsilon^{I}(\mathbf{h},\mathbf{y})$ and $\varepsilon^{II}(\mathbf{h},\mathbf{y})$:	peak broadenings
$\varepsilon^{III}(\mathbf{h},\mathbf{y})$:	peak shifts

For non-textured (isotropic) samples

Triaxial state

$$\varepsilon^I(h,y) = \frac{1+\nu}{E}\left[\left(\sigma_\phi - \sigma_{33}\right)\sin^2\psi + \left(\sigma_{13}\cos\phi + \sigma_{23}\sin\phi\right)\sin 2\psi\right] - \frac{\nu}{E}\sigma_{ii}$$

$$= \frac{\left\langle d_h(\varphi,\psi)\right\rangle_{V_d} - d_{h,0}}{d_{h,0}}$$

$$\sigma_{ii} = \sigma_{11} + \sigma_{22} + \sigma_{33}$$

$$\sigma_\phi = \sigma_{11}\cos^2\varphi + \sigma_{12}\sin 2\varphi + \sigma_{22}\sin^2\varphi - \sigma_{33}$$

Assuming σ_{33}=0 and small penetration depth

$$\varepsilon^I(h,y) = \frac{1+\nu}{E}\sigma_\phi\sin^2\psi - \frac{\nu}{E}\left(\sigma_{11} + \sigma_{22}\right)$$

linear $\sin^2\psi$ law

But non-linear behaviour is observed: Textured (anisotropic) samples; anisotropic plasticity; thermal anisotropy …

Dolle (J. Appl. Cryst., 12, 489, 1979) analyzed the problem in general, then Noyan and Nguyen (plastic deformation), Barral et al. (texture connection) …

For textured (anisotropic) samples

Arithmetic means:
- Voigt model: ε_{ij} is homogeneous, σ^{kl} not, upper bound for $<C_{ijkl}>$
- Reuss model: σ^{ij} is homogeneous, ε_{kl} not, lower bound for $<C_{ijkl}>$
- Hill model: neither ε_{ij} nor σ^{kl} are homogeneous, $<C_{ijkl}>$ “in between”

Inversion property is violated: $<C_{ijkl}> \neq <S_{ijkl}>^{-1}$

Geometric means: Inversion property is math property: $<C_{ijkl}> \neq <S_{ijkl}>^{-1}$

Scalar case (isotropic):

$$\left(\overline{E}^{geo}\right)^{-1} = e^{-\sum_{i=1}^{N} \nu_i \ln E_i} = e^{\sum_{i=1}^{N} \nu_i \ln E_i^{-1}} = \overline{\left(E^{-1}\right)}^{geo}$$

Geometric mean of elastic tensors

Elastic tensors are diagonally symmetric, but not diagonal !: need to diagonalise them first: $C^{(\lambda)}$ with $b_{ij}^{(\lambda)}$ eigentensors

$$C_{ijk\ell} = \sum_{\lambda=1}^{6} C^{(\lambda)} \mathbf{b}_{ij}^{(\lambda)} \mathbf{b}_{k\ell}^{(\lambda)}$$

$$\left(\ln C\right)_{ijk\ell} = \sum_{\lambda=1}^{6} \ln(C^{(\lambda)}) \mathbf{b}_{ij}^{(\lambda)} \mathbf{b}_{k\ell}^{(\lambda)} = \ln\left[\prod_{\lambda=1}^{6} (C^{(\lambda)})^{\mathbf{b}_{ij}^{(\lambda)} \mathbf{b}_{k\ell}^{(\lambda)}}\right]$$

Which are weighted over orientations:

$$C_{ijkl}^{Macro} = \overline{C_{ijkl}}^{geo} = e^{\overline{\ln C}_{i'j'k'l'}} = e^{\langle \Theta \rangle_{ijk\ell,i'j'k'\ell'} (\ln C)_{i'j'k'l'}}$$

$$\langle \Theta \rangle_{ijk\ell,i'j'k'\ell'} = \int_{g} \Theta_{i}^{i'}(g) \Theta_{j}^{j'}(g) \Theta_{k}^{k'}(g) \Theta_{\ell}^{\ell'}(g)\ f(g)\ dg$$

Satisfying Hooke's law $\sigma^{ij,M} = C_{ijk\ell}^{M}\, \varepsilon_{k\ell}^{M}$ with $C_{ijk\ell}^{M} = (C_{ijk\ell}^{-1,M})^{-1}$

Multiphase sample

For simplicity, take the isotropic case (N phases ϕ_n with phase fractions ν_n):

Voigt: $$E_M = \sum_{n=1}^{N} \nu_n E_n$$ and $$E_M \neq \left(E_M^{-1}\right)^{-1}$$

Reuss: $$E_M^{-1} = \sum_{n=1}^{N} \nu_n E_n^{-1}$$ and $$E_M^{-1} \neq \left(E_M\right)^{-1}$$

Geo: $$\ln E_M = \sum_{n=1}^{N} \nu_n \ln E_n$$

$$E_M = e^{\sum_{n=1}^{N} \nu_n \ln E_n}$$ and $$E_M = \left(E_M^{-1}\right)^{-1}$$

Matthies *et* Humbert (J. Appl. Cryst. 1995) for single phase, Matthies (Sol. Stat. Phen. 2010)

LAYERING

Layered systems

Problem 3

Layer, Rietveld and QTA: correlations: f(g), thicknesses and structure

f(g):
- Pole figures need corrections for abs-vol
- Rietveld also to correct intensities

layers:
- unknown sample true absorption coefficient μ
- unknown effective thickness (porosity)

Layering

Asymmetric Bragg-Brentano

$$C_\chi^{\text{top film}} = g_1\left(1 - \exp\left(-\mu T g_2 / \cos\chi\right)\right) / \left(1 - \exp\left(-2\mu T / \sin\omega\cos\chi\right)\right)$$

$$C_\chi^{\text{cov.layer}} = C_\chi^{\text{top film}}\left(\exp\left(-g_2 \sum \mu_i' T_i' / \cos\chi\right)\right) / \left(\exp\left(-2\sum \mu_i' T_i' / \sin\omega\cos\chi\right)\right)$$

Probes μT

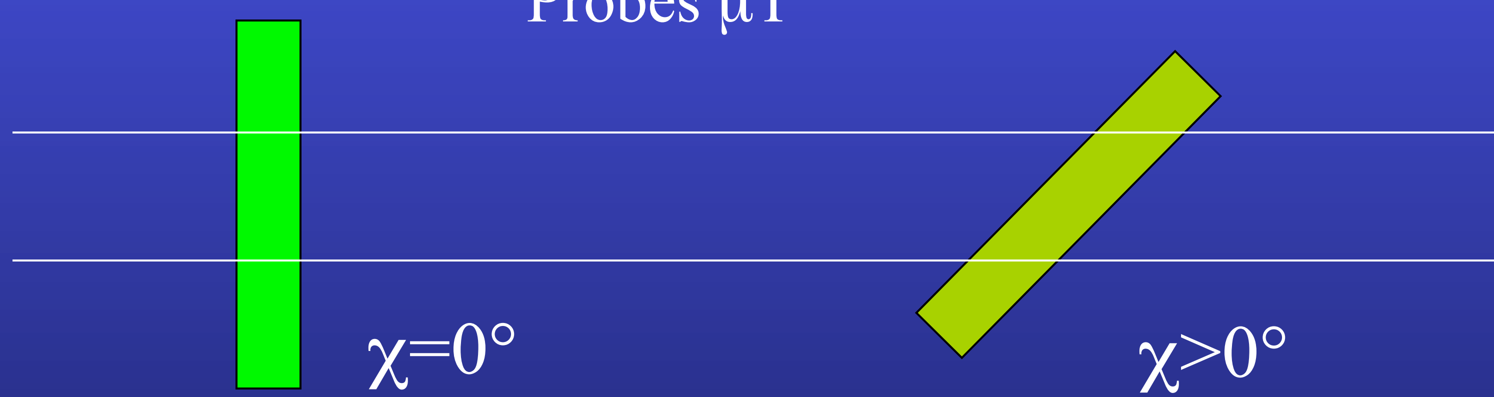

STANDARDS

Al_2O_3 « standard » powder

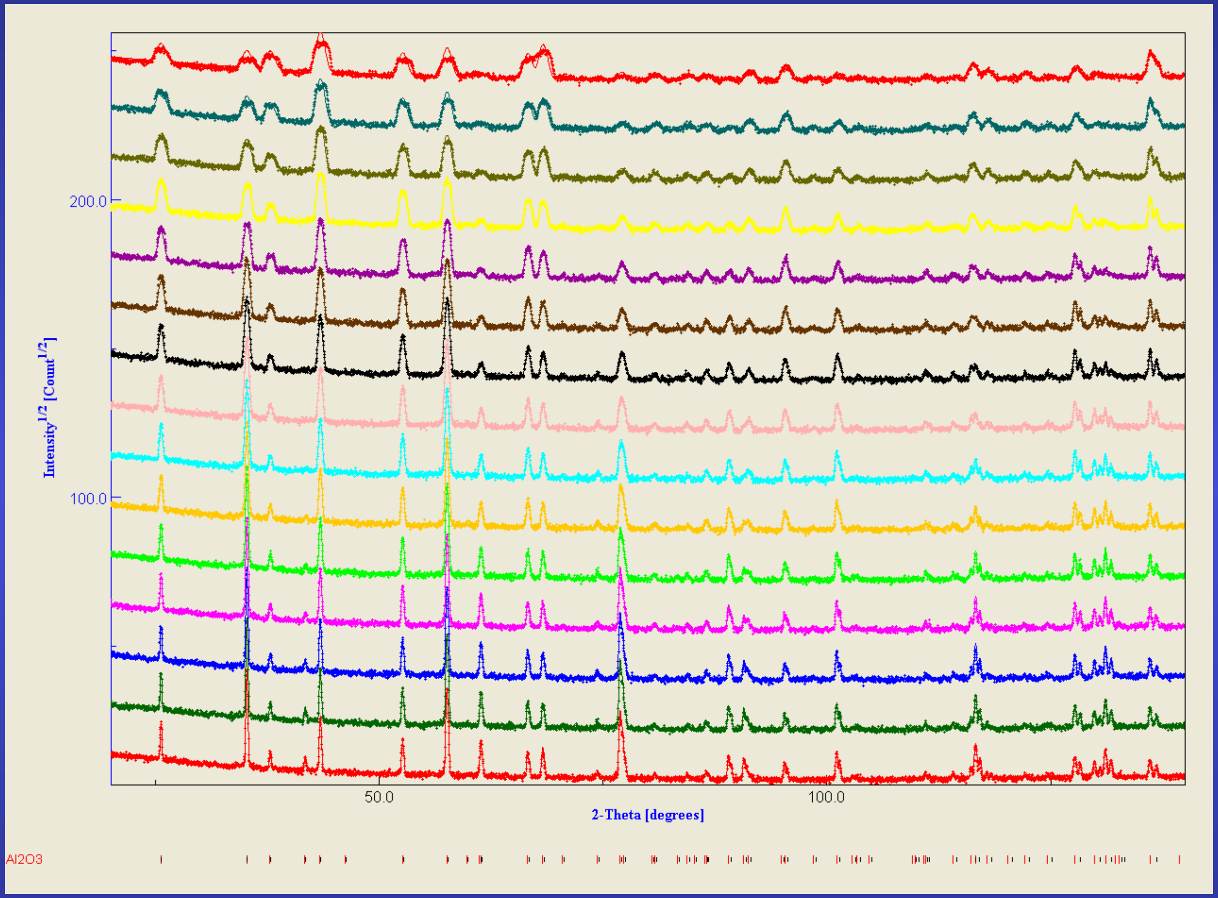

2θ-scans:
GoF = 1.92
R_W = 15.60 %
R_B = 11.94 %

θ−2θ-scans:
GoF = 1.86
R_W = 16.11 %
R_B = 12.40 %

15 diagrams x 5 mn (fibre texture): 1.25 h
936 diagrams x 5 mn (non symmetric texture): 3.25 days

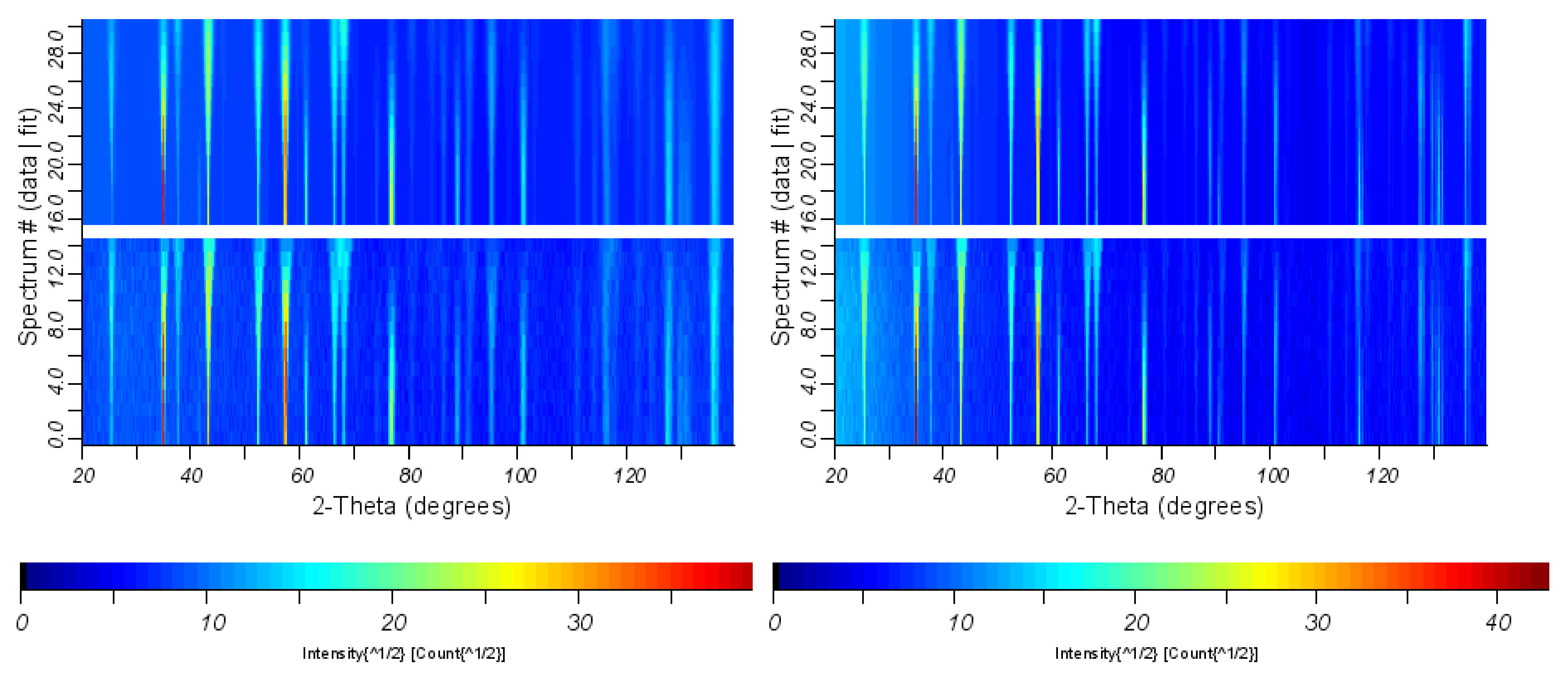

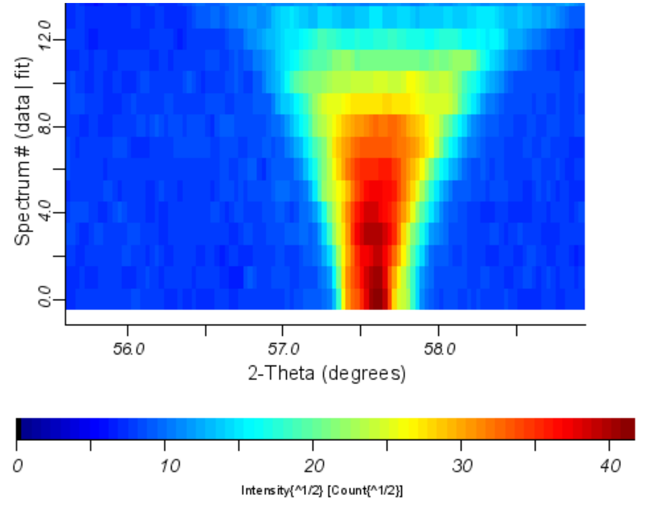

-70 microns x shift in χ

And texture !!

XRR

Specular reflectivity: **q**=(0,0,z)

- Fresnel:

$$R(\mathbf{q}) = \left| \frac{q_z - \sqrt{q_z^2 - q_c^2 + \frac{32 i \pi^2 \beta}{\lambda^2}}}{q_z + \sqrt{q_z^2 - q_c^2 + \frac{32 i \pi^2 \beta}{\lambda^2}}} \right|^2 \delta q_x \delta q$$

- matrix:

$$R^{flat} = \frac{r_{0,1}^2 + r_{1,2}^2 + 2 r_{0,1} r_{1,2} \cos 2 k_{Z,1} h}{1 + r_{0,1}^2 r_{1,2}^2 + 2 r_{0,1} r_{1,2} \cos 2 k_{Z,1} h}$$

- Born approximation:
  Electron Density Profile

$$R(q_z) = r.r^* = R_F(q_z) \left| \frac{1}{\rho_s} \int_{-\infty}^{+\infty} \frac{d\rho(z)}{dz} e^{i q_z z} dz \right|^2$$

- Roughness:

$$R^{rough}(q_z) = R(q_z) \exp(-q_{z,0} q_{z,1} \sigma^2) \quad \text{Low-angles (reflectivity)}$$

$$S_R = 1 - p \exp(-q) + \mathrm{p} \exp\left(\frac{\text{-q}}{\sin\theta} \right) \quad \text{high-angle (Suortti)}$$

CPS scans

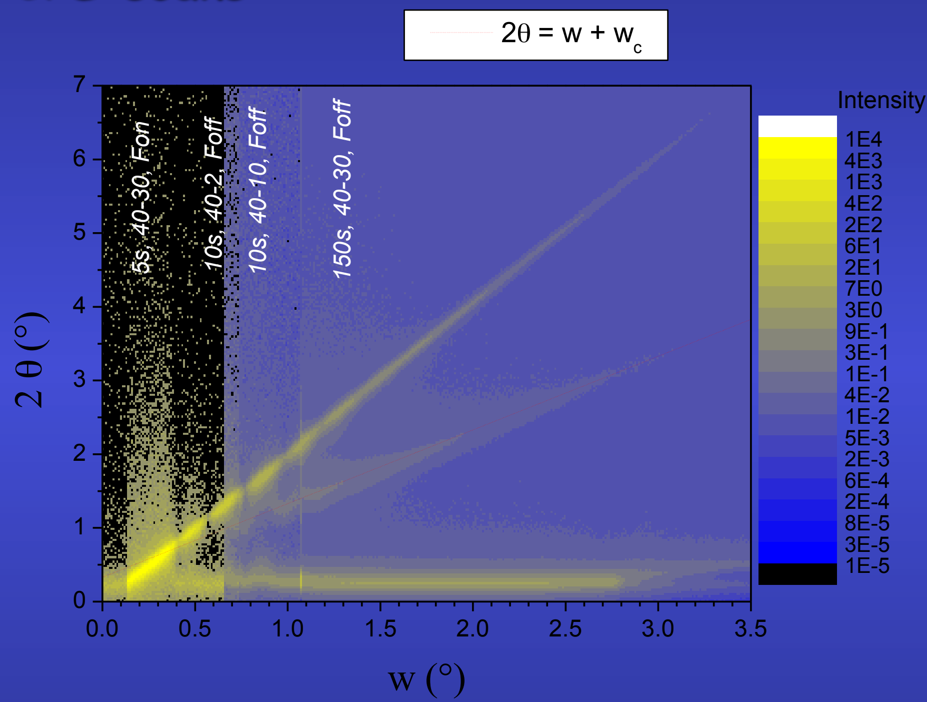

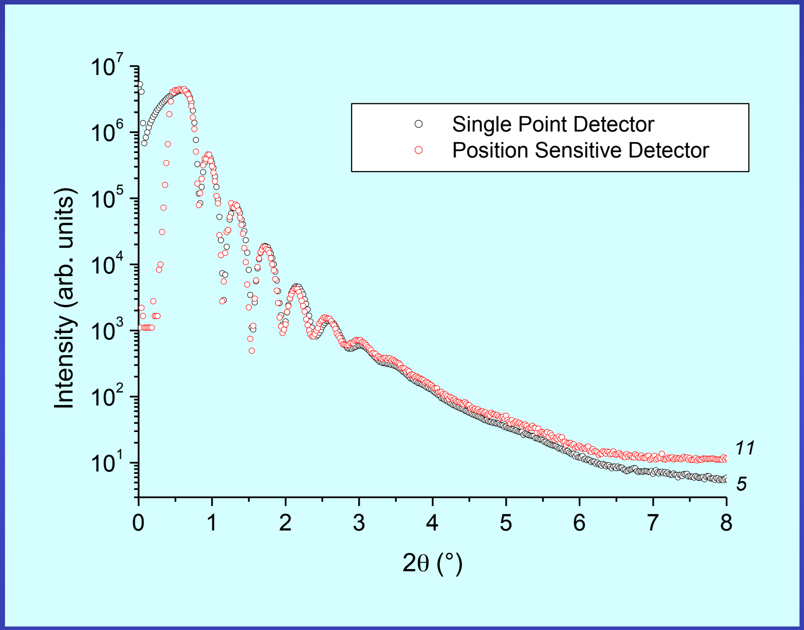

Useful for having bot specular and off-specular signals in one scan

XRF/XRR/XRD

Experimental Set-ups

↳ Laboratory combined XRF & XRR set-up

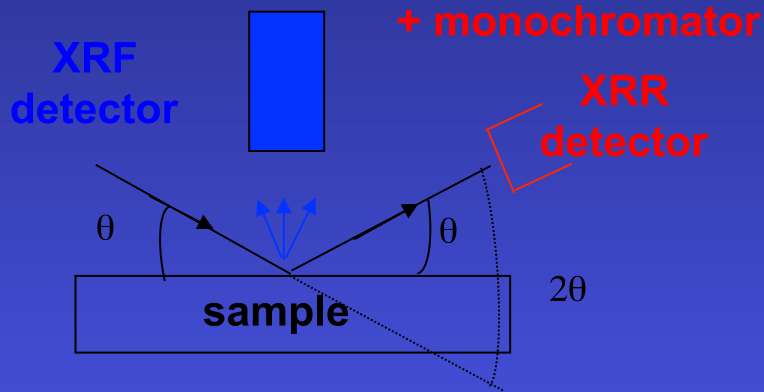

X-Pert panalytical diffractometer

⅄ XRF detector = silicon drift detector
(25 mm²/500 µm, 0.5mm Be window)

↳ XRF Instrumental f

simulation of polychromatic X-ra

detector response (escap

→ full correction for losses due to air and Be

Energy resolution versus X-ray energy @ 5.9 keV (*www.amptek.com*)

126 eV FWHM with the Mn K_{α} line but < 50 eV FWHM at low energy.

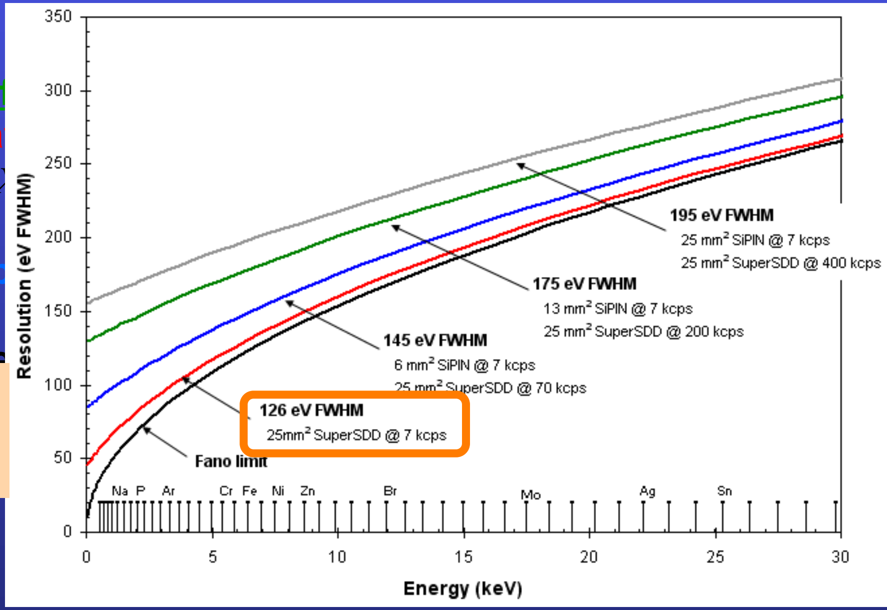

IO/Ag/IO textured samples ➔ intensited must be corrected :

$$I_{hkl}(2\theta, \chi, \varphi) = I_{hkl}(2\theta)\, P_{hkl}(\chi, \varphi)$$

$P_{hkl}(\chi, \varphi)$ → Orientation Distribution Function (ODF): WIMV method used in MAUD

Experimental need

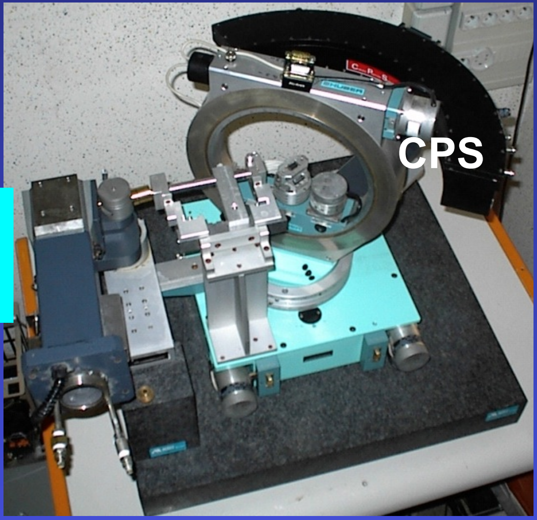

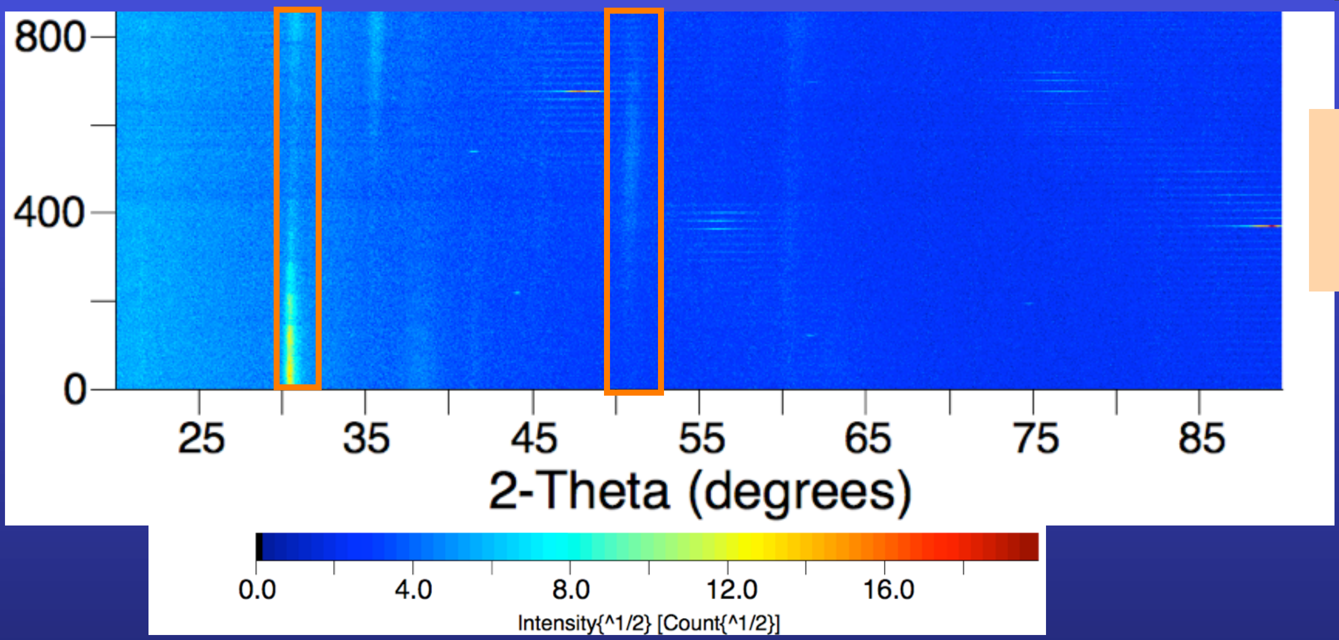

By changing (χ, φ): peaks position moves ➔ residual stress

Combined XRR, XRD & GiXRF Analysis

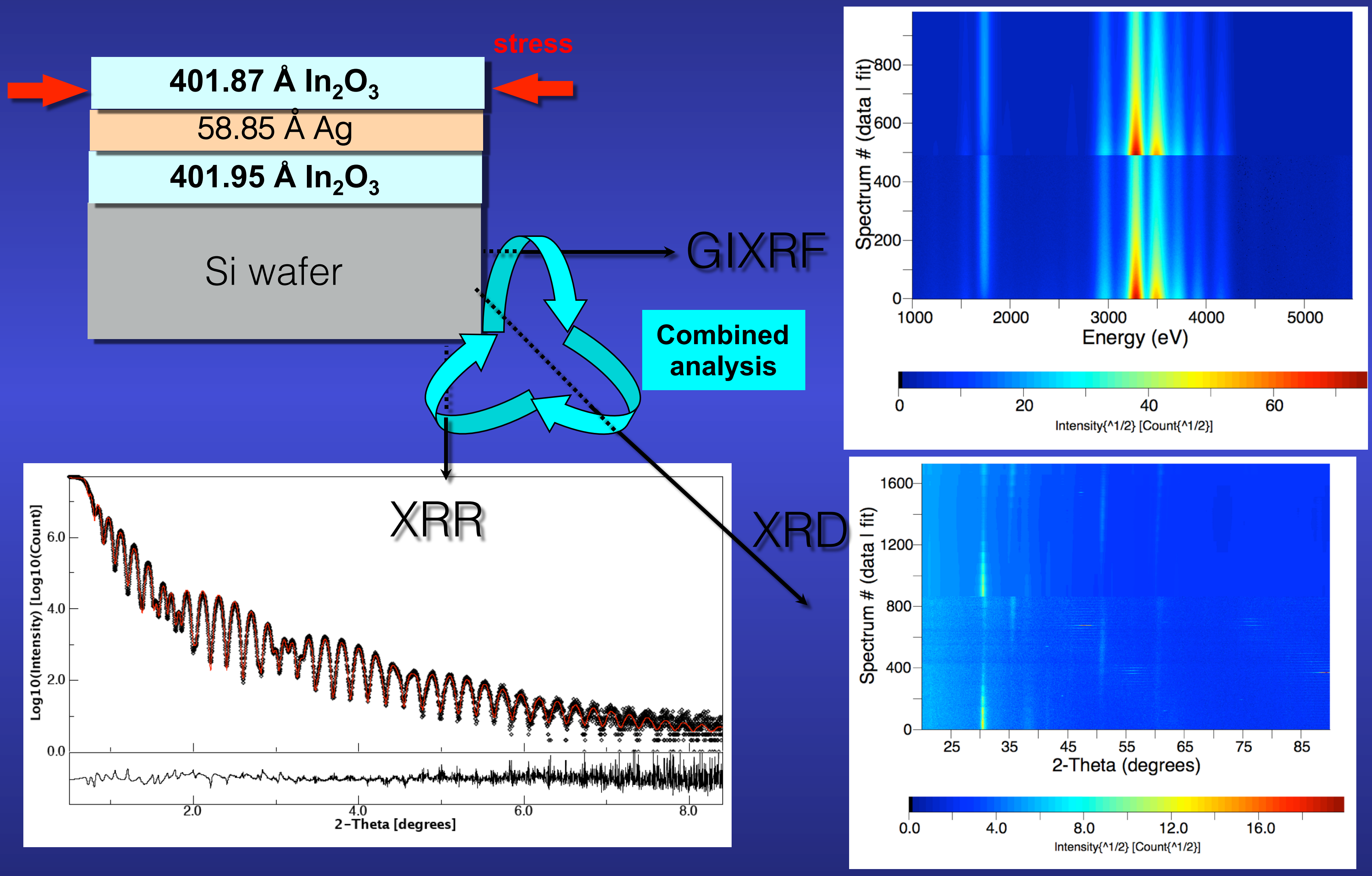

XRR

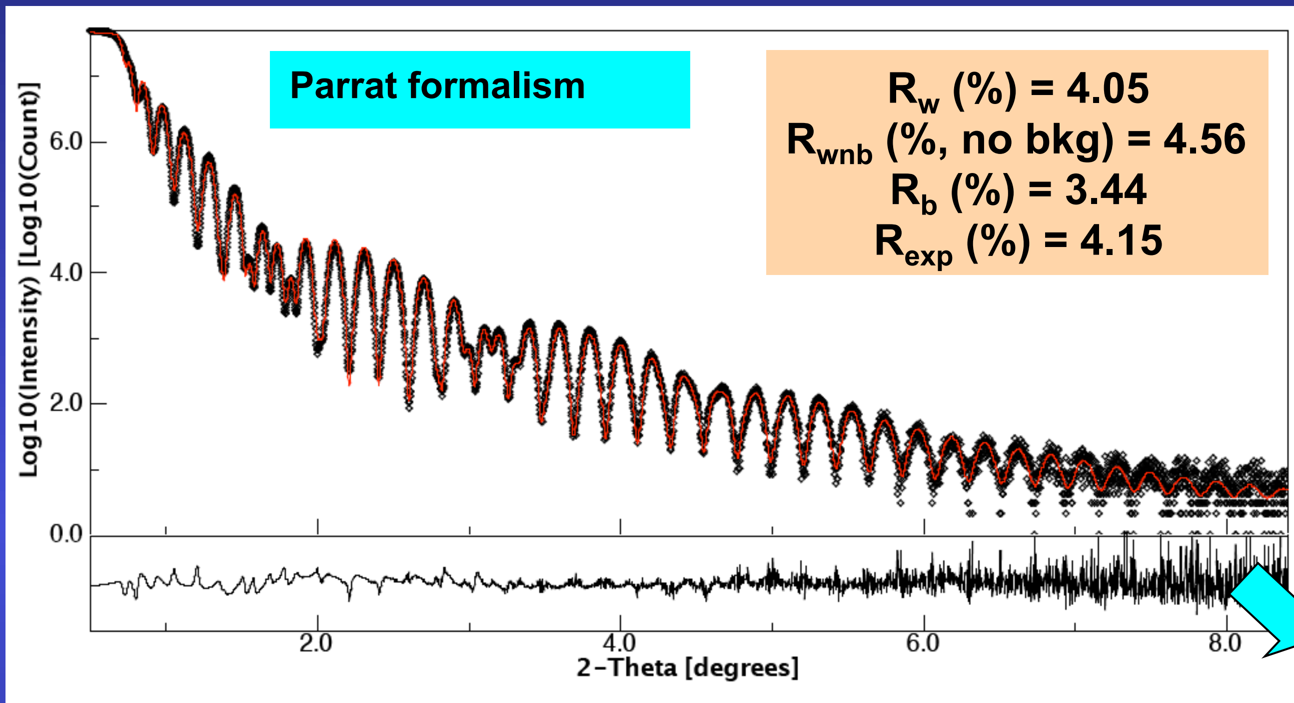

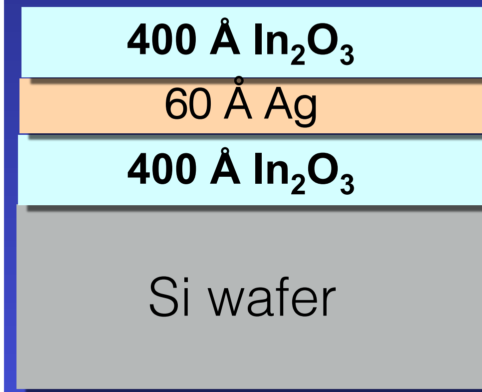

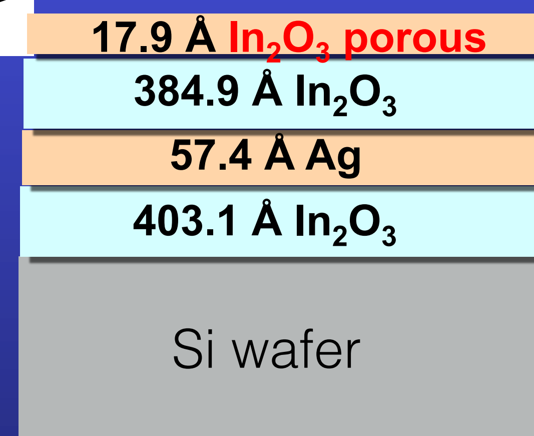

Highly porous In_2O_3 layer

Top layer: q_c = 0.0294 Å^{-1}; roughness r =0.38nm

Top In_2O_3: q_c = 0.0504 Å^{-1}; r =2.06 nm

Ag : q_c = 0.0576 Å^{-1}; r =0.26 nm

Bottom In_2O_3: q_c = 0.04889 Å^{-1}; r =6.74 nm

Si wafer: q_c = 0.0313 Å^{-1}; r = 0.73 nm

XRD

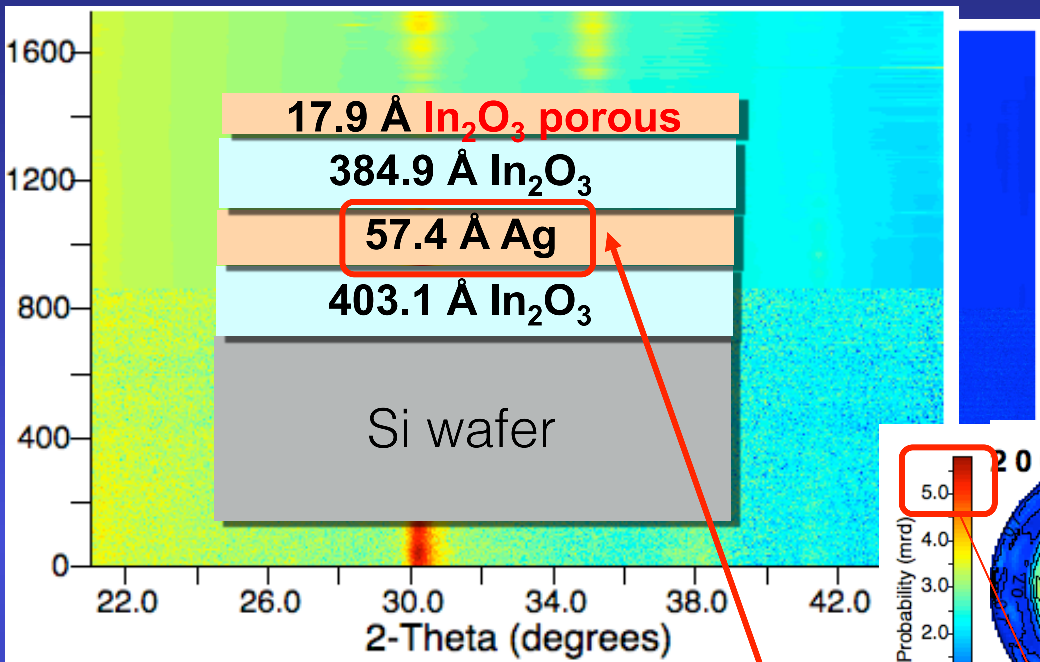

R_w (%) = 23.97
R_{wnb} (%, no bkg) = 58.31
R_b (%) = 18.71
R_{exp} (%) = 22.04

In_2O_3

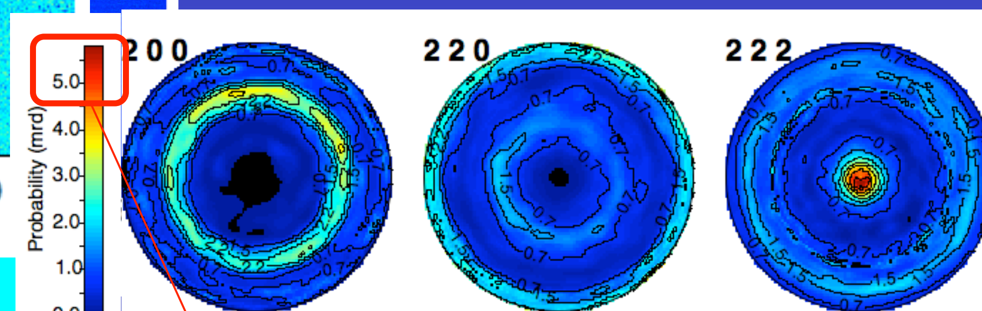

5 m.r.d.

Refined Ag phase parameters

- Isotropic crystallite size = 56.4 (1.3) Å
- Cell parameter: a = 4.0943(7) Å

Ag:

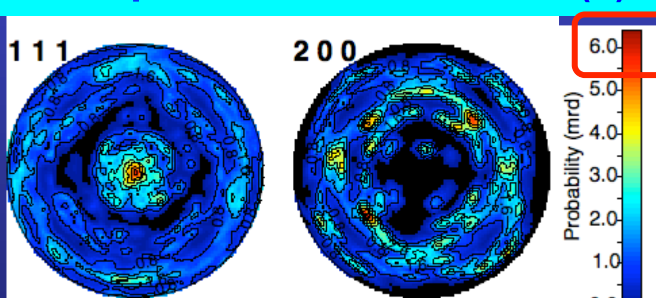

Refined In_2O_3 phase parameters

- σ_{xx} = - 1 GPa (in-plane compressive stress)
- Isotropic crystallite size = 153.2(5) Å
- Cell parameter: a = 10.2104(5) Å

GiXRF

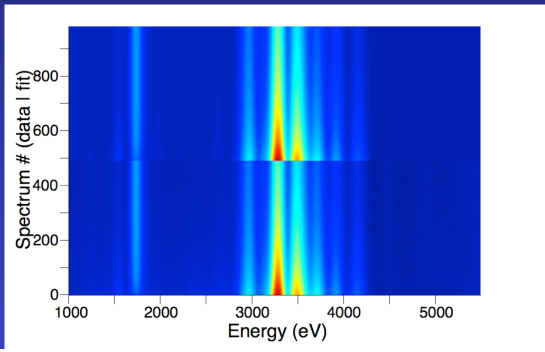

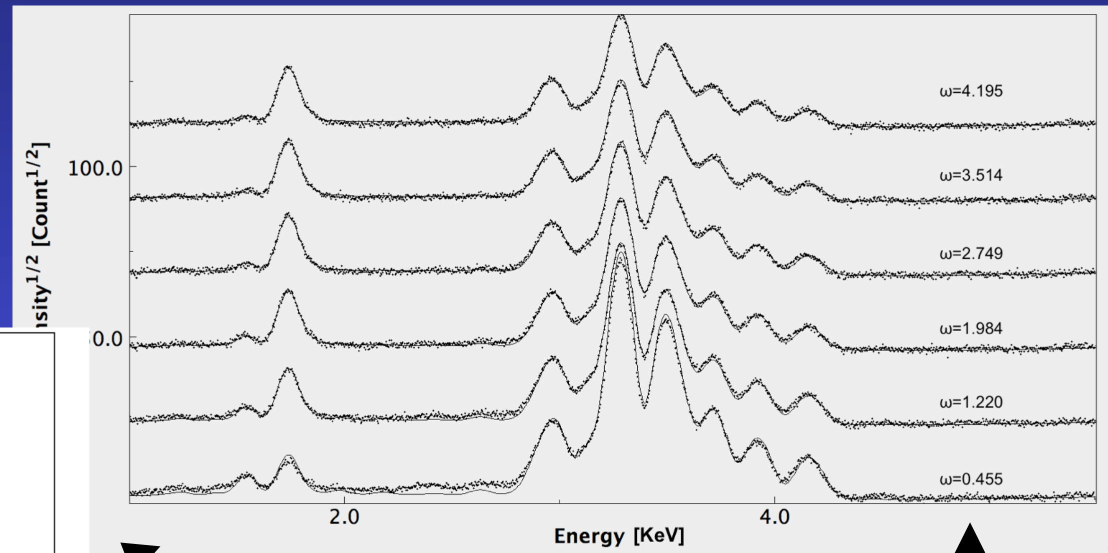

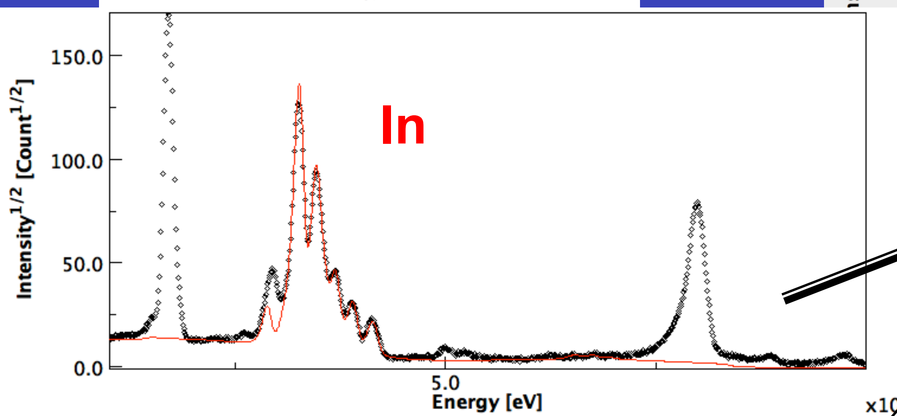

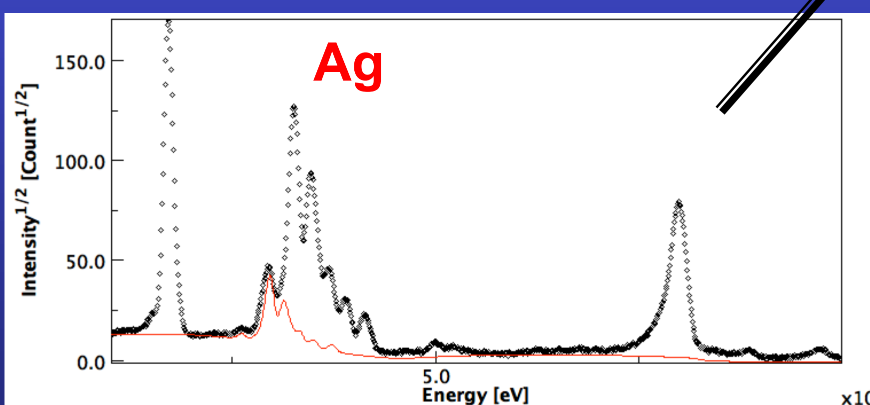

No presence of contaminant observed

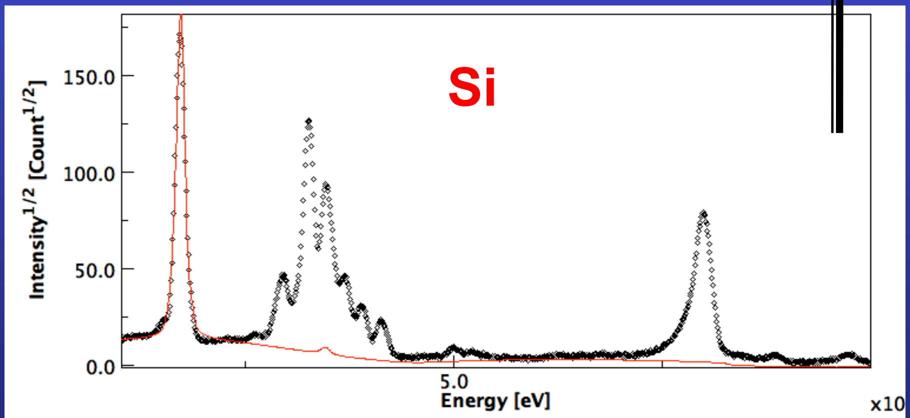

FPSM

Full-Pattern Search-Match

www.iutcaen.unicaen.fr

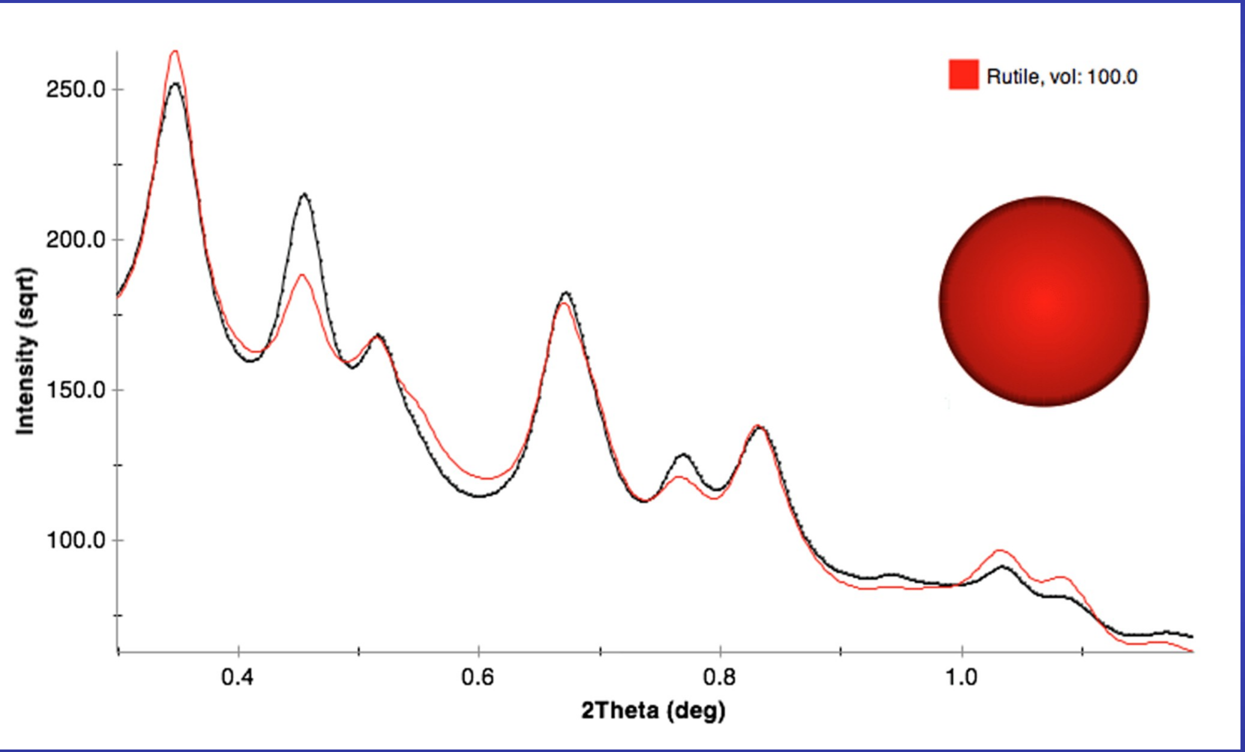

Rutile nanocrystalline Electron Powder Diffraction pattern

A site for open FPSM

Diffraction pattern and sample composition

Upload diffraction pattern: [ ] Parcourir...

Atomic elements in the sample: O Al Ca F Zn

☐ Sample nanocrystalline

Experiment details

Radiation:

◉ X-ray tube: Cu

○ Other : x-ray Wavelength (Å): 1.540598

Instrument geometry:

◉ Bragg-Brentano (theta-2theta)

○ Bragg-Brentano (2theta only), omega: 10

○ Debye-Scherrer

○ Transmission

Instrument broadening function: Medium

Search and quantify

☐ Extra output (for debugging)

Structures database: CODstructures

1 min later
>275000 COD
structures

Found phases and quantification:

Phase ID	name	vol. (%)	wt. (%)	crystallites (Å)	microstrain
9004178	Zincite	16.8284	23.9708	2148.26	0.00028435
9009005	Fluorite	42.5522	33.9388	2117.08	0.000363147
9007498	Corundum	37.2197	37.2493	1889.82	0.000267779
2300112	zinc_oxide	3.39971	4.84114	1754.74	6.98311e-05

Final Rietveld analysis, Rw: 0.159468, GofF: 1.95869

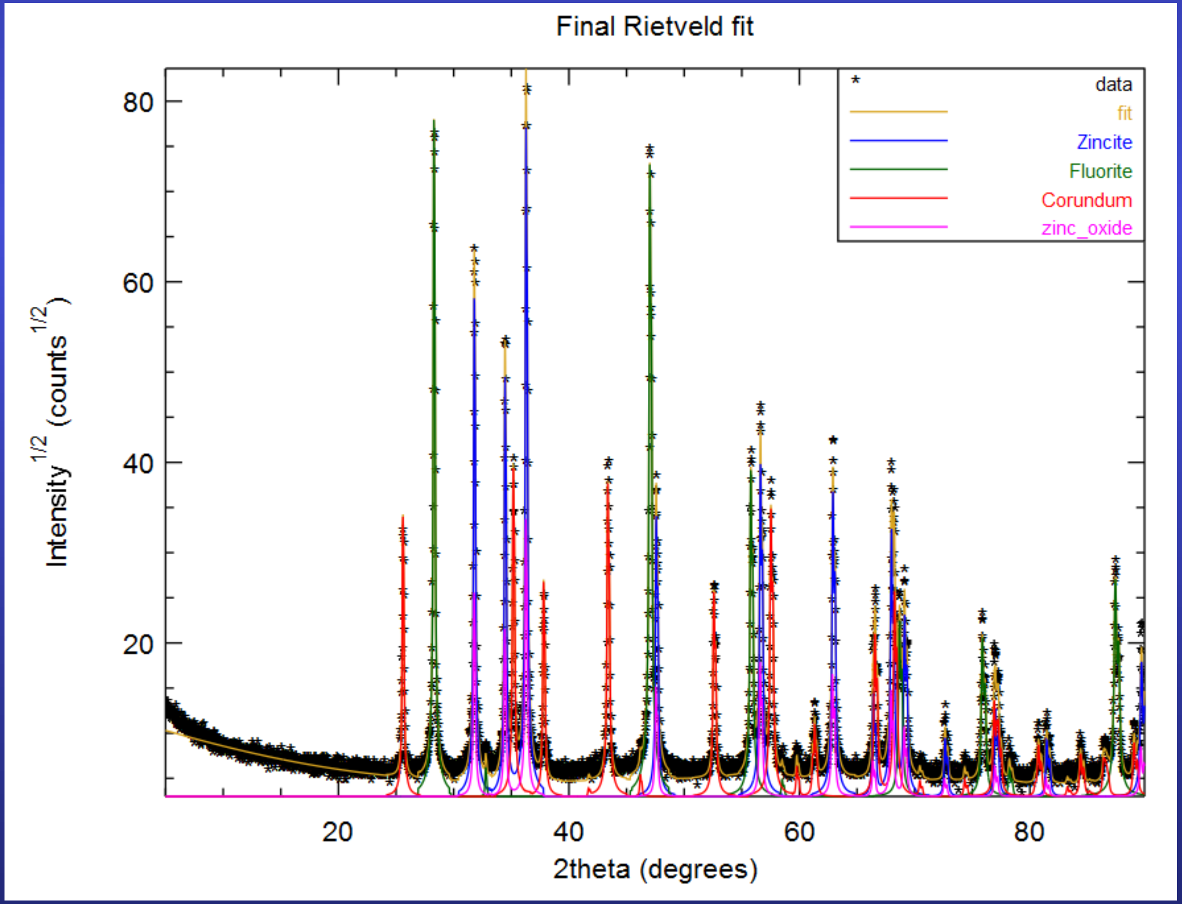

CaCO3 - mollusks

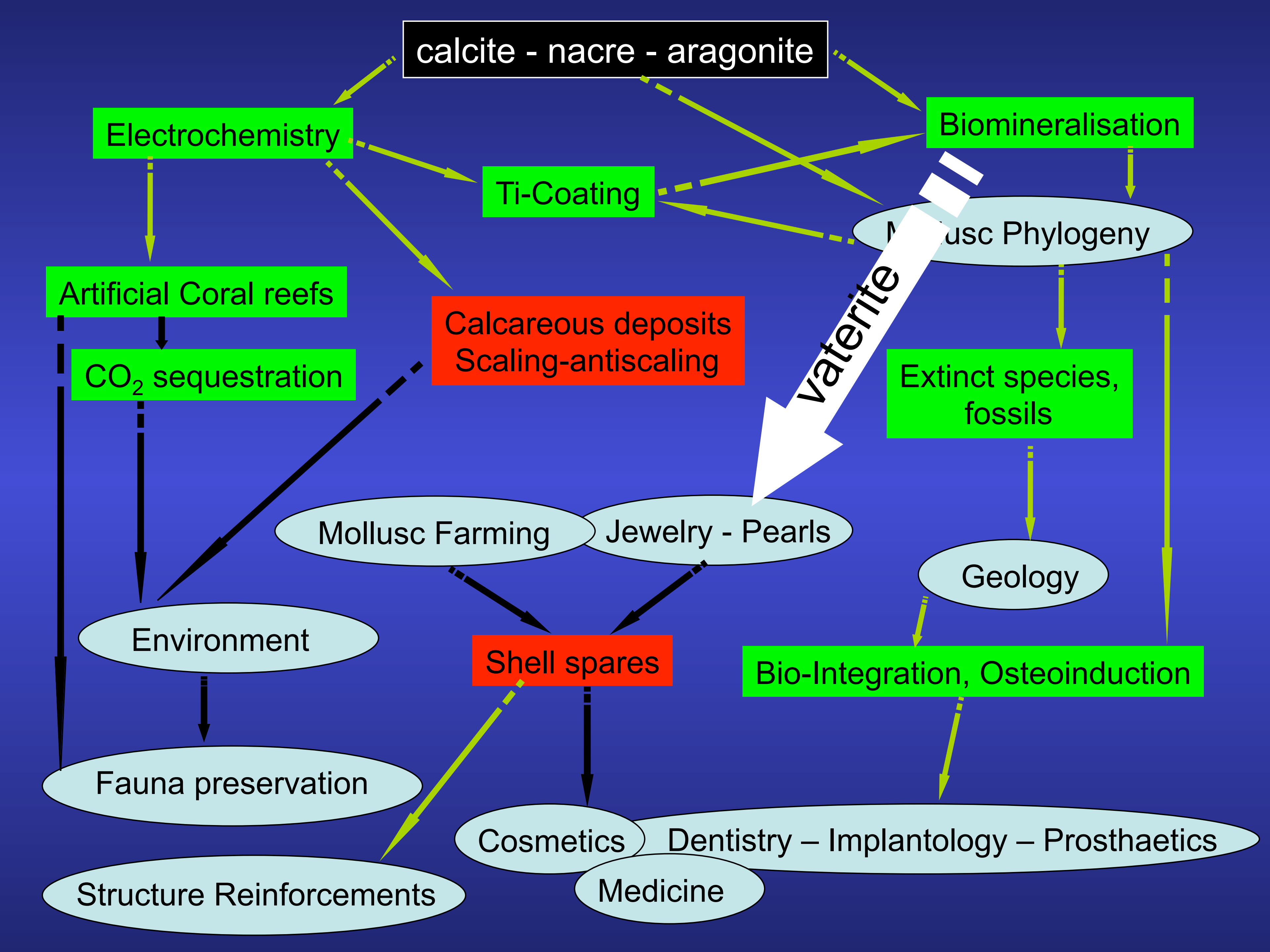
calcite - nacre - aragonite
Electrochemistry
Biomineralisation
Ti-Coating
usc Phylogeny
vaterite
Artificial Coral reefs
Calcareous deposits
Scaling-antiscaling
CO_2 sequestration
Extinct species, fossils
Mollusc Farming
Jewelry - Pearls
Geology
Environment
Shell spares
Bio-Integration, Osteoinduction
Fauna preservation
Cosmetics
Dentistry – Implantology – Prosthaetics
Medicine
Structure Reinforcements

Aplanarity of carbonate groups in $CaCO_3$: $\Delta Z_{C\text{-}O1} = c(z_C - z_{O1})$

T, pH →

Mineral

calcite	aragonite	vaterite
0 Å	0.05744 Å +2 kJ/mol	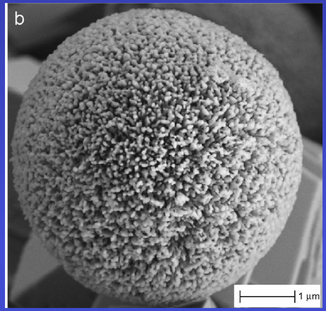

Biogenic

calcite	*aragonite*	*vaterite*
	Intermediate or more distorted	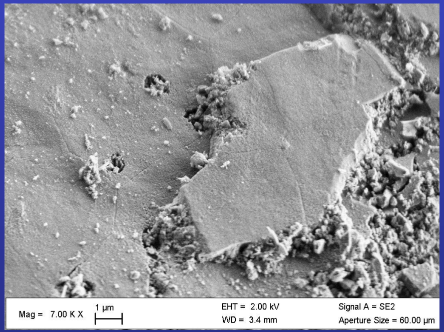

[Mg2+], inter/intracrystalline molecules →

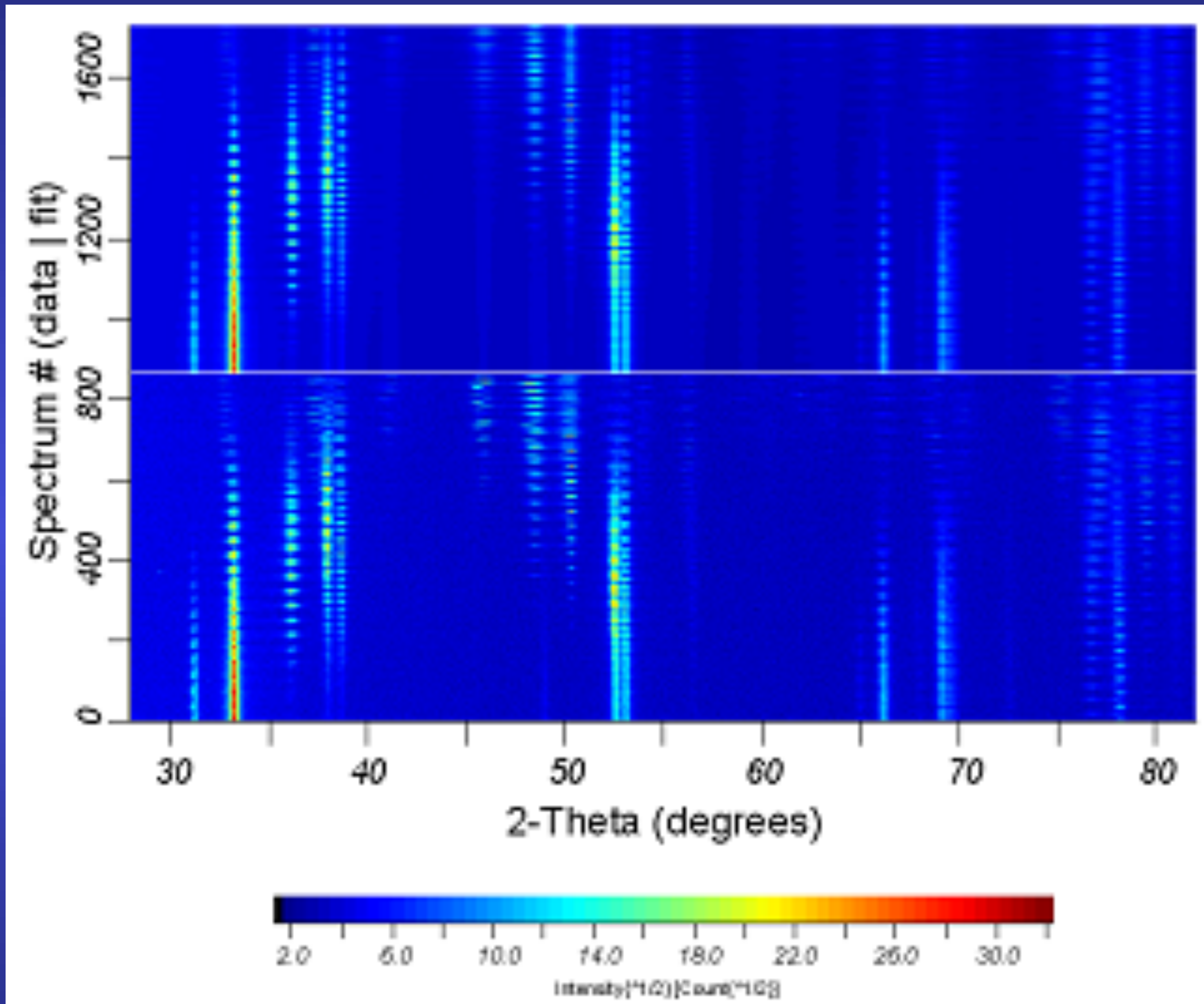

refined

experiments

GoF:1,72
Rw: 28,0%
Rexp:21,3%

for all (χ,φ) sample orientations

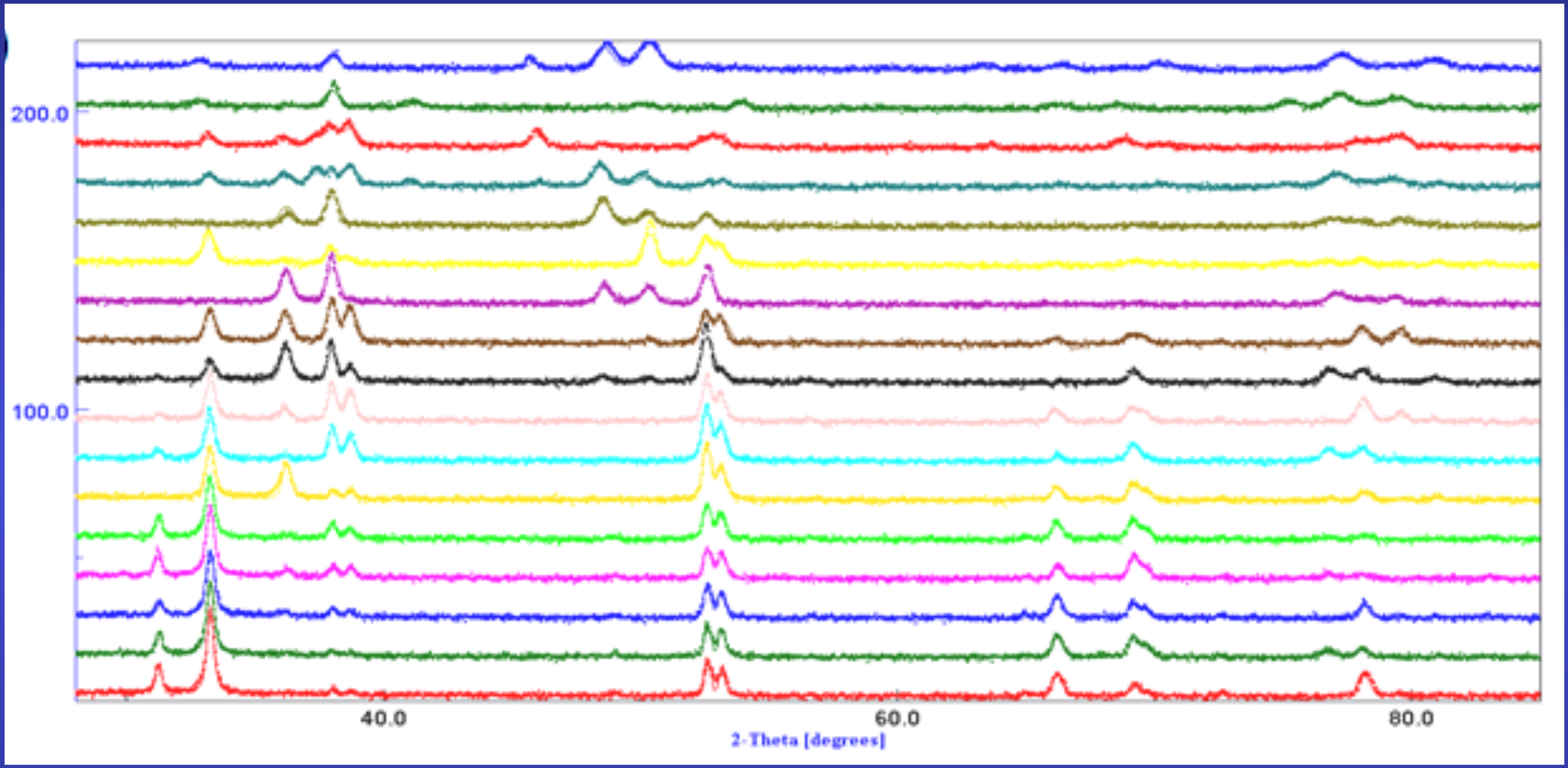

IRC layer of *Charonia lampas lampas* for selected (χ,φ) sample orientations

Aragonitic layers in mollusc shells

Gastropods — *Crossed lamellar layers*

Charonia lampas lampas (triton or trumpet cousin)

Columnar Nacre

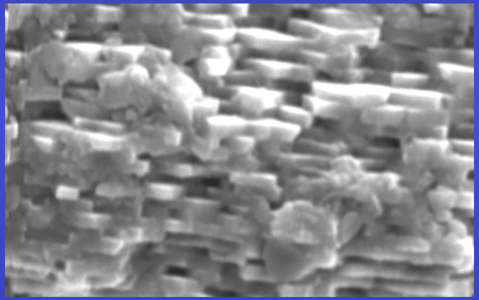

Haliotis tuberculata (common abalone)

Bivalves — *Sheet Nacre*

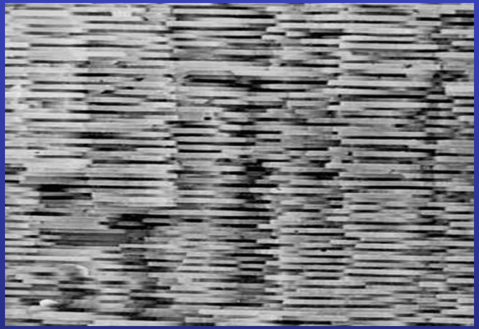

Pinctada maxima (Mother of pearl oyster)

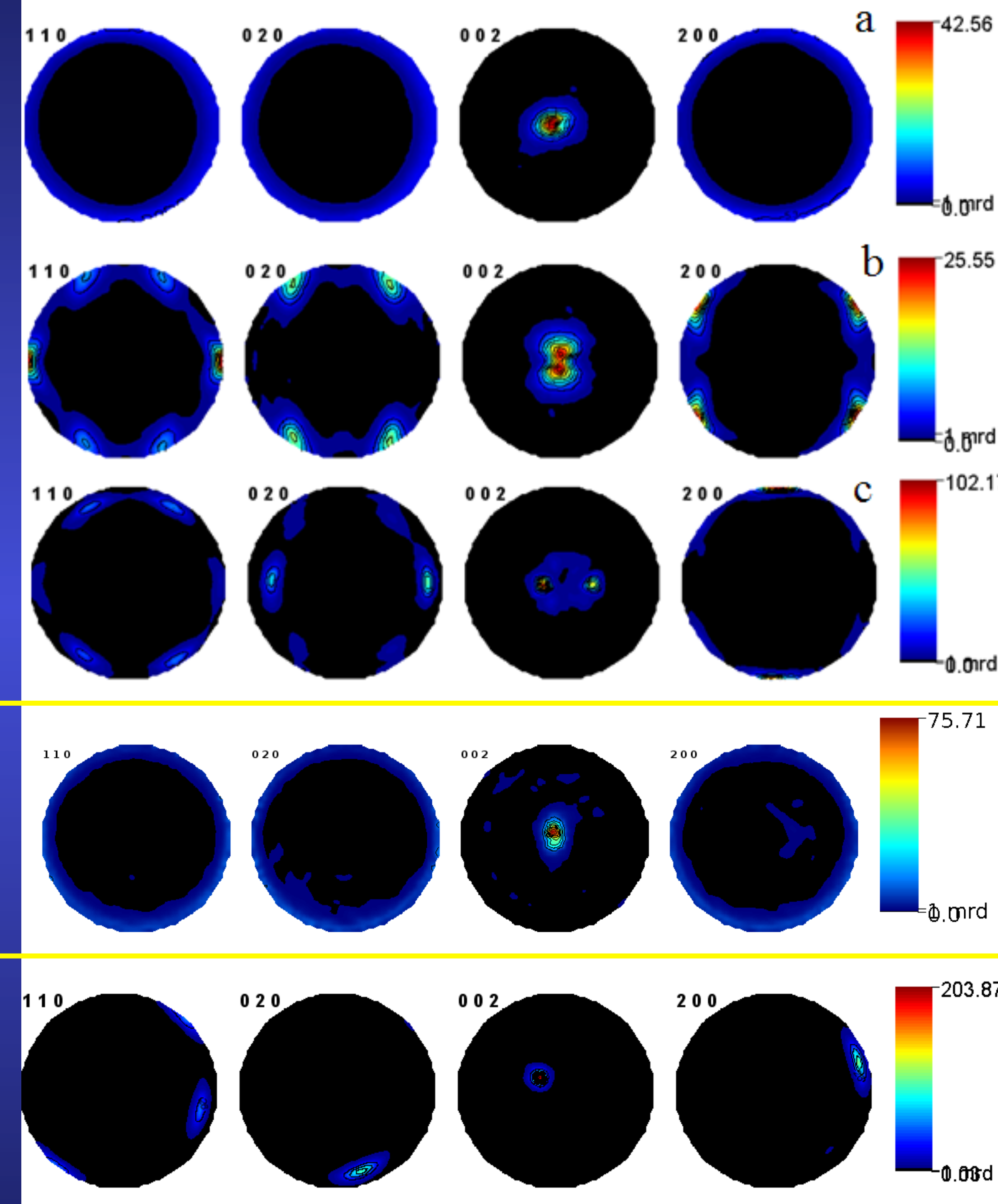

Outer CL
43 mrd^2

Interm Radial CL
47 mrd^2

Inner Com CL
721 mrd^2

Inner Columnar Nacre
211 mrd^2

Inner Sheet Nacre
1100 mrd^2

Unit-cell distortions

	OCL	*Charonia* IRCL	ICCL	*Pinctada* ISN	*Haliotis* ICN
a (Å) b (Å) c (Å)	4,98563(7) 8,0103(1) 5,74626(3)	4,97538(4) 7,98848(8) 5,74961(2)	4,9813(1) 7,9679(1) 5,76261(5)	4,97071(4) 7,96629(6) 5,74804(2)	4.9480(2) 7.9427(6) 5.7443(6)
Δa/a Δb/b Δc/c	0,0047 0,0053 0,0004	0,0026 0,0026 0,0010	0,0038 0,0000 0,0033	0.0017 -0.0002 0.0007	-0.0029 -0.0032 0.0007
ΔV/V (%)	1,05	0,62	0,71	0.22	-0.60

Anisotropic cell distortion - depends on the layer
Only nacres exhibit (**a**,**b**) contraction
Due to inter- and intra-crystalline molecules
Distortions and anisotropies larger than pure intra- effect (Pokroy et al. 2007)

Elastic stiffnesses

Single crystal	**160 37.3 1.7 87.2 15.7 84.8 41.2 25.6 42.7**
ICCL	**96.5 31.6 13.7 139 9.5 87.8 29.8 36.6 40.2**
RCL	**130.1 32.6 10.3 103.3 14.1 84.5 36.3 31.1 40.5**
OCL	**111.1 32.9 13.2 119 11.8 84.8 32.8 34.6 40.9**

Structural distortions in aragonitic biogenic ceramic composites

Aplanarity of carbonate groups in $CaCO_3$

$$\Delta Z_{C\text{-}O1} = c(z_C - z_{O1})$$

Calcite	*Biogenic aragonite*	*Mineral aragonite*
0 Å	*Intermediate ?*	*0.05744 Å*

Atomic Structures

		Geological reference	*Charonia lampas* OCL	*Charonia lampas* IRCL	*Charonia lampas* ICCL	*Strombus decorus* mixture	*Pinctada maxima* ISN
Ca	y z	0.41500 0.75970	0.41418(5) 0.75939(3)	0.414071(4) 0.76057(2)	0.41276(9) 0.75818(8)	0.4135(7) 0.7601(8)	0.41479 (3) 0.75939 (2)
C	y z	0.76220 -0.08620	0.7628(2) -0.0920(1)	0.76341(2) -0.08702(9)	0.7356(4) -0.0833(2)	0.7607(4) -0.0851(7)	0.7676 (1) -0.0831 (1)
O1	y z	0.92250 -0.09620	0.9115(2) -0.09205(8)	0.9238(1) -0.09456(6)	0.8957(3) -0.1018(2)	0.9228(4) -0.0905(9)	0.9134 (1) -0.09255 (7)
O2	x y z	0.47360 0.68100 -0.08620	0.4768(1) 0.6826(1) -0.08368(6)	0.4754(1) 0.68332(9) -0.08473(5)	0.4864(3) 0.6834(2) -0.0926(1)	0.4763(6) 0.6833(3) -0.0863(7)	0.4678 (1) 0.68176 (7) -0.09060 (4)
ΔZ_{C-O1} (Å)		**0.05744**	**0.00029**	**0.04335**	**0.1066**	**0.031**	**0,054**

Carbonate group aplanarity specific to a given layer
Aplanarity decreases from inner to outer shell layers (CL layers)
-> up to quite ΔZ=0 outside (nearly the calcite value)
Average aplanarity on the whole shell = geological reference (Strombus)
In Haliotis nacre: large ΔZ=0.08, + strong anisotropy: less stable nacre

Pearls - CCD

Hyriopsis cumingi (freshwater mussel), China

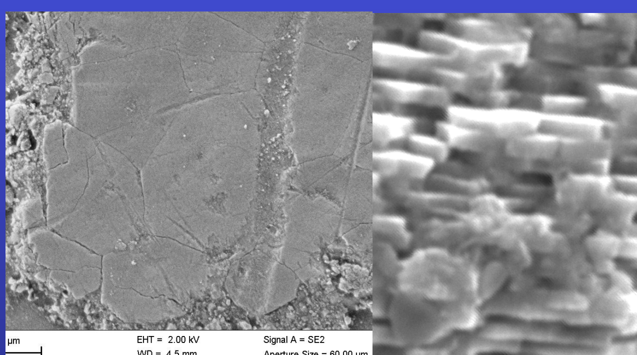

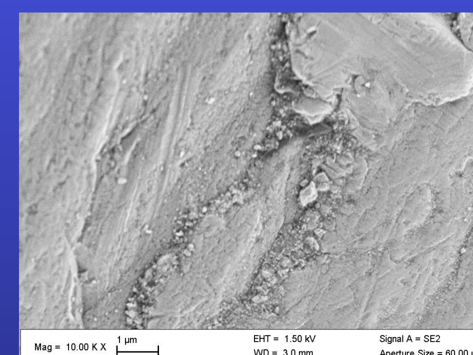

sheet nacre (aragonite)

vaterite defect

INEL « large » beam

864 diagrams
2-days acquisition
250 mm goniometer

$\chi^2 = 1.01$
Rw = 53.9 %

a = 4.9542(2) Å
b = 7.9593(3) Å
c = 5.7258(2) Å

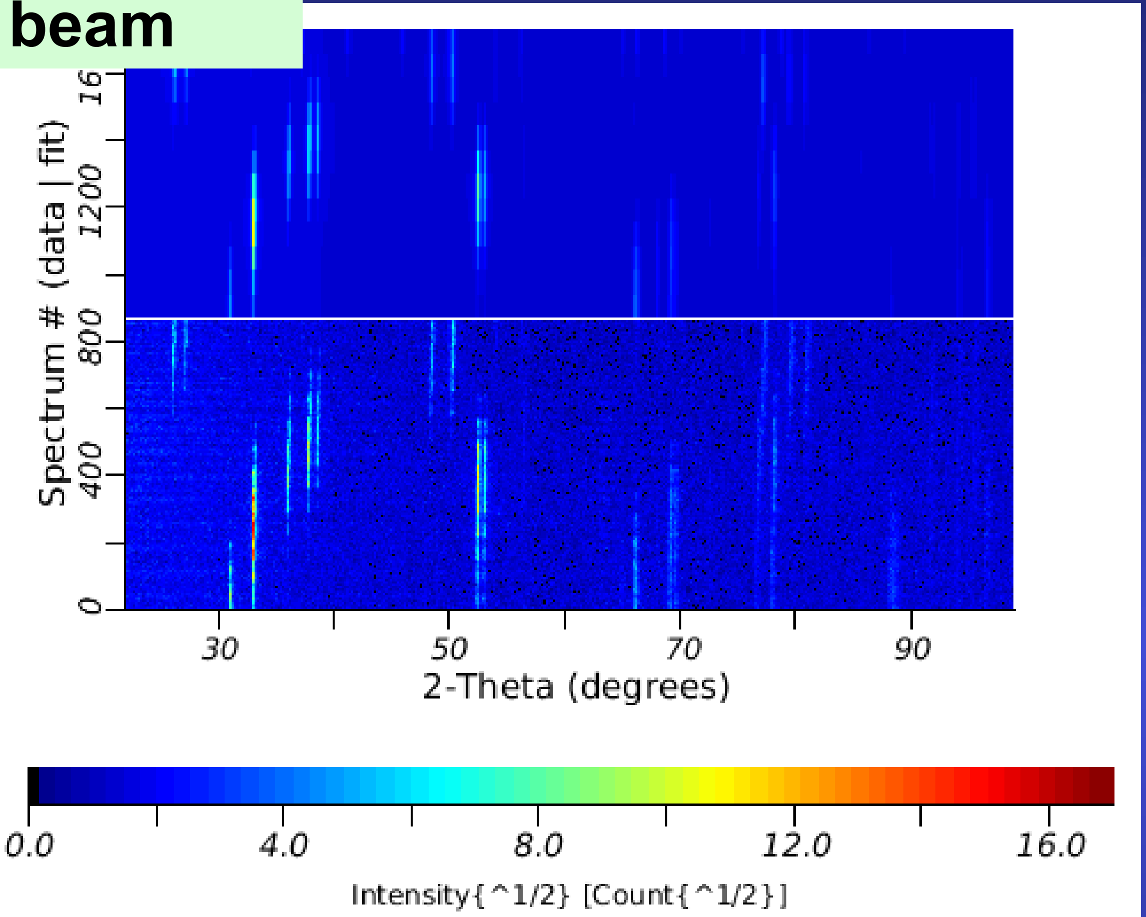

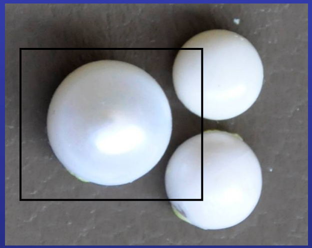

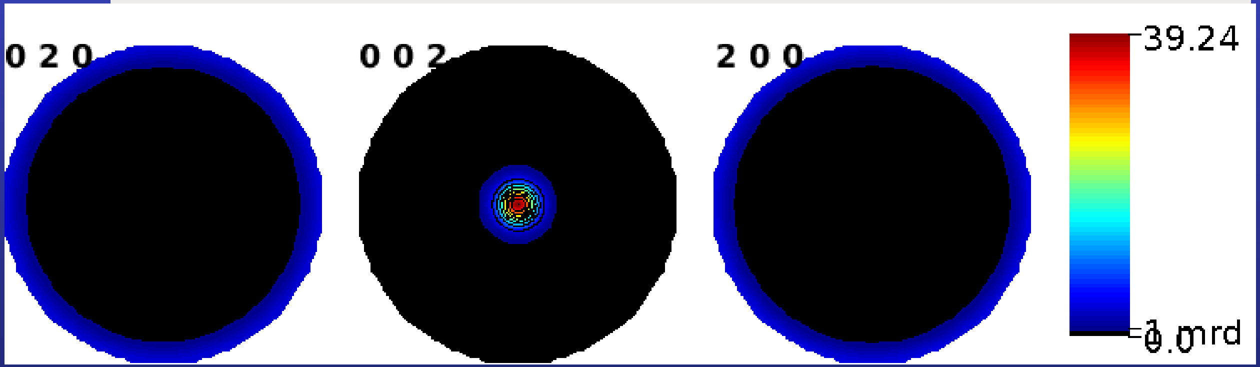

Bruker CCD + «small» InCoatec μsource

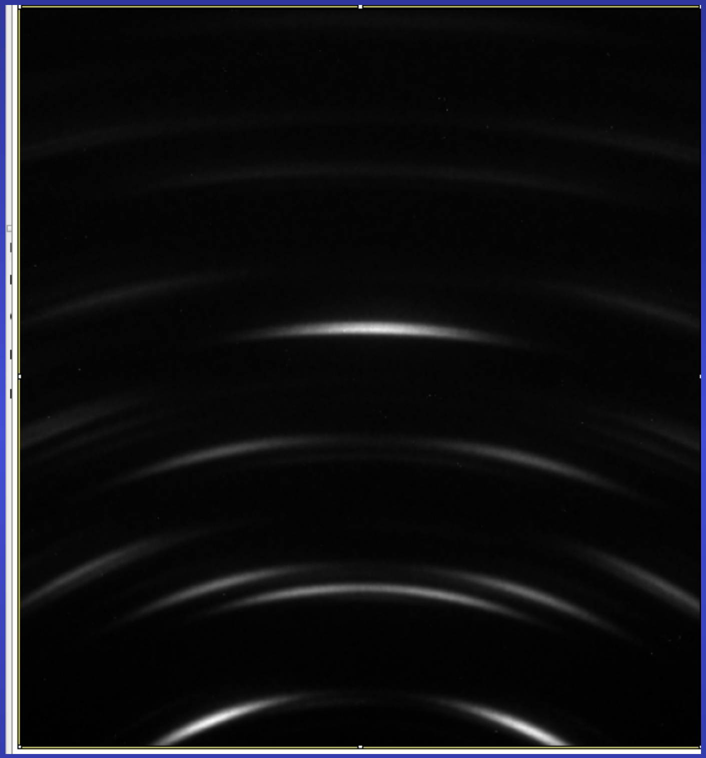

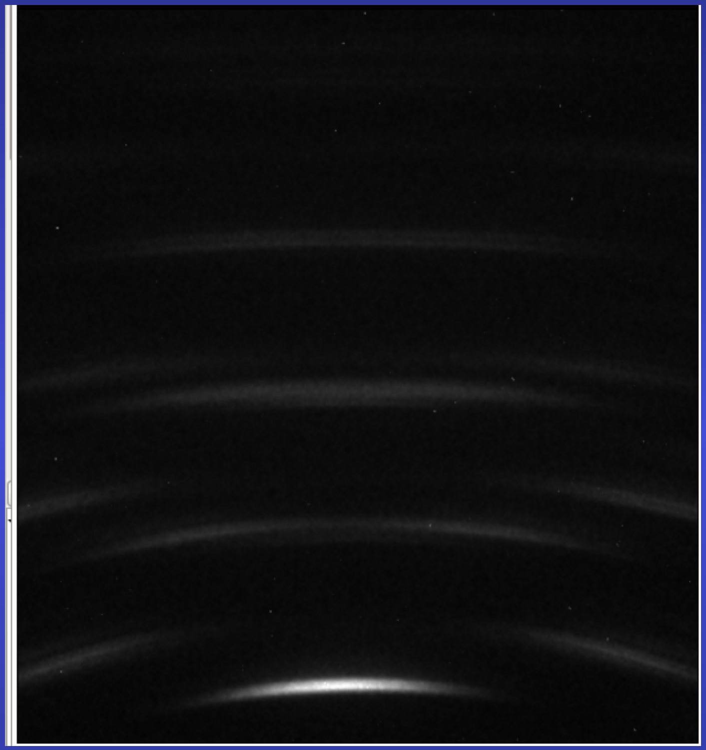

Reflection geometry
72 images
2-hours acquisition
60 mm sample-CCD distance

Compromises:
- resolution/pole figure coverage
- pixel size/distance
- wavelength/nb of lines

Standard component

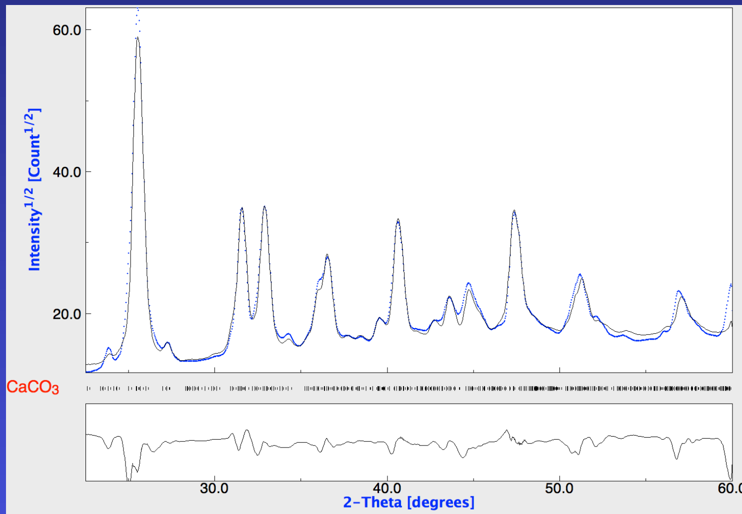

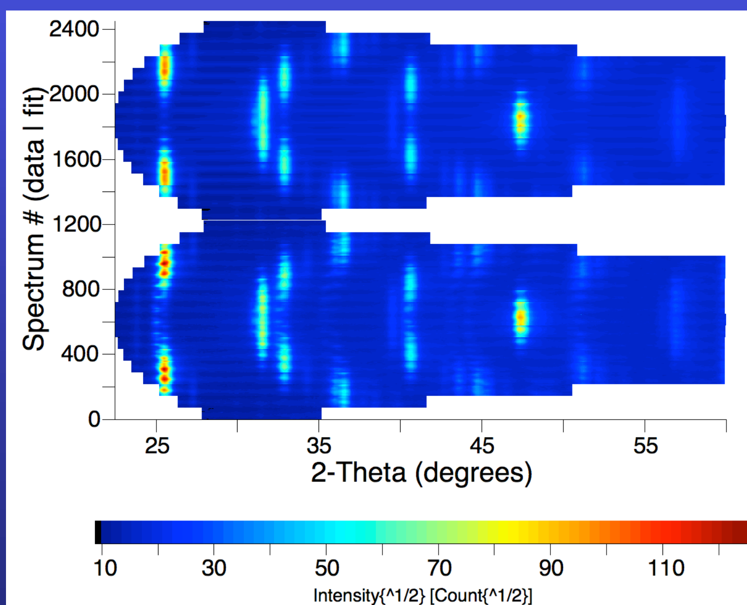

EWIMV

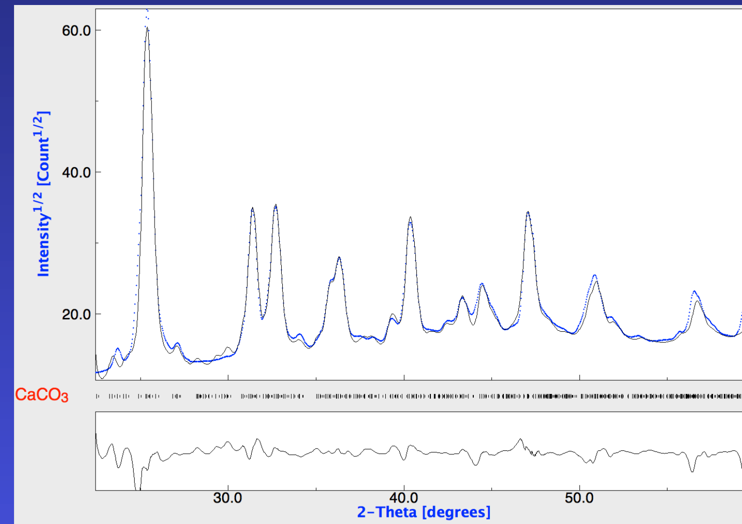

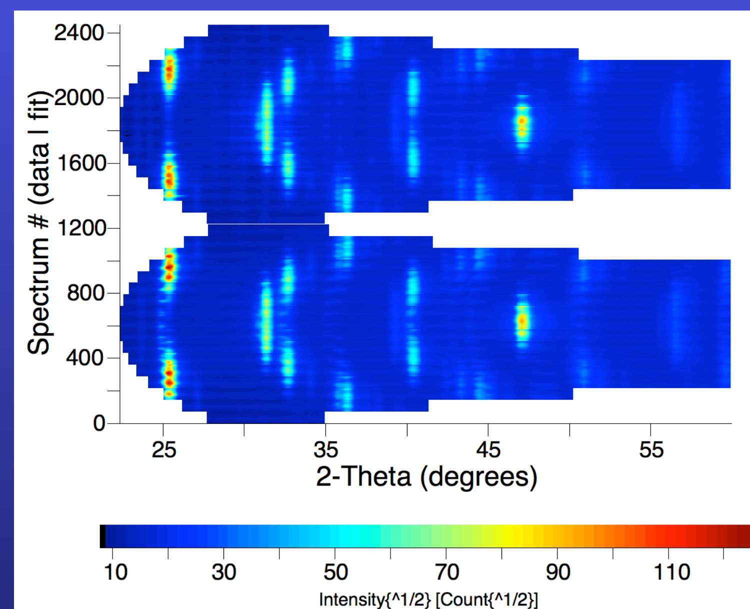

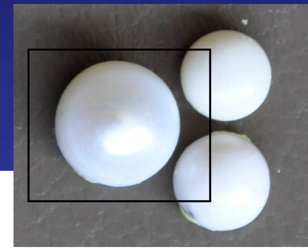

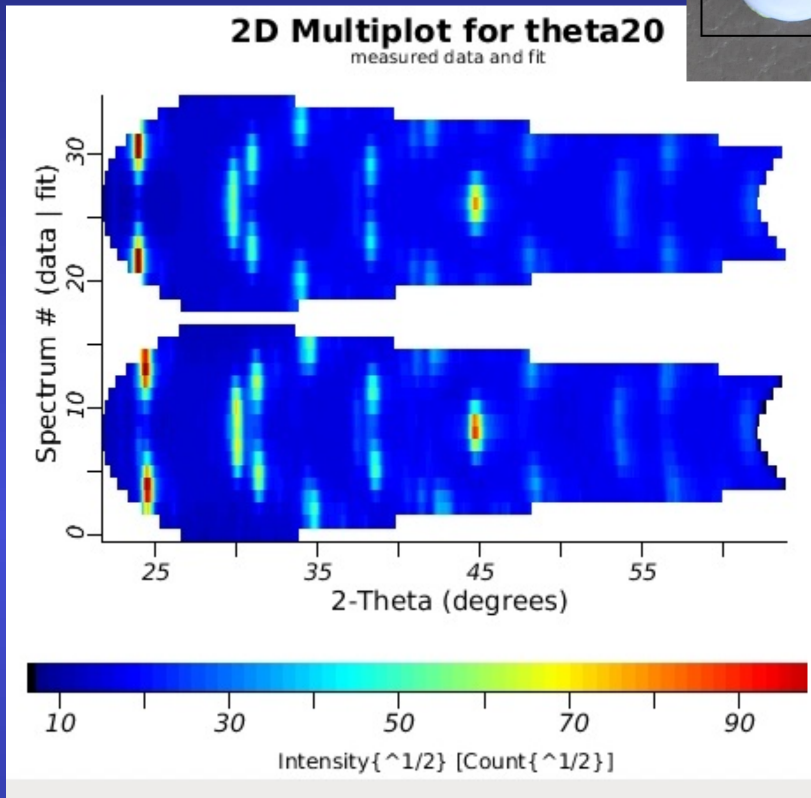

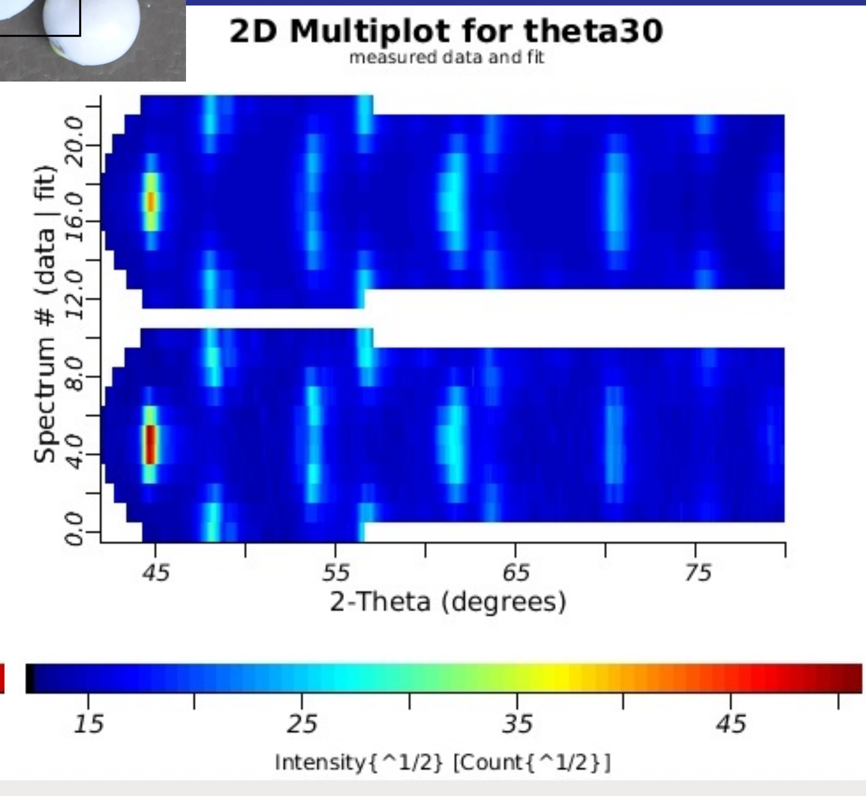

Refinement of:
- image centre (x,y) and tilts (xt,yt)
- sample-CCD distance

χ^2 = 3.7
Rw = 18.5 %

Imperfect control of pearl symmetry:
- volume/absorption corrections
- center of rotation
- Biso compensation

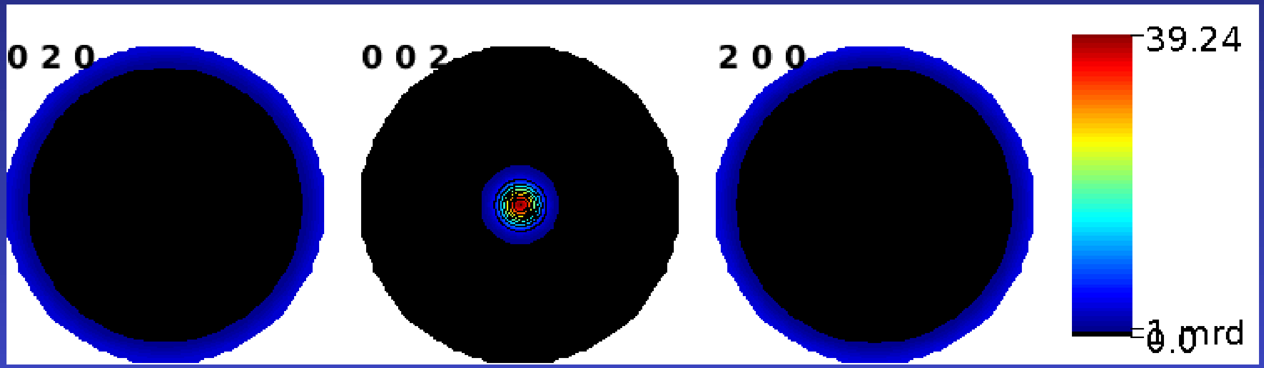

INEL

1h fit
1.5 Gb RAM

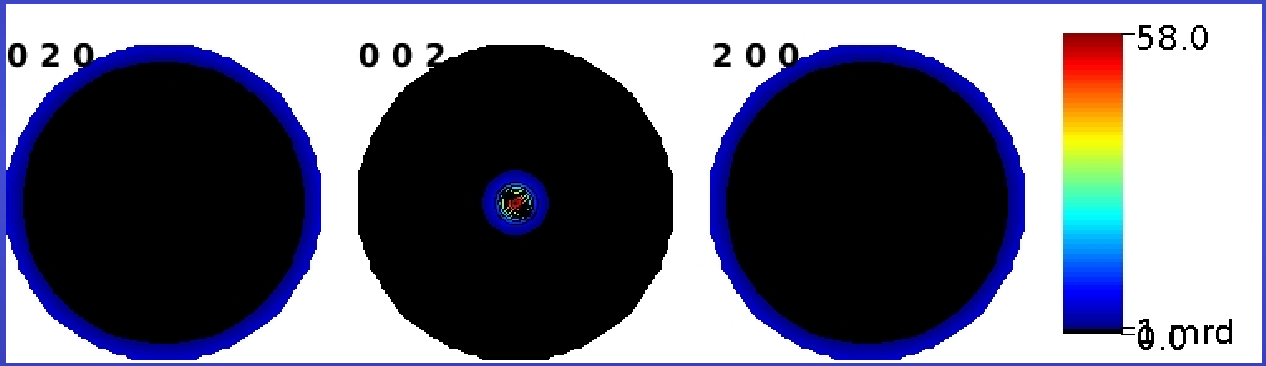

Bruker

5h fit
13 Gb RAM
4 cores
8 thread
parallelised

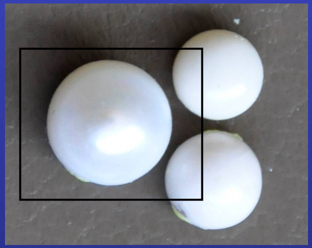

a = 5.049(3) Å
b = 8.324(6) Å
c = 5.592(4) Å

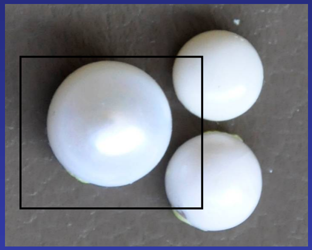

equator

$\chi^2 = 1.05$
Rw = 59.2 %

a = 4.9785(2) Å
b = 7.9801(3) Å
c = 5.7258(2) Å

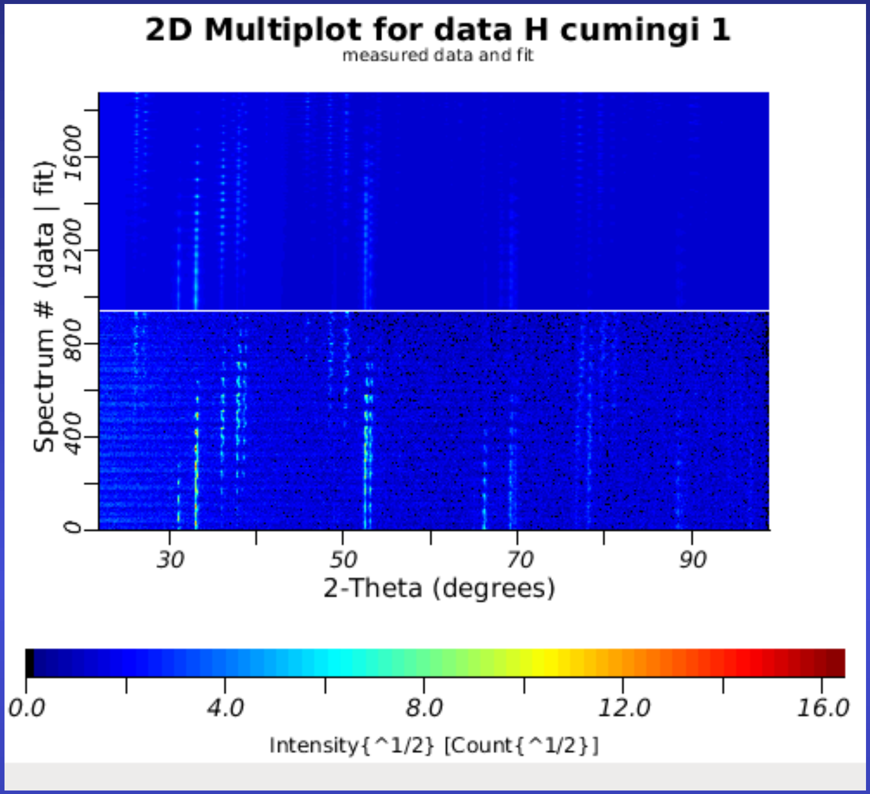

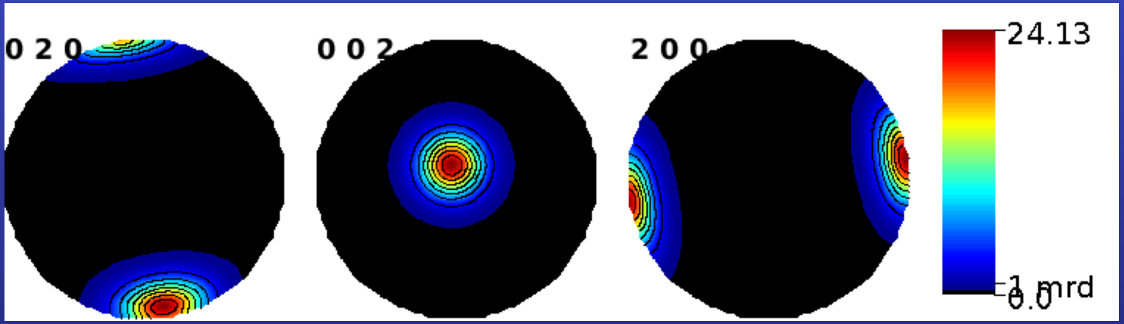

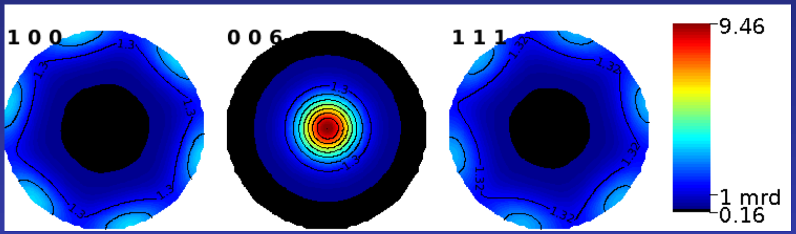

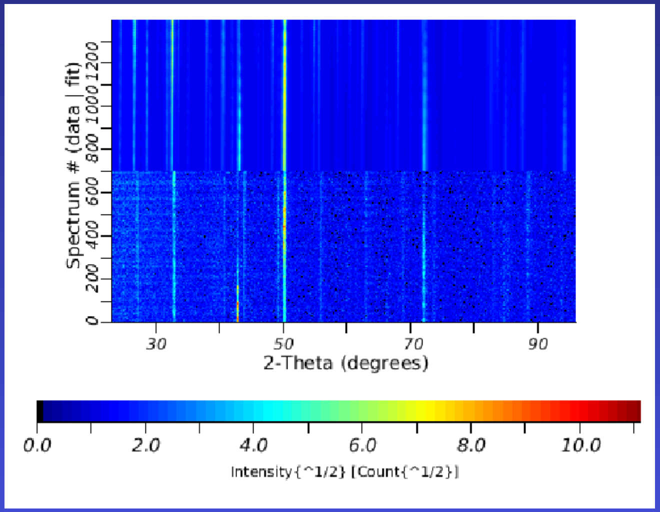

$P6_3/mmc$
Ama2
C2/c
C-1

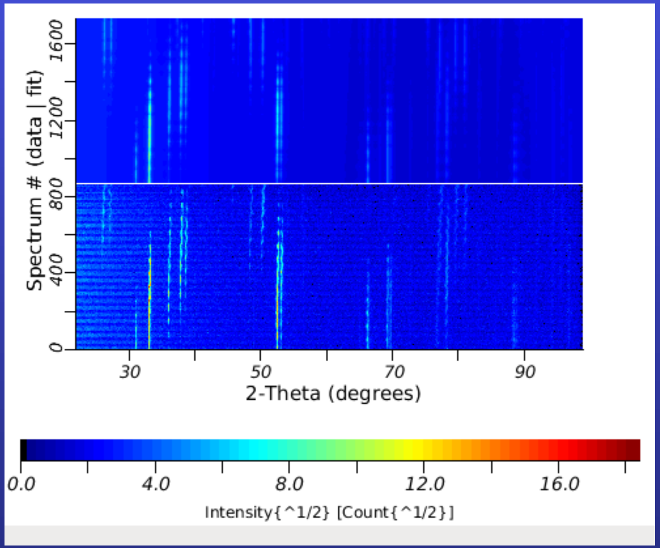

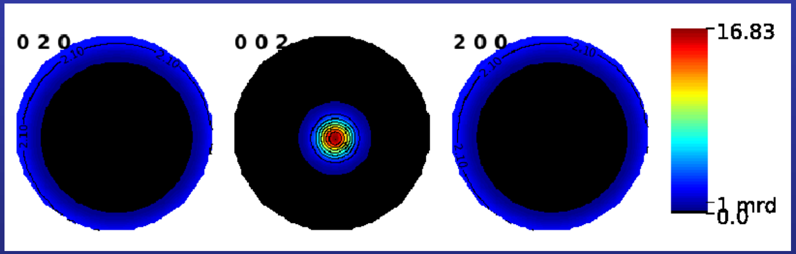

EDP

Intensity-spectra extraction

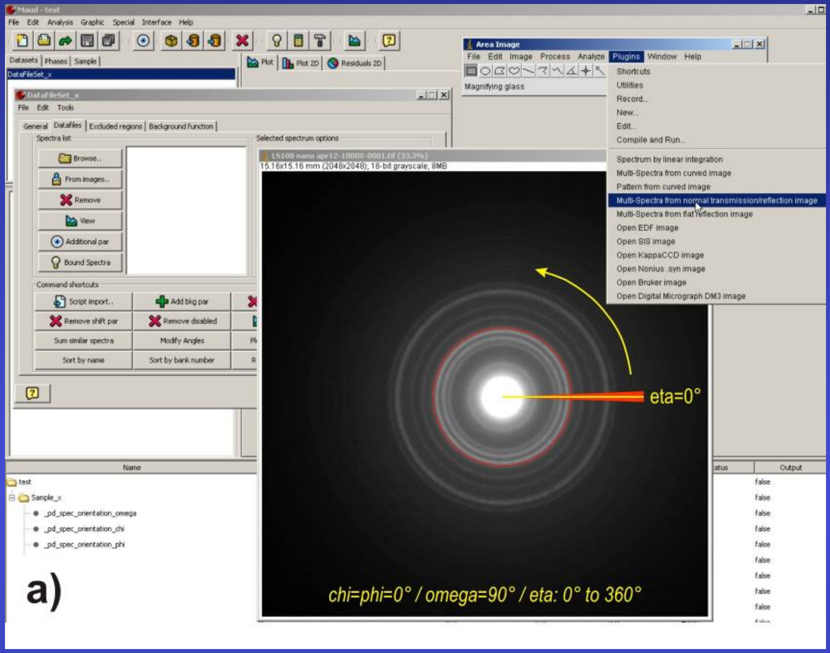

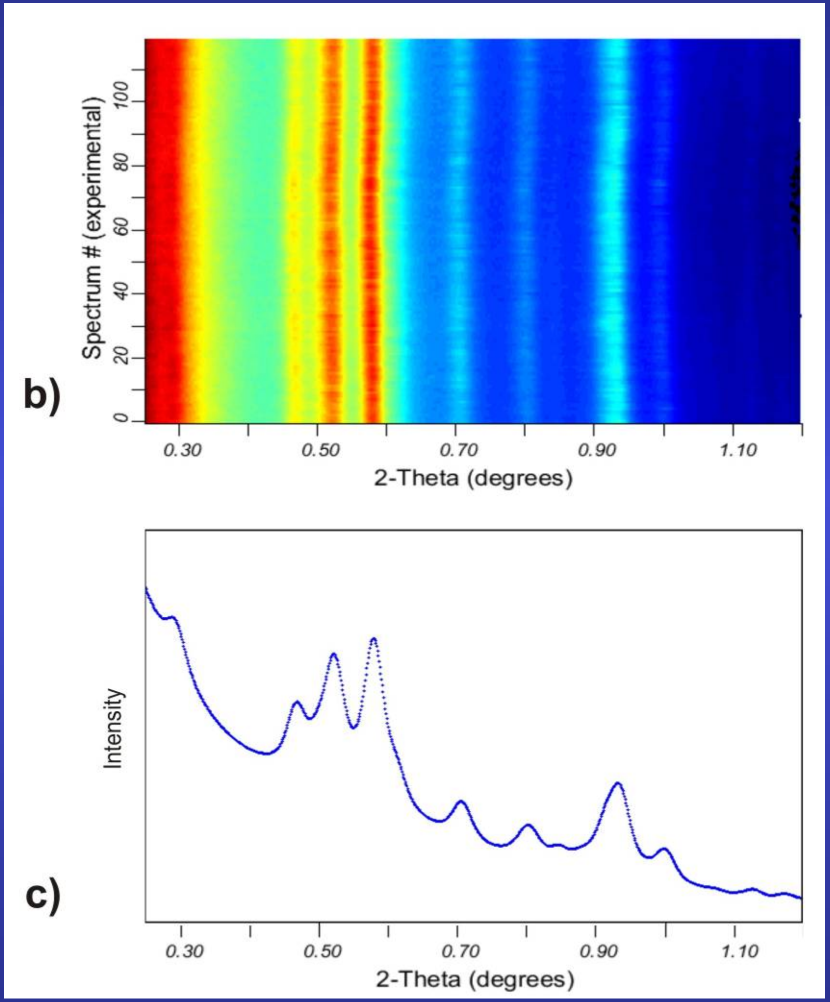

EDP: Microstructure of nanocrystalline materials: TiO2 rutile

► *quantitative analysis of electron diffraction ring pattern ?*

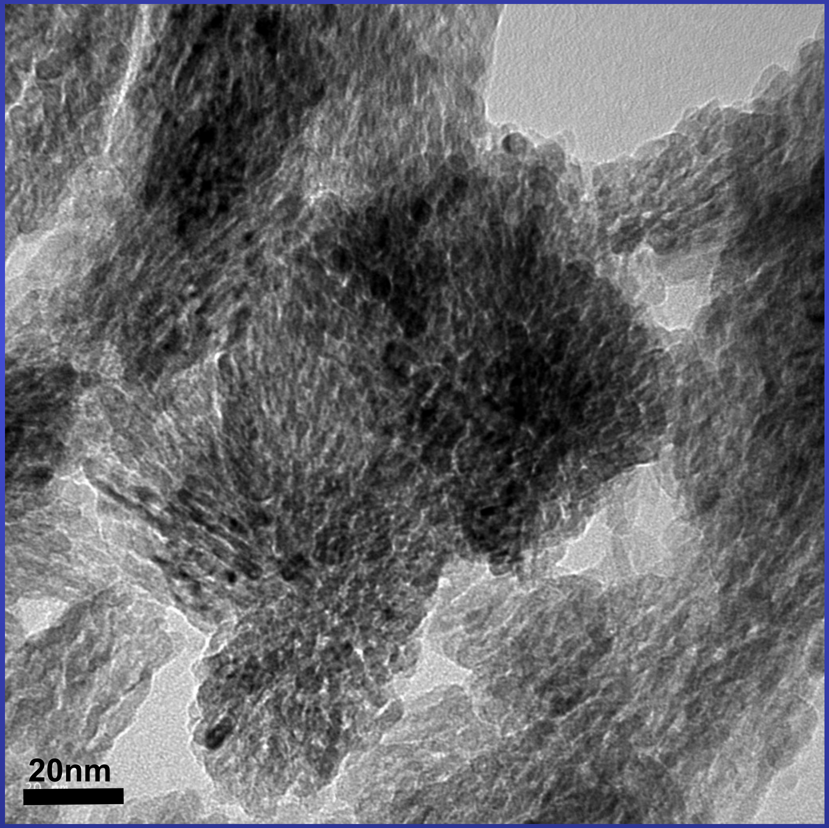

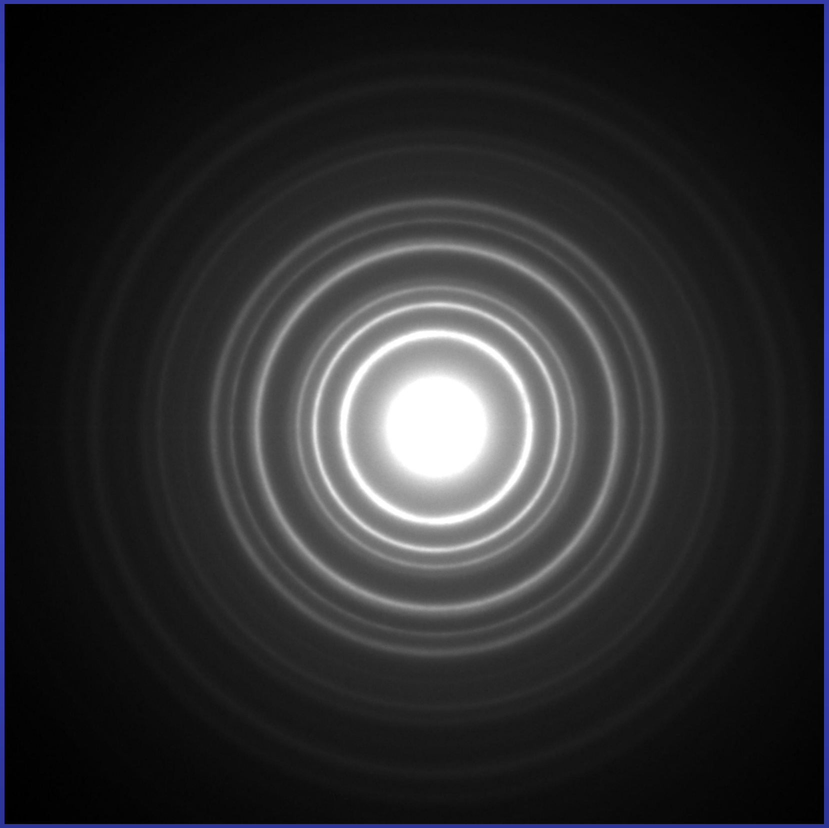

FEI Tecnai G2 (300kV) with an Ultrascan 1000 (2048x2048 14µm pixels)

Paterns taken from +25° to -25° (step 5°) tilts: thin film prepared for TEM plan view

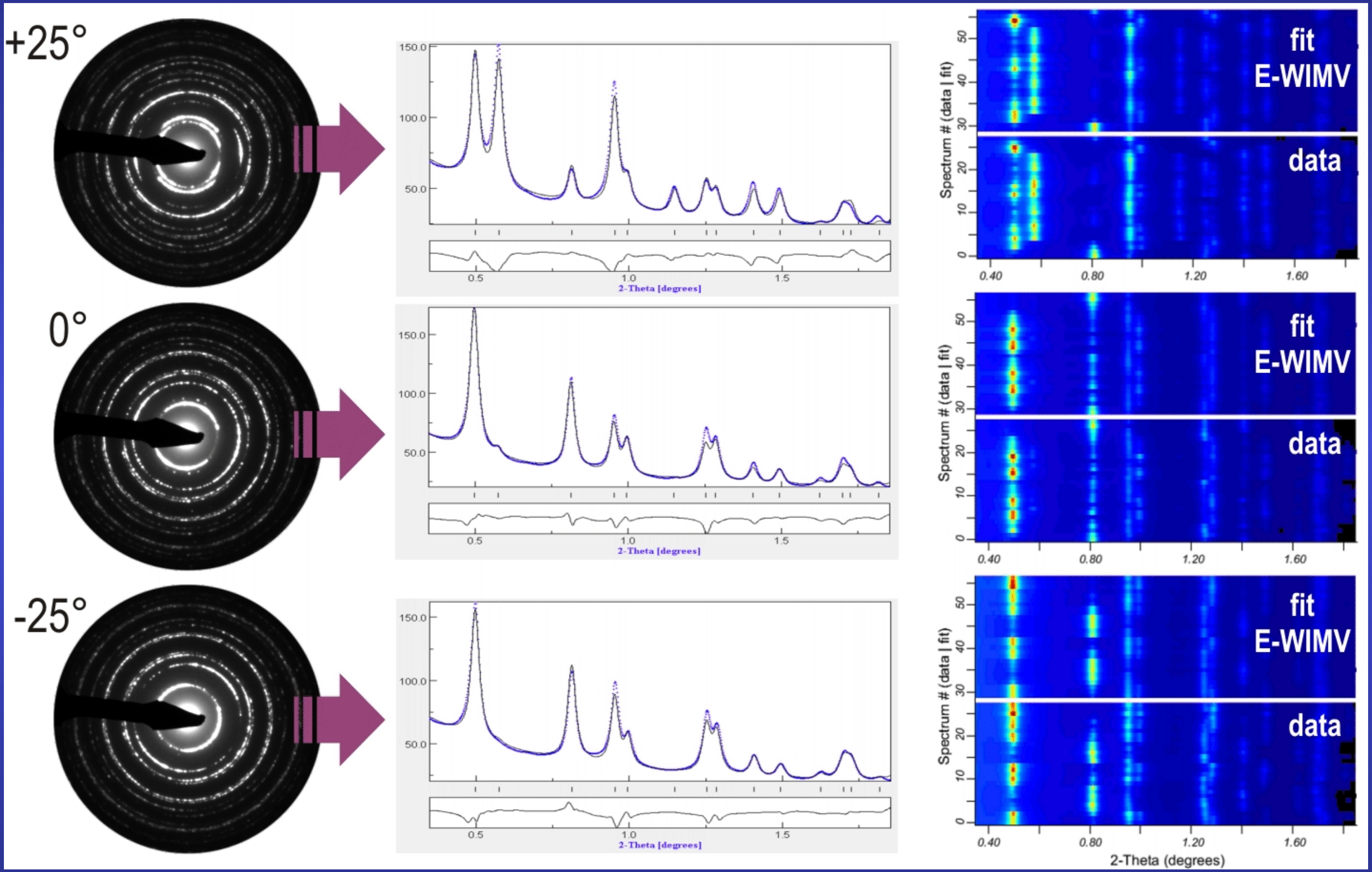

3 out of 11 EPD, 1D and 2D plots. Pattern matching (Pawley)

Pawley pattern matching

EWIMV Fiber component

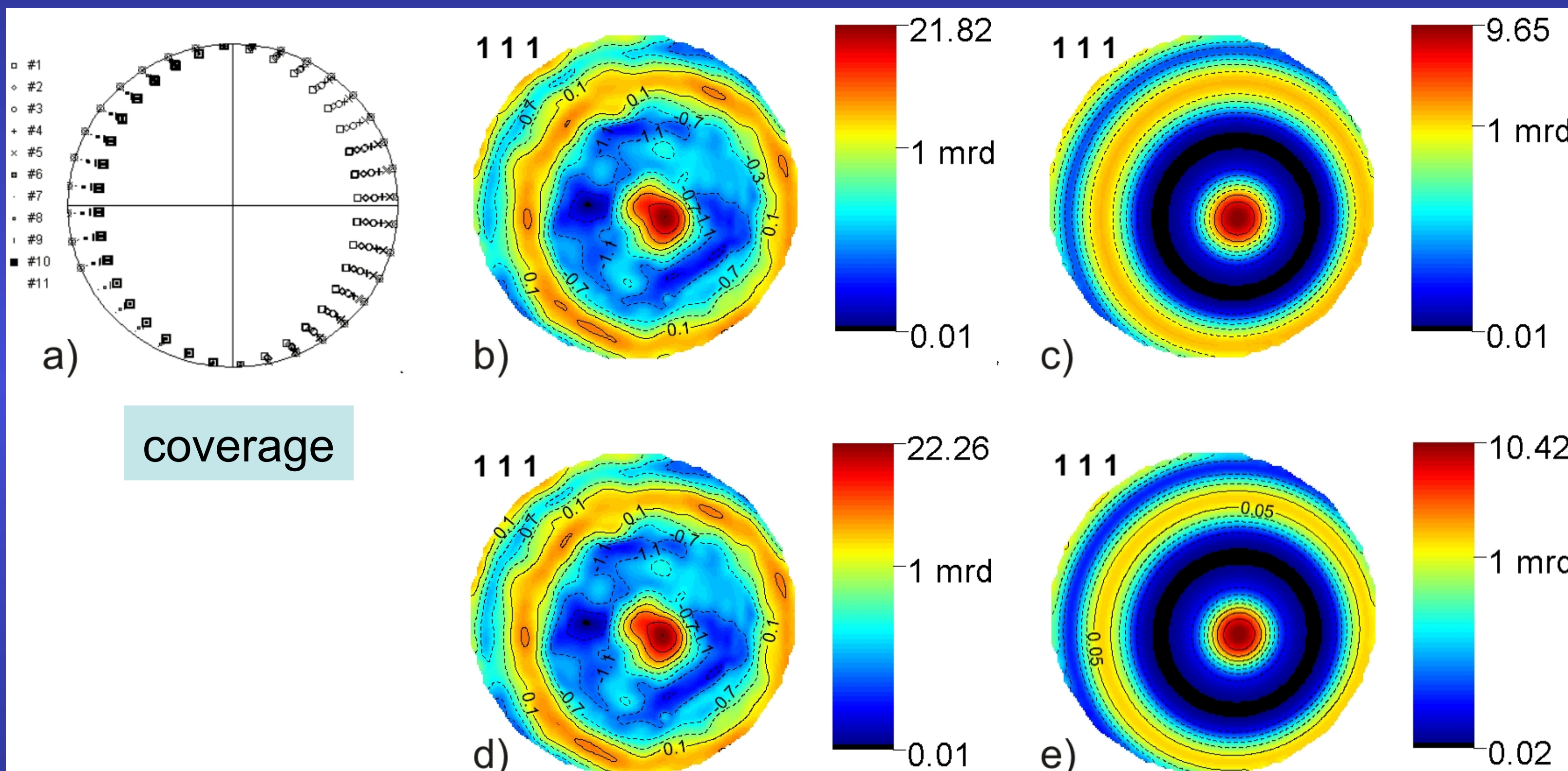

EWIMV Fiber component

2-beams dynamical (Blackman)

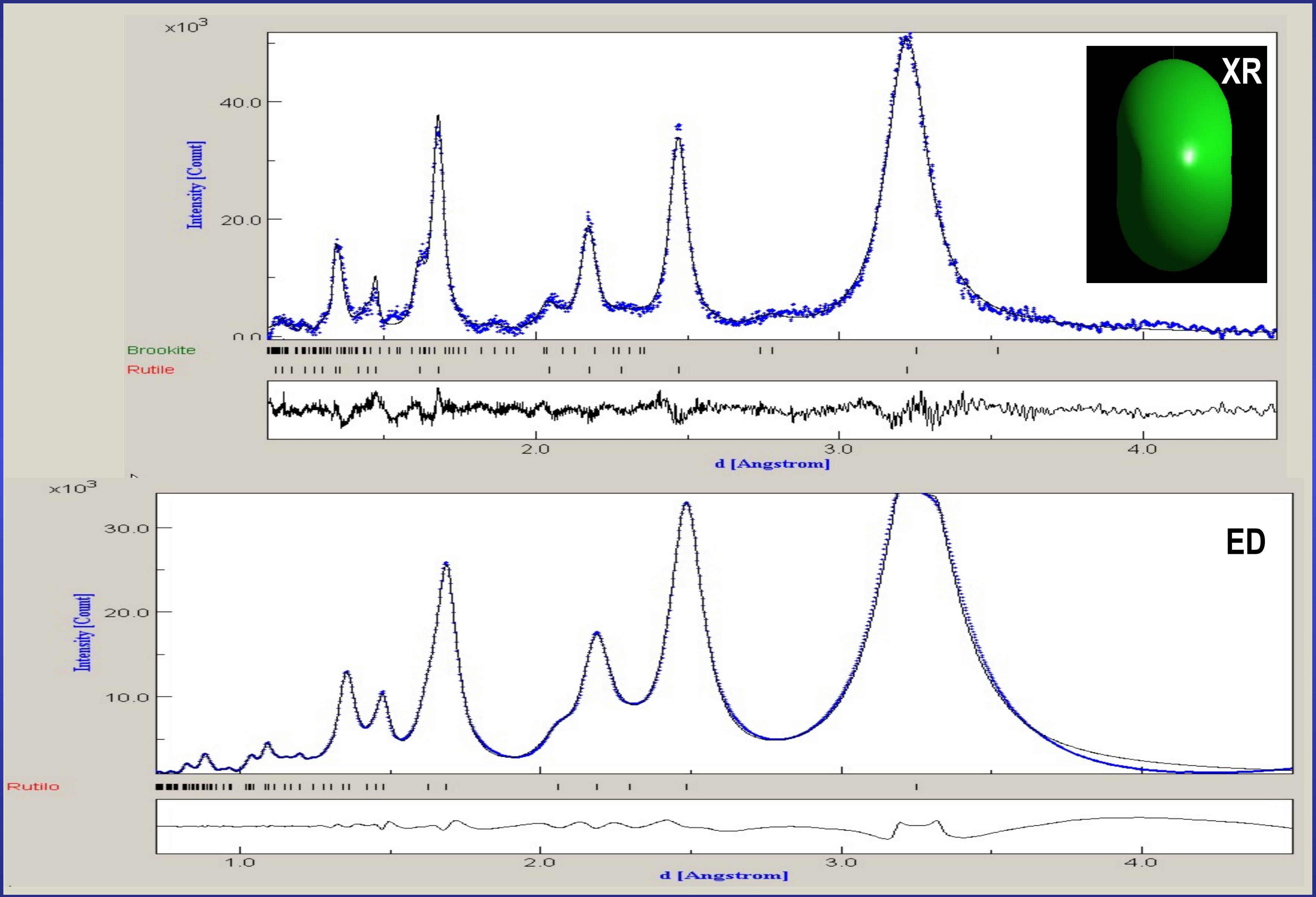

x10^3
40.0
20.0
0.0
Intensity [Count]
XR
Brookite
Rutile
2.0
3.0
4.0
d [Angstrom]
x10^3
30.0
20.0
10.0
Intensity [Count]
ED
Rutilo
1.0
2.0
3.0
4.0
d [Angstrom]

Line broadening: anisotropic sizes

Mn_3O_4 nanopowders (polyol process)

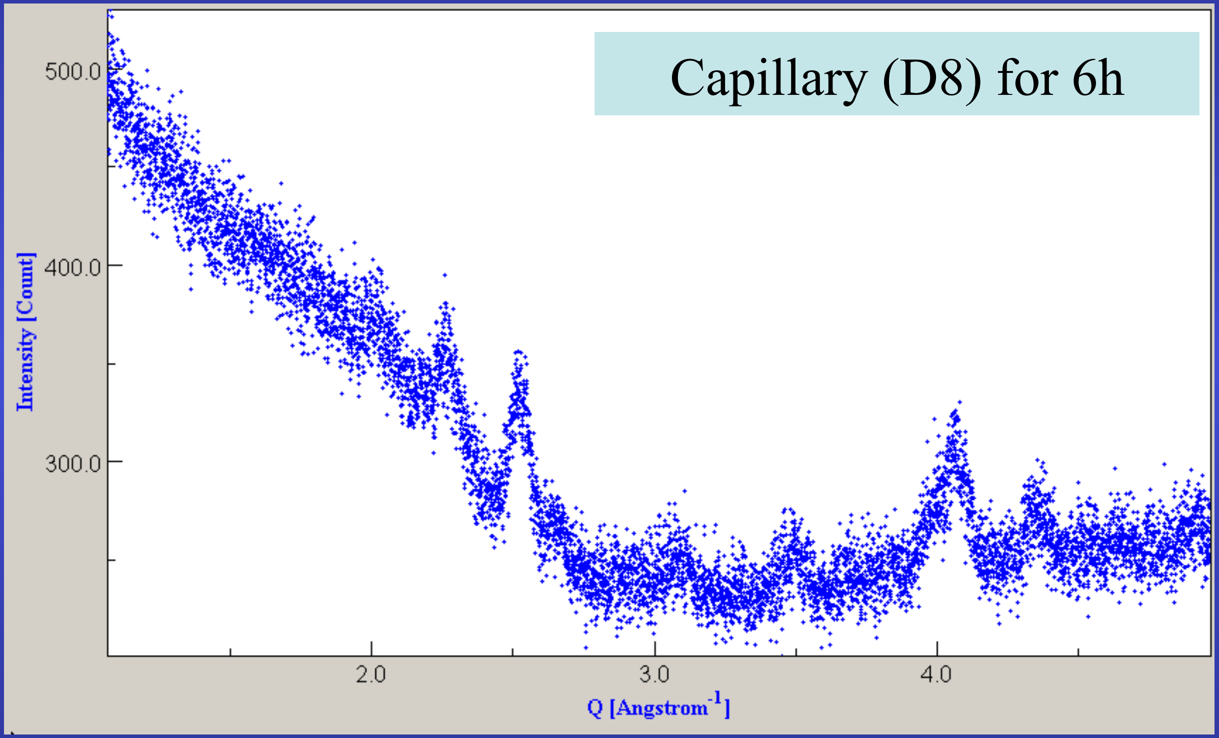

Reflection for 3h (100mg)

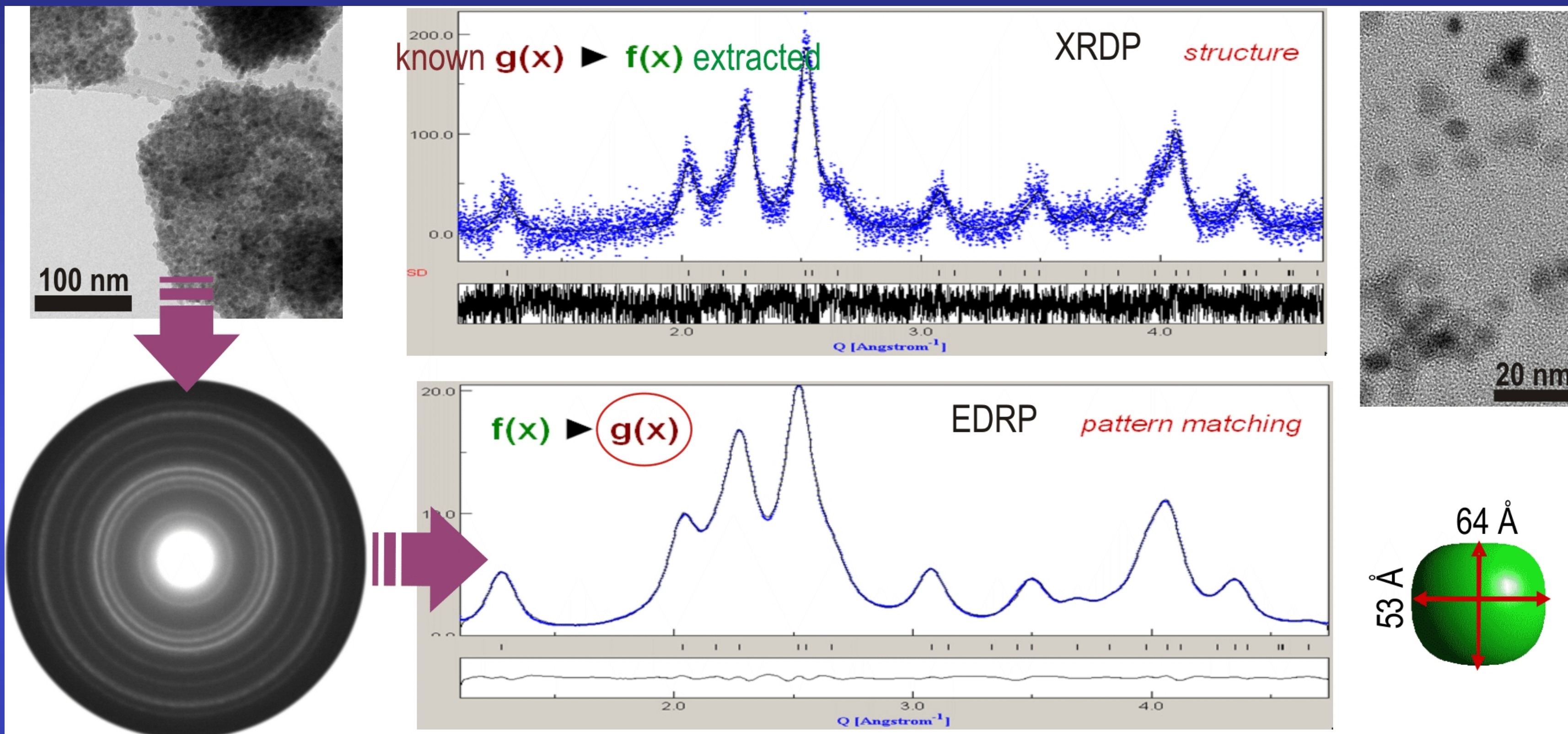

TEM in seconds (few μg)

$$\langle R_h \rangle = R_0 + R_1 P_2^0(x) + R_2 P_2^1(x)\cos\varphi + R_3 P_2^1(x)\sin\varphi + R_4 P_2^2(x)\cos 2\varphi + R_5 P_2^2(x)\sin 2\varphi + \ldots$$

TiO_2 nanopowders

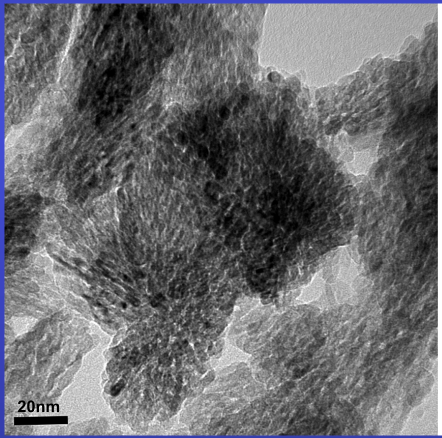

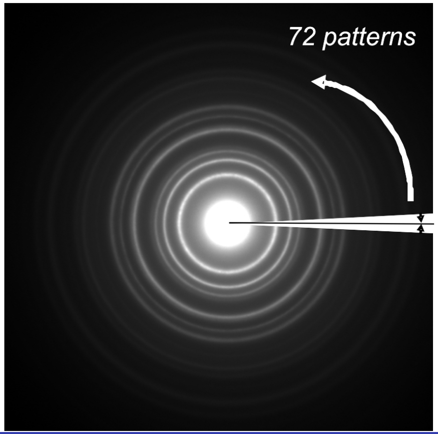

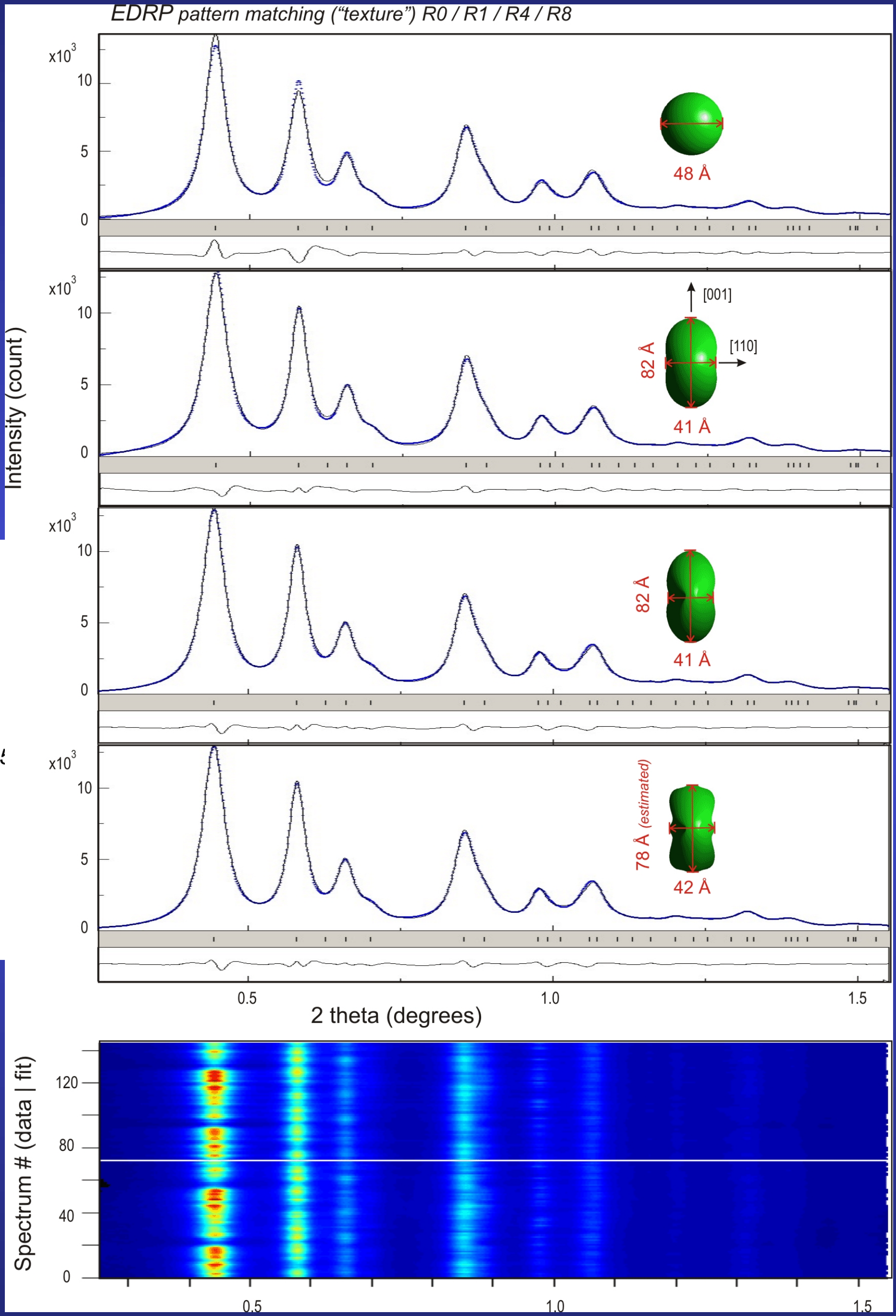

Popa $R_0 + R_1$

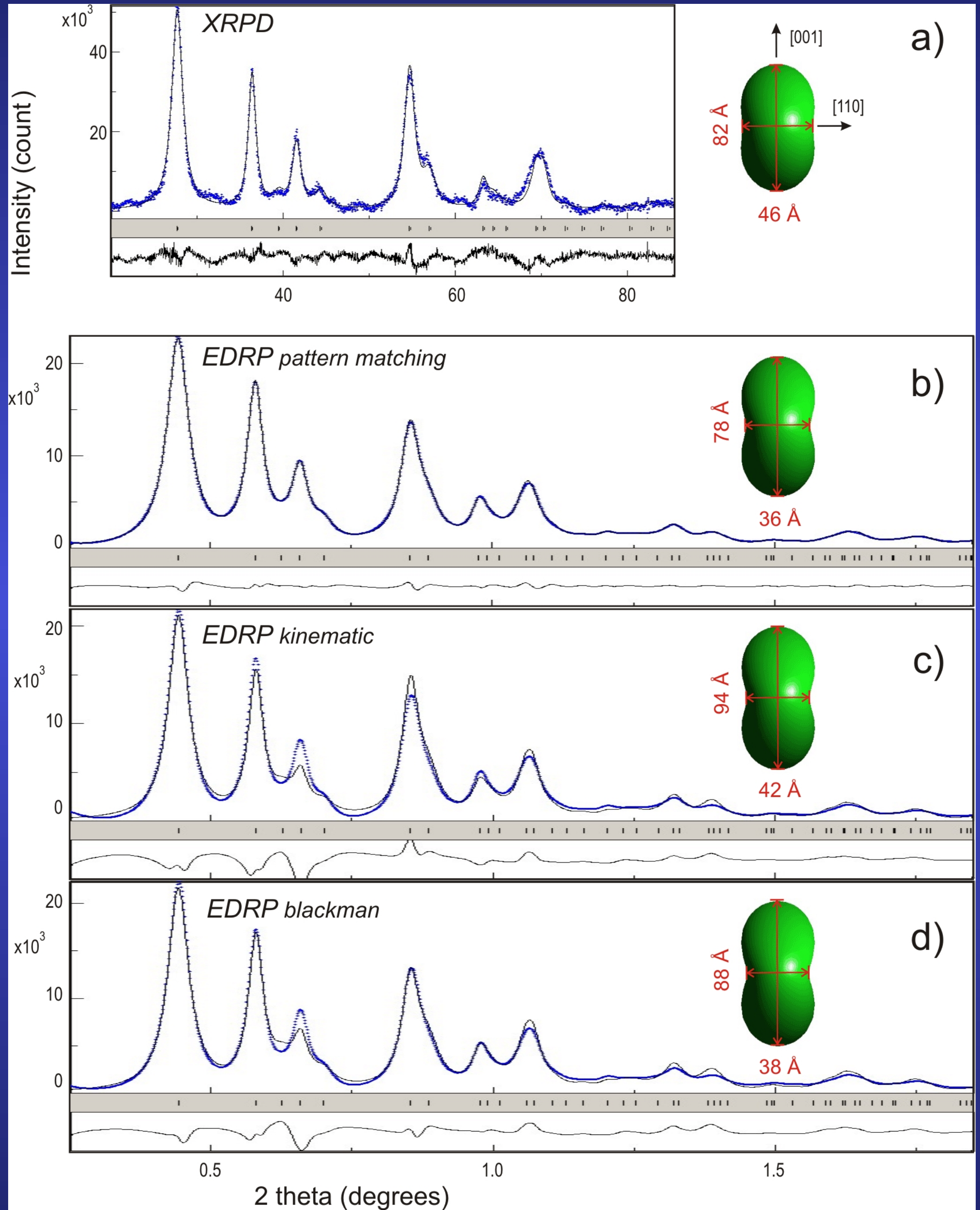

XRPD
EDRP pattern matching
EDRP kinematic
EDRP blackman
a)
b)
c)
d)
[001]
[110]
82 Å
46 Å
78 Å
36 Å
94 Å
42 Å
88 Å
38 Å
Intensity (count)
2 theta (degrees)

Popa up to R_4

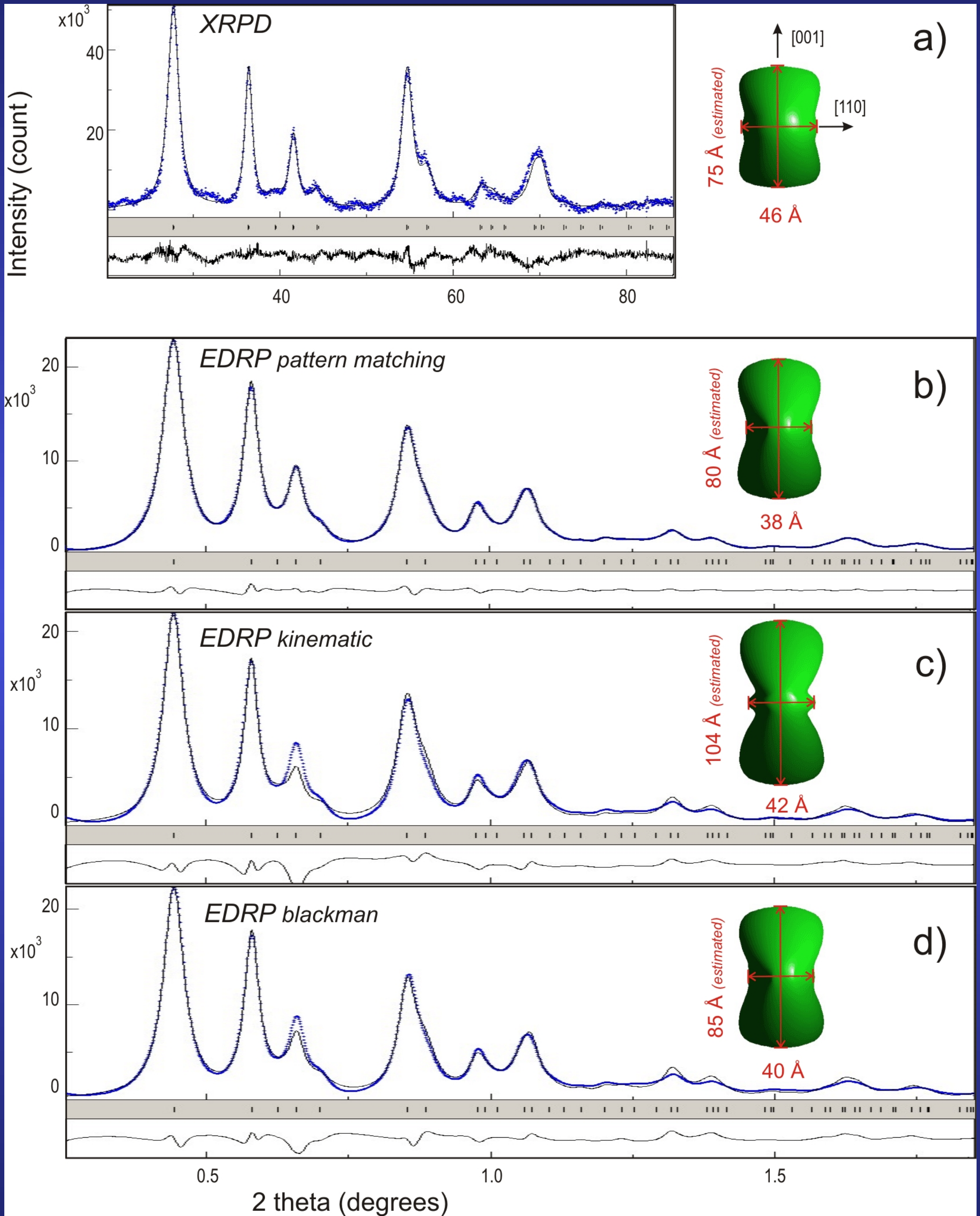

x10^3
40
20
XRPD
Intensity (count)
40
60
80
a)
[001]
[110]
75 Å (estimated)
46 Å
EDRP pattern matching
20
x10^3
10
0
b)
80 Å (estimated)
38 Å
EDRP kinematic
c)
104 Å (estimated)
42 Å
EDRP blackman
d)
85 Å (estimated)
40 Å
0.5
1.0
1.5
2 theta (degrees)

QTA: local vs global

Pt thin film on Si

a) 6 µm diameter selected area, b) EPD and c) 2D plot.

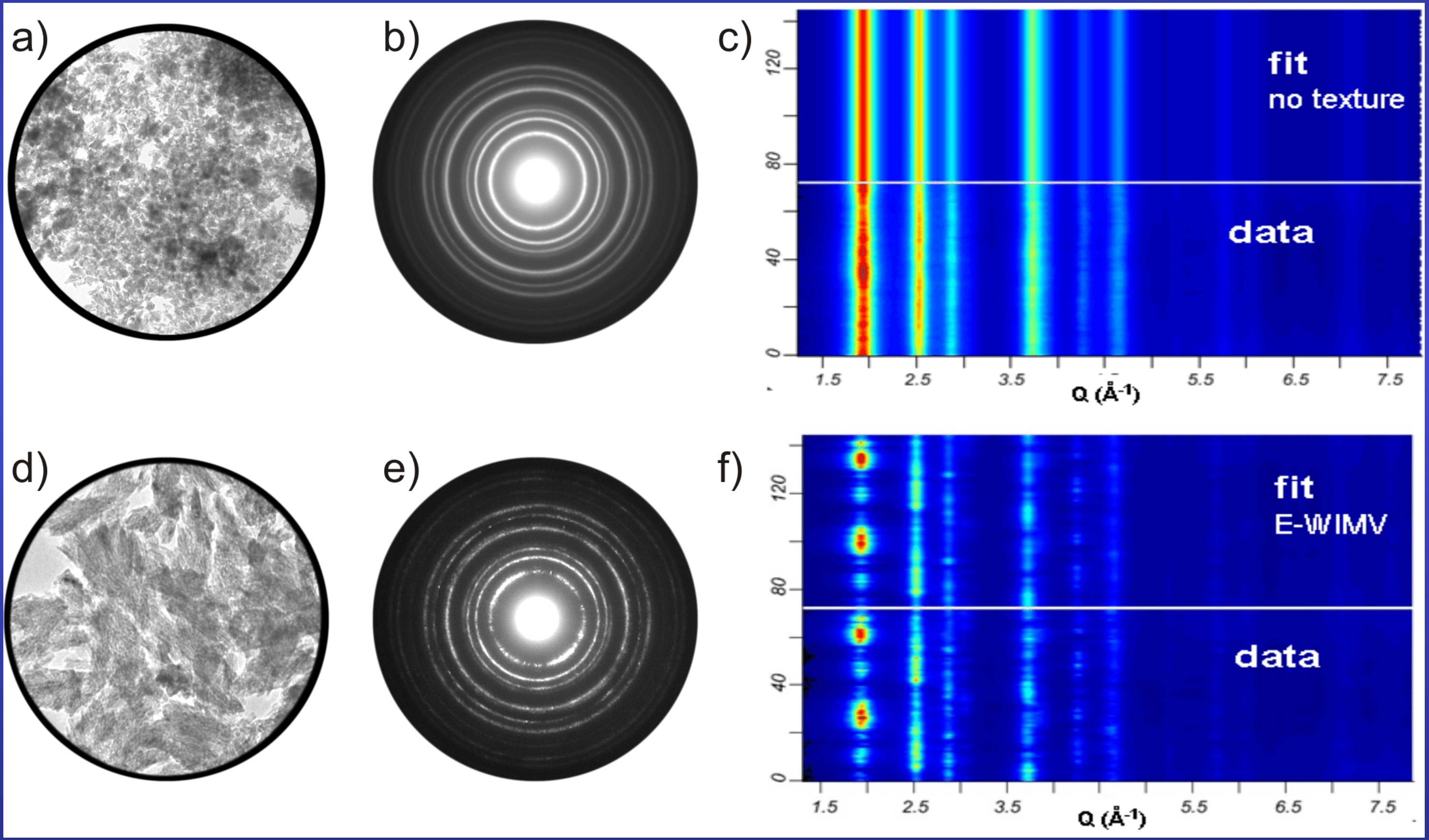

d) 0.5 µm diameter selected area, e) EPD and f) 2D plot

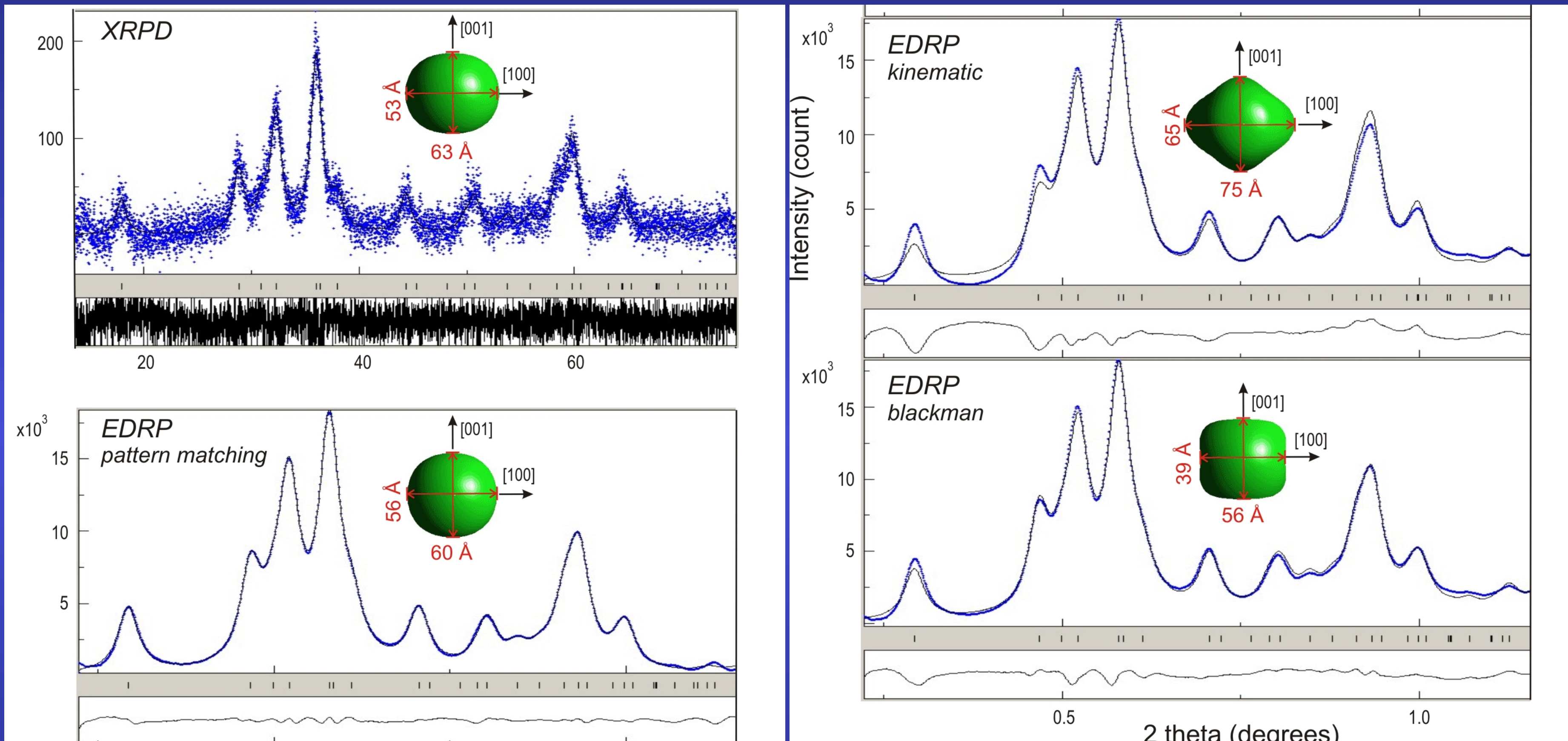

XRPD
[001]
[100]
53 Å
63 Å
200
100
20
40
60
EDRP
pattern matching
x10³
15
10
5
56 Å
60 Å
EDRP
kinematic
65 Å
75 Å
Intensity (count)
EDRP
blackman
39 Å
56 Å
0.5
1.0
2 theta (degrees)

BULKS

Bi-2212

Bi2212 + Secondary phases ⟶ Bi2223

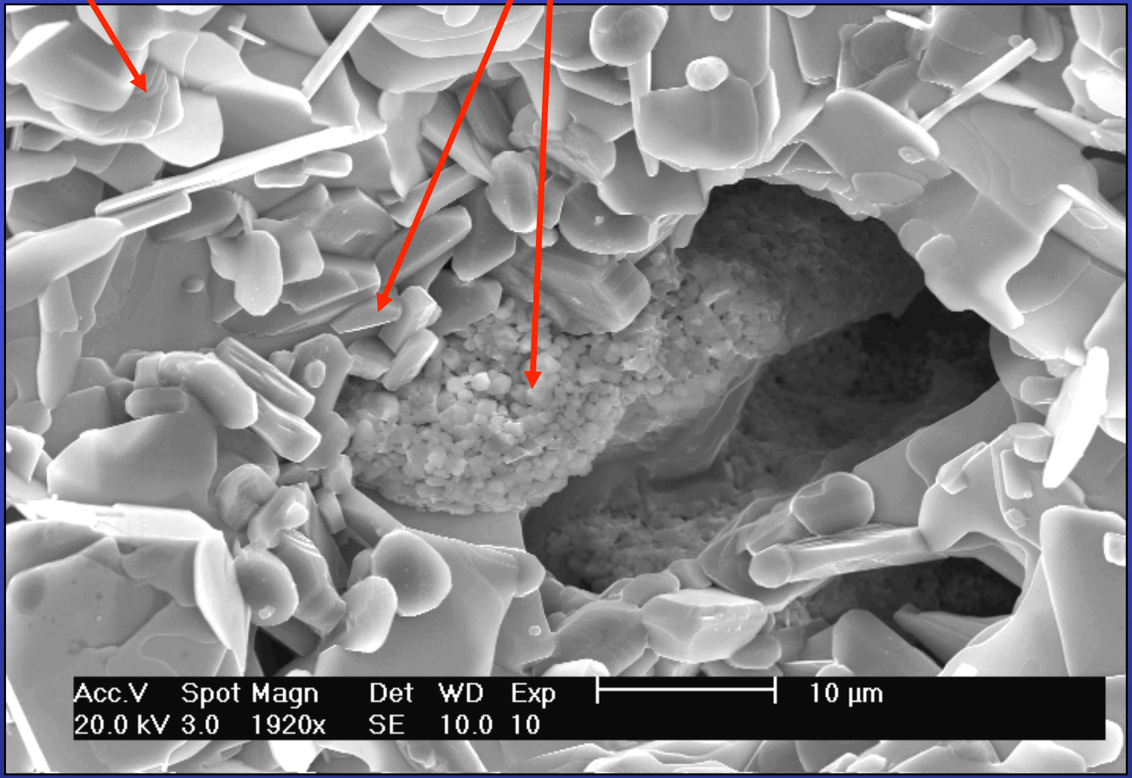

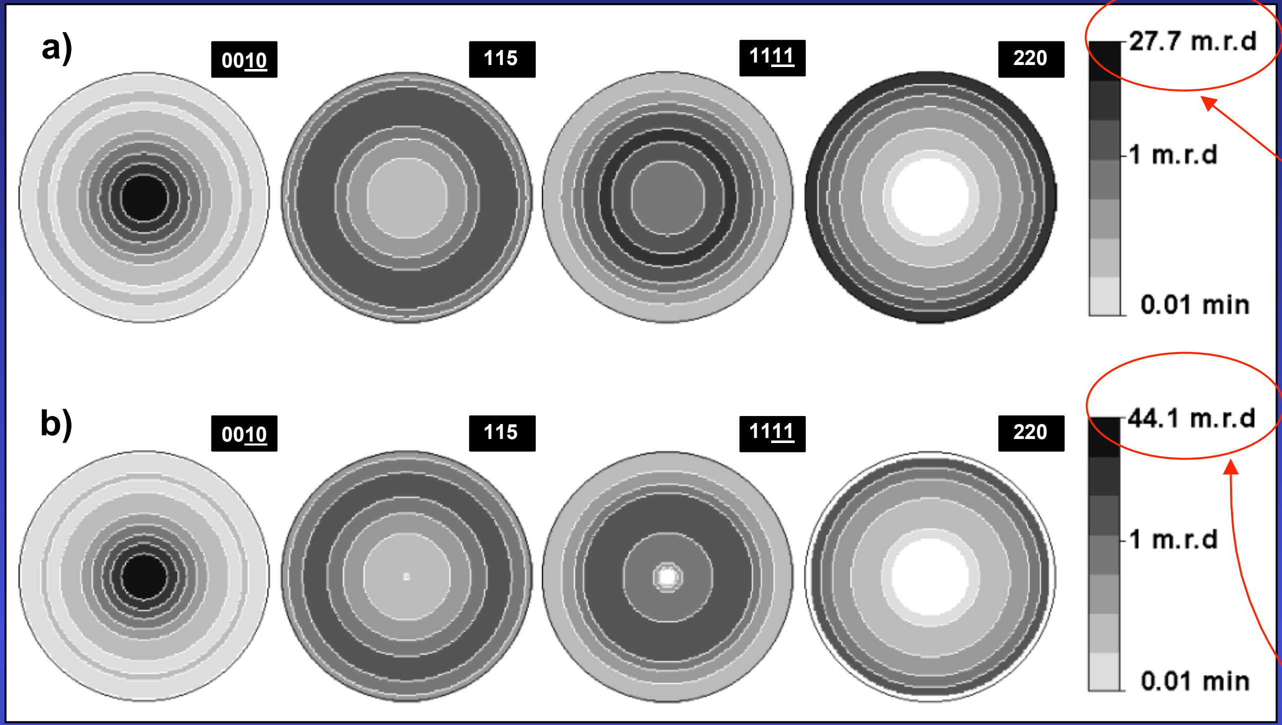

Recalculated (WIMV)

Extracted (Le Bail)

Logarithmic density scale, equal area projection

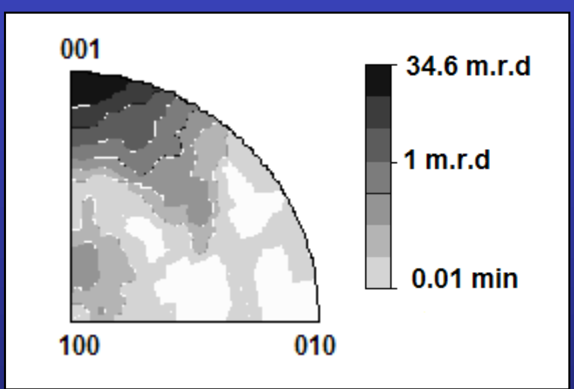

Logarithmic density scale, equal area projection

Stacking faults and/or intergrowth on the c-axis →New periodicities and peaks characterized with intermediate c parameters.

However, no algorithm is included to solve intergrowths in the combined approach.

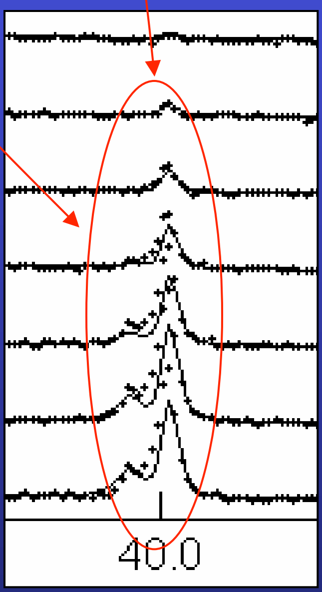

Bi2223 compounds

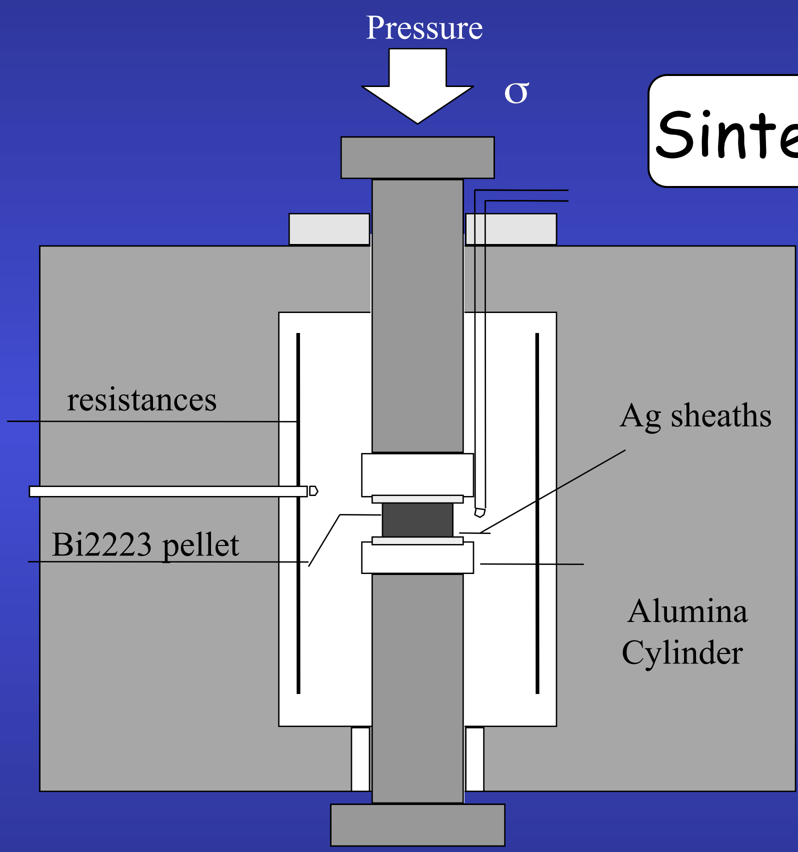

Sinter-Forging

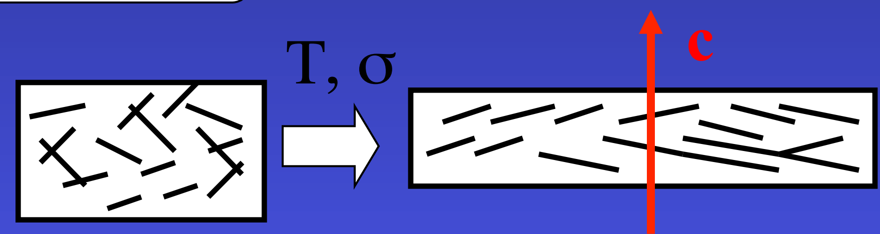

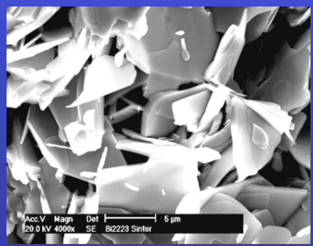

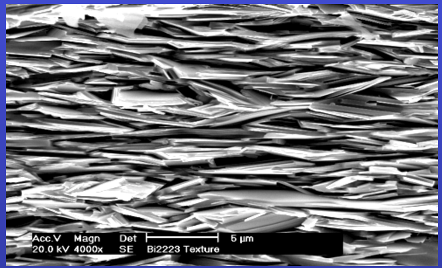

Grain alignment ⇒ ↗ Jc

(00ℓ) Texture

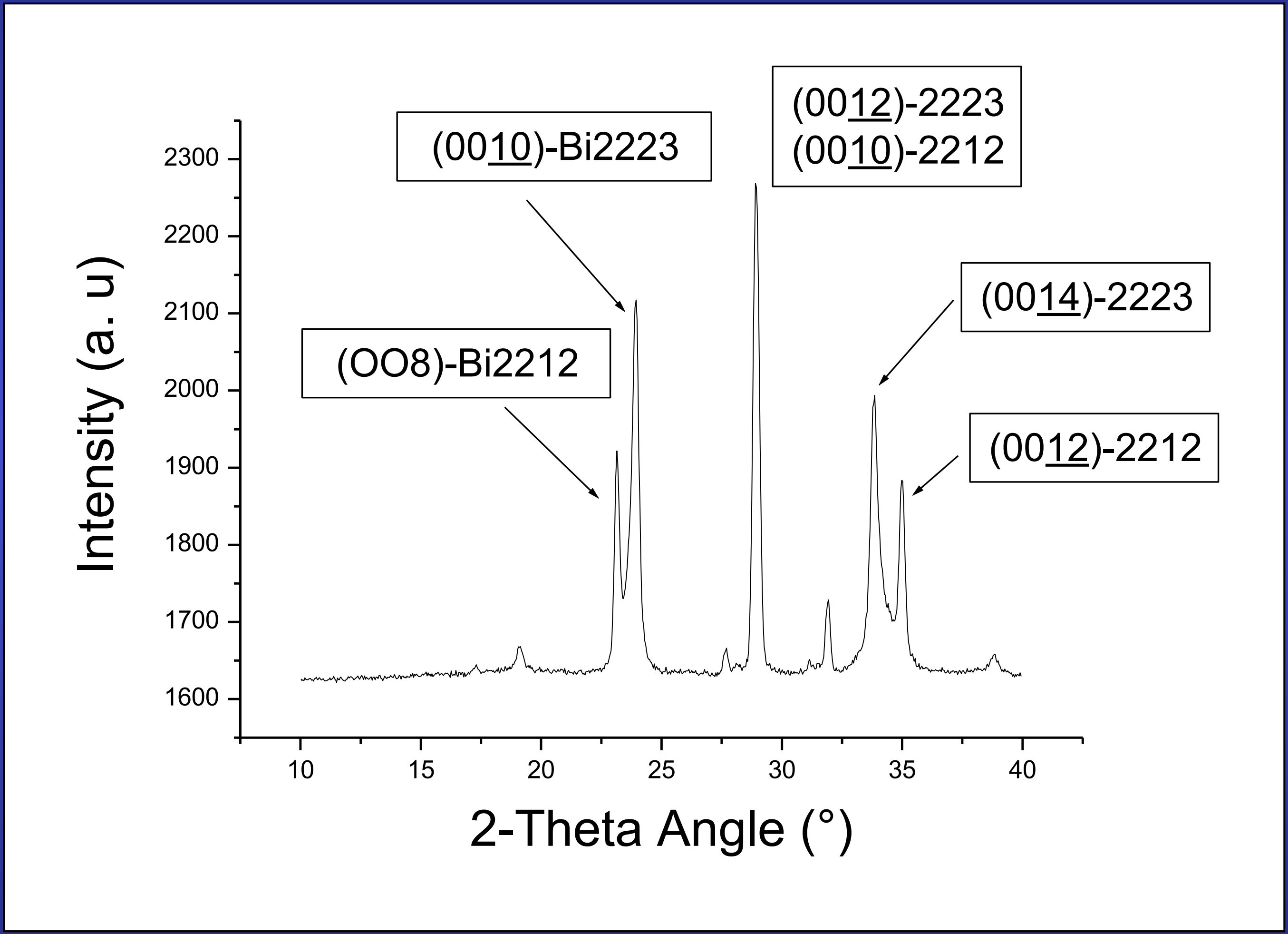

(0010)-Bi2223
(0012)-2223
(0010)-2212
(0014)-2223
(OO8)-Bi2212
(0012)-2212
Intensity (a. u)
2300
2200
2100
2000
1900
1800
1700
1600
10
15
20
25
30
35
40
2-Theta Angle (°)

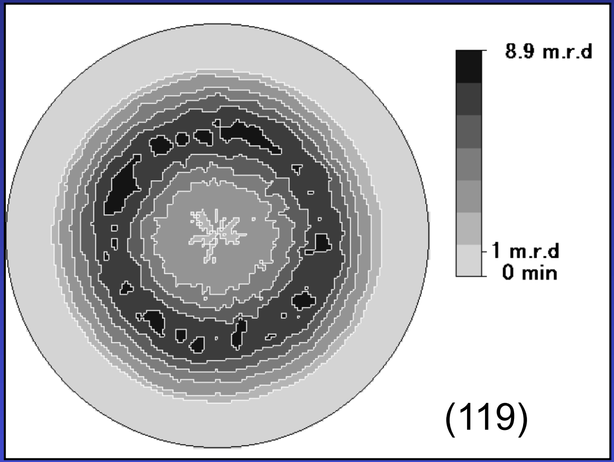

Combined Analysis

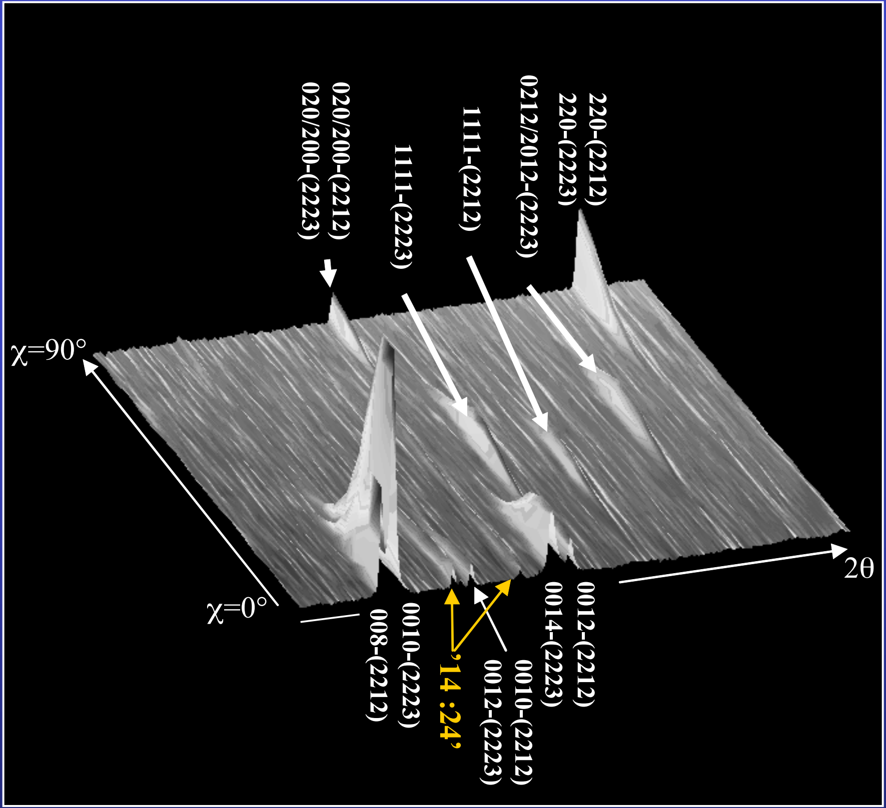

- *Neutrons*
- Sample: ~70 mm^3
- 2θ patterns for χ=0° to 90°
- No φ rotation (fibre texture).

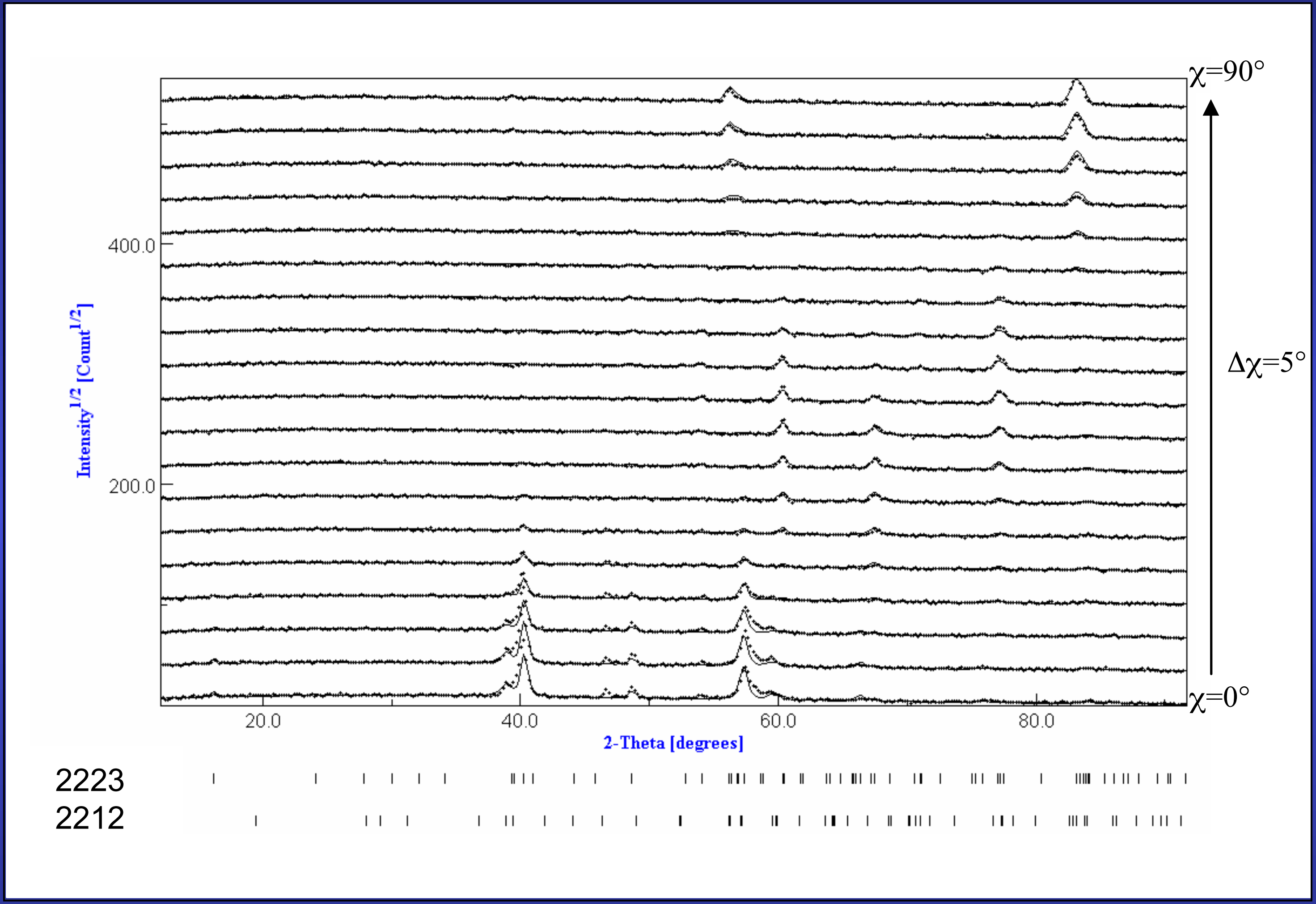

Rw=9.12
RP=16.24

Effect of the sinter-forging treatment on the texture development, crystal growth, transport properties

Sinter-forging dwell time (h)	*Orientation Distribution Max (m.r.d.)*		*% Bi2223*	*Cell parameters (Å)*		*Crystallite size Bi2223 (nm)*	*Rb (%)*	*Rw (%)*	*Rexp (%)*	*RP0 (%)*	*RP1 (%)*	*J_c (A/cm^2)*
	Bi2212	*Bi2223*		*Bi2223*	*Bi2212*							
20	21.8	20.7	59.9±1.3	a=5.419(3) b=5.391(3) c=37.168(3)	a=5.414(3) b=5.393(3) c=30.800(3)	205±7	7.56	11.1	4.55	17.74	10.56	12500
50	24.1	24.4	72.9±2.9	a=5.419(3) b=5.408(3) c=37.192(3)	a=5.416(3) b=5.396(3) c=30.806(3)	273±10	7.54	11.37	4.58	17.05	11.04	15000
100	31.5	25.2	84.4±4.6	a=5.410(3) b=5.405(3) c=37.144(3)	a=5.412(3) b=5.403(3) c=30.752(3)	303±10	5.4	8.04	3.69	13.54	9.31	19000
150	65.4	27.2	87.0±4.1	a=5.417(3) b=5.403(3) c=37.199(3)	a=5.413(3) b=5.407(3) c=30.792(3)	383±13	6.13	9.12	4.8	16.24	12.25	20000

↗ Texture strength

↗ *Sinter-forging Time* ⇒ ↗ % Bi2223 ⇔ ↗ J_c

↗ Crystallite Size

E. Guilmeau et al., JAC

FILMS

AlN/Pt/TiO_x/Al_2O_3/Ni-Co-Cr-Al

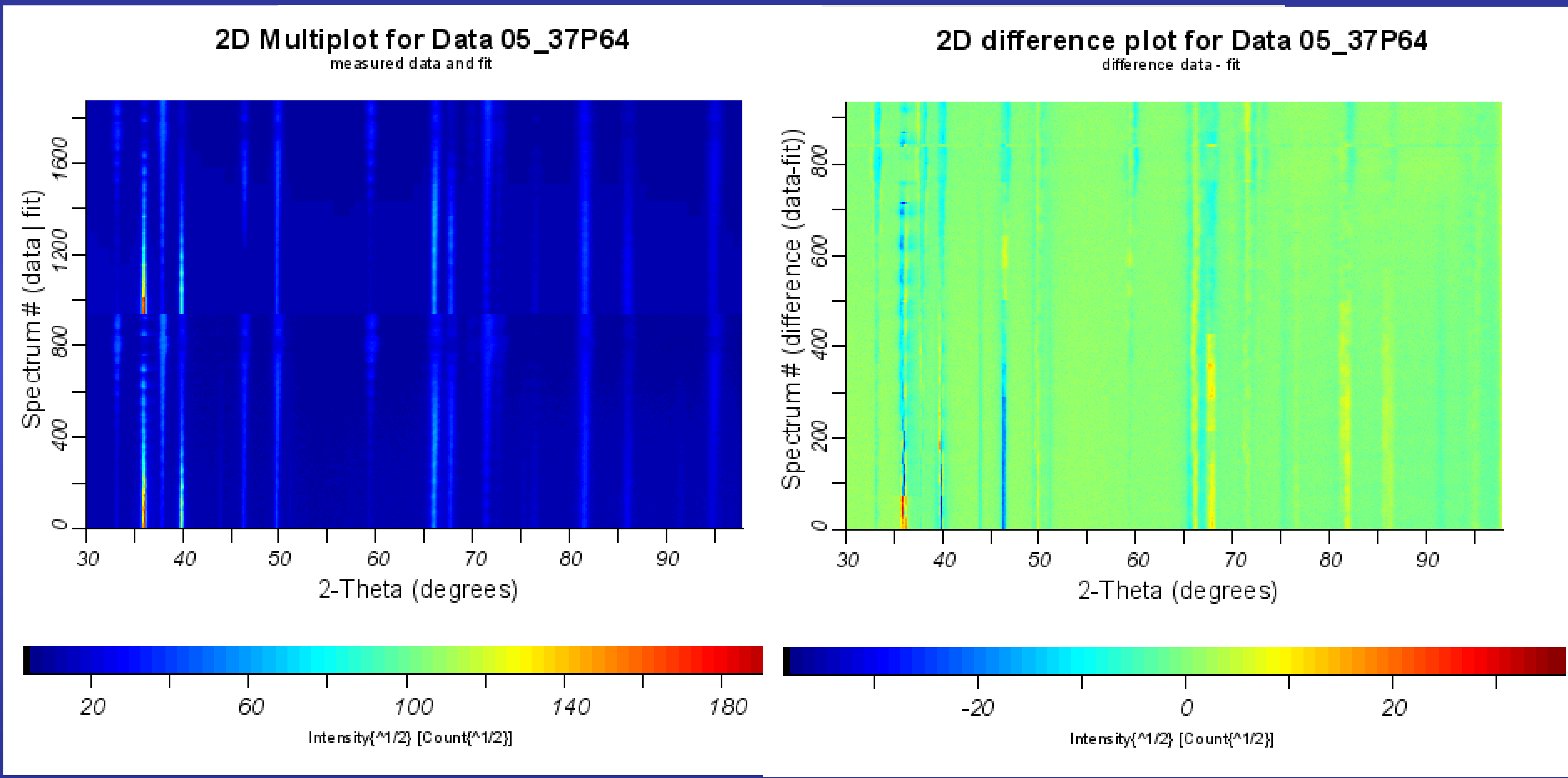

Rw (%) = 24.120445
Rexp (%) = 5.8517213

T(AlN) = 14270(3) nm
T(Pt) = 430(3) nm

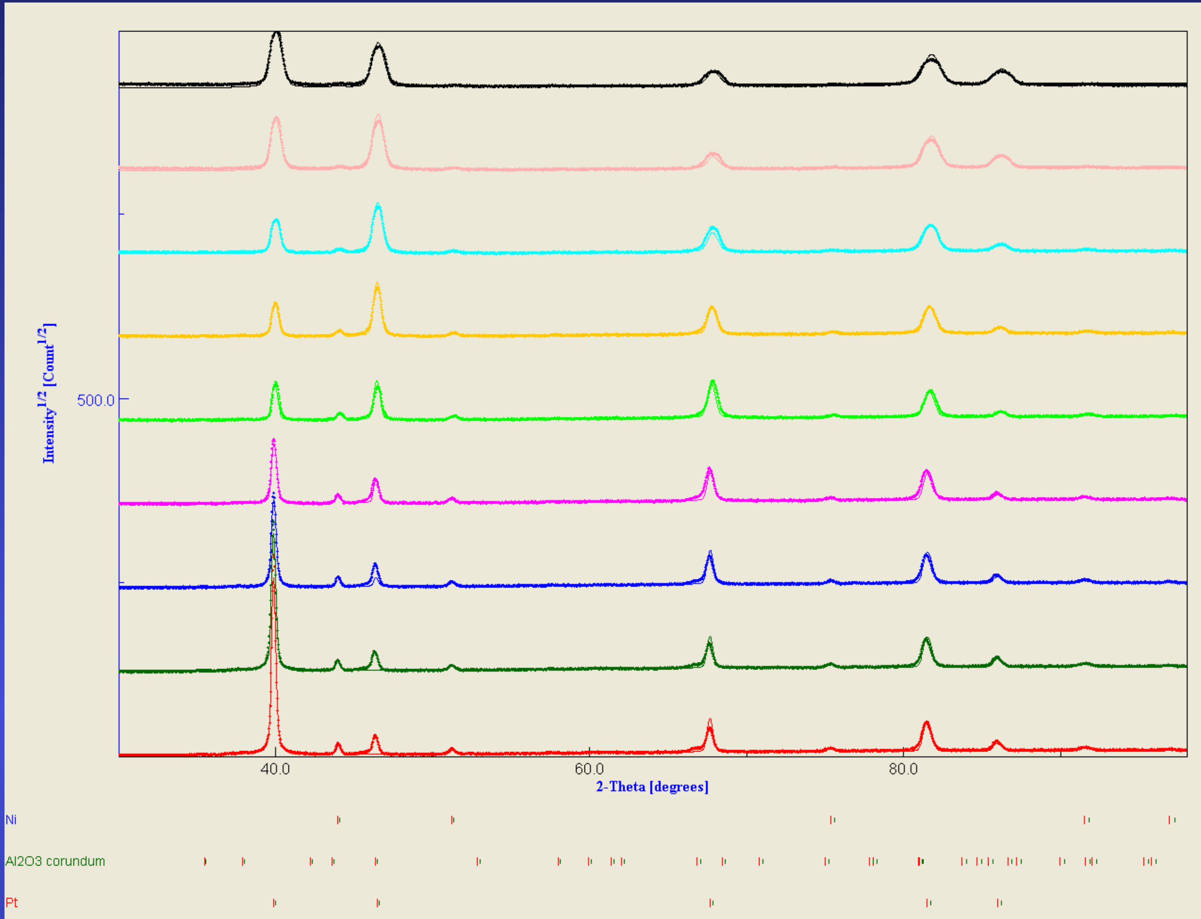

(χ,φ) randomly selected diagrams

Al_2O_3

a = 4.7562(6) Å
c = 12.875(3) Å
T= 7790(31) nm
<t> = 150(2) Å
<ε> = 0.008(3)

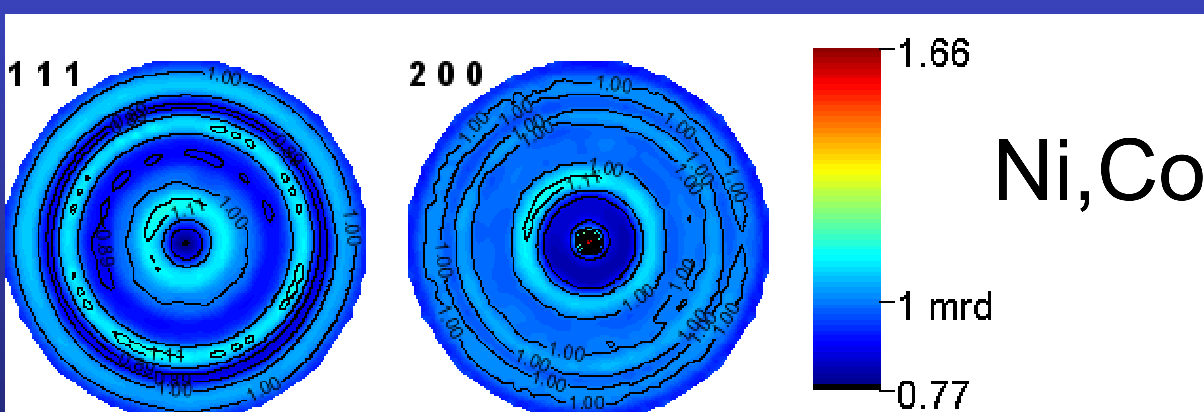

a = 3.569377(5) Å
<t> = 7600(1900) Å
<ε> = 0.00236(3)
σ_{11} = -328(8) MPa
σ_{22} = -411(9) MPa

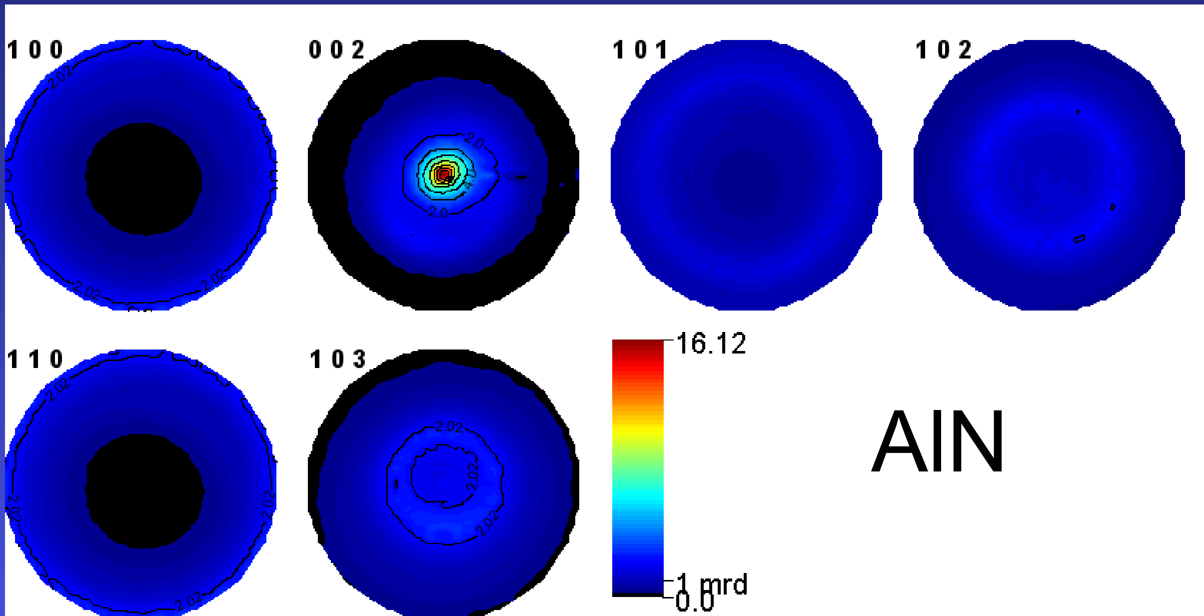

Rw (%) = 4.1

a = 3.11203(1) Å
c = 4.98252(1) Å
T = 14270(3) nm
<t> = 2404(8) Å
<ε> = 0.001853(2)
σ_{11} = -1019(2) MPa
σ_{22} = -845(2) MPa

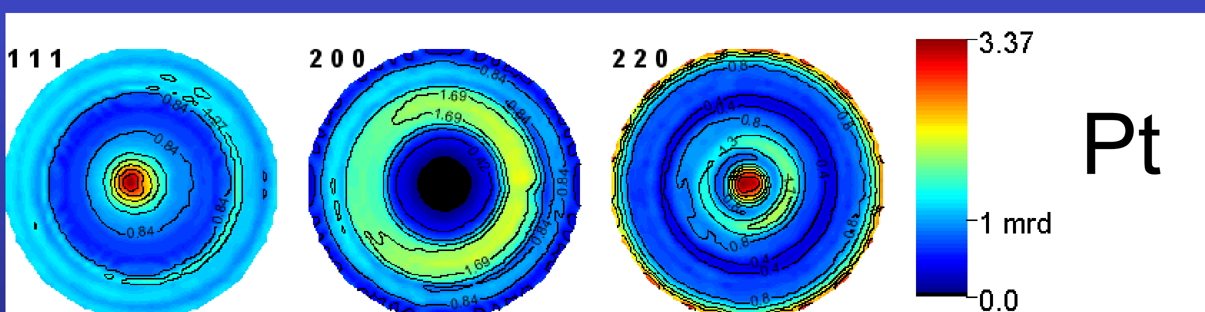

Rw (%) = 33.3

a = 3.91198(1) Å
T = 1204(3) nm
<t> = 2173(10) Å
<ε> = 0.002410(3)
σ_{11} = -196.5(8)
σ_{22} = -99.6(6)

Substrate bias vs stress-texture evolution

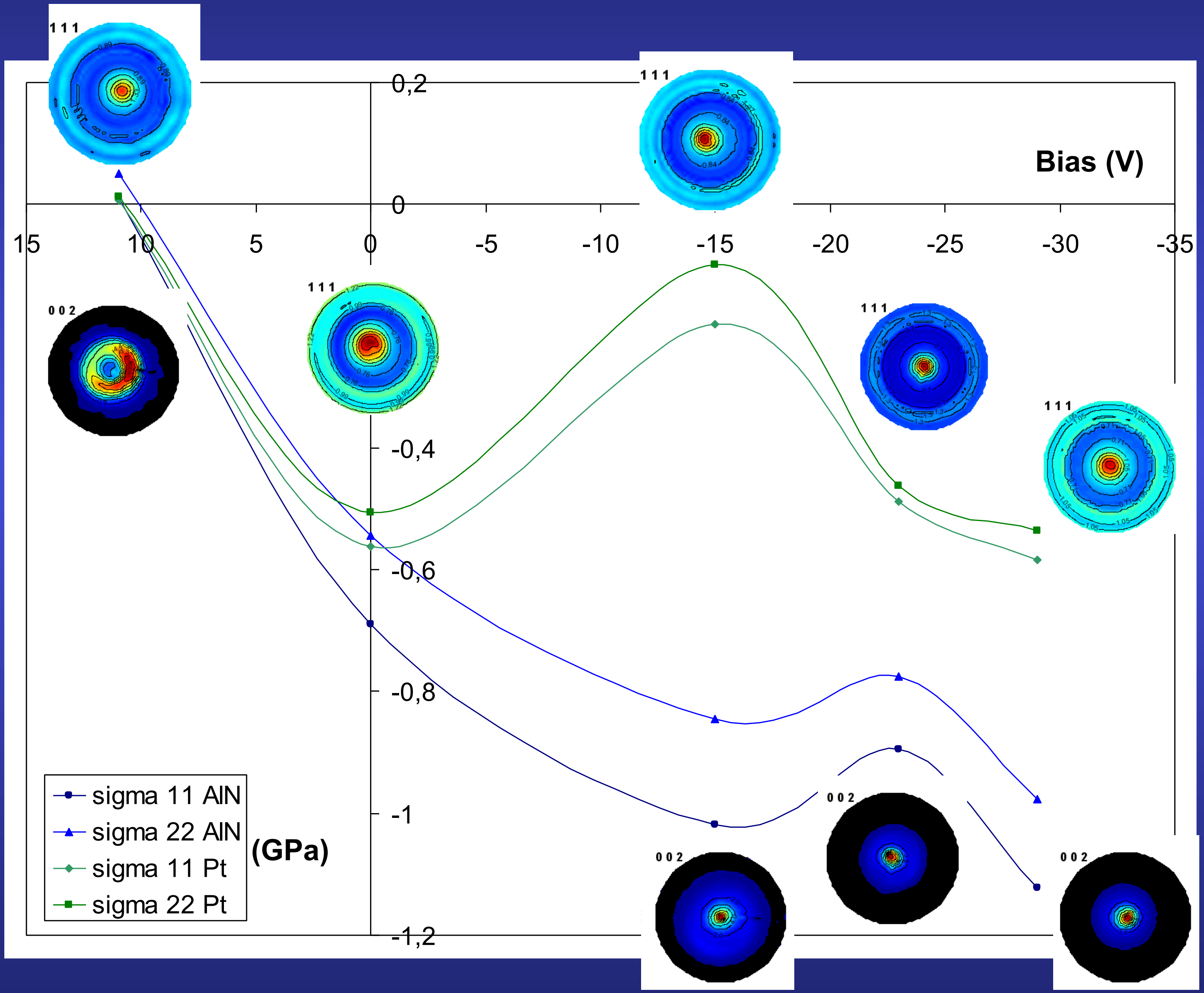

Si nanocrystalline thin films

M. Morales, Caen

Silicon thin films deposition by reactive magnetron sputtering:

- power density 2W/cm^2
- total pressure: $p_{total} = 10^{-1}$ Torr
- plasma mixture: H_2 / Ar, pH_2 / p_{total} = 80 %
- temperature: 200°C
- substrates: amorphous SiO_2 (a-SiO_2)
  (100)-Si single-crystals
- target-substrate distance (d)
  - a-SiO_2 substrates: d = 4, 6, 7, 8, 10, 12 cm
    films A, B, C, D, E, F
  - (100)-Si: d = 6, 12 cm
    films G, H

Aim: quantum confinement, photoluminescence properties

Typical refinement

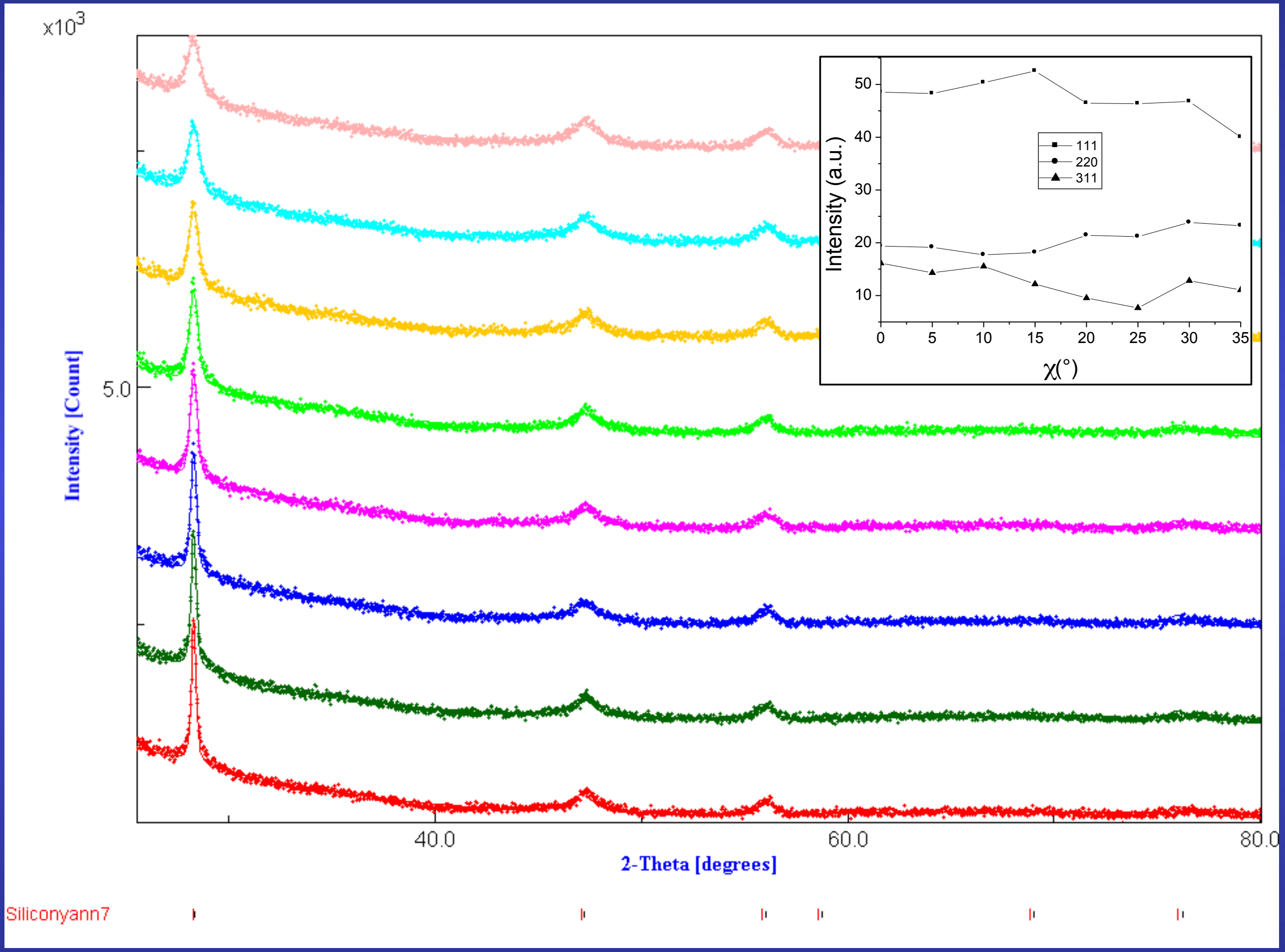

χ = 35°

χ = 0°

broad, anisotropic diffracted lines, textured samples

Refinement Results

Sample	d (cm)	a (Å)	RX thickness (nm)	Anisotropic sizes (Å)			Texture parameters			Reliability factors (%)			
				<111>	<220>	<311>	Maximum (m.r.d.)	minimum (m.r.d.)	Texture index F^2 (m.r.d^2)	RP_0	R_w	R_B	R_{exp}
A	4	5.4466 (3)	---	94	20	27	1.95	0.4	1.12	1.72	4.0	3.7	3.5
B	6	5.4439 (2)	711 (50)	101	20	22	1.39	0.79	1.01	0.71	4.9	4.3	4.2
C	7	5.4346 (4)	519 (60)	99	40	52	1.72	0.66	1.05	0.78	4.3	4.0	3.9
D	8	5.4461 (2)	1447 (66)	100	22	33	1.57	0.63	1.04	0.90	5.5	4.6	4.5
E	10	5.4462 (2)	1360 (80)	98	20	25	1.22	0.82	1.01	0.56	5.0	3.9	4.0
F	12	5.4452 (3)	1110 (57)	85	22	26	1.59	0.45	1.05	1.08	4.2	3.5	3.7
G	6	5.4387 (3)	1307 (50)	89	22	28	1.84	0.71	1.01	1.57	5.2	4.7	4.2
H	12	5.4434 (2)	1214 (18)	88	22	24	2.77	0.50	1.12	2.97	5.0	4.5	4.3

Mean anisotropic shape

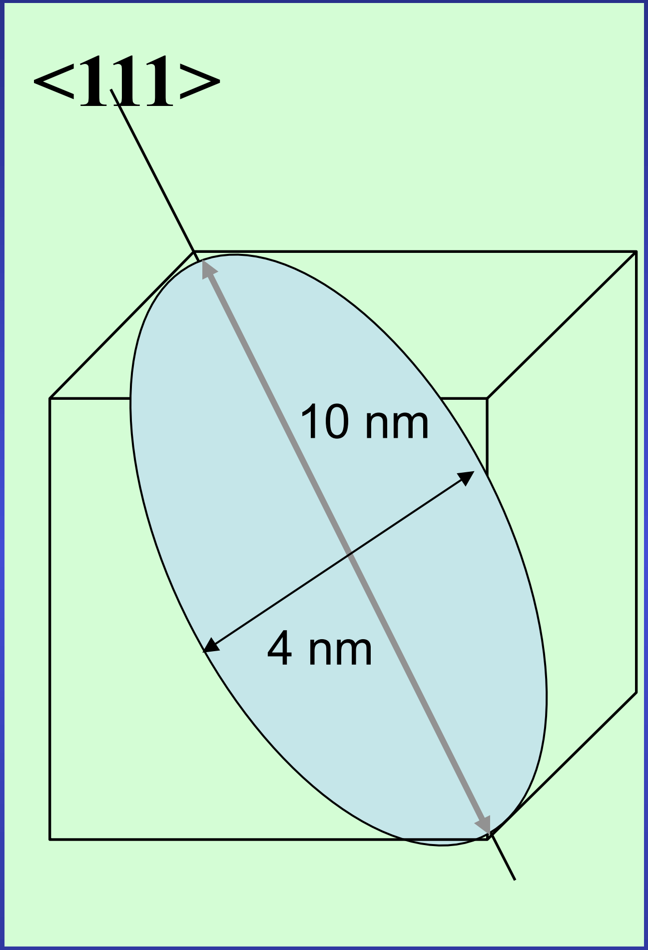

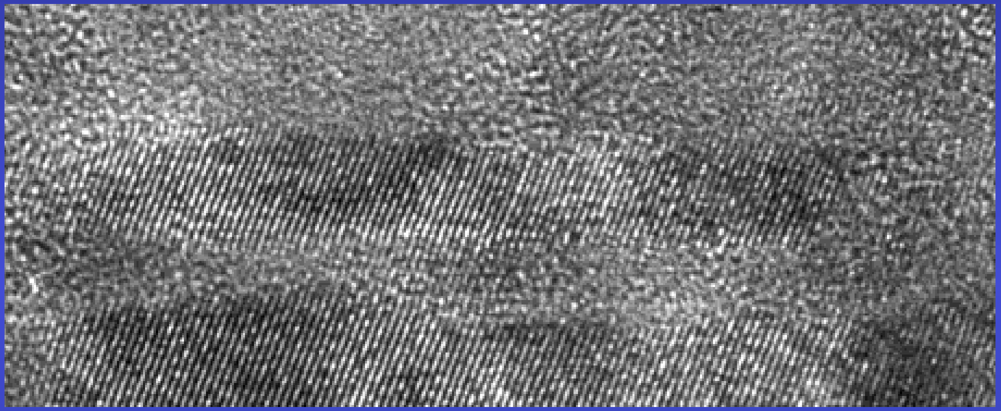

Schematic of the mean crystallite shape for Sample D represented in a cubic cell, as refined using the Popa approach and exhibiting a strong elongation along <111>, and TEM image

001 Inverse Pole Figures

a-SiO_2

(100)-Si

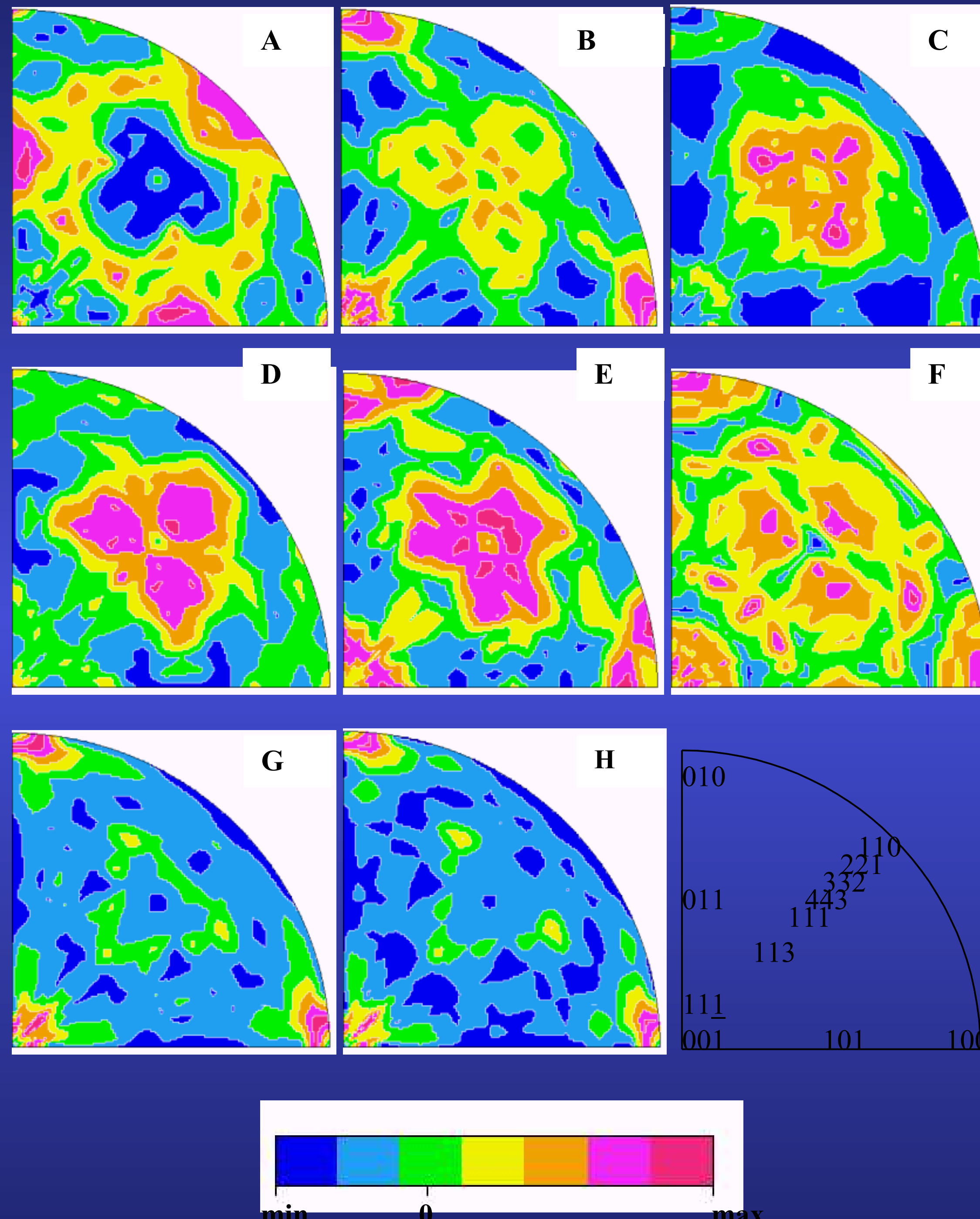

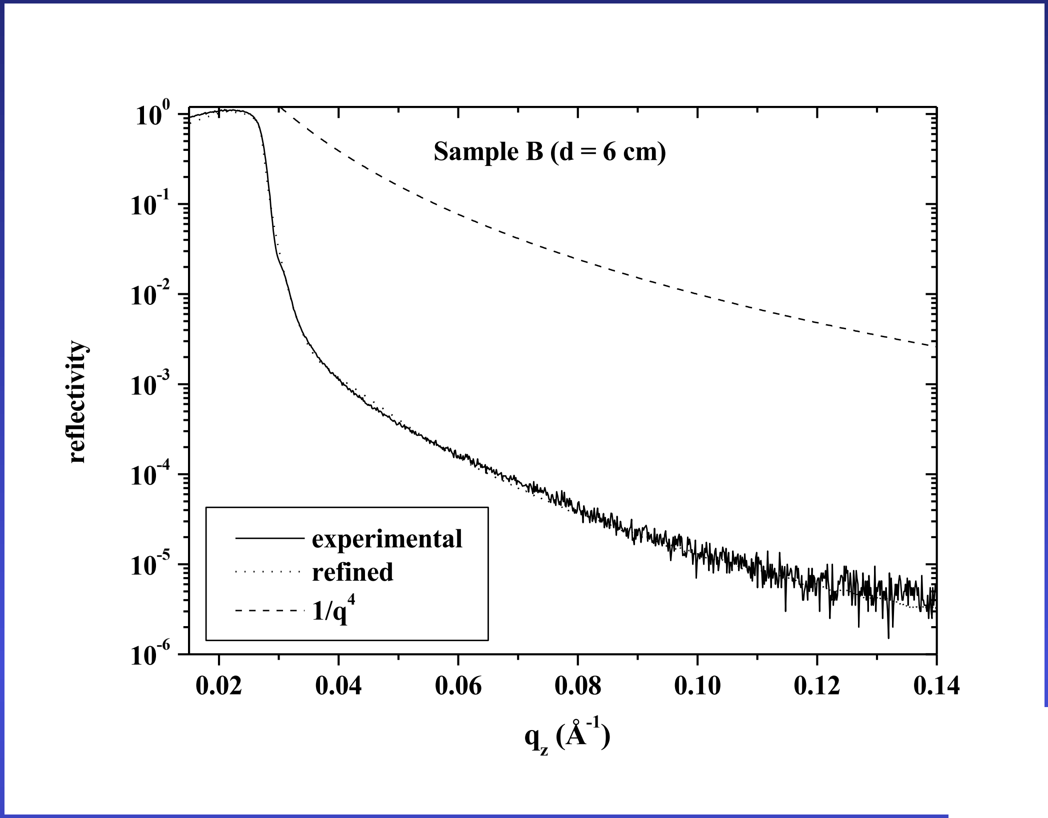

XRR:

Roughness governed

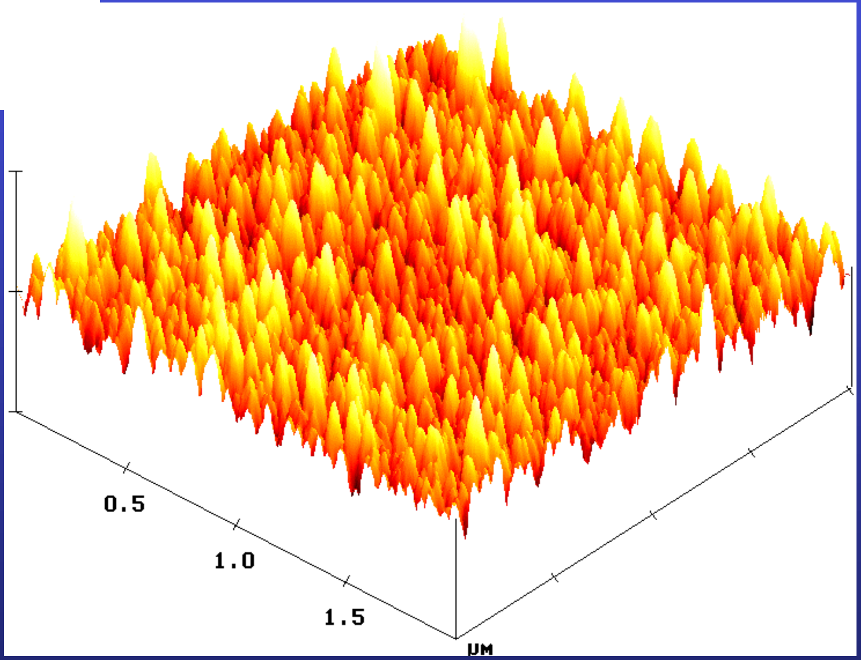

AFM:

homogeneous roughness

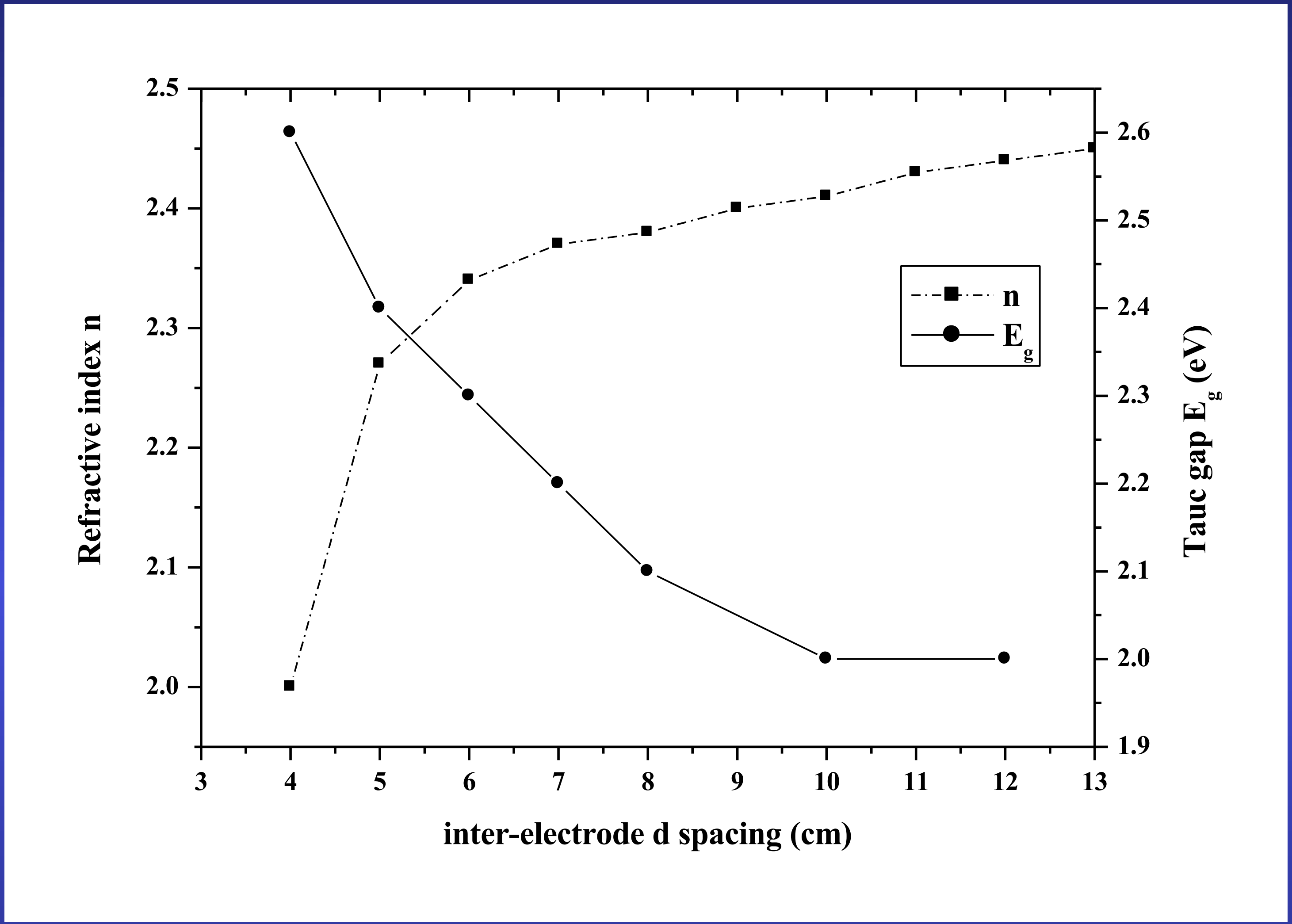

↳ Refractive index linked to film porosities:

Larger target-sample distances: increased compacity due to lower nanopowder filling

Ferroelectric PCT films

J. Ricote, Madrid

thin films:

$(Ca_{0.24}Pb_{0.76})TiO_3$ sol-gel synthesised solutions deposited by spin coating on a substrate of $Pt/TiO_2/Si$, with and without a treatment at 650ºC for 30 min.

All films are crystallised at 700ºC for 50 s by Rapid Thermal Processing (RTP; 30ºC/s).
A series is also recrystallised at 650ºC for 1 to 3 h.

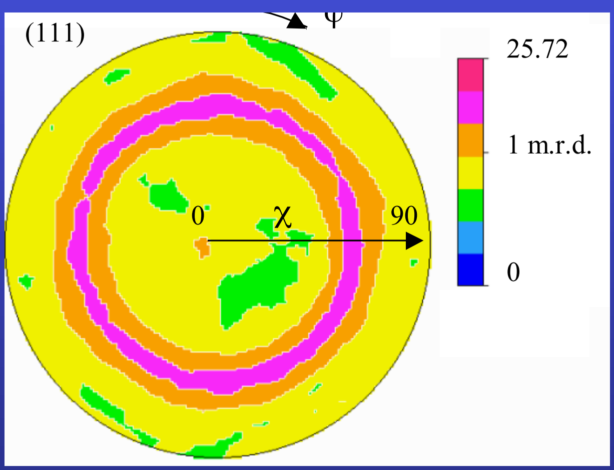

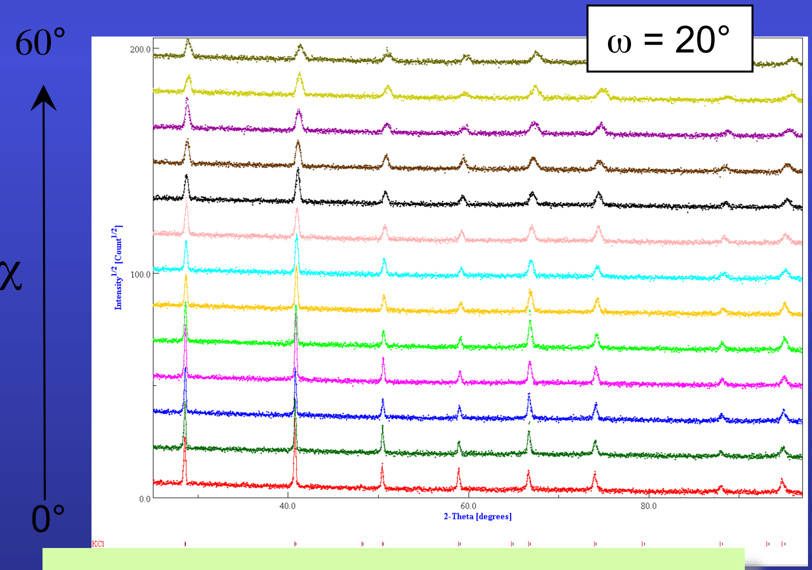

Refinement of individual spectra

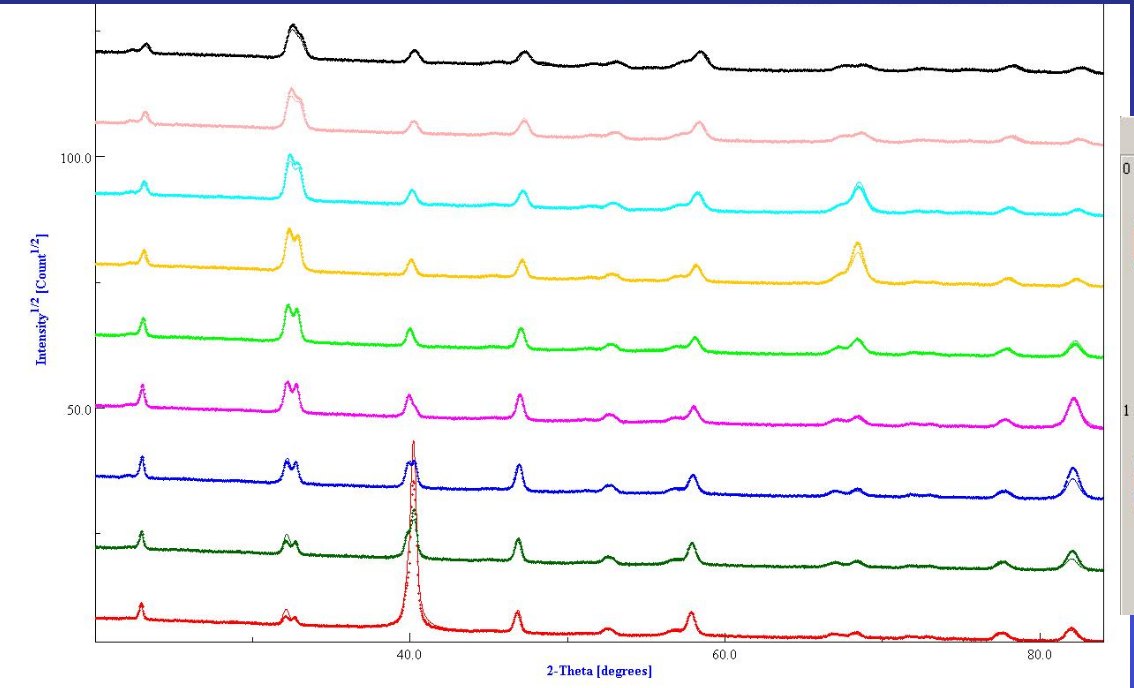

PCT

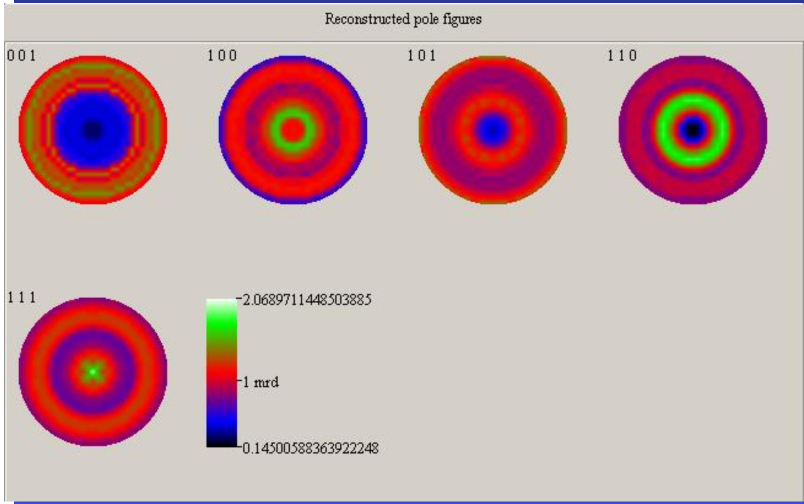

a = 3.9156(1) Å
c = 4.0497(3) Å
T = 2525(13) Å
t_{iso} = 390(7) Å
ε = 0.0067(1) rms

Pt

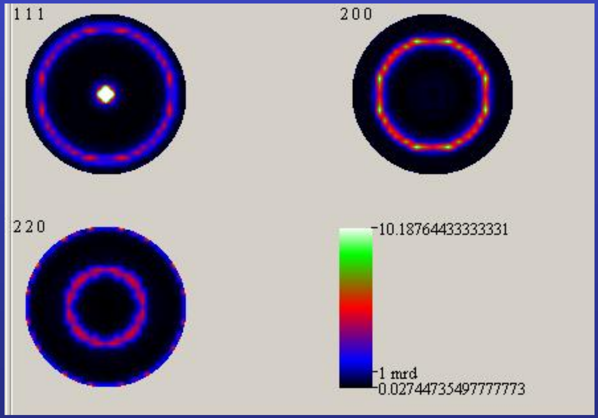

a = 3.9108(1) Å
T = 457(3) Å
t_{iso} = 458(3) Å
ε' = 0.0032(1) rms

R_W = 13%; R_B = 12%; R_{exp} = 22%.(Rietveld)
R_W = 5%; R_B = 6% (E-WIMV)

Atom	Occupancy	x	y	z
Pb	0.76	0.0	0.0	0.0
Ca	0.24	0.0	0.0	0.0
Ti	1.0	0.5	0.5	0.477(2)
O1	1.0	0.5	0.5	0.060(2)
O2	1.0	0.0	0.5	0.631(1)

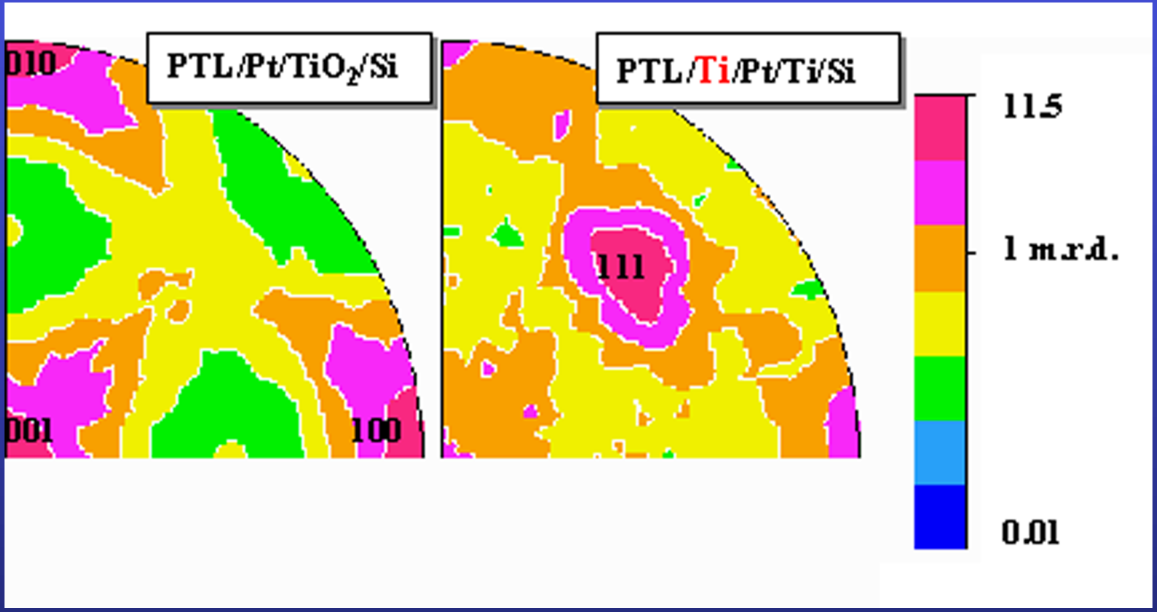

Compliance coefficients $[10^{-3}\ GPa^{-1}]$	$PbTiO_3$ single crystal (data set A)	Film random orientation	PCT-Si <001> contrib≈17%	PLT <001> contrib.≈49%	PCT-Mg <001> contrib.≈68%
s_{11}	6.5	10.1	10.5	10.0	9.7
s_{22}	6.5	10.0	10.5	10.0	9.7
s_{33}	33.3	9.8	9.0	10.3	11.3
s_{44}	14.5	13.2	12.8	12.9	13.1
s_{55}	14.5	13.2	12.8	13.0	13.1
s_{66}	9.6	13.4	14.0	13.5	12.7
s_{12}	-0.35	-3.3	-3.5	-3.2	-3.0
s_{21}	-0.35	-3.3	-3.5	-3.2	-3.0
s_{13}	-7.1	-3.2	-3.1	-3.4	-3.6
s_{31}	-7.1	-3.2	-3.1	-3.4	-3.6
s_{23}	-7.1	-3.2	-3.1	-3.4	-3.6
s_{32}	-7.1	-3.2	-3.1	-3.4	-3.6
s_{33}/s_{11}	5.1	0.97	0.86	1.03	1.16
s_{13}/s_{12}	20.3	0.97	0.89	1.06	1.20

Geometric mean average + biaxial stress state

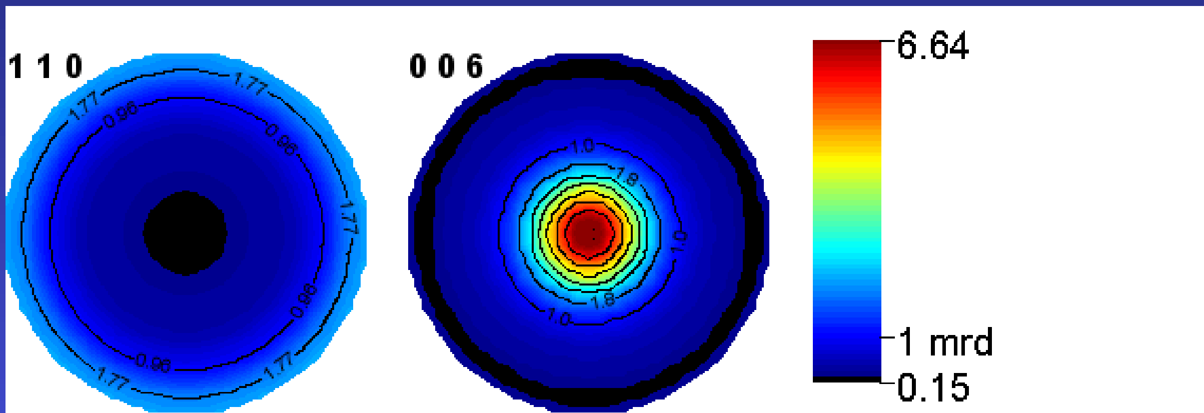

R_W (%) = 9.23
R_B (%) = 7.40

a = 4.75611(6) Å
c = 12.9806(1) Å

z_{Al} = 0.35266(3) Å
x_O = 0.6923(2) Å

Cyclic-fibre texture assumed

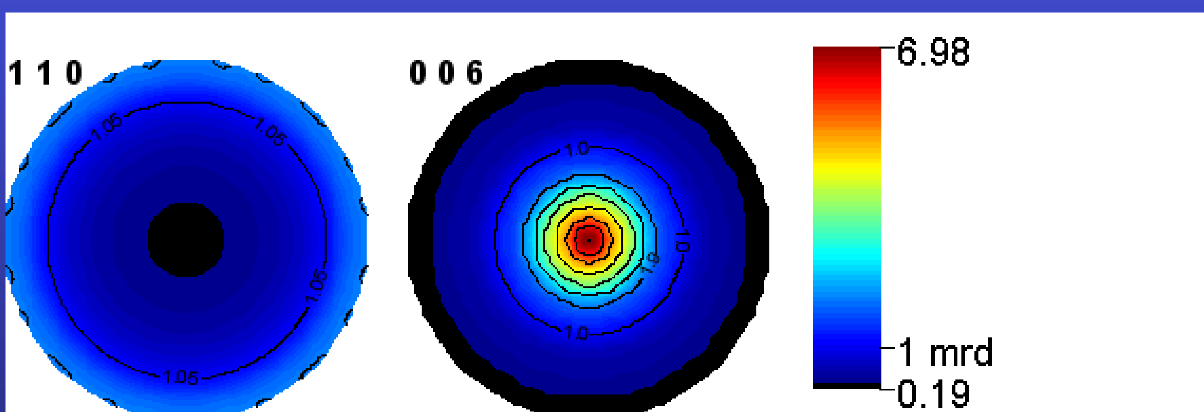

R_W (%) = 7.14
R_B (%) = 5.64

a = 4.75874(3) Å
c = 12.99373(7) Å

z_{Al} = 0.35225(2) Å
x_O = 0.6943(2) Å

Limitations of the simple Quantitative Texture Analysis

Structural parameters are difficult to obtain due to:

Substrate influence:
overlapping of reflections from the film and the substrate

TEXTURE effects:
peaks that do not appear at low χ angles

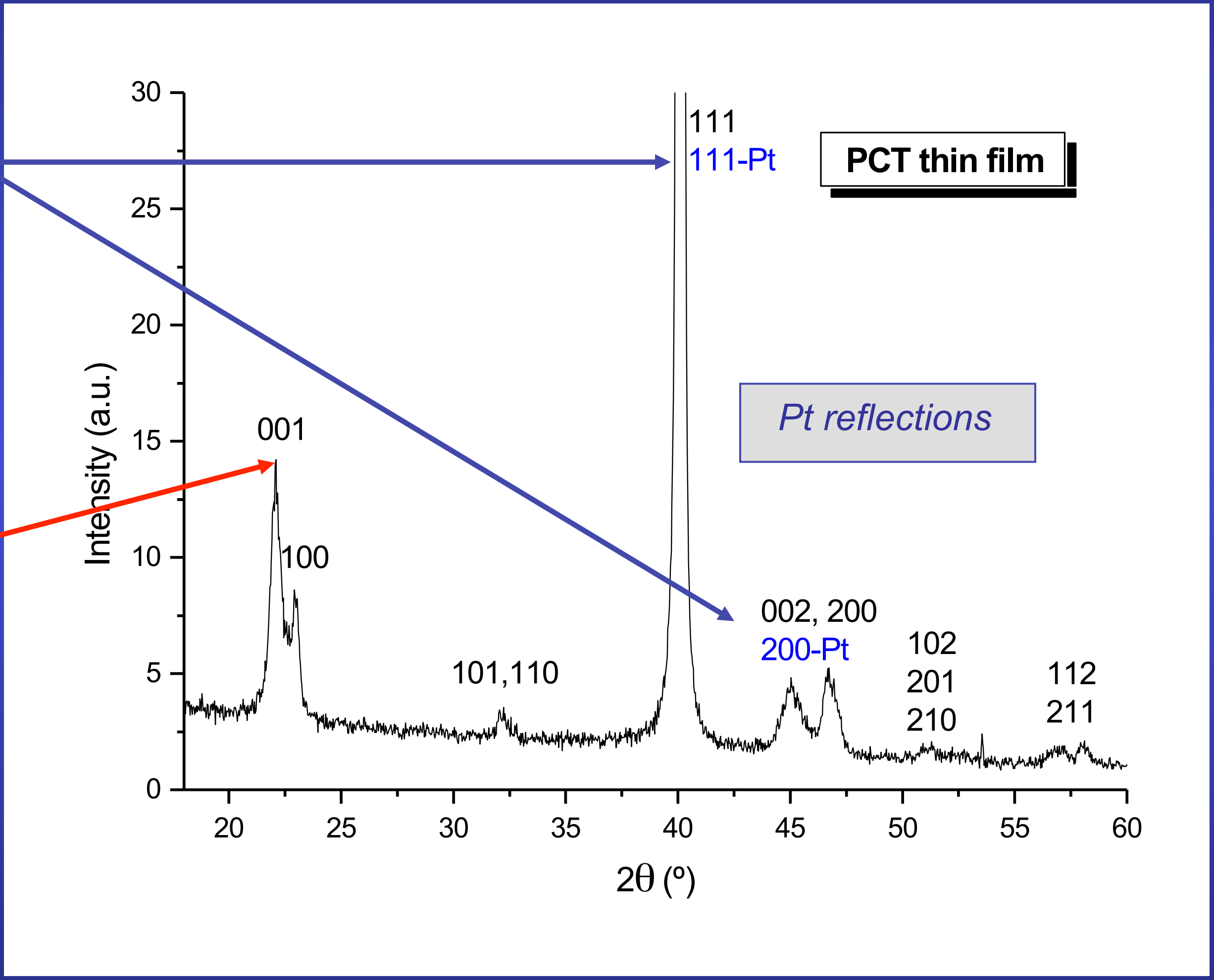

Structural parameters

Pt layer

	a (Å)	thickness (nm)	R factors (%)
non-treated substrate			
Pt	3.9108(1)	45.7(3)	R_W=13, R_B=12, R_{exp}=22
annealed substrate			
Pt	3.9100(4)	46.4(3)	R_W=8, R_B=14, R_{exp}=21
Pt (Recryst. 1h)	3.9114(2)	47.8(3)	R_W=9, R_B=20, R_{exp}=21
Pt (Recryst. 2h)	3.9068(1)	46.9(3)	R_W=9, R_B=14, R_{exp}=22
Pt (Recryst. 3h)	3.9141(4)	47.5(9)	R_W=27, R_B=12, R_{exp}=21

Annealing of the substrate does not introduce significant variations on the structure of the Pt layer

PTC film

	a (Å)	c (Å)	thickness (nm)
on non-treated substrate			
PCT	3.9156(1)	4.0497(6)	272.5(13)
on annealed substrate			
PCT	3.8920(6)	4.0187(8)	279.0(9)
PCT (Recryst. 1h)	3.8929(2)	4.0230(4)	266.1(11)
PCT (Recryst. 2h)	3.8982(2)	4.0227(4)	258.4(9)
PCT (Recryst. 3h)	3.9001(4)	4.0228(11)	253.6(29)

Recrystallisation reduces the stress on the film, and, increases the lattice parameters

Structural, microstructural and texture quantitative characterisation of ferroelectric thin films by the combined method

Analysis of the X-ray diffraction diagrams of a PCT film on $Pt/TiO_2/Si$

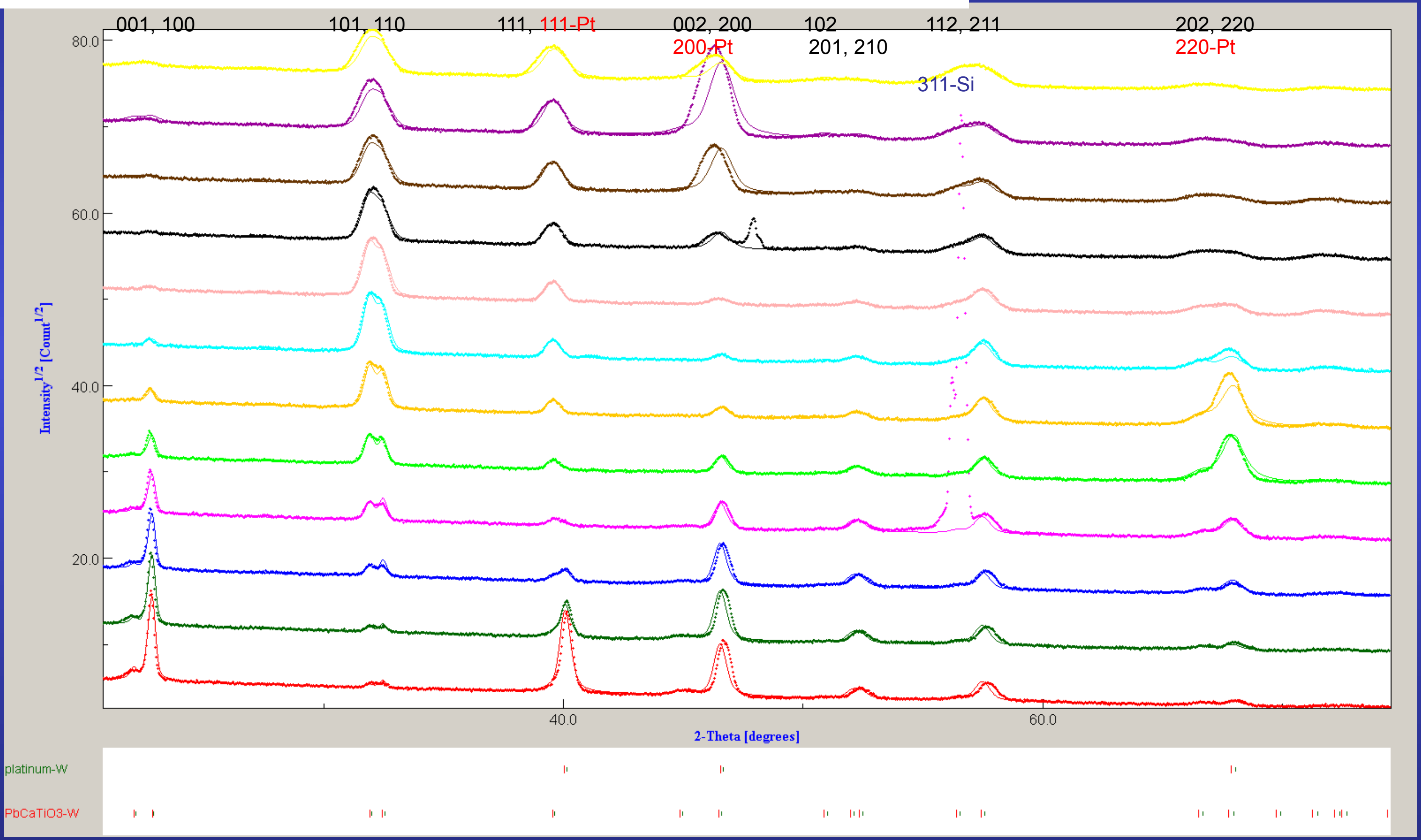

R_W = 13%; R_B = 12%; R_{exp} = 22%.(Rietveld)
R_W = 5%; R_B = 6% (E-WIMV)

Substrate influence on Residual Stress and Texture

Tensile stress

PCT on $Pt/TiO_2/(100)Si$

PCT on $Pt/(100)MgO$

PCT on $Pt/(100)SrTiO_3$

Compressive stress

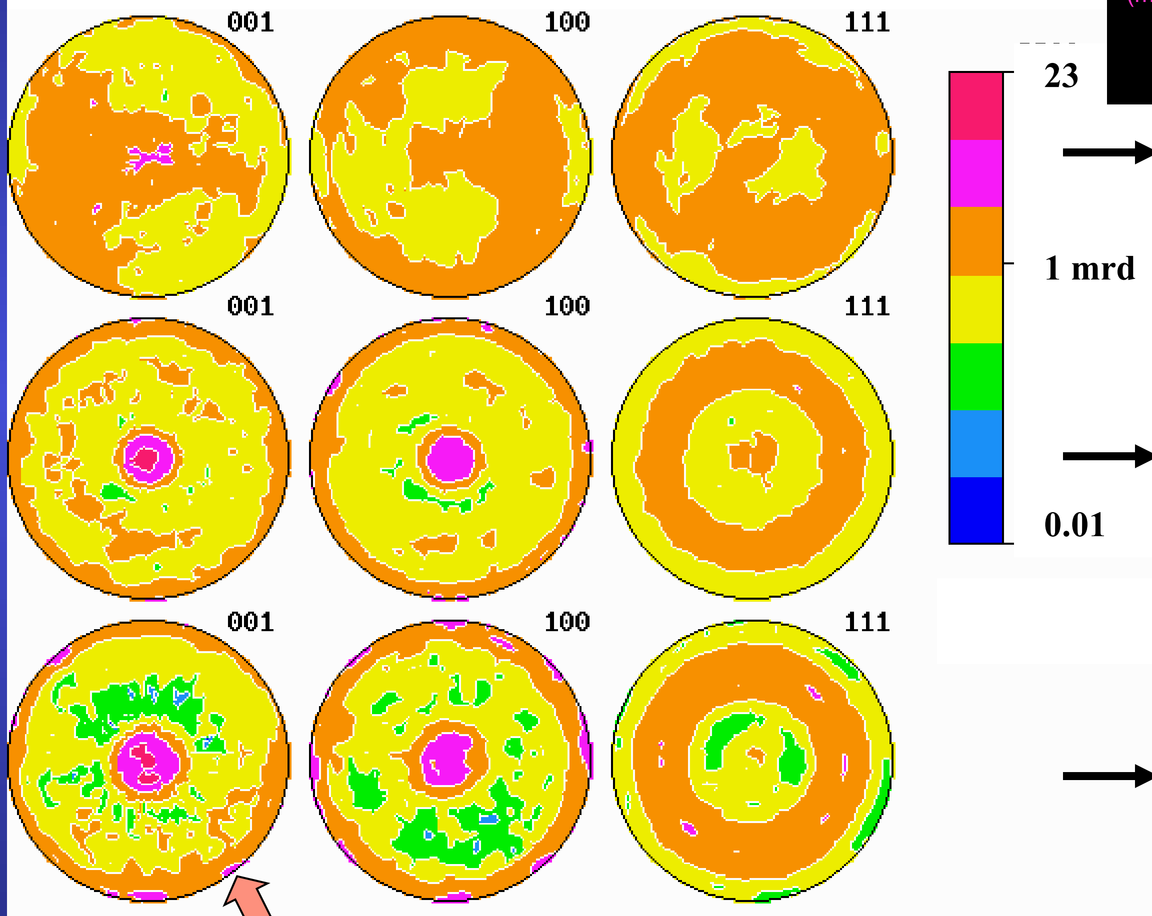

Enhancement of <001> texture

Texture Index (m.r.d.^{2})	Pyroelectric Coefficient (10^{-8}C cm^{-2} K^{-1})
2.1	0.3
5.1	1.5
7.9	1.1

Ferroelectric PMN-PT films

J. Ricote, DMF-Madrid

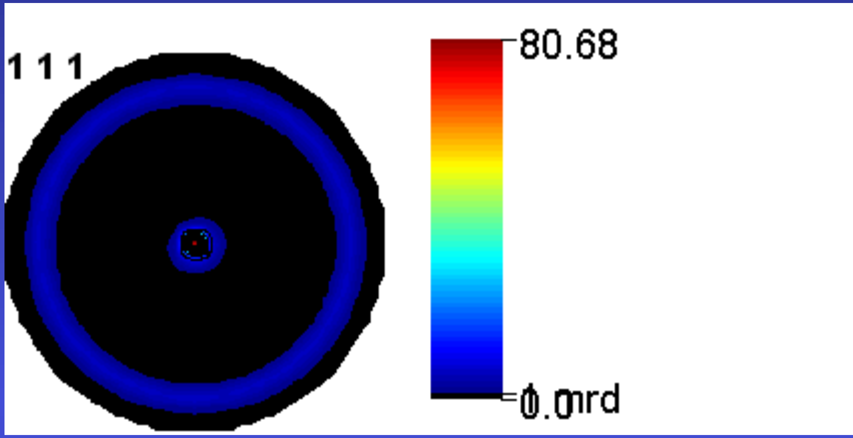

Pt

a = 3.91172(1) Å
T = 583(5) Å
t_{iso} = 960(1) Å
ε = 0.0032(1) rms
σ_{11}= 0.639(1) GPa
σ_{22}= 0.651(1) GPa
σ_{12}= -0.009(1) GPa

$Pb_{0.7} (Mg_{1/3}Nb_{2/3})O_3$-$Pb_{0.3}TiO_3$ /$Ti0_2$/Pt/Si-(100)

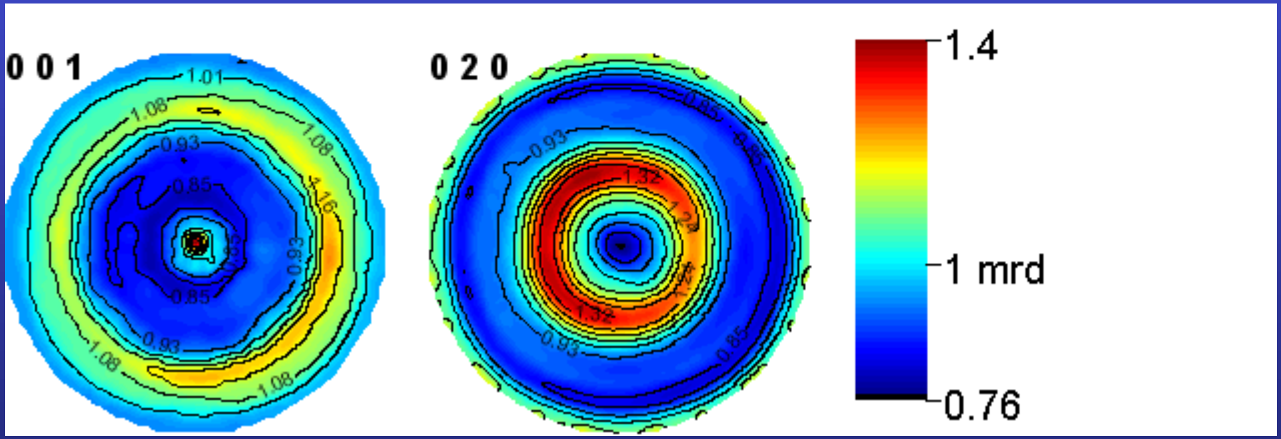

a = 5.67858(9) Å
b = 5.69038(9) Å
c = 3.99558(4) Å
β = 90.392(1) Å
T = 1322(9) Å
t_{iso} = 1338(2) Å
ε = 0.0067(1) rms

ZnSe:Cr^{2+} films
N. Vivet, PhD

conditions:

♦ $20 \leq T_d \leq 385°C$
♦ P_{RF} = 50-200W
♦ P_{Ar} = 0.5 Pa and 2 Pa
♦ d = 7 and 10 cm

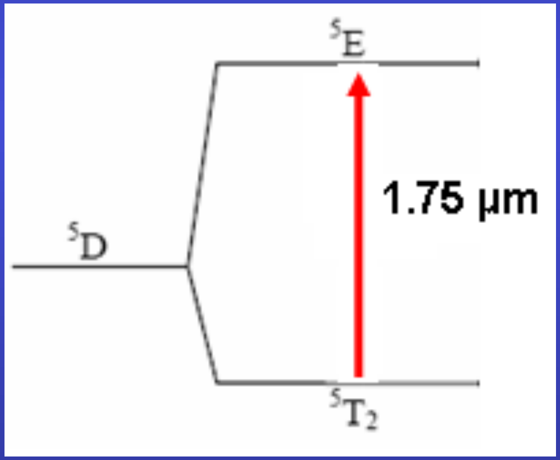

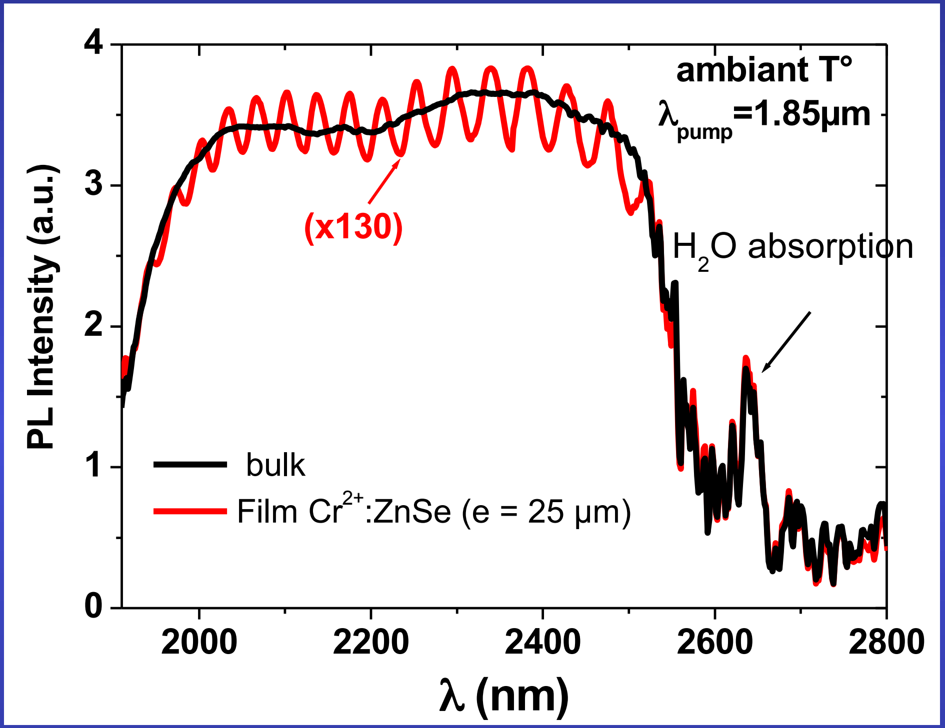

♦ **Large emission band centred at 2200nm: $^5E \rightarrow {}^5T_2$ transition (Cr^{2+})**

♦ **Single crystals and thin films: similar spectra**

111 Peak shifts

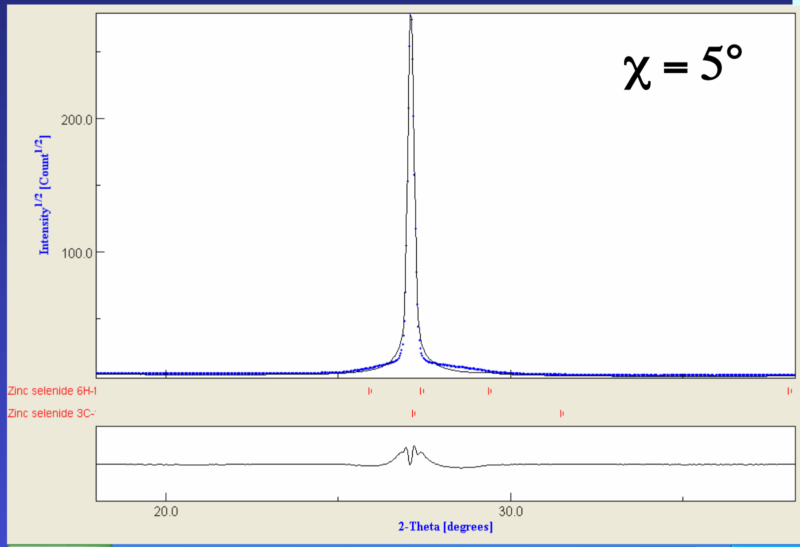

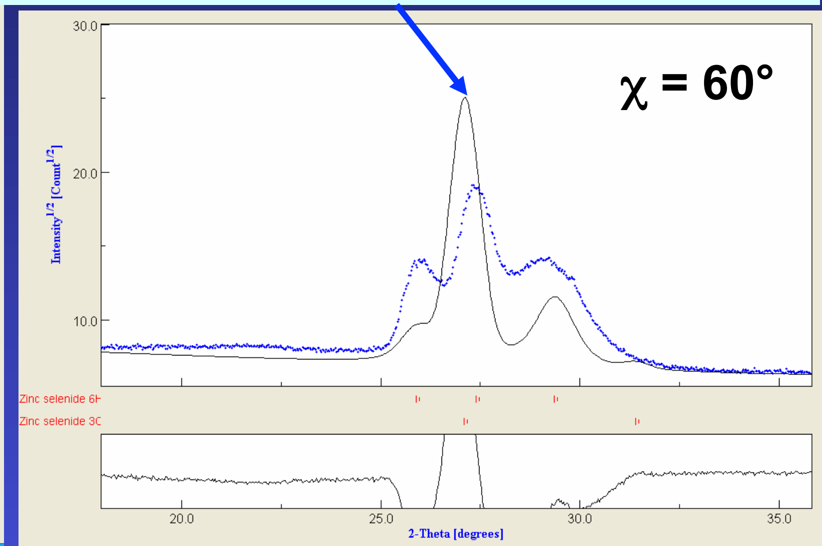

Residual stresses and/or stacking faults

Anisotropic sizes

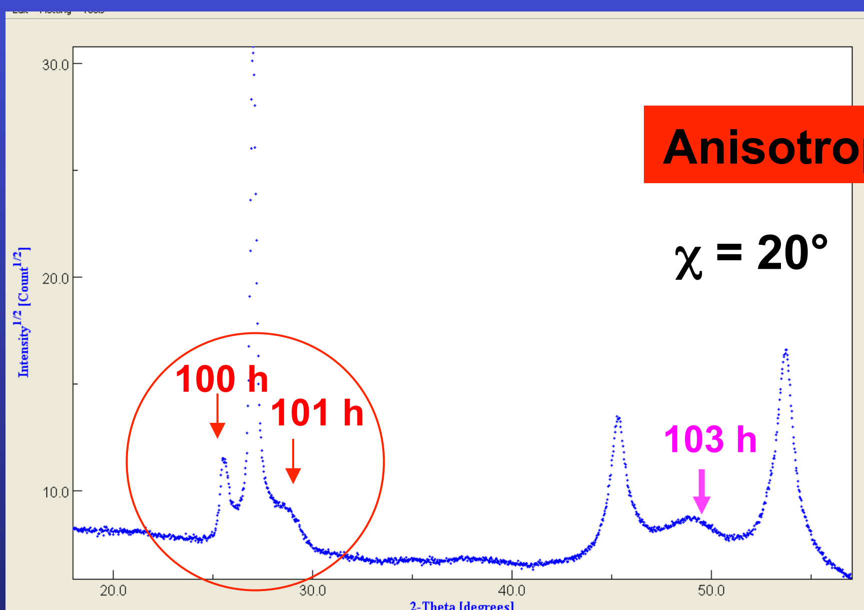

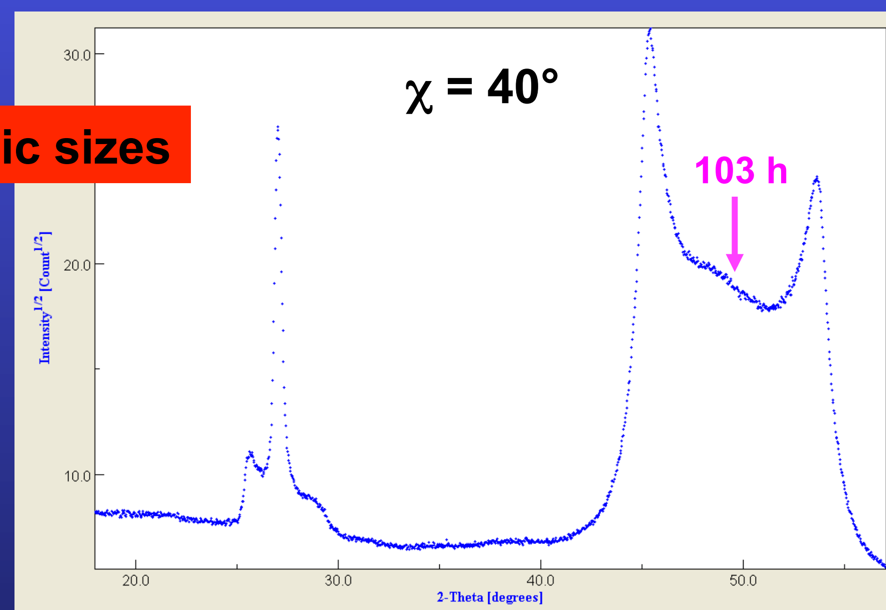

Fibre Texture + 2 polytypes (6H and 3C) + anisotropic sizes + residual stresses and/or stacking faults + layering

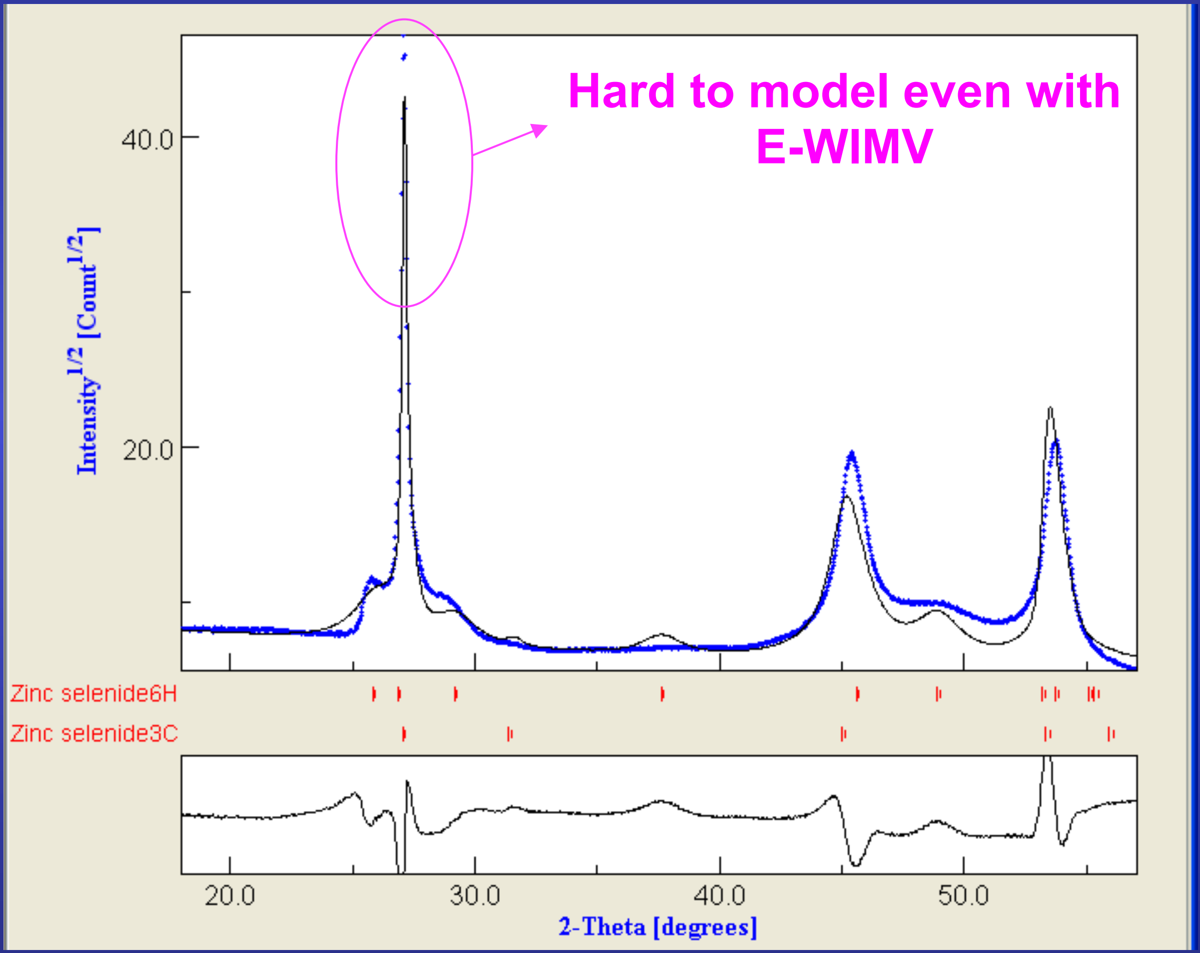

Sum diagram: ω =13.65°, P_{RF} = 200W

Gold thin films

Crystallite size (Å) along	Film thickness					
	10nm	**15nm**	**20nm**	**25nm**	**35nm**	**40nm**
[111]	176	153	725	254	343	379
[200]	64	103	457	173	321	386
[202]	148	140	658	234	337	381

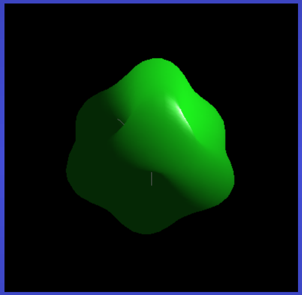

10 nm

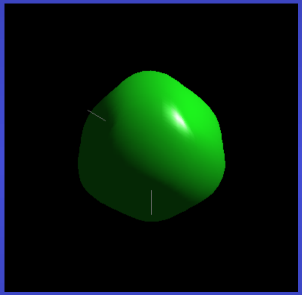

15 nm

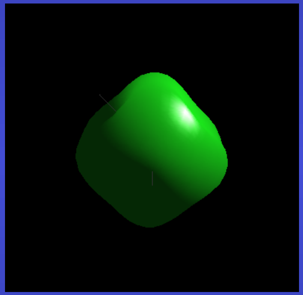

20 nm

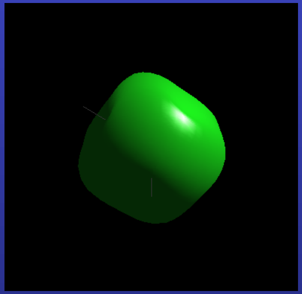

25 nm

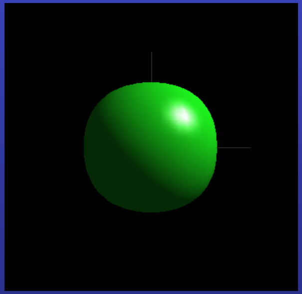

35 nm

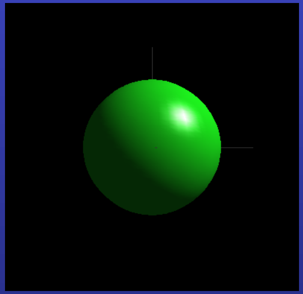

40 nm

$Zr_{0.8}Ca_{0.2}O_2$ film orthorhombic texture

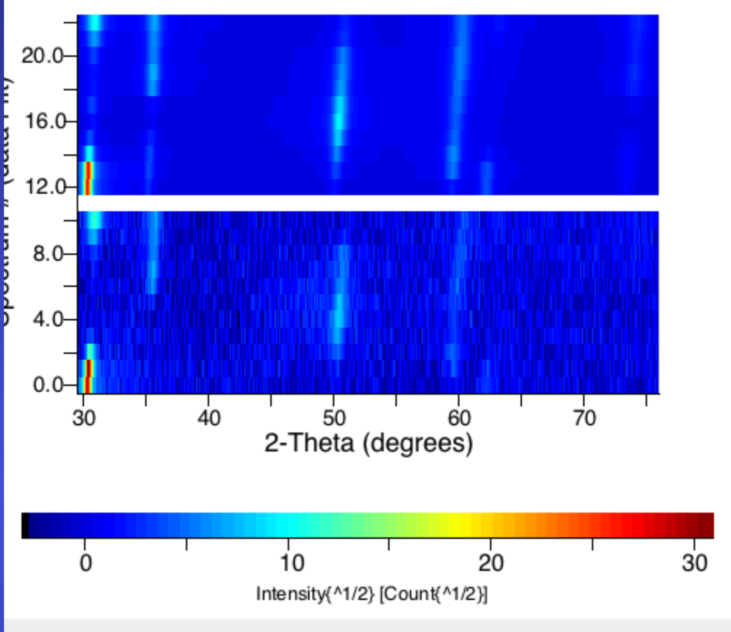

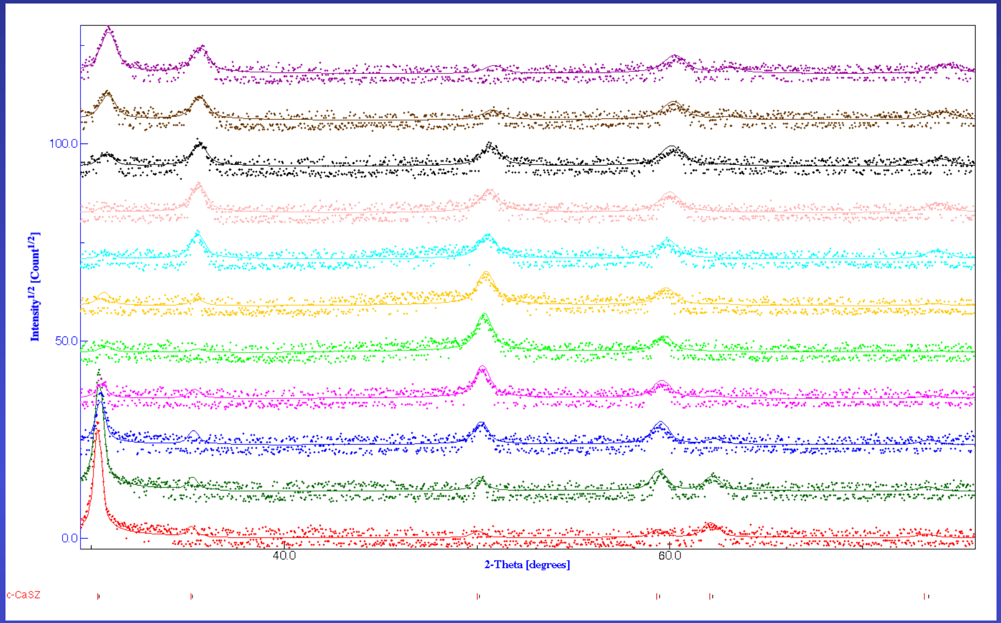

a = 5.146(2) Å
<t> = 106(2) Å
<ε> = 0.00333(5)
$\sigma_{11} = \sigma_{22}$ -2.62(8) GPa